January 2014

Evaluation and Modeling of Internal Water Storage Zone Performance in Denitrifying Bioretention Systems

Thomas Joseph Lynn
University of South Florida, tjlynn@mail.usf.edu

Follow this and additional works at: http://scholarcommons.usf.edu/etd

Part of the Civil Engineering Commons, and the Environmental Engineering Commons

Evaluation and Modeling of Internal Water Storage Zone Performance in Denitrifying

Bioretention Systems

by

Thomas J. Lynn

Dedication

I dedicate this dissertation to my mother, my father, my grandmother Agnes and Dr.

Sunil Saigal.

Acknowledgments

I would like to thank all of my committee members, Dr. Sarina Ergas, Dr. Daniel Yeh, Dr. Mahmood Nachabe, Dr. Valerie Harwood, and Dr. John Kuhn and my outside chair, Dr. Kamal Alsharif, for their interest in my doctoral research. In particular, I am very grateful for having Dr. Ergas mentor me on a weekly basis. I would also like to thank Dr. James Mihelcic and Dr. Manriker Gunaratne for creating a path for me to begin and complete my research. I would like to thank Dr. Nachabe (+10 years), Dr. Yeh (10 years) and Dr. Audrey Levine for educating and/or mentoring me during my undergraduate and graduate studies and/or professional development. I would like to thank Harold Barrineau, Randall Cooper, John Early, Daryl Flatt, Mary French, Jim Jones, Jon Kramer, Steven Lopes, and Larry Szabrak for encouraging my professional development. I would like to thank Richard Allan, Irene Chen, Bill and Marge Gelatka, Jim Schwinn and Bob Vincent for their encouragement. I would like to thank John Lynn Jr. for being my personal computer technician and Jim Lynn for checking up on me. I would like to thank Veronica Aponte Morales, Robert Bair, Qais Banihani, Suzie Boxman, Ivy Drexler, Kim Hutton, Maureen Kinyua, Lucie Krayzelova, Eunyoung Lee, Alex Lin, Ryan Locicero, Emma Lopez, Valerie Mauricio-Cruz, Thanh Nguyen, Oscar Pena, James Poulin, Laurel Rowse, Laura Rodriguez-Gonzalez, Kevin Slaughter, Laurie Walker and Dr. Pauline Wanjugi for assisting me during my research. I would also like to thank the National Science Foundation, the Southwest Florida Water Management District, the Tampa Bay Estuary Program and the University of South Florida College of Engineering for their support.

Table of Contents

ii

iii

List of Tables

v

vii

viii

ix

x

xi

xiv

xv

List of Figures

Abstract

Nitrate (NO_3^-) loadings from stormwater runoff promote eutrophication in surface waters. Low Impact Development (LID) is a type of best management practice aimed at restoring the hydrologic function of watersheds and removing contaminants before they are discharged into ground and surface waters. Also known as rain gardens, a bioretention system is a LID technology that is capable of increasing infliltration, reducing runoff rates and removing pollutants. They can be planted with visually appealing vegetation, which plays a role in nutrient uptake. A modified bioretention system incorporates a submerged internal water storage zone (IWSZ) that includes an electron donor to support denitrification. Modified (or denitrifying) bioretention systems have been shown to be capable of converting NO_3^- in stormwater runoff to nitrogen gas through denitrification; however, design guidelines are lacking for these systems, particularly under Florida-specific hydrologic conditions.

The experimental portion of this research investigated the performance of denitrifying bioretention systems with varying IWSZ medium types, IWSZ depths, hydraulic loading rates and antecedent dry conditions (ADCs). Microcosm studies were performed to compare denitrification rates using wood chips, gravel, sand, and mixtures of wood chips with sand or gravel media. The microcosm study revealed that carbon-containing media, acclimated media and lower initial dissolved oxygen concentrations will enhance NO_3^- removal rates. The gravel-wood medium was observed to have high NO_3^- removal rates and low final dissolved organic

carbon concentrations compared to the other media types. The gravel-wood medium was selected for subsequent storm event and tracer studies, which incorporated three completely submerged columns with varying depths. Even though the columns were operated under equivalent detention times, greater NO_3^- removal efficiencies were observed in the taller compared to the shorter columns. Tracer studies revealed this phenomenon was attributed to the improved hydraulic performance in the taller compared to shorter columns. In addition, greater NO_3^- removal efficiencies were observed with an increase in ADCs, where ADCs were positively correlated with dissolved organic carbon concentrations.

Data from the experimental portion of this study, additional hydraulic modeling development for the unsaturated layer and unsaturated layer data from other studies were combined to create nitrogen loading model for modified bioretention systems. The processes incorporated into the IWSZ model include denitrification, dispersion, organic media hydrolysis, oxygen inhibition, bio-available organic carbon limitation and Total Kjeldahl Nitrogen (TKN) leaching. For the hydraulic component, a unifying equation was developed to approximate unsaturated and saturated flow rates. The hydraulic modeling results indicate that during ADCs, greater storage capacities are available in taller compared to shorter IWSZs Data from another study was used to develop a pseudo-nitrification model for the unsaturated layer. A hypothetical case study was then conducted with SWMM-5 software to evaluate nitrogen loadings from various modified bioretention system designs that have equal IWSZ volumes. The results indicate that bioretention systems with taller IWSZs remove greater NO_3^- loadings, which was likely due to the greater hydraulic performance in the taller compared to shorter IWSZ designs.

However, the systems with the shorter IWSZs removed greater TKN and total nitrogen loadings due to the larger unsaturated layer volumes in the shorter IWSZ designs.

Chapter 1:

Introduction

Stormwater runoff is a major source of surface water degradation in the United States (Akan and Houghtalen, 2003). Urbanization increases impervious areas, which intensifies nitrogen runoff to downstream surface waters. Excessive nitrogen runoff promotes eutrophication, which is known to contribute to fish kills, loss of biodiversity, hypoxic zones, seagrass mortality, physical interferences with recreation and rapid filling of surface water bodies (Vaccari et al, 2006; Cameron et al., 2010; Moorman et al., 2010).

Best Management Practices (BMPs) have been developed in an attempt to control nitrogen loadings from urban areas. BMPs were originally created to control flooding in developed areas; however, the Federal Clean Water Act, passed in 1972, facilitated the understanding of how non-point sources (e.g., stormwater runoff) contribute to surface water pollution (Gurr and Nnadi, 2009). Consequently, BMPs were modified to provide treatment, which has been further enhanced through the development of Low-Impact-Development (LID) technologies. LID is one category of BMPs, which more closely focuses on maintaining or restoring the pre-development hydrologic and water quality characteristics of a site (Dietz, 2007; Viesmann et al. 2009).

One type of LID technology are bioretention systems, also known as "raingardens", "bioinfiltration" or bioswales (Davis et al., 2006). Bioretention systems have the capability of reducing runoff volumes, attenuating peak flows and removing solids, organics, metals, phosphorous and various forms of nitrogen (Davis et al., 2006). As a unique advantage compared with other LID technologies, bioretention systems can be modified to include a denitrification zone, or submerged internal water storage zone (IWSZ), for removing nitrate (NO_3^-) (Kim et al., 2003; Brown et al., 2011). Denitrification in the IWSZ occurs because portions of the zone can become anoxic as aerobic and facultative microorganisms utilize dissolved oxygen in a submerged IWSZ that is supplied with an electron-donor (e.g. wood chips, elemental sulfur) (Kim et al., 2003; Davis et al., 2009; Ergas et al., 2010).

There is a lack of information available to provide IWSZ design guidance for bioretention systems. Most prior research on modified bioretention systems has focused on evaluating denitrification performance in relation to one or two design parameters (e.g., hydraulic loading rate, IWSZ depth) (Kim et al., 2003; Lucas et al., 2007b; Zinger et al, 2007; Lucas et al 2011a). In addition, a simple mathematical model for calculating nitrate (NO_3^-) removal in IWSZs has not been developed (Collins et al., 2010). Such a model should be able to predict performance in IWSZs with varying depth, detention time, antecedent dry conditions (ADCs), and hydraulic and NO_3^- loading rates. Development of this model will allow designers to accurately estimate NO_3^- load reductions from modified bioretention systems.

In addition to improving bioretention IWSZ design guidance, my research begins the groundwork for designing a wet detention via bioretention (biodetention) "treatment train". This

2

unique system takes advantage of the elevation difference between on-site and downstream water elevations to promote nitrification in the sand layer, where subsequent denitrification occurs in the IWSZ. Where appropriate, this system can be designed so that bioretention precedes wet detention as implemented by Sarasota County, in Sarasota, FL (Connor, personal communication, May 17, 2012). As later discussed, nitrogen loadings from wet detention systems are of particular concern for sub-tropical regions, such as Florida.

The overall goal of this research was to provide guidelines for the design of the IWSZ in bioretention systems. The following research questions and objectives were used to guide this research:

- How do biological processes affect the dynamic performance of IWSZs?

    - Investigate NO_3^- removal performance using unacclimated and acclimated media.

    - Investigate NO_3^- removal performance under aerobic and anoxic environments.

    - Investigate NO_3^- removal performance under varying ADCs.

    - Investigate NO_3^- removal performance under varying influent NO_3^- concentrations.

    - Investigate NO_3^- removal performance under varying hydraulic loading rates.

- How do hydraulic processes affect the dynamic performance of IWSZs?

    - Evaluate the hydraulic performance of IWSZs.

    - Refine the general equations used to calculate Pe to produce more accurate results.

    - Evaluate the removal efficiency for NO_3^- and other water quality parameters of three IWSZs with varying depths that were operated with equal detention times.

3

- Can a mechanistic-based nitrogen load reduction model be developed for modified bioretention system designers?

  - Develop a simplified approach to model saturated and unsaturated flows through modified bioretention systems using SWMM-5 software.

  - Develop a nitrogen transformation model that can be used with SWMM-5.

  - Conduct a case study that evaluates annual nitrogen load reductions by implementing various bioretention system designs.

4

Chapter 2:

Literature Review

2.1 Overview

This chapter briefly describes the issues and processes that affect nitrogen removal in bioretention and other related treatment systems. Section 2.2 describes the variable nature of stormwater runoff from both a water quality and water quantity perspective. Section 2.3 describes how bioretention and related systems are used to control nitrogen loadings. Section 2.4 describes the various nitrogen transformation processes that occur within each layer in a bioretention system. Section 2.5 more thoroughly describes how solid lignocellulosic material promotes nitrate (NO_3^-) removal in the internal water storage zone (IWSZ) of bioretention systems. Separate literature reviews are also provided in Chapters 3, 4 and 5 where more emphasis is focused on the biological, hydraulic and modeling aspects of bioretention systems, respectively.

2.2 Stormwater Runoff Sources and Characteristics

In undeveloped areas, stormwater runoff is created when the rainfall rate exceeds the infiltration rate (in general terms) of a given surface. The volume and rate of stormwater runoff can be estimated if the climate type, season, region, soil type, land cover, topography, rainfall intensity and rainfall duration for a given surface is known (Bedient and Huber, 2002). However, in developed areas, the volume and rate of stormwater runoff is intensified by

www.manaraa.com

increases in impervious surfaces, tree removal, surface leveling, soil flipping, surface compaction and conveyance of runoff through stormwater pipes and channels (Akan and Houghtalen, 2003).

Increases in stormwater runoff also impair surface water quality. During dry weather conditions, pollutants build up on land surfaces (Akan and Houghtalen, 2003). During a rainfall event, these pollutants are carried away from runoff and contribute to surface water degradation. The pollutants originate from a number of sources. including fertilizer use, animal and bird feces, automobiles, street litter, street sweepings, herbicide and pesticide residues, eroded soil from construction sites and atmospheric deposition (Viesmann et al., 2009; Akan and Houghtalen, 2003; Luell et al., 2011).

Nitrogen speciation characteristics of stormwater runoff are highly variable (see Pitt et al., 2005). Factors affecting runoff quality in stormwater include: pollutant sources, land use, land use density, hydrology, antecedent dry conditions (ADCs) (time between storm events) and time of sampling during a rainfall event. Water quality characteristics of stormwater runoff are usually quantified as event mean concentrations (EMC), because the pollutant concentration of runoff changes during a rainfall event. An EMC is the total pollutant mass taken up by runoff divided by the volume of runoff (Bertrand-Krajewski et al., 1998). The "first flush", or first one-half to one inch of runoff, normally contains the highest concentrations of pollutants. Stormwater treatment regulations often require stormwater systems to be designed to treat the first flush.

6

Stormwater runoff water quantity characteristics are extremely variable due to the range of sub-processes involved. Small rainfall events dominate the total number of rainfall events. In Florida, approximately 88% of all rainfall events generate less than one inch of rainfall, which means >88% generate less than one inch of runoff (Harper and Baker, 2007). As discussed previously, ADCs have an impact on pollutant concentrations in runoff. Harper and Baker (2007) compiled a list of precipitation data from Florida and found average antecedent dry periods of 4.12 and 1.89 days for the dry and wet season, respectively. This information is useful in determining the minimum time between storm events that generate runoff, which is primarily dependent on specific site characteristics.

2.3 Best Management Practices

Best management practices (BMPs) are used to alleviate the detrimental effects of stormwater runoff (Viesmann et al., 2009). There are two types of BMPs: structural and nonstructural. Structural BMPs are physically manufactured or natural technologies and include: ponds (e.g., retention and detention), LID (also included in non-structural BMPs), gross pollutant removal devices (e.g., baffle boxes and hydrodynamic separators) and erosion control measures (e.g., rip rap and vegetation). Nonstructural BMPs are human activities related to stormwater management, such as planning, inspection, public education, compliance/enforcement and operations and maintenance. Both structural and non-structural BMPs are inter-related and essential for effectively managing stormwater runoff.

The total nitrogen and NO_3^- removal performance of various BMPs can be found in the International Stormwater Best Management Practices Database (2010). Based on these data,

media filters have the best TN removal performance (41%), but are poor in NO_3^- removal. Like bioretention systems, media filters are known to clog, which increases maintenance requirements. The International Stormwater Best Management Practices Database (2010) also provides interesting information regarding runoff influent values. Total nitrogen influent concentrations for detention ponds and media filters are almost 1 mg/L higher than the other reported BMPs. This may have occurred because detention ponds and media filters are used in many high water table environments, such as Florida. Low elevation differences between the ground surface and the water table often require engineers to design inlets and pipes to convey on-site runoff to wet detention systems. In the case where highly impervious areas are desired for small sites with low infiltration (high water table), media filters are used. Both of these examples reduce and/or eliminate the potential for runoff to be pretreated by pervious vegetated areas before being discharged into a BMP area.

A wet detention system is a pond that can detain or attenuate runoff to reduce downstream flooding. A critical issue for wet detention systems is its limitation in removing nutrients. The main nitrogen removal mechanism is sedimentation. After most of the sedimentation has taken place, additional nitrogen removal is inhibited (Schueler, 1987). This may occur because other natural nitrogen removal mechanisms require anoxic zones and a bio-available electron donor to function. Schuler (1987) developed an empirical equation that relates the detention time with TN removal efficiency for wet detention systems. The equation indicates a negligible increase in TN removal efficiency for detention times greater than 14 days and TN removal efficiencies are less than 50%. This presents a significant challenge if a proposed

development is located in a high water table environment and TN removal efficiency requirements are greater than 50%.

2.3.1 Low Impact Development

Another form of a structural BMP is LID. The intention of LID is to minimize the hydrologic impact created by development (Dietz, 2007). LID strategies often involve developing stormwater management systems within infrastructure, which serves another purpose for a development. Pavement, roof tops, gardens and storage reservoirs are examples of infrastructure than can be used for LID with permeable pavement, green roofs, bioretention systems and rain barrels, respectively (Dietz, 2007; Masi et al., 2011). LID or "treatment train" designs of LID and wet detention systems may be an ideal strategy for both controlling flooding and removing pollutants in high water table environments, such as Florida.

2.3.2 Bioretention Systems

Bioretention systems are emerging as a preferred BMP (Davis et al., 2009). Bioretention systems were originally designed for reducing runoff volumes by enhancing infiltration (Morzaria-Luna et al., 2004). However, a number of studies have reported additional benefits of bioretention through surface water attenuation and pollutant removal (Morzaria-Luna et al., 2004). Many bioretention studies have confirmed the removal of suspended solids, phosphorus, heavy metals, oil and grease, chlorides and fecal indicator bacteria (Davis et al., 2009).

The majority of bioretention studies have focused on conventional systems. Conventional systems have multiple layers which include: a ponding area, vegetation, mulch, top

9

soil, and sand layers, as shown in Figure 2.1. Davis et al. (2006) performed laboratory studies on conventional bioretention systems with sampling ports constructed at varying depths. One of the experiments in the study used a 4.1 cm/hr synthetic storm event lasting for six hours. Overall, TKN removal efficiencies between 74 and 83% were observed, with 42 to 63% of the TKN removal occurring in the mulch layer. In addition, TN removal efficiencies between 66 and 83% were measured. However, effluent NO_3^- concentrations from all sampling ports were greater than the influent. When the flow rate was reduced to 2 cm/hr, 19 to 79% NO_3^- removal was observed in the lower port. The decrease in the flow rate most likely created anoxic conditions in the lower section; thereby, creating a mechanism for denitrification.

Various types of bioretention configurations are shown in Figure 2.2. Conventional bioretention systems are best for infiltration and/or if the surrounding soil characteristics are sandy, as shown in Figure 2.2a. Bioretention systems sometimes include a gravel layer or geotextile fabric encompassing the discharge pipe to prevent clogging, as shown in Figures 2.2b and 2.2c (Davis et al., 2009). Also, overflow weirs are sometimes used to ensure that the water surface elevation does not exceed the depth of the ponding area to prevent on-site flooding. Conventional bioretention systems with under-drains can incorporate impermeable liners and are good for reducing on-site flooding, reducing groundwater contamination and/or if soil characteristics are poorly-drained, as shown in Figure 2.2b (PGC, 2007). Modified bioretention systems can incorporate impermeable liners and are desired for attenuation, reducing groundwater contamination, NO_3^- removal and/or if soil characteristics are poorly-drained, as shown in Figure 2.2c (PGC, 2007).

Nitrogen removal efficiencies from conventional and modified bioretention system studies can be found in Collins et al. (2010). Both systems (conventional and modified) have similar sedimentation, filtration and nitrification performance. TKN is removed through all of these processes, which can explain why median TKN removal efficiencies of conventional (44.4%) and modified (54.1%) bioretention systems are comparable. However, the main advantage of modified bioretention systems is NO_3^- removal performance. Unlike TKN, median NO_3^- removal efficiencies for modified systems (65%) are greater than conventional systems (8%). Denitrification can occur in conventional systems, but the lack of a carbon source and anoxic conditions greatly inhibits NO_3^- removal. The numerous reports of negative NO_3^- removal efficiencies for conventional systems (Collins et al., 2010) provide insight to this phenomenon.

Many water quality treatment processes occur in bioretention systems. Bioretention design guidelines provide information on how physical, chemical and biological processes can be incorporated into the system; however, little research has focused on providing design guidance for the IWSZ. Brown et al. (2011) observed longer IWSZ retention times (greater depths) increase total nitrogen and phosphorus removal; however, this study compared two field bioretention systems with different media layers, vegetative covers, IWSZ depths and runoff volumes when comparing two bioretention cells. Laboratory studies by Kim et al. (2003) and Zinger et al. (2007a) were more controlled, which provides greater insight.

Kim et al. (2003) developed the modified bioretention system by incorporating an IWSZ with carbon-containing media under the sand layer. The NO_3^- removal performance of various

11

sand-mixed electron donor media types can be found elsewhere (Kim et al., 2003; Gibert et al., 2010). A decrease in NO_3^- removal efficiency was observed with higher flow rates and/or influent NO_3^- concentrations. A lag period before NO_3^- removal was observed when the columns were drained and then operated after 30 and 84-day dormant periods. However, nearly complete nitrate removal was observed when the columns were left submerged and then operated after 7 and 37-day dormant periods (or ADCs). The authors concluded that newspaper was the best electron-donor and that near complete NO_3^- removal efficiency could be achieved if stormwater remained in the IWSZ for more than seven days.

The study by Kim et al. (2003) has some drawbacks. The water source used in the study was dechlorinated tap water, with additional inputs of total dissolved solids, NO_3^- and phosphorous, and no added organic carbon. Nitrate removal rates in the control columns could have been greater if organic carbon was included in the source water because a carbon source could be used for denitrification. Also, this study considered the NO_3^- mass loading rate (mg/day-N) as the prime independent variable of interest; however, designers also need to know NO_3^- removal efficiency with respect to IWSZ depth (or volume). For example, two bioretention systems could have the same NO_3^- mass loading rate, but have different IWSZ depths. In this case, the NO_3^- removal efficiency of each system will be different, as indicated by Zinger et al. (2007).

Zinger et al. (2007a) performed mesocosm studies on modified bioretention units with different sand-mixed carbon sources (no carbon, pea straw and red-gum) and IWSZ depths (0, 15, 45 and 60 cm). An IWSZ depth of 45 cm was observed to be the optimum depth with TN

and NO_3^- removal efficiencies of 74 and 99 percent, respectively. However, TN removal efficiencies for all units were between 70 and 74%. In addition, declining removals of ammonia and org-N were observed with increasing IWSZ depth. The authors reasoned that the decreases in ammonia and organic nitrogen occurred because mineralization was inhibited by the anoxic conditions present in the IWSZ.

Little detail was provided in the study by Zinger et al. (2007a). The study did show how the IWSZ depth affects different nitrogen species, but did not consider varying nitrogen loading rates or detention times. In addition, the study investigated one storm event type, which was a slug load of the average runoff volume from a storm event. This is a concern because it is impossible to know the difference in removal performance between the discharged portion retained in the IWSZ from the previous storm event and the runoff portion entering and leaving the system on the same day. In addition, nitrogen species removal performance is likely to change with different storm event types, making the usefulness of the data limited.

Though much research has been performed on bioretention systems, peer-reviewed studies have yet to focus on bioretention system performance in high water table environments. In addition, poor NO_3^- removal performance has been observed when a permanently saturated IWSZ is not incorporated into the system (Davis et al., 2001; Hsieh and Davis, 2005a; Hsieh and Davis, 2005b; Davis et al., 2006; Dietz and Clausen, 2006; Hunt et al., 2006; Hsieh et al., 2007; Lucas and Greenway, 2011b). Both of these issues can be solved by introducing an impermeable liner around the IWSZ. Such inclusion would prevent bioretention systems from draining (lowering) the water table and enhance NO_3^- removal performance.

2.3.3 Denitrification Beds

Schipper et al. (2010) conducted a brief review of denitrifying bioreactors, which use carbon sourced treatment systems to promote denitrification. Denitrification walls, beds and layers are three types of denitrifying bioreactors, of which, denitrification beds most resemble an IWSZ in bioretention systems. Denitrification beds are filled with wood chips and are used for a variety of concentrated NO_3^- discharges including wastewater and tile/drain discharges from agriculture. At times, denitrification beds use an impermeable liner.

Critical information can be gathered from denitrification bed research. Moorman et al. (2010) observed wood chip decompositions of 75 and 13 percent after nine years of operation when compared to areas under occasional and permanent anoxic conditions, respectively. Media saturation affects system longevity from the loss of carbon substrate and increases dissolved organic carbon leaching as carbon is washed out of the system. In addition, the use of un-acclimated media has not limited system performance as denitrifiers present in soil and water eventually colonize the systems when a favorable environment is provided (Schipper et al., 2010). Cameron and Schipper (2010) found little difference in denitrification performance in regards to wood chip media size (4 to 61 mm) and type (softwood; hardwood or eucalyptus).

2.4 Nitrogen Removal Mechanisms in Bioretention System Media

Sedimentation, immobilization, filtration, nitrification, plant uptake and denitrification are processes that remove nitrogen in bioretention systems (USEPA 1999; Lucas and Greenway 2011b). During a storm event, stormwater runoff flows into and fills the ponding area where larger particles containing particulate organic nitrogen (org-N) settle. Particulate org-N can also

14

be physically removed, or filtered, in the mulch and/or sand layers. Soluble org-N can be

hydrolyzed to ammonium by plants or microorganisms in the sand layer. Also, as runoff flows

through the mulch layer, some of the ammonium (NH_4^+) is immobilized by plants and

microorganisms to organic nitrogen for protein synthesis (Kadlec and Wallace, 2009) or

adsorbed to negatively charged sites on clay particles. Runoff from the mulch layer is then

conveyed to the unsaturated sand layer where aerobic conditions enable NH_4^+ to be nitrified to

NO_3^-. When runoff enters the root zone (within the sand layer), or rhizosphere, NO_3^- can be

removed by plant uptake (Recous et al., 1992).

The final removal mechanism involves denitrification, where NO_3^- is converted to

nitrogen gas in a saturated layer or IWSZ. Denitrification is a microbial respiratory process

where nitrogen oxides are converted to nitrogen gas in the absence of oxygen (Rittman and

McCarty, 2001). Specific enzymes regulate denitrification through a series of four sequential

steps and are shown in Philippot et al. (2007). Numerous genera of denitrifying microorganisms,

as well as some archeae and fungi, have been identified and include: *Firmicutes*, *Actinomycetes*,

Bacteriodes, *Aquifaceae*, *Proteobacteria Alphaproteobacteria*, *Betaproteobacteria*,

Gammaproteobacteria and *Epsilonproteobacteria* (Philippot et al., 2007). Denitrification can be

viewed as a communal process since many denitrifying microorganisms do not produce all of the

enzymes required to complete denitrification (Zumft, 1997).

There are two other biological nitrogen oxide removal processes that should not be

confused with denitrification. These processes are dissimilatory nitrate reduction (DRNA) and

anaerobic ammonia oxidation (ANAMMOX) (Vaccari et al., 2006). DRNA is a process where

15

NO_3^- is reduced to ammonia under anoxic conditions with high organic carbon to electron acceptor ratios (Tiedje et al., 1982). ANAMMOX is a process where ammonia serves as an electron donor, nitrite serves as an electron acceptor and the product of the reaction is nitrogen gas. DRNA and denitrification use the same genes (*Nap* and *Nar*) to reduce NO_3^- to NO_2^- (Wallenstein et al., 2006); however, DRNA does not use nitrite reductase genes (*nirK* and *nirS*). Previous studies have not evaluated the presence of ANAMMOX activity in bioretention systems; however, Zhu et al. (2013) studied ANAMMOX activity in riparian zones and observed that ANAMMOX contributed between 11 and 35% of the total of nitrogen gas production.

Research investigating the expression of denitrifying genes in the IWSZ of bioretention systems has yet to be performed. However, Chen et al. (2013) quantified nitrifying and denitrifying genes in the sand (nitrifying) and mulch layer of bioretention systems and observed that the quantity of denitrifying genes decreased as a function of media depth. The controlling factor was possibly the decrease in available dissolved organic carbon with depth. Warnecke et al. (2011) investigated denitrifying communities in denitrification beds, which are similar to IWSZs, and indicated that microbial denitrifcation (instead of DRNA or ANNAMOX) was the primary NO_3^- removal mechanism. The authors observed differing denitrifying gene quantities corresponding to the use of varying solid organic substrates in the denitrification bed.

2.5 Bioavailability of Lignocellulosic Media

Denitrification is a process that requires the presence of an electron donor such as a soluble bioavailable organic substrate or elemental sulfur. A general denitrification

16

stoichiometric reaction that uses soluble organic carbon is shown below (Rittman and McCarty, 2001).

$$38CH_2O + 12NO_3^- + 12H^+ \rightarrow 4C_5H_7O_2N + 18CO_2 + 4N_2 + 30H_2O \qquad (2.1)$$
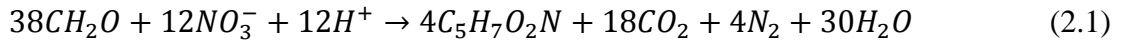
Wastewater denitrification systems often utilize soluble organic carbon sources, which include methanol, acetate and glycerol (Rittman and McCarty, 2001). However, the organic carbon can be in the form of a solid substrate. The use of solid substrates can be advantageous for two reasons: (1) they can act as biofilm carriers; and (2) they release bioavailable organic carbon to the biofilm at a relatively constant rate (Chu and Wang, 2013). Solid organic carbon materials with their corresponding denitrification performance from various denitrifying bioreactor and modified bioretention studies can be found in Gibert et al. (2010).

Denitrification with solid substrates requires an additional step to solubilize the solid substrate through a process called hydrolysis (Chu and Wang, 2013). Hydrolysis occurs when bacteria excrete extracellular enzymes that break down solid substrates into molecules that are small enough to pass through the bacteria's cell wall (Rittman and McCarty, 2001). Organic solid substrates can be manufactured or obtained from nature. Manufactured solid substrates can be useful to ensure a relatively constant effluent water quality and decrease unwanted residuals or by-products from substrate hydrolysis. In addition, research identifying biochemical processes that occur during hydrolysis may be easier to conduct with manufactured compared to natural solid substrates (Shen et al., 2013). Natural substrates are more economical, but have the potential to create effluent water quality issues, such as carry-over of dissolved organic carbon into the effluent, color changes and high ammonia concentrations (Shen et al., 2013).

17

Prior studies investigating denitrification with various manufactured solid substrates suggests that certain species of bacteria are capable of thriving on specific types of solid substrates and environments. Mergaert et al. (2001) observed that *Pseudomonas* was more prevalent under aerobic conditions, while *Acidovorax facilis* and strains similar to *Brevundimonas* dominated under anoxic conditions with PHB as the biofilm carrier and sole carbon source. Shen et al. (2013) observed that approximately 53% of the biofilm consisted of *Diaphorobacter* and *Acidovorax* when starch/polycaprolactone was the carbon source. Additional studies by Kobayashi et al. (1999) and Zhang (2010) showed that *Diaphorobacter* and *Acidovorax* are also capable of depolymerizing other solid organic substrates.

Natural solid substrates are more complex than manufactured substrates. Natural organic solid substrates include wood, compost, leaves and native soil (Gibert et al., 2008). Wood is most commonly used for passive denitrification systems, which include denitrification beds and IWSZs in modified bioretention systems (FAWB, 2008; Schipper et al., 2010). Wood is primarily composed lignocellulose, which consists of three polymers, cellulose, hemi-cellulose and lignin (Perez et al., 2002). These polymers have different structural characteristics. Cellulose is a glucose polymer with α-1,4-linkages, hemicellulose is a heteropolysaccharide polymer and lignin is an amorphous heteropolymer (Malherbe et al., 2002; Perez et al., 2002). The general composition of cellulose, hemi-cellulose and lignin for lignocellulosic materials are different (Betts et al., 1991). The rate of hydrolysis from hemi-cellulose is known to occur fastest, followed by cellulose and then lignin (Malherbe and Cloete, 2002). In addition, the biodegradation of these polymers requires different enzymes (Rittman and McCarty, 2001).

18

Lignocellulose hydrolysis has been identified as the rate-limiting step for the production of biofuels and paper and the degradation of wastes from silage (Malherbe and Cloete, 2002). As a result, a large number of studies have focused on understanding lignocellulosic material hydrolysis. However, much of this research has focused on aerobic rather than anaerobic processes, and the basic mechanisms for hydrolysis are different in anaerobic and aerobic environments (Leschine et al., 1995; Tomme et al., 1995). Generally, aerobic environments allow hydrolysis rates to increase, while anaerobic environments allow bacteria and fungi to utilize hydrolyzed material more efficiently (Malherbe and Cloete, 2002).

Cellulose hydrolysis is the most studied lignocellulosic polymer for use in mesophilic anaerobic environments. Enzymes that depolymerize cellulose in anaerobic environments are organized in multi-enzymatic complexes called cellulosomes (Desvaux, 2006). Enzymes found in cellulosomes are known to include endoglucanase, cellobiohydrolase and xylanase (Leschine, 1995). The products of cellulose depolymerization include cellobiose, cellodextrines and glucose which can be metabolized in biofilms (Leschine, 1995; Desvaux, 2006).

Anaerobic bacteria and fungi are known to produce extracellular enzymes that hydrolyze cellulose and include *Bacteroides cellulosolvens*, *Cellulomonas spp.*, *Clostridium cellulolyticum*, *Clostridium cellulovorans*, *Clostridium papyrosolvens*, *Fibrobacter succinogenes*, *Ruminococcus albus* and *Neocallimastix frontalis* (a rumen fungus) (Leschine, 1995). These organisms exhibit several other capabilities: *Clostriduium cellulovorans* is capable of utilizing other carbon sources found in wood, such as xylan and pectin (Kosugi et al., 2001); the cellulosomes of *Clostridium cellulolyticum* are known to facilitate bacterial adhesion onto solid

19

substrates (Desvaux, 2006); in nitrogen-limited environments, *Cellulomonas spp.* can utilize

ammonium from solid cellulosic substrates for synthesis (Young et al., 2012); and some

cellulolytic bacteria, such as *F. succinogenes*, do not produce cellulosomes (Schwartz, 2001).
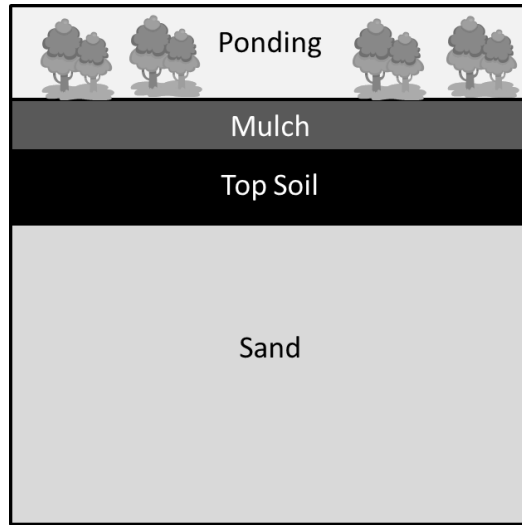
Figure 2.1. A layer profile schematic of a conventional bioretention system.
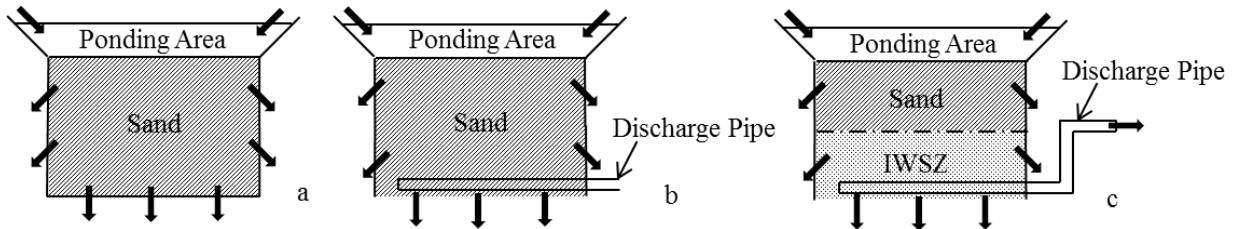
Figure 2.2. Various bioretention system configurations: (a) conventional bioretention; (b) conventional bioretention with an under-drain; (c) modified bioretention.

Biological Processes in Internal Water Storage Zones of Bioretention Systems[1]

3.1 Introduction

Urban stormwater runoff is one of the primary sources of impairment to surface waters in the United States (USEPA, 2000). Urban runoff contains nutrients, such as nitrogen and phosphorus, which promote eutrophication. Eutrophication is known to contribute to toxic algal blooms, reduced fish yields and biodiversity, development of hypoxic zones, decreased property values and reduced recreational use of surface waters (Smith, 2003). Low Impact Development technologies, such as bioretention systems, can be used to reduce eutrophication by controlling nitrogen loadings from urban areas (Ahiablame et al., 2012). A bioretention system is a stormwater treatment system that is capable of increasing infiltration, reducing runoff rates and removing pollutants (Dietz, 2007).

A number of nitrogen transformation processes occur in bioretention systems including: nitrification, denitrification, immobilization, mineralization, plant uptake and filtration (Lucas and Greenway, 2011). Previous studies have reported that conventional bioretention systems achieve a median of 8% nitrate (NO_3^-) removal (see review by Collins et al., 2010). This has led to the development of a modified bioretention system, which includes an internal water storage

---

[1] Note: Portions of this chapter are being prepared for submission to the Journal of "Environmental Engineering Science". The co-authors of the manuscript included Thomas Lynn, Daniel Yeh and Sarina Ergas. Research questions and experimental design were developed by Thomas Lynn and Sarina Ergas. Thomas Lynn performed laboratory work. Thomas Lynn and Sarina Ergas drafted the paper. Data interpretation and comments were provided by all authors.

zone (IWSZ) containing an electron donor to promote denitrification (Kim et al., 2003). Factors that have been reported to affect NO_3^- removal in IWSZs include: influent NO_3^- concentration, oxidation reduction potential (i.e., aerobic/anoxic conditions), detention time and electron donor availability (Kim et al., 2003; Smith, 2008; and Ergas et al., 2010). Other factors that may be important include biofilm acclimation, antecedent dry conditions (ADC), IWSZ depth, electron donor hydrolysis rate and transport of influent dissolved organic carbon (DOC), decaying vegetation and/or plant exudates from the surface to the IWSZ (Kim et al., 2003; Chun et al., 2009; Zhang et al., 2011; Chu and Wang, 2013).

Bioretention systems are operated on an intermittent basis where the number of days between storm events is referred to as the ADCs. Prior peer-reviewed studies investigating the effect of ADCs on NO_3^- removal in the IWSZ is limited. Kim et al. (2003) studied ADCs of 7 and 37 days and observed low initial effluent NO_3^- concentrations. Effluent NO_3^- concentrations gradually increased, but were lower than influent NO_3^- concentrations. Cho et al. (2011) observed that NO_3^- leaching occurs as a result of increased ADCs; however, their study evaluated conventional bioretention systems with under-drains, rather than modified bioretention systems. Zinger et al. (2007b) compared NO_3^- removal performance of biofilters with and without a submerged zone at ADCs between one and eight weeks. After an ADC of two weeks, NO_3^- removal in biofilters with a submerged zone was greater than in biofilters without a submerged zone.

In order to promote denitrification in the IWSZ, a sufficient amount of bioavailable organic carbon needs to be present. This organic carbon may come from the influent

22

stormwater, plant exudates, decaying plant roots and/or solid carbon-containing material added to the IWSZ. Guidance on providing a solid carbon-containing material to the IWSZ is usually given in terms of a volume percentage of material; for example, specifying that five percent of the IWSZ media should be comprised of hardwood chips (FAWB, 2008). However, solid sources of organic carbon must first be hydrolyzed into soluble compounds before bacteria can utilize the material as an electron-donor (see review by Desvaux, 2006). During ADCs, the hydrolysis process could increase bio-available carbon concentrations and affect NO_3^- removal efficiencies. Studies investigating organic carbon hydrolysis in IWSZs of bioretention systems have not been conducted previously.

After years to decades of operation, bio-available organic carbon in the IWSZ media will be depleted. To maintain high NO_3^- removal rates, IWSZ media will then need to be replaced. However, the lifespan of biodegradable additives remains unknown (Grebel et al., 2013), and is important for understanding how bioretention systems should be designed (Laurenson et al., 2013). Knowledge of hydrolysis rates in IWSZs can be used to develop conservative design guidelines and estimate the longevity of solid organic carbon sources. Moorman et al. (2010) evaluated carbon degradation in denitrifying bioreactors, which are similar to IWSZs, and observed high organic carbon degradation in unsaturated compared to saturated environments. This suggests that hydrolysis rates are faster in aerobic compared to anoxic environments (see review by Malherbe and Cloete, 2002).

The overall goal of this research was to investigate the dynamic performance of IWSZs in microcosms and bench-scale bioretention systems.   The specific objectives of this study were to

23

estimate the longevity of eucalyptus wood chips as carbon substrates in IWSZs and to investigate NO_3^- removal performance under the following conditions: 1) unacclimated and acclimated media; 2) aerobic and anoxic environments; 3) varying ADCs; 4) varying influent NO_3^- concentrations; and 5) varying hydraulic loading rates. Although field bioretention systems include vegetation, a mulch layer, a sand layer and an IWSZ layer, this study focused solely on processes that occur in the IWSZ layer in the absence of removal mechanisms influenced by surface vegetation.

3.2 Materials and Methods

3.2.1 Materials

The source water used for this study was local stormwater runoff from a pond at the Botanical Gardens at the University of South Florida, Tampa campus. Stormwater was spiked with KNO_3 to achieve a feed NO_3^--N concentration above 2 mg/L to mimic nitrified stormwater runoff (Schueler, 2003). Influent characteristics for each of the studies that were conducted can be found in Tables 3.2 through 3.4 of the results section. For all acclimated studies, microoganisms present in the source water was the inoculant. All studies were performed in the laboratory at approximately 22°C. The media types in the microcosm studies consisted of >1 mm sand (Seffner Rock and Gravel, Tampa, FL), 0.6 to 1.3 cm pea gravel (Seffner Rock and Gravel, Tampa, FL), 1.3 to 2.5 cm eucalyptus wood chips (Sarasota County, Sarasota, FL), 2:1 (vol/vol) mixture of sand and eucalyptus wood chips and a 2:1 (vol/vol) mixture of gravel and eucalyptus wood chips. The selected ratio for the media mixtures was used to reduce buoyancy issues. Eucalyptus is a hardwood and was chosen over other organic carbon media because it is

24

locally available and was expected to have a greater longevity than softwood media (Yang et al., 2007).

3.2.2 Microcosm Study

The microcosm study was used to investigate the NO_3^- removal performance from un-acclimated and acclimated media in aerobic and anoxic environments. In this study, biofilm acclimation refers to daily addition of influent stormwater over a one month period to seed the media with indigenous bacteria. Microcosm studies were performed in two phases. During Phase 1, the following five media types were tested under acclimated and unacclimated conditions: sand, gravel, wood, sand-wood and gravel-wood. Unacclimated microcosm tests were performed on the first day that the source water was added to the media. During Phase 2, the gravel-wood medium was tested under both anoxic and aerobic conditions. In addition, a gravel-wood microcosm, with the media initially dried at 105°C for four hours, was used as an inactivated control. Microcosms were set up in one liter glass bottles. The volume of media mixture placed into each microcosm was 750 mL. During Phase 2, mean dissolved oxygen (DO) concentrations in the source water for the aerobic and anoxic microcosms were 5.2 and 1.0 mg/L, respectively. The microcosms were sealed and placed in the dark. Samples were collected every hour and analyzed as described below. Incubation periods for all acclimated and unacclimated microcosms were 6 and 12 hours, respectively. All experiments were carried out in triplicate with the exception of the single unacclimated microcosms.

3.2.3 Column Study

A schematic of the laboratory setup for the column study is shown in Figure 3.1. Experiments were carried out in a completely submerged 12.7 cm ID acrylic column to mimic an IWSZ with a depth of 45 cm. The gravel-wood media (bulk porosity = 0.42) was supported by a 7.6 cm under-drain layer of pea gravel to prevent clogging. A comparison of the NO_3^- removal performance from the column used in this study with two other columns with different depths (see Chapter 4). Stormwater was pumped from the reservoir using a Cole Parmer Masterflex L/S peristaltic pump (Thermo Fisher Scientific, Waltham, Massachusetts).

Storm events were set up to simulate a storm that discharges runoff into the bioretention ponding area as a slug load, which causes the hydraulic loading rate to decrease over time as the pond area drains (for approximately 36 hours). To achieve this, the hydraulic loading rates (or detention times) were varied over time by manually adjusting the pump flow valves. Note that detention time versus storm duration values are shown in the results section. Eleven storm events were investigated in the column study, as shown in Table 3.1. ADCs are defined as the time period between the end of a previous storm event to the beginning of the next storm event. Storm Events (SE) #1, 2, 3, 4, 5 and 9 were operated under the same hydraulic loading conditions and were used to investigate the effect of varying ADCs. Storm Event #4 (ADC of 8 days and hydraulic loading rate of 8.3 cm/hr) was also used as a base case to compare SE #6 and SE #7, which were operated with a higher influent NO_3^- concentration (4 mg/L NO_3^--N) and higher average hydraulic loading rates (32.2 cm/hr), respectively. Storm Events #8, 10 and 11 were operated at constant detention times of one, two and three hours, respectively.

26

3.2.4 Analytical Methods

Standard Methods (Standard Methods, 2012) were used to measure dissolved organic carbon (DOC) (Method 5310B), total nitrogen (TN) (4500-N), total suspended solids (TSS) (2540D) and volatile suspended solids (VSS) (2540D). Anion (NO_3^-, nitrite [NO_2^-], phosphate [PO_4^{3-}], sulfate [SO_4^{2-}]) and ammonium (NH_4^+) concentrations were measured by ion chromatography (USEPA, 1997), using an 850 Professional Ion Cromatograph (Metrohm AG, Herisau, Switzerland). A Shimadzu TOC-V CSH Total Organic Carbon / Total Nitrogen Analyzer (Shimadzu Scientific Instruments, Columbia, Maryland) was used to measure non-purgeable organic carbon (NPOC) and TN. NPOC concentrations were used to estimate DOC concentrations. TKN concentrations were calculated by difference $TN - [NO_3^--N + NO_2^--N]$. An Orion 5 Star (Thermo Scientific Inc., Beverly, Massachusetts) meter with a calibrated probe was used to measure pH and DO. Method detection limits for DOC, TN, NO_3^--N, NO_2^--N , $PO_4^{3-}-P$, $SO_4^{2-}-S$, NH_4^+-N were 0.11, 0.03, 0.01, 0.04, 0.02, 0.01 and 0.07 mg/L, respectively.

3.2.5 Statistical Analysis

Differences in NO_3^- removal performance during the microcosm studies were evaluated using two-way analysis of variance (ANOVA). It was assumed that the observed NO_3^- removal was due to denitrification and that other NO_3^- removal mechanisms (such as adsorption or biosynthesis) were negligible; however, no confirmation studies, such as studies using isotope tracers, were carried out. Denitrification rate constants for all media types and environmental conditions were estimated by minimizing the sum of squares residuals between the data and the model and then using linear regression to calculate the coefficient of determination (r^2). During the column study, flow weighted influent and effluent concentrations were calculated for each

27

storm event and were used to calculate the mean mass removal efficiencies. Differences in TN

removal performance between storm event types were evaluated using two-way ANOVA. Initial

effluent sample data (water initially retained in the IWSZ before the storm event) and effluent

sampling data where NO_3^- removal efficiency was observed to exceed 95% were excluded.

3.2.6 Data Analysis

Denitrification kinetics were assumed to follow a first-order reaction rate with DO

inhibition (Wild et al., 1995):

$$k_1 = k \frac{K_{O_2}}{K_{O_2} + S_{O_2}} \qquad (3.1)$$

where k_1 = first-order denitrification rate constant that was calculated from the data obtained

from the anoxic or aerobic microcosms (hr^{-1}); k = first-order denitrification rate constant (hr^{-1});

K_{O2} = oxygen inhibition coefficient (mg/L); and S_{O2} = initial DO concentration (mg/L). Values

of k and K_{O2} were calibrated using data from the aerobic and anoxic microcosms with the wood-

gravel media.

The IWSZ longevity estimate was calculated by extrapolating data from the gravel-wood

anoxic and aerobic microcosms in Phase 2. Based on the column study results, biological sulfate

reduction was assumed to occur. In addition, the rate at which DOC dissolves into the

microcosm pore waters was assumed to be equal to the hydrolysis rate. The following

parameters that affect DOC concentrations: DOC hydrolysis rate (DOC_h (mg/L-hr)), mass of

DOC consumed per mass of NO_3^--N consumed ($\gamma_{C/N}$ (g/g)), mass of DOC consumed per mass of

oxygen consumed ($\gamma_{C/O}$ (g/g)) and mass of DOC consumed per mass of SO_4^{2-}-S consumed ($\gamma_{C/S}$

(g/g)) were estimated according to the DOC mass balance equation shown in Equation 3.2.

28

$$DOC_I - \frac{\Delta O \times \gamma_{C/O}}{f_{e,O}} - \frac{\Delta N \times \gamma_{C/N}}{f_{e,N}} - \frac{\Delta S \times \gamma_{C/S}}{f_{e,S}} + DOC_h \times \tau = DOC_E \qquad (3.2)$$

where DOC_I and DOC_E are the initial and final DOC concentrations (mg/L); ΔN, ΔO and ΔS are

the differences in the initial and final NO_3^--N, DO and SO_4^{2-}-S concentrations (mg/L),

respectively; τ is the incubation time (6 hr); and $f_{e,O}$, $f_{e,N}$, and $f_{e,S}$ are factors that account for the

stoichiometric relationship between DOC and DO, NO_3^--N and SO_4^{2-}-S as electron acceptors,

respectively. Assumed values of $f_{e,O}$, $f_{e,N}$, and $f_{e,S}$ were 0.4, 0.5 and 0.92, respectively, and were

based on typical values observed in wastewater treatment systems (Rittman and McCarty, 2001)

because values in stormwater systems are unknown. Based on stoichiometric relationships, ΔN

and ΔS are equal to 2.86ΔO and 2.00ΔO, respectively (see Section 4.9 in USEPA, 2010). These

ratios were inserted into Equation 3.2 and the terms $\gamma_{C/N}$ and $\gamma_{C/S}$ were replaced with $\gamma_{C/O}$, as

shown in Equation 3.3.

$$DOC_I - \frac{\Delta O \times \gamma_{C/O}}{0.4} - \frac{\Delta N \times \left(\frac{2.86\Delta O}{\Delta N}\right)\gamma_{C/O}}{0.5} - \frac{\Delta S \times \left(\frac{2.00\Delta O}{\Delta S}\right)\gamma_{C/O}}{0.92} + DOC_h \times \tau = DOC_E \qquad (3.3)$$

3.3 Results

3.3.1 Microcosm Study

Results from the unacclimated microcosms are shown in Table 3.2. Increased

concentrations of Org-N, DOC, PO_4^{3-} and SO_4^{2-} were observed for all media types, with the

highest final concentrations observed in the wood-containing media. Increased concentrations of

NO_2^- and NH_4^+ and a decrease in pH were also observed in the wood-containing media. NO_3^-

removal was observed in wood-containing microcosms after six to twelve hours.

29

Results from the microcosms after acclimation are shown in Table 3.2. Six hours after stormwater addition, NO_3^- removal efficiencies of 1, -4, 100, 84 and 100% were observed for the sand, gravel, wood, sand-wood and gravel-wood media, respectively. NO_3^- removal performance from the gravel-wood media was significantly higher than the sand-wood media; and the wood only media was significantly higher than the gravel-wood media (p-value<0.05). First-order denitrification rate constants (hr^{-1}) of 0.75, 0.27 and 0.57 were calibrated for wood, sand-wood and gravel-wood media, respectively. Final NH_4^+ concentrations were below the detection limit for all media types.

A comparison of the water quality characteristics of gravel-wood microcosms under initial aerobic, anoxic and inactivated conditions are shown in Table 3.3 and Figure 3.2. Within six hours of stormwater addition, NO_3^- removal efficiencies of 97 and 80% were observed for the anoxic and aerobic microcosms, respectively. NO_3^- removal was significantly lower in aerobic compared to anoxic microcosms (p-value<0.05); however, both microcosms exhibited first-order kinetics ($r^2 = 0.98$ and 0.94, respectively). Mean initial DO concentrations of 5.2 mg/L in the aerobic microcosms were reduced to 1.6 and 0.1 mg/L within one and six hours, respectively. Values for k and K_{O2} from Equation 3.1 were calculated as 0.54 hr^{-1} and 2.18 mg/L, respectively.

Leaching of NH_4^+ was not observed under either condition. Final DOC concentrations were not significantly different in the anoxic (4.9 mg/L) compared to aerobic (4.6 mg/L) microcosms (p-value=0.05). Low (3%) and no (0%) removal of SO_4^{2-} were observed in the anoxic and aerobic microcosms, respectively. Mean TSS and VSS removal efficiencies of -1,048 and -1,737% were observed in the anoxic microcosms, respectively; while -587 and -492%

30

were observed in the aerobic microcosms, respectively. Relatively high final concentrations of NH_4^+, Org-N, TOC, PO_4^{3-} and SO_4^{2-}, were observed in the inactivated control microcosms.

Data from the gravel-wood media anoxic and aerobic microcosms were used to estimate the longevity of eucalyptus in IWSZs. Substituting data from the anoxic microcosm into Equation 3.3 yields:

$$3.93\frac{mg}{L} - \frac{1.0\frac{mg\,O}{L}\times\gamma_{C/O}}{0.4} - \frac{1.90\frac{mg\,N}{L}\times\left(\frac{2.86\Delta O}{\Delta N}\right)\gamma_{C/O}}{0.5} - \frac{1.22\frac{mg\,S}{L}\times\left(\frac{2.00\Delta O}{\Delta S}\right)\gamma_{C/O}}{0.92} + DOC_h \times 6\,hr = 4.90\frac{mg}{L}$$

(3.4)

Substituting data from the aerobic microcosm into Equation 3.3 yields:

$$3.86\frac{mg}{L} - \frac{5.1\frac{mg\,O}{L}\times\gamma_{C/O}}{0.4} - \frac{1.57\frac{mg\,N}{L}\times\left(\frac{2.86\Delta O}{\Delta N}\right)\gamma_{C/O}}{0.5} - \frac{0.05\frac{mg\,S}{L}\times\left(\frac{2.00\Delta O}{\Delta S}\right)\gamma_{C/O}}{0.92} + DOC_h \times 6\,hr = 4.58\frac{mg}{L}$$

(3.5)

Equations 3.4 and 3.5 were solved simultaneously to find the following values: $\gamma_{C/O}$ (0.043 g/g), $\gamma_{C/N}$ (0.123 g/g), $\gamma_{C/S}$ (0.086 g/g) and DOC_d (0.28 mg/L-hr). Assuming the following for eucalyptus: an empirical formula of $CH_{1.864}O_{0.515}N_{0.089}S_{0.003}$ in which 19.18 (wt%) of the material is fixed carbon (Sulaiman and Lee, 2012), the fixed carbon did not hydrolyze and a density of 400 g/L (determined experimentally), the estimated longevity of the media is 34 years. In calculating this value, it was assumed that saturation conditions were maintained in the IWSZ and the hydrolysis rate was constant at 0.28 mg/L-hr.

31

3.3.2 Column Study

Overall water quality results from the column study are shown in Table 3.4. Average mass removal efficiencies for NO_3^-, TKN and TN were 85, -43 and 66%, respectively. Influent and effluent NH_4^+ concentrations were consistently below the detection limit of 0.07 mg/L. Removal of PO_4^{3-}, SO_4^{2-}, TSS and VSS, decrease in pH and production of DOC was also observed.

Mean water quality results for SE #'s 1-5 and 9 are shown in Figure 3.3. After the initial pore water volume was discharged, mean effluent NO_3^--N concentrations decreased from 0.39 to 0.02 mg/L when the detention time increased from one to nine hours (Figure 3.3a). However, the mean effluent DOC concentration decreased from 58.8 to 5.2 mg/L as the detention time increased to four hours and then increased to 6.1 mg/L during the nine hour detention time (Figure 3.3b).

Water quality results for SE #4 (8 day ADC) and SE #5 (0 day ADC) are shown in Table 3.4 and Figure 3.4. NO_3^- removal efficiencies for the initial effluent samples taken from these storm events were greater than 98%. Overall NO_3^- mass removal efficiencies for SE #4 and SE #5 were 97 and 86%, respectively, as shown in Table 3.4. For the one hour detention time effluent samples (2nd sample taken), the NO_3^- removal efficiencies for SE #4 and SE #5 were 77 and 52%, respectively. The weighted mean effluent DOC concentration from SE #5 (11.5 mg/L) was greater than SE #4 (5.3 mg/L). The influent DOC concentration for both storm events was 4.9 mg/L. In addition, weighted mean effluent DOC concentrations from SE #2, SE #3 and SE #9 were all greater than SE #5.

32

Nitrogen speciation data that compares the effect of varying influent NO_3^--N concentrations from SE #4 (2 mg/L NO_3^--N) and SE #6 (4 mg/L NO_3^--N) are shown in Table 3.4 (additional data not shown). TN removal efficiencies were significantly higher in SE #4 than SE #6 (p-value<0.01); however, the difference in the overall TN mass removal efficiency was only 3%. The highest effluent NO_2^--N concentrations (0.36 to 0.44 mg/L) were observed from the two, three and four hour detention time samples taken during SE #6, while NO_2^--N concentrations from all of the other samples from SE #4 and SE #6 were below 0.12 mg/L. Weighted mean effluent TKN concentrations for SE #4 and SE #6 were greater than influent TKN concentrations by 0.06 and 0.14 mg/L, respectively.

Water quality data comparing low (SE #4) with high (SE #7) flow rate storm events are shown in Table 3.4 and Figure 3.5. As expected, the TN removal efficiency was significantly higher in SE #4 than SE #7 (p-value<0.01). TKN and TSS removal efficiencies were also higher in SE #4 compared with SE #7.

Results from the constant flow storm events (SE #8, SE #9 and SE #11) are shown in Table 3.4 and Figure 3.6. Steady-state effluent NO_3^- concentrations were not observed for any of these storm events even after nine IWSZ pore volumes were discharged. In SE #8, NO_3^- removal efficiencies from samples taken after 1.25, 5 and 9 pore volumes were discharged were 90, 43 and 31%, respectively. In SE #11, NO_3^- removal efficiencies slowly declined from 85 to 78% with respect to the samples taken during the 8th and 28th pore volume discharged, respectively.

33

3.4 Discussion

3.4.1 Microcosm Study

The unacclimated microcosm results (Table 3.2) provide insight into expected IWSZ performance during start-up. Cameron and Schipper (2012) evaluated unacclimated media and observed similar results with respect to increases in NH_4^+-N and Org-N concentrations and decrease in pH for carbon-containing media; however, increases in DOC, PO_4^{3-}-P and SO_4^{2-}-S were not reported. Increases in effluent nutrient concentrations during start-up periods are a cause for concern, since typical nutrient concentrations in stormwater runoff are relatively low. However, NO_3^- removal appeared to commence within twelve hours of stormwater addition, most likely due to the presence of denitrifying bacteria in the wood chips. This provides confidence that IWSZs will begin to denitrify even without inoculation with bacteria (such as biomass from a wastewater treatment facility). The carbon-containing media results can also be used to evaluate the effluent water quality characteristics from the mulch layer that is typically included in bioretention systems. The high final concentrations of NH_4^+, Org-N and PO_4^{3-} that were observed in the carbon-containing media microcosms provide evidence that the mulch layer negatively impacts the water quality performance of bioretention systems.

The acclimated microcosm results (Table 3.2) provide data on the maximum expected denitrification kinetics from the IWSZ media after bioretention systems have been in the field for a number of storm events. The results from the sand and gravel medium indicated that NO_3^- removal did not occur in absence of a carbon source. This is in contrast with the results observed by Gibert el al. (2008); however, their study was conducted over several days with influent DOC concentrations greater than 30 mg/L. Differences in NO_3^- removal rates in sand-wood and gravel-

34

wood media provide evidence that the physical characteristics (grain size, porosity, surface area, etc.) of the media play a role in IWSZ denitrification rates. Due to its higher porosity, a higher total mass of NO_3^- was added to the gravel-wood medium than the sand-wood medium during the acclimation period. This may have increased the denitrifying bacteria population and improved NO_3^- removal in the gravel-wood medium. However, this phenomenon would not be expected to occur in nutrient-rich waters, such as wastewater because the sand-wood medium would provide more surface area for biofilm attachment, which utilizes NO_3^- at a higher rate.

Although the highest NO_3^- removal rates were observed with the wood only medium, the gravel-wood media was selected for further evaluation in microcosm and column studies for the following reasons: (1) a relatively high denitrification rate constant in comparison to the sand-wood media; (2) the structural stability of the gravel in the gravel-wood media, as compared to the wood only media, mitigates IWSZ compression that could potentially decrease IWSZ hydraulic conductivity over time; (3) the permeability of the gravel-wood media is greater than sand-wood media; and (4) the mean effluent DOC concentration of gravel-wood media (4.1 mg/L) was less than wood media (6.8 mg/L).

The results from the anoxic and aerobic microcosms are useful for comparing how influent DO concentrations affect NO_3^- removal rates. In this study, higher DO concentrations decreased NO_3^- removal rates. Varying results have been obtained in previous studies investigating the effect of DO on NO_3^- removal rates in IWSZs. Smith (2008) evaluated effluent concentrations of NO_3^- and DO at varying flow rates and observed that complete DO removal was required before NO_3^- was completely removed. However, Clark and Pitt (2009) investigated the

35

effect of aerobic and anoxic microcosms with different medium types (compost, sand, peat and granular activated carbon) and observed NH_4^+ release and negligible NO_3^- removal in anoxic microcosms, while NO_3^- production was observed in aerobic microcosms. The findings from Clark and Pitt (2008) were similar to the observations in unacclimated and inactivated microcosms in this study. DO inhibition has received more attention in wastewater compared to stormwater treatment. For wastewater, K_{O2} values between 0.1 and 0.2 mg/L have been reported in the literature (Barker and Dold, 1997), and are lower than the results from this study. The anoxic and aerobic results from this study provide evidence that DO concentrations limit NO_3^- removal rates to a lower degree than in wastewater treatment systems.

The microcosm study results show that microbial communities were capable of utilizing the DOC released from the eucalyptus wood chips as an electron donor with different electron acceptors. DO is utilized preferentially, NO_3^- is consumed when DO concentrations are reduced below the inhibitory concentration and finally SO_4^{2-} is utilized at low oxidation reduction potential. Note that oxidation reduction potential or production of SO_4^{2-} reduction products was not measured.

3.4.2 IWSZ Longevity

Internal water storage zone longevity may depend on whether wood-containing media is temporarily or permanently saturated. The hydrolysis process is different in aerobic (un-saturated) compared to anaerobic or anoxic (saturated) environments. Aerobic hydrolysis produces more energy but intermediate products can be lost through the process (Malherbe and Cloete, 2002). Anaerobic hydrolysis is more efficient because membrane-bound enzyme

36

complexes form a barrier around solid substrates (e.g. cellulose), which prevents the loss of intermediate products (Malherbe and Cloete, 2002). This could explain why high final TKN, PO_4^{3-} and DOC concentrations were only observed in the un-acclimated and inactivated control microcosms, since they both were exposed to aerobic conditions before the experiment began. In addition, Rovira and Vallejo (2002) evaluated eucalyptus degradation in unsaturated soil and observed that 45 to 70% of the organic carbon was degraded within two years. Therefore, it is recommended that IWSZs should be designed to maintain saturated conditions to increase longevity and reduce intermediate product leaching.

Bioretention systems are passive systems that should be designed to blend into nature and operate for an extended period of time. The estimated service life of IWSZs (~34 years) provides evidence that carbon will be available for at least a decade. In the field, the actual service life could be reduced due to physical (e.g., erosion), chemical (e.g., changes in temperature) and biological (e.g., if more accurate values of $f_{e,O}$, $f_{e,N}$ and $f_{e,S}$ for stormwater systems were used) processes that were not included in the estimate from this study. For instance, if $f_{e,O}$, $f_{e,N}$ and $f_{e,S}$ were approximately equal to one in electron acceptor deficient environments, then the longevity estimate would be 16 years. However, IWSZ longevity may be longer if the hydrolysis rate decreases over time (Malherbe and Cloete, 2002), whereas, this study assumed a constant hydrolysis rate. Robertson et al. (2008) observed decreased NO_3^- removal (20 to 50% the initial rate) in a denitrifying bioreactor containing 20% sawdust and 80% sand (w/w) that was in operation for 15 years. Furthermore, Christianson et al. (2012) reviewed longevity estimates in denitrifying bioreactor studies that ranged between 9 and 72 years. The

37

results from this and previous studies imply that permanently saturated carbon-containing IWSZs will supply bio-available carbon over multiple decades of operation.

3.4.3 Column Study

The column study results (Table 3.4) indicate that IWSZs can affect multiple water quality parameters. Results of nitrogen speciation showed that IWSZs consistently removed NO_3^- over multiple storm events, and that a slight production in TKN (up to 0.2 mg/L) resulted in lower TN removal efficiencies. The overall PO_4^{3-} results (Table 3.4) provide evidence that IWSZs are capable of removing phosphorus. Barrett et al. (2013) also observed PO_4^{3-} removal and suggested that dissolved phosphorus may have precipitated as calcium hydroxyapatite during ADCs; however, the results from this study show PO_4^{3-} production during the longest ADC storm event (SE #9). Future research investigating the mechanism(s) for PO_4^{3-} removal in IWSZs is recommended. SO_4^{2-} removal was observed during SE #1 through SE #10, possibly due to biological SO_4^{2-} reduction. Elgood et al. (2010) studied NO_3^- removal in denitrifying bioreactors and observed similar results with respect SO_4^{2-} reduction. The column study results (Table 3.4) were similar to the microcosm study results (Table 3.3) with the exception of the lower TSS and VSS removal efficiencies in the microcosms, most likely because the TSS and VSS samples from the microcosms were quickly drained prior to analysis. The overall TSS and VSS results from the column study indicate that gravel-containing IWSZs can be utilized for other stormwater treatment applications such as a 'polishing' filter for removing TSS in wet detention systems. Problems with clogging were not observed during this study since the IWSZ inlet water elevation did not increase. Hatt et al. (2007) evaluated the performance of a gravel filter and

38

observed clogging throughout their study. However, their study incorporated an underlain layer of fine sand, which may have induced system clogging.

The column experiments were developed to mimic the temporal flows that occur in real bioretention systems, as shown in Figures 3.3-3.5. During a storm event, runoff is conveyed to the bioretention ponding area, where the ponding elevation reaches its maximum height. In this period, the IWSZ flow rate is high; hence, short detention times were utilized for the initial stage of this experiment. After a storm event, runoff no longer enters the ponding area, while the ponding elevation decreases and conveys runoff through the IWSZ. At this stage, water initially retained in the IWSZ is discharged and is followed by runoff from the storm event. During this period, the flow rate decreases until the water elevation reaches the top elevation of the IWSZ. This experiment used pumps controlled by timers so there are step decreases in flow rate over each storm event rather than continuous decreases.

Mean effluent DOC data (Figure 3.3b) is useful for understanding how DOC dynamics could affect the NO_3^- removal performance of IWSZs. High DOC concentrations that were observed during the initial period of the storm events could have increased NO_3^- removal rates. NO_3^- removal rates may have then decreased as excess DOC was flushed out of the system; however, the increase in detention time may have played a larger role by reducing effluent NO_3^- concentrations (Figure 3.3a). When the detention time increased even further, NO_3^- was almost completely removed and effluent DOC concentrations increased due to the greater hydrolysis rate compared to the DOC consumption rate. Increased DOC concentrations in the IWSZ pore waters may then be available for next storm event, as the intermittent cycle continued.

39

Water quality data from SE #4 (8 day ADC) and SE #5 (0 day ADC) (Figure 3.4) are useful for comparing how varying ADCs affect IWSZ performance. The initial low effluent NO_3^- concentration during SE #4 was expected because water leaving the reactor had been retained in the IWSZ during ADCs. Kim et al. (2003) observed similar results and suggested that mixing of the influent and IWSZ initial pore water volume occurs over time, which causes the IWSZ NO_3^- removal efficiency to decrease. This could explain why low NO_3^- removal was observed in the one hour detention time sample for SE #5, since this storm event began immediately after SE #4. However, the difference in NO_3^- removal efficiencies over the duration of SE #4 and SE #5 indicates that higher initial DOC concentrations from SE #4 increased NO_3^- removal. In addition, effluent DOC results from SE #2, SE #3 and SE #9 (ADCs $\geq$ 4 days) are similar to SE #4 compared to SE #5. Warneke et al. (2011) also observed that higher bioavailable carbon in denitrification beds will yield greater NO_3^- removal rates. The results from this study provide evidence that the influent and water previously retained in the IWSZ simultaneously dilute influent NO_3^- concentrations and flush out retained DOC over multiple IWSZ pore volumes, which decreases NO_3^- removal efficiency over time. After the initial IWSZ pore water and excess DOC have been flushed out of the reactor, detention time plays a more dominant role in NO_3^- removal.

Nitrogen speciation removal efficiency data from SE #4 (Influent NO_3^--N = 2 mg/L) and SE #6 (4 mg/L) are useful for comparing how varying influent NO_3^- concentrations affect IWSZ performance (Table 3.4). A slight increase in effluent NO_2^- concentrations during SE #6 may have been due to partial denitrification at the higher influent NO_3^- loading rate. Storm Event #6

40

produced a higher percentage of TKN compared to SE #4; however, the actual TKN concentration produced was relatively low compared to influent NO_3^--N concentrations. These results provide evidence that NO_3^- is removed more efficiently during storm events with lower influent NO_3^- concentration, but the difference in TN removal efficiency is relatively small. This is important because seasonal fertilizer application rates can alter influent NO_3^- concentrations (Vidon et al., 2009).

The results from the low (SE #4) and high flow rate (SE #7) storm events show that an increase in IWSZ detention time increases NO_3^- removal and plays a significant role in increasing TN removal efficiencies (Table 3.4; Figure 3.5), as previously observed in other studies (Kim et al., 2003; Smith, 2008; Ergas et al., 2010; Lucas and Greenway, 2011; Lee et al., 2013). In addition, increased TKN production observed during SE #7 suggests that biofilm is washed out at higher flow rates. These results provide evidence that low hydraulic loading rates will reduce effluent NO_3^- and TKN concentrations. In addition, the TSS results revealed that lower hydraulic loading rates also improve TSS removal, which was expected.

The constant flow storm event (SE #8, SE #9 and SE #11) results provide a general framework for how multiple processes affect NO_3^- removal in IWSZs, as shown in Table 3.4 and Figure 3.6. As previously discussed, water mixing and DOC flushing will contribute to the decrease in NO_3^- removal efficiency over time; however, these processes are only expected to occur during the initial IWSZ pore volumes discharged. A phenomenon that could explain the longer term decrease in NO_3^- removal efficiency is the effect of mass transfer of substrates into the biofilm. When IWSZs are initially charged, a high substrate concentration gradient exists

41

between the IWSZ pore water and biofilm boundary layer. During IWSZ operation, substrate concentration gradients decrease, thereby decreasing substrate mass transfer rates and reducing NO_3^- removal rates over time.

3.4.4 Implications for Full-Scale Bioretention System Design

Understanding where and how nitrogen species transformation processes occur is important in developing design strategies for bioretention systems. The results from this study consistently show that NO_3^- removal was greater than TN removal. There are two reasons for this: (1) the IWSZ was saturated, which prevented TKN oxidation and (2) the saturated wood-chip media in the IWSZ leached TKN. In full-scale bioretention systems, nitrification in the sand layer will likely increase TKN oxidation and plant uptake or microbial processes in the rhizosphere will likely increase TN   removal. Thus, higher TN removal efficiencies would likely occur if bioretention systems containing sand and plant layers were evaluated.

Plant uptake is considered to be a dominant TN removal mechanism during bioretention operation if an efficient nitrification/denitrification process is unavailable (Payne et al., 2013). Reported plant uptake rates vary between 0.5 and 180 g TN/m^2/yr, with the highest values representing nutrient-rich wetlands (Payne et al., 2013). Davis et al. (2006) and Greenway and Lucas (2010) estimated bioretention plant uptake values of 75 and 65 g N/m^2/yr, respectively. TN removal rates for the gravel and wood media evaluated in this study were between 600 and 1,600 g TN/m^2/yr. Thus, inclusion of an IWSZ containing a gravel-wood media could increase TN removal rates and decrease the bioretention footprint required to remove TN.

The results from this study also provide insight on the potential impact that IWSZs have on downstream waters. Due to oxygen uptake in the IWSZ, effluent DO is low. In addition, excess DOC washed out of the IWSZ may be consumed by aerobic bacteria, preventing reaeration. If IWSZs are designed significantly larger than what is needed to reduce NO_3^-, then DO levels in downstream waters may decrease and impact aquatic ecosystems. Because of this, understanding the characteristics of DOC sources (mulch, soil, plant decay and exudates, and IWSZ carbon-containing media) and sinks (adsorption, plant uptake and microbial decomposition) and their rates is vital in determining how IWSZ effluent could impact downstream surface waters.

3.5 Conclusions

Processes that control NO_3^- removal in IWSZs of modified bioretention systems were investigated using mixtures of wood, sand and gravel media. Based on the results from this study, the following conclusions were drawn:

- Unacclimated media export TKN, DOC and PO_4^{3-}, but once media are acclimated they export only TKN and DOC to a smaller degree and remove NO_3^- at higher rates. These results also indicate that the mulch layer exports high amounts of TKN and PO_4^{3-} and should not be included in bioretention system designs.

- The gravel-wood media was selected for further evaluation due to good hydraulic properties and the observed increase in NO_3^- removal rates and low DOC production compared to the sand-wood and wood media.

- NO_3^- removal was positively correlated with antecedent dry conditions (ADCs) and detention time and negatively correlated with influent NO_3^- concentration and storm duration.

- Hydrolysis increased IWSZ pore water DOC concentrations during ADCs and improved NO_3^- removal efficiency during IWSZ operation.

- It was estimated that permanently saturated IWSZs will act as a carbon source to promote denitrification for approximately 34 years.

Table 3.1. Storm event ADCs, durations and characteristics used for the column study.

Storm Event	ADC (days)	Duration (hr)	Notes
1	0	37.5	Began one day after acclimation period
2	16	37.5	
3	4	37.5	
4	8	37.5	
5	0	37.5	Began immediately after storm event #4
6	8	37.5	Influent NO_3-N $\approx$ 4 mg/L
7	8	11.25	High flow rates
8	8	9	Constant 1 hr detention time
9	30	37.5	
10	N/A[a]	18	Constant 2 hr detention time
11	N/A[a]	86.25	Constant 3 hr detention time

[a] Not measured

44

Table 3.2. Results from the acclimated (top value) and unacclimated (bottom value) microcosm experiments during Phase 1. All parameter values are in mg/L with the exception of pH; acclimated microcosm standard deviation values are shown in parenthesis; and BDL is below detection limit.

Parameter	Initial	Wood	Sand-Wood	Gravel-Wood	Sand	Gravel
NO_3^--N	1.94 (0.06)	BDL	0.30 (0.09)	BDL	1.94 (0.06)	2.04 (0.11)
	1.85	1.34	1.74	1.69	2.14	2.58
NO_2^--N	BDL	BDL	BDL	BDL	BDL	BDL
	0.06	0.62	0.33	0.25	BDL	BDL
NH_4^+-N	BDL	BDL	BDL	BDL	BDL	BDL
	BDL	14.83	4.37	11.26	BDL	BDL
Org-N	0.2 (0.1)	0.3 (0.0)	0.3 (0.1)	0.3 (0.1)	0.4 (0.1)	0.2 (0.1)
	0.4	10.4	11.1	0.4	1.5	1.4
TN	2.2 (0.1)	0.3 (0.0)	0.7 (0.1)	0.4 (0.0)	2.3 (0.2)	2.2 (0.1)
	2.4	27.2	17.6	13.6	3.7	4.0
DOC	2.9 (0.2)	6.8 (1.2)	4.6 (1.0)	4.1 (0.5)	3.5 (0.6)	3.0 (0.3)
	3.5	372.3	142.9	123.1	13.4	14.3
PO_4^{3-}-P	0.09 (0.02)	0.09 (0.02)	BDL	0.04 (0.02)	0.13 (0.02)	0.13 (0.00)
	0.14	49.58	12.81	13.58	0.41	0.25
SO_4^{2-}-S	20.5 (2.1)	17.9 (2.0)	20.5 (1.8)	18.9 (2.1)	20.9 (2.6)	20.5 (2.4)
	23.7	41.6	34.0	32.3	27.6	26.4
pH	8.0 (0.3)	7.0 (0.1)	7.2 (0.1)	7.5 (0.2)	7.6 (0.5)	7.7 (0.2)
	8.4	5.5	6.7	6.4	8.7	8.7

Table 3.3. Results from the anoxic, aerobic and inactivated control microcosms experiments during Phase 2. All parameter values are in mg/L with the exception of pH; standard deviation values are shown in parenthesis; BDL is below detection limit; only the initial DO concentration for the aerobic microcosms is shown. Initial anoxic DO concentrations were 1.0 mg/L.

Parameter	Initial	Anoxic	Aerobic	Inactivated control
NO_3^--N	1.96 (0.00)	0.06 (0.05)	0.39 (0.18)	1.90 (0.03)
NO_2^--N	0.02 (0.00)	0.03 (0.00)	0.04 (0.00)	0.04 (0.00)
NH_4^+-N	BDL (-)	BDL (-)	BDL (-)	0.95 (0.06)
Org-N	0.4 (0.17)	0.4 (0.02)	0.3 (0.04)	1.9 (0.06)
TN	2.4 (0.15)	0.5 (0.03)	0.7 (0.18)	4.8 (0.06)
DOC	3.9 (0.05)	4.9 (0.23)	4.6 (0.32)	71.4 (5.0)
PO_4^{3-}-P	0.12 (0.00)	0.09 (0.00)	0.08 (0.01)	0.74 (0.09)
SO_4^{2-}-S	35.5 (0.2)	34.2 (0.3)	35.6 (0.2)	50.8 (1.0)
DO	5.2 (0.7)	0.0 (0.0)	0.1 (0.2)	-
pH	7.7 (0.11)	-	-	-

Table 3.4. Overall storm event influent and effluent water quality characteristics during the column study. Flow weighted influent and effluent concentrations (mg/L) are shown with the standard deviation (mg/L) in parenthesis and the total mass removed (%) in brackets. Flow weighted effluent values are shown for pH.

	NO_3^--N	TKN	TN	PO_4^{3-}-P	SO_4^{2-}-S	TSS	VSS	DOC	pH
Influent	2.13 (0.55)	0.3 (0.1)	2.5 (0.6)	0.12 (0.03)	65.3 (5.7)	6.1 (2.2)	1.8 (0.7)	4.8 (0.4)	7.6 (0.3)
Storm #									
1	0.28 [86]	0.4 [-24]	0.7 [68]	0.03 [70]	50.3 [8]	2.4 [57]	0.4 [74]	5.9 [-37]	6.9
2	0.05 [97]	0.4 [7]	0.5 [79]	0.03 [73]	51.6 [16]	2.8 [38]	0.5 [68]	22.0 [-368]	6.8
3	0.08 [96]	0.5 [-45]	0.6 [75]	0.04 [60]	57.1 [14]	1.8 [55]	0.3 [76]	6.8 [-42]	7.0
4	0.06 [97]	0.5 [-17]	0.6 [76]	0.04 [73]	62.0 [12]	1.9 [67]	0.2 [87]	11.5 [-130]	6.9
5	0.25 [86]	0.5 [-12]	0.8 [65]	0.04 [68]	71.4 [-2]	2.6 [69]	0.6 [61]	5.3 [3]	7.0
6	0.40 [89]	0.4 [-49]	1.1 [73]	0.06 [54]	58.1 [13]	2.6 [70]	0.8 [65]	11.2 [-115]	7.1
7	0.84 [62]	0.4 [-53]	1.3 [49]	0.04 [74]	56.6 [13]	3.2 [38]	1.0 [41]	9.0 [-94]	7.0
8	0.81 [58]	0.5 [-103]	1.4 [38]	0.08 [49]	58.9 [12]	-	-	11.2 [-146]	-
9	0.06 [97]	0.5 [-55]	0.6 [75]	0.16 [-29]	64.5 [14]	-	-	16.7 [-251]	7.0
10	0.39 [80]	0.5 [-234]	1.0 [55]	0.01 [86]	58.2 [5]	-	-	5.6 [-21]	-
11	0.33 [84]	-	-	0.00 [100]	63.4 [-3]	-	-	-	-
Overall	0.32 [85]	0.5 [-43]	0.9 [66]	0.07 [59]	59.3 [9]	2.5 [59]	0.6 [68]	10.5 [-119]	7.0
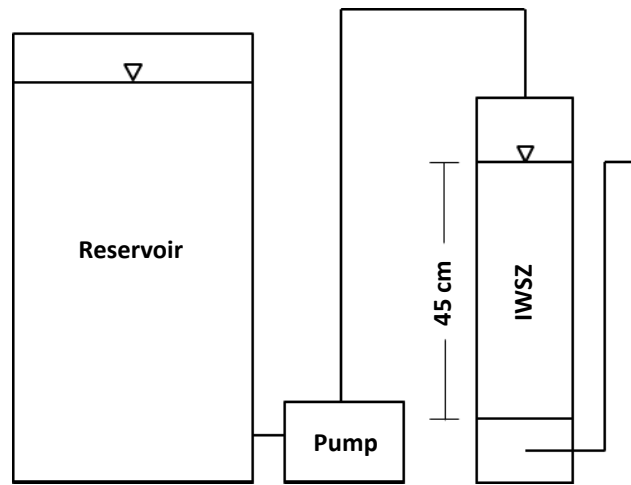
Figure 3.1. General laboratory setup for the storm event studies.
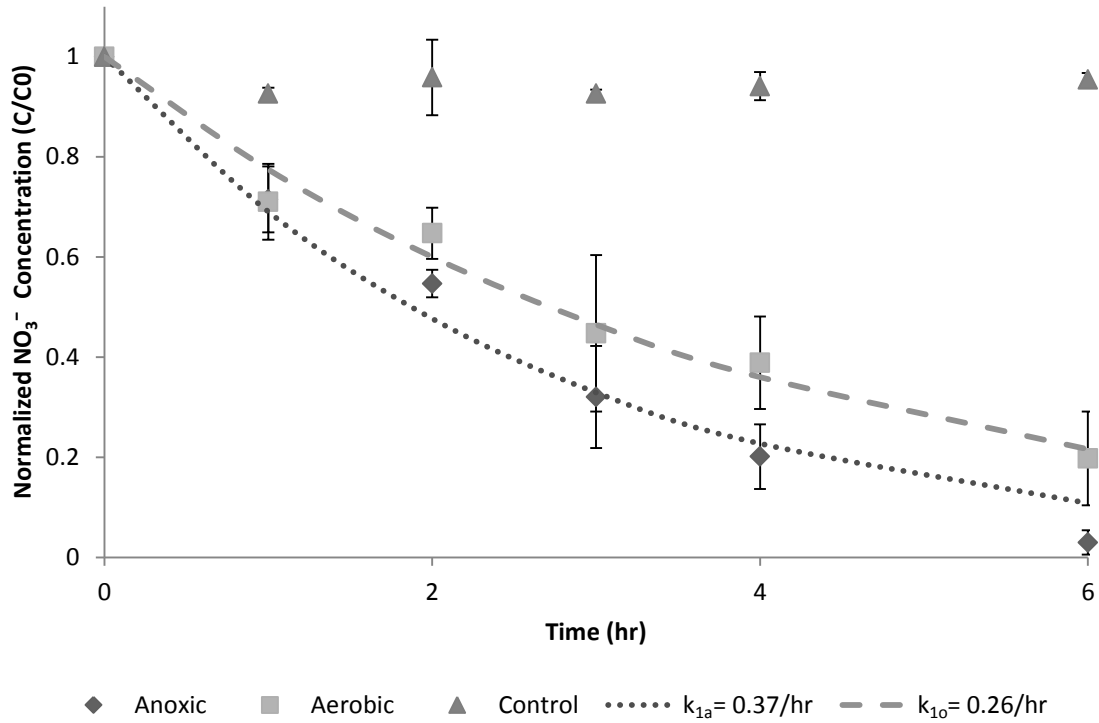
Figure 3.2. Normalized NO_3^- concentrations over time in gravel-wood microcosms incubated under anoxic, aerobic and inactivated control conditions. Lines represent denitrification models for the anoxic (k_{1a}) and aerobic (k_{1o}) microcosms. Error bars represent standard deviations of triplicate microcosms.

47
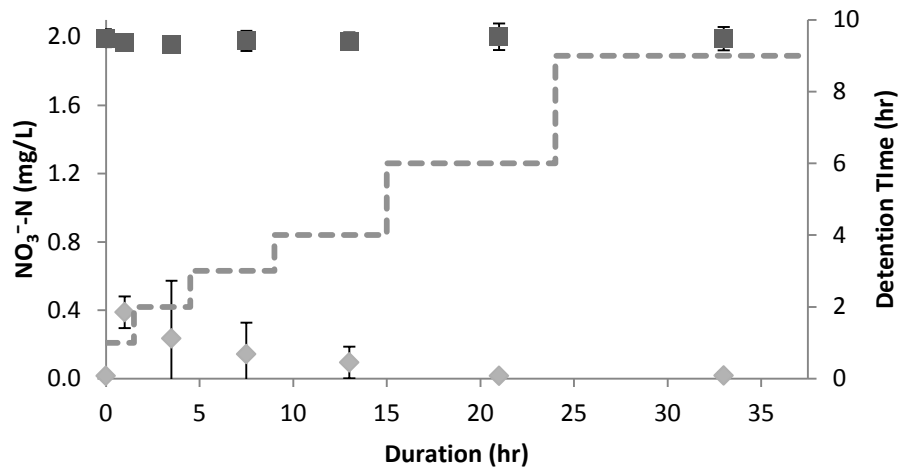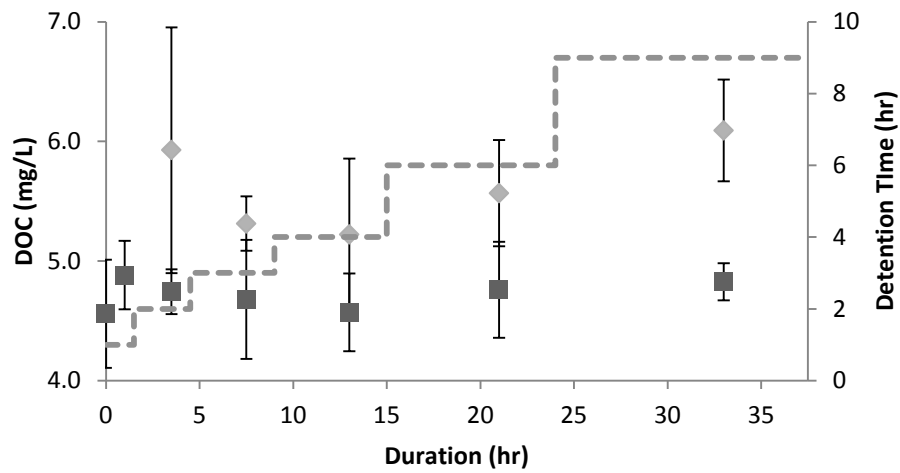
Figure 3.3. Mean NO_3^--N (a) and DOC (b) concentrations for SE #'s 1-5 and 9, which were operated under the same hydraulic loading conditions. Effluent DOC data from the initial pore water (58.8 mg/L) and one hour detention time (24.4 mg/L) samples are not shown. Error bars represent standard deviations.

48
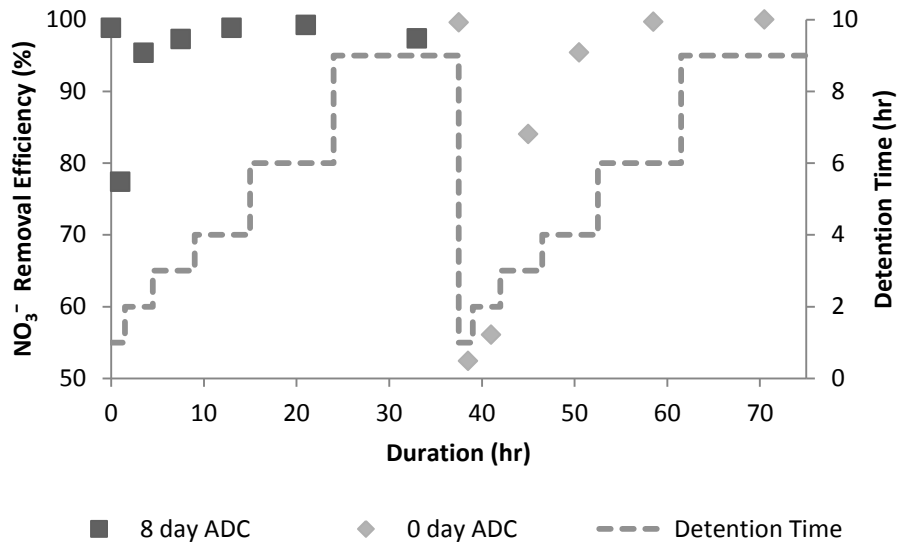
Figure 3.4. NO_3^- removal efficiency data comparing the effects of varying ADCs from SE #4 (8 day ADCs) and SE #5 (0 day ADCs).
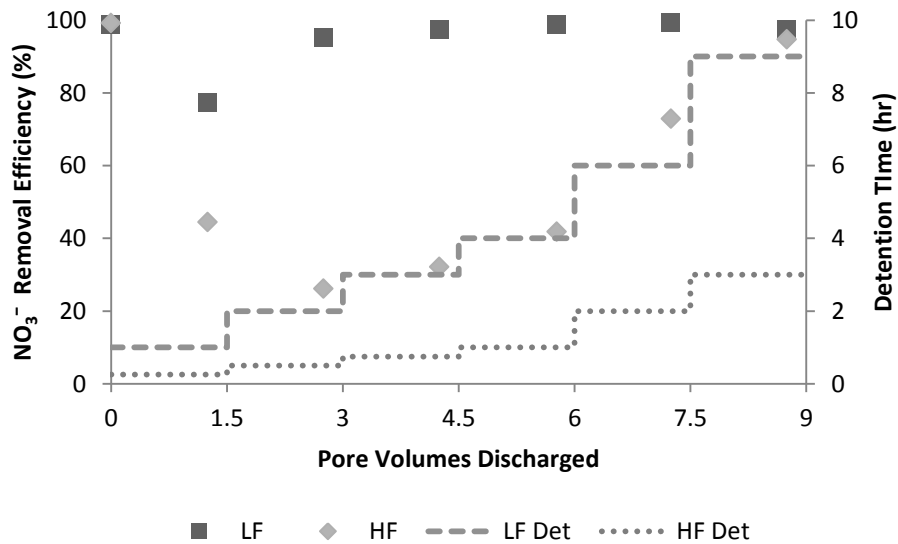
Figure 3.5. NO_3^- removal efficiency data comparing low and high flow storm events. LF, HF and "Det" values represent the low flow storm event (SE #4), high flow storm event (SE #7) and detention time, respectively.

49
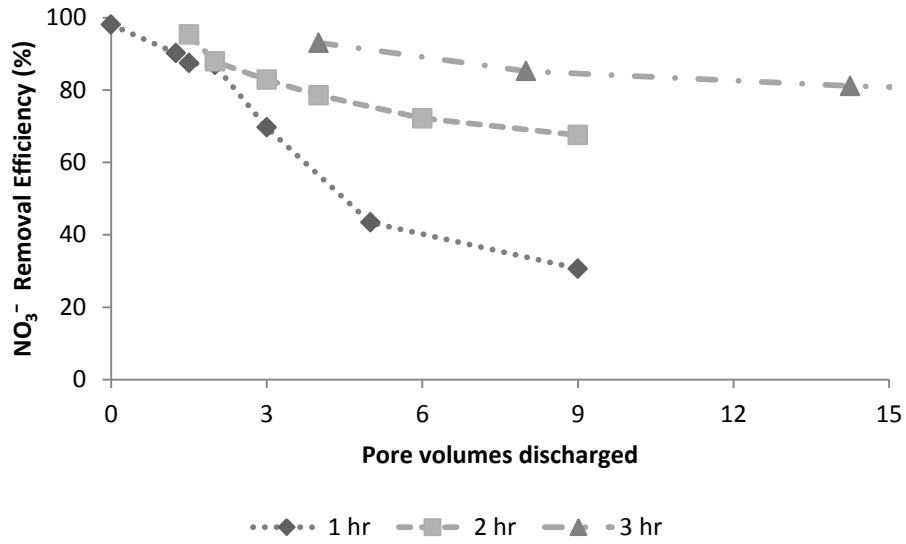
Figure 3.6. Nitrate removal efficiency data comparing storm events SE #8 (1 hr), SE #10 (2 hr) and SE #11 (3 hr) with a constant detention time. SE #11 sample data after 15 pore volume were discharged are not shown.

Dynamic Processes in Internal Water Storage Zones of Bioretention Systems[2]

4.1 Introduction

Bioretention systems are Low Impact Development (LID) technologies that minimize the hydrologic impact created by development (Dietz, 2007). Bioretention systems were originally designed to reduce runoff volumes by enhancing infiltration; however, additional benefits of bioretention include pollutant removal and surface water attenuation (Morzaria-Luna et al., 2004). A number of bioretention studies have confirmed that these systems achieve high removal efficiencies for suspended solids, phosphorus, heavy metals, oil and grease and fecal indicator bacteria (Hsieh and Davis, 2005; Davis et al., 2006; Ergas et al., 2010; Zhang et al., 2011; Zhang et al., 2012). In addition, modified bioretention systems have been developed that enhance the removal of nitrate (NO_3^-) by incorporating a submerged internal water storage zone (IWSZ) that includes an organic carbon source to promote denitrification (Collins et al., 2010; Lucas and Greenway, 2011).

Modified bioretention systems are passive systems that operate intermittently with varying hydraulic loading rates. During a storm event, runoff is conveyed into the ponding area, where the water elevation reaches the highest level near the end of a storm event. This creates a

---

[2] Note: Portions of this chapter have been submitted and are under review for publication to "*Journal of Environmental Engineering – ASCE*". The co-authors of the manuscript included Thomas Lynn, Mahmood Nachabe and Sarina Ergas. Research questions and experimental design were developed by Thomas Lynn and Sarina Ergas. Thomas Lynn performed laboratory work. Thomas Lynn and Sarina Ergas drafted the paper. Data interpretation and comments were provided by all authors.

hydraulic gradient that allows runoff from the ponding area to flow through the IWSZ. After a storm event, the water elevation decreases in the ponding area, and causes the IWSZ hydraulic loading rate to decrease. To gain a better understanding on proper design of IWSZs, previous studies have focused on evaluating NO_3^- removal as a function of the hydraulic loading rate (Kim et al., 2003; Smith, 2008; Ergas et al., 2010; Lee et al., 2013). Their results indicate that lower hydraulic loading rates (or higher detention times) increase NO_3^- removal efficiency. However, even on a macro-scale, NO_3^- removal in IWSZs is a function of the dispersion coefficient (D; cm^2/s) and the denitrification rate constant in addition to the hydraulic loading rate.

Due to the hydrodynamic nature of IWSZs, understanding dispersion and how it affects water quality performance is essential. Prior published studies on the effect of dispersion in IWSZs on NO_3^- removal are unavailable; however, dispersion has been studied in related systems, such as conventional bioretention systems and denitrifying bioreactors. Chun et al. (2009) developed a transport model based on laboratory data for denitrifying bioreactors. Grismer et al. (2012) performed a tracer study on conventional bioretention systems using various media types. Both studies found that estimated D values varied for each data set.

There are two general equations that can be used to calculate D in porous media (e.g. IWSZs), as shown in Equation 4.1 (Gunn and Pryce, 1969) and Equation 4.2 (Bear, 1972).

$$D = \frac{D_m}{\tau} + \frac{1}{2}\text{v}d \tag{4.1}$$

$$D = \tau D_m + \alpha_L \text{v} \tag{4.2}$$

where D_m is the molecular diffusion coefficient (cm^2/s); τ is the tortuosity factor ($2^{0.5}$); v is the pore velocity (cm/s); d is the average particle diameter of the media (cm); and α_L is the

52

longitudinal dispersivity (cm). Equations 4.1 and 4.2 can be rewritten to include the Peclet

Number, which is a dimensionless number that can be used to quantify whether advection or

dispersion dominate transport processes (Crittenden et al., 2005). In Equation 4.1, the Peclet

Number is equal to Pe_L ($Pe_L = vd/D$; Gunn and Pryce, 1969); however, in Equation 4.2, the

Peclet Number is equal to Pe (Pe $= L/ \alpha_L$ or vL/D; Kramer and Westererp, 1963), where L is the

length or depth (cm). Equations 4.1 and 4.2 both predict that higher pore velocities increase D.

However, there are three fundamental differences between Equation 4.1 and 4.2: (1) Equation

4.1 calculates the Peclet Number as a function of d instead of L; (2) Equation 4.1 assumes that

the Peclet Number varies with a change in pore velocity, while Equation 4.2 assumes that the

Peclet Number is constant (Charbeneau, 2006); and (3) the diffusive terms are calculated

differently. Due to these fundamental differences, an additional investigation that evaluates how

D varies with v is warranted.

   Although the Facility for Advancing Water Biofiltration (FAWB) recommends an IWSZ

depth of 45 cm, only a few published studies have rigorously evaluated how depth affects the

water quality performance of bioretention systems with IWSZs. Brown and Hunt (2011)

performed a field study of modified bioretention systems and observed higher total nitrogen

removal with IWSZ depths of 0.73-1.03 m compared with 0.57-0.87 m. However, the systems

utilized different media types. Zinger et al. (2007) performed a laboratory study and observed

higher NO_3^- removal efficiencies with IWSZ depths of 45 and 60 cm compared with 15 cm.

Results from these studies indicate that taller IWSZs improve NO_3^- removal efficiency; however,

neither of these studies compared the performance of these IWSZs with equal detention times.

53

As a result, these studies only provide evidence that greater detention times, rather than a specific IWSZ depth, improve NO_3^- removal efficiency.

The overall goal of this research was to investigate the dynamic performance of IWSZs in bioretention systems. The specific objectives of this study were to: (1) evaluate the hydraulic performance of IWSZs; (2) refine the general equations used to calculate D to produce more accurate results; and (3) evaluate the removal efficiency for NO_3^- and other water quality parameters of three IWSZs with varying depths that were operated with equal detention times. Temperature, plant uptake and nitrification also play a direct and/or indirect role in IWSZ performance; however, these factors were not considered in this study.

4.2 Materials and Methods

4.2.1 Experimental Setup

A schematic of the laboratory setup for the column study is shown in Figure 4.1. Source water used for this study was local stormwater runoff from a pond at the University of South Florida, Tampa. Stormwater was spiked with KNO_3 to achieve a NO_3^--N concentrations of 2 mg/L to mimic nitrified stormwater runoff (Schueler, 2003). All studies were performed at room temperature (approximately 22°C). A 2:1 (vol/vol) mixture of 0.6 to 1.3 cm pea gravel (Seffner Rock and Gravel, Tampa, FL) and 1.3 to 2.5 cm eucalyptus wood chips (Sarasota County, Sarasota, FL) was used. The porosity was 0.42. The media type used in this study was based on a prior study (see Chapter 3) showing that high NO_3^- removal could be achieved with this mixture. Experiments were carried out in three 12.7 cm ID acrylic columns with depths of 30, 45 and 60 cm. The gravel and wood medium in each column was supported by a 7.6 cm under-

drain layer of pea gravel to prevent clogging. The discharge pipes were 1.3 cm ID schedule 40

PVC. The discharge pipes were designed to collect water from the under-drain layer and to

discharge effluent above the IWSZ layer to completely submerge the medium. The pump used

for this study was a Cole Parmer Masterflex L/S Economy Drive (Thermo Fisher Scientific,

Waltham, Massachusetts), which was controlled by manually adjusting the pump flow valves.

4.2.2 Tracer Study

Three tracer tests were conducted for each column, while maintaining constant IWSZ

detention times of one, three and four hours. Prior to the start of each test, four pore volumes of

influent without the tracer were flushed through the columns to remove compounds that could

alter baseline conductivity measurements. The tracer tests proceeded by spiking the influent

with 2, 3 and 4 liters of a 200 mg/L potassium chloride (KCl) solution into the 30, 45 and 60 cm

columns, respectively. Influent without tracer was fed to the columns for the remaining time of

each tracer test. Samples were collected from the outlets of the columns and conductivity was

measured as described below. The conductivity value was adjusted to account for the

background conductivity of the influent and was converted to KCl concentration based on a

calibration curve.

Data from the tracer tests were used to estimate dispersive parameters that included: D,

t_{50}, Morrill Dispersion Index (MDI) and Pe. The term t_{50} is the time when 50% of the tracer

mass has passed through the column. The MDI describes the hydraulic characteristics of a

reactor as compared to ideal plug flow (MDI = 1) and complete mixed flow reactors (MDI ≈ 22)

(Tchobanoglous et al., 2003). The Pe is particularly useful because the degree of dispersion in a

55

reactor can be predicted if Pe is known; for instance, Pe values less than 4 and greater than 20 indicate high and low dispersion, respectively (Tchobanglous et al., 2003).

The one-dimensional convective-dispersive solute transport equation (Van Genutchen and Alves, 1982) was used to estimate D and Pe:

$$R\frac{\partial C}{\partial t} = D\frac{\partial^2 C}{\partial x^2} - \mathrm{v}\frac{\partial C}{\partial x} \tag{4.3}$$

where R is the retardation coefficient; C is the tracer concentration (mg/L); t is time (s); and x is the distance from the IWSZ inlet. The retardation coefficient in Equation 4.3 was set to one based on the assumption that adsorption of the KCl tracer onto the media was negligible.   The appropriate initial and boundary conditions for Equation 4.3 (Delgado, 2006) are:

$$C(x, 0) = C_1 \tag{4.4a}$$

$$\left(-D\frac{\partial C}{\partial x} + \mathrm{v}C\right)\Big|_{x=0} = \begin{cases} \mathrm{v}C_0 & 0 < t < t_0 \\ 0 & t \geq t_0 \end{cases} \tag{4.4b}$$

$$\frac{\partial C}{\partial x}(L, t) = 0 \tag{4.4c}$$

where C_1 is the initial tracer concentration in the column (mg/L); C_0 is the tracer solution concentration that was used in the study; and t_0 is the time at which the tracer solution was no longer applied to the columns. An approximate solution to Equation 4.3 modified from the solution presented in Genutchen and Alves (1982) to include Pe yields:

$$C(x, t) = \begin{cases} C_1 + (C_0 - C_1) \times A(x, t) & 0 < t < t_o \\ C_1 + (C_0 - C_1) \times A(x, t) - C_o \times A(x, t - t_0) & t \geq t_0 \end{cases} \tag{4.5a}$$

where

$$A(x,t) = \frac{1}{2}erfc\left[\frac{x-vt}{2\sqrt{\frac{vL}{tPe}}}\right] + \sqrt{\frac{vtPe}{\pi L}} \times exp\left[-\frac{Pe(x-vt)^2}{4vLt}\right] - \frac{1}{2}\left(1 + \frac{xPe}{L} + \frac{vtPe}{L}\right) \times exp^{\left(\frac{xPe}{L}\right)} \times erfc\left[\frac{x+vt}{2\sqrt{\frac{vL}{tPe}}}\right] + \sqrt{\frac{4vtPe}{\pi L}} \times$$

$$\left[1 + \frac{Pe}{4L}(2L - x + vt)\right]exp\left[Pe - \frac{Pe(2L-x+vt)^2}{4vLt}\right] - \frac{Pe}{L}\left[2L - x + \frac{3vt}{2} + \frac{Pe}{4L}(2L - x + vt)^2\right]exp^{(Pe)}erfc\left[\frac{2L-x+vt}{2\sqrt{\frac{vL}{tPe}}}\right]$$

<div align="right">(4.5b)</div>

The L value for each column was adjusted to include the length of the under-drain layer. The dispersive characteristics of the under-drain and IWSZ layers were assumed to be equal. Equation 4.5 was used to estimate D and Pe values for each tracer test.

4.2.3 Theory

The general equations to estimate D (Equations 4.1 and 4.2) were refined to estimate D using experimental data from the tracer study. The theory assumes that the Peclet Number (using the term Pe) is a function of the Reynolds Number (Re; $Re = qd/v$), where q is the superficial velocity (flow rate divided by the cross-sectional area of the column; cm/s); and v is the kinematic viscosity (cm^2/s). Expressions that relate Pe and Re were tested to evaluate which expression yielded the highest correlation with the experimental data. The general equation that was used to evaluate the expressions was:

$$Pe = Pe(Re) \tag{4.6}$$

After the highest correlated expression was selected, Equation 4.6 was then used to solve for D, using:

$$D = \frac{vL}{Pe(Re)} \tag{4.7}$$

To account for extreme conditions (i.e. $Re \rightarrow 0$), the term Pe_o was inserted into Equation 4.7:

<div align="center">57</div>

$$D = \frac{vL}{Pe(Re) + Pe_0} \tag{4.8}$$

where Pe_0 is defined as the hypothetical Pe value when a reactor is operating under no flow conditions. To account for no flow conditions, a diffusive term (D_m/τ) and a Re dead constant (10^{-6}) was inserted into Equation 4.8, to yield:

$$D = \frac{D_m}{\tau} + \frac{vL}{Pe(Re + 10^{-6}) + Pe_0} \tag{4.9}$$

4.2.4 Column Study

Eleven storm events were investigated in the column study as shown in Table 3.1 (see page 44). Eight of the storm events were set up to simulate a storm that discharges runoff into the bioretention ponding area as a slug load, while the other three storm events were set up to simulate a constant flow of runoff. The detention times were varied by manually adjusting the pump flow valves for a specific period of time. The term ADC was defined as the time period between the end of a previous storm event to the beginning of the next storm event.

4.2.5 Analytical Methods

Standard Methods (Standard, 2012) were used to measure dissolved organic carbon (DOC) (Method 5310B), total nitrogen (TN) (4500-N), total suspended solids (TSS) (2540D) and volatile suspended solids (VSS) (2540D). Anion (NO_3^-, nitrite [NO_2^-], phosphate [PO_4^{3-}] and sulfate [SO_4^{2-}]) and ammonium (NH_4^+) concentrations were measured by ion chromatography (USEPA, 1997) using an 850 Professional Ion Cromatograph (Metrohm AG, Herisau, Switzerland). A Shimadzu TOC-V CSH Total Organic Carbon / Total Nitrogen Analyzer (Shimadzu Scientific Instruments, Columbia, Maryland) was used to measure non-purgeable organic carbon (NPOC) and total nitrogen (TN). NPOC concentrations were used to estimate

58

DOC concentrations. Total Kjeldahl Nitrogen (TKN) concentrations were estimated by

difference TKN ≈ TN − [NO_3^--N + NO_2^--N]. An Orion 5 Star (Thermo Scientific Inc., Beverly,

Massachusetts) meter with a calibrated probe was used to measure pH, dissolved oxygen and

conductivity. Method detection limits for DOC, TN, NO_3^--N, NO_2^--N , PO_4^{3-}-P, SO_4^{2-}-S, NH_4^+-N

were 0.11, 0.03, 0.01, 0.04, 0.02, 0.01 and 0.07 mg/L, respectively.

4.2.6 Statistical Analysis

The estimated Pe and D values for each tracer test were determined by using a nonlinear

least-squares method by minimizing the sum of square residuals (SSR) (Kemmer and Keller,

2012) between the experimental data and the convective-dispersive solute transport model.

Fisher's F Distribution 95% confidence intervals were used to determine Pe confidence intervals

(Kemmer and Keller, 2012). The following analyses were determined through linear regression

to calculate the coefficient of determination (r^2): potential relationships between an expression

containing Pe and another containing the Reynolds Number (Re); the best-fit Pe_0 value; and the

relationship between the final expression that was used to calculate D (in the form of Eq. 9) and

the D values determined from the tracer study data. During the column study, flow weighted

influent and effluent concentrations were used to calculate mass removal efficiency. Storm event

TN removal efficiency data from the three IWSZs were compared using two-way analysis of

variance.

4.3 Results

The results from a typical tracer test that was performed during this study are shown in

Figure 4.2. During the one hour detention time tracer tests (Figure 4.2a), 95% of the tracer mass

59

was recovered before 3.3 pore volumes had discharged. Breakthrough from all columns occurred at approximately 0.8 pore volumes discharged. During the four hour detention time tracer tests (Figure 4.2b), 95% of the tracer mass was recovered before 6.1 pore volumes had discharged. In addition, breakthrough from the 30 and 60 cm columns occurred at 0.5 and 0.7 pore volumes discharged, respectively.

The dispersive parameters that were calculated from the tracer test data are shown in Table 4.1. The one hour detention time Pe values for all of the columns were between 12 and 15, which indicate moderate dispersion. However, during the three and four hour detention time tracer tests, moderate dispersion was observed in the 45 and 60 cm columns and high dispersion was observed in the 30 cm column. The lowest MDI values for each column were observed during the one hour detention time tracer tests. During the one hour detention time tracer tests, t_{50} for each column was similar (1.8 to 2.0 hr); however, during the three and four hour detention time, t_{50} for the 30 cm column was at least 0.7 hr less than the 45 and 60 cm columns. The D value was only observed to increase with a decrease in detention time (or increase in velocity) during the 60 cm column tracer tests.

The following relationships between Pe and Re were evaluated using the tracer test data: (1) Pe versus Re (r^2=0.62); (2) 1/Pe versus 1/Re (r^2=0.84); (3) Pe versus 1/Re (r^2=0.88); and (4) ln Pe versus 1/Re (r^2=0.94; Figure 4.3). The fourth relationship had the highest correlation and results in:

$$Pe = C_1 e^{-\left(\frac{C_2}{Re}\right)} \tag{4.10}$$

where the initial estimates for the constants C_1 and C_2 were 21.4 and 0.32, respectively. Pe_0

values of 0, 0.25, 0.5 and 1.0 were tested in Eq. 8. The most appropriate Pe_0 value was chosen

using the following criteria: verifying that large D values are not calculated at low Re values; and

by limiting the change of the 'best-fit' r^2 value (from when $Pe_0 = 0$) between the data and

Equation 4.8 to less than 0.05. Based on these criteria a Pe_0 value of 0.5 was determined.

Equation 4.10 was inserted into Equation 4.9 with the appropriate parameters to yield:

$$D = \frac{D_m}{\tau} + \frac{vL}{20e^{-\left(\frac{0.34}{Re+10^{-6}}\right)}+0.5} \qquad (4.11)$$

The r^2 value between Equation 4.11 and the estimated D values from the experimental data

(Equation 4.4) was 0.76.

A summary of the overall water quality results from the storm event studies with the

three columns are shown in Table 4.2. All of the columns removed NO_3^-, TN,

PO_4^{3-}, SO_4^{2-}, TSS and VSS and produced TKN and DOC. NO_3^- removal efficiencies from the 45

and 60 cm columns were greater than from the 30 cm column. Overall TN removal efficiency

from the 30 cm column was significantly less than the 45 and 60 cm columns (both p-

values<0.01). Overall TN removal efficiency was not significantly different between the 45 cm

and 60 cm columns (p-value=0.38).

NO_3^- removal efficiency data from SE #4, SE #6, and SE #7 are shown in Figure 4.4.

During these storm events, NO_3^- removal efficiencies from the 30 cm column samples were lower

than the 45 and 60 cm column samples when the detention time was 2 hr or greater; however,

NO_3^- removal efficiencies from each column were similar when the detention time was less than 2

hours. NO_3^- removal dynamics for every column and during each of these storm events were otherwise similar. High NO_3^- removal efficiencies (>95%) and effluent DOC concentrations (data not shown) were observed in the first samples as the initial pore water was flushed from the system. Lower NO_3^- removal efficiencies and effluent DOC concentrations were then observed in the second samples as the influent mixed with the initial pore water. Thereafter, higher NO_3^- removal efficiencies were observed when the detention time increased. In addition, effluent DOC concentrations decreased to or were lower than influent DOC concentrations over the initial five samples taken.

NO_3^- removal efficiency data from the constant two hour detention time storm event (SE #10) are shown in Figure 4.5. During this storm event, NO_3^- mass removal efficiencies of 73, 80 and 90% were observed from the 30, 45 and 60 cm columns, respectively. However, during the constant one hour detention time storm event (SE #8) NO_3^- mass removal efficiencies of 59, 58 and 59% were observed from the 30, 45 and 60 cm columns, respectively.

4.4 Discussion

The tracer study data (Figure 4.2) can be useful in understanding how detention time and depth affect the hydraulic performance of IWSZs. In terms of pore volumes discharged, breakthrough during the four hour detention time tracer tests (Figure 4.2b) occurred earlier than during the one hour detention time tracer tests (Figure 4.2a). This indicates that lower detention times increase the hydraulic efficiency of IWSZs. Moreover, during the one hour detention time tests, breakthrough from each column occurred at similar pore volumes discharged; however, during the four hour detention time tests, breakthrough from the 30 cm column occurred earlier

than from the 60 cm column. This indicates that at high detention times, the hydraulic efficiency

of taller IWSZs is greater than for shorter IWSZs; however, at low detention times the hydraulic

efficiencies of shorter and taller IWSZs are similar.

Analysis of the tracer study results (Table 4.1) also provides evidence that greater depths

and lower detention times improve the hydraulic efficiency of IWSZs. The highest Pe and

lowest MDI values observed during the one hour detention time tracer tests indicates that a

decrease in detention time increases hydraulic efficiency. Similar t_{50} values observed during the

one hour detention time tracer tests provide additional evidence that the hydraulic efficiency for

each column was similar; however, at higher detention times, the hydraulic efficiency decreases

when the IWSZ depth decreases. The fundamental theory for Equations 4.1 and 4.2 could be

applied to the results obtained from the 60 cm column, where D increased with an increase in

velocity (decrease in detention time). However, D did not increase with an increase in velocity

in the 30 and 45 cm columns. This provides an example of how Equation 4.1 does not produce

accurate results with experimental data (Delgado, 2006). In addition, the results of this study

indicate that Pe changes with a change in Re (Figure 4.3) or pore velocity, which conflicts with

the fundamental theory used in developing Equation 4.2.

The tracer study results provide new insights into the dynamic nature of IWSZs in

bioretention systems. At higher flow rates, the hydraulic efficiency increases; however,

denitrifying bacteria have less time to respire NO_3^-. At lower flow rates, the hydraulic efficiency

decreases; however, denitrifying bacteria have more time to respire NO_3^-. In addition, the tracer

study results indicate that an increase in IWSZ depth improves hydraulic efficiency, which

63

increases NO_3^- removal efficiency. The combined effects of these phenomena can be understood by analyzing the SE #6 NO_3^- removal efficiency data shown in Figure 4.4b. For the 30 cm column, the difference in NO_3^- removal efficiency between the one and four hour detention time samples was only 6%; however, in the 60 cm column, the difference was 23%.

Data from the tracer study were used to develop a novel equation for calculating D. Equation 4.10 implies that as Re increases, Pe increases. This indicates that at higher flow rates, advection dominates over dispersion (Tchobanoglous et al., 2003). Thus, higher flow rates cause the system to operate closer to ideal plug flow conditions. This is also shown in the experimental data provided in Table 4.1, where higher Pe values were observed during lower detention times (high flow rates) compared to higher detention times. Equation 4.11 included the term "Pe_0" that was developed primarily for modeling purposes. The addition of Pe_0 allows Pe→Pe_0 as Re→0, which would prevent the calculation of large D values when Re is small ($0.05 < Re < 0.1$).

The method used to estimate D from the tracer test data was constrained to one independent variable. Chun et al. (2009) estimated D by allowing the denitrification decay constant, the velocity and D to change in order to fit data to their model, while other studies followed a similar approach (Zhang et al., 2010; Herbert, 2011; Delay et al., 2013). Grismer et al. (2012) estimated D by setting D as the only independent variable. However, their study assumed the porosity and pore water volume for their reactor. The results from these studies would have greater validity if D was the only independent variable and if all critical parameters were measured, rather than estimated.

The overall water quality results (Table 4.2) are useful for comparing how different IWSZ depths affect the overall performance of IWSZs. Significantly lower TN removal efficiencies were observed from the 30 cm column, indicating that the hydraulic efficiency of IWSZs decreases with a decrease in depth. Similar results were observed for each IWSZ with respect to the removal or production of water quality constituents other than NO_3^-. These results provide evidence that multiple processes occur in IWSZs including: dispersion; denitrification; TKN production; phosphate reduction; sulfate reduction; filtration; and hydrolysis.

NO_3^- removal efficiency data from SE #4 (Figure 4.4a) shows how varying IWSZ depths affect NO_3^- removal. In the 45 and 60 cm columns, NO_3^- removal efficiency increased with increasing detention time. Previous studies have also observed a positive correlation between NO_3^- removal efficiency and detention time (Kim et al., 2003; Smith, 2008). However, this was not observed when comparing the one and two hour detention time samples taken from the 30 cm column. The 30 cm column results could be explained by the mixing of the influent and water previously retained in the IWSZ, which resulted in higher NO_3^- removal efficiencies during the initial operating period (Kim et al., 2003). Another hypothesis could be that lower effluent DOC concentrations from the two hour detention time samples limited NO_3^- removal efficiency. However, both of these explanations would also infer that the 30, 45 and 60 cm columns would have similar NO_3^- removal efficiencies, which was not the case in this study. Differences in NO_3^- removal efficiency from IWSZs with varying depths was likely due to dispersion, where lower hydraulic efficiencies were observed in the 30 cm column compared to the 45 and 60 cm columns. These results provide evidence that taller IWSZs require less media volume than shorter IWSZs to remove the same amount of NO_3^-.

NO_3^- removal efficiency data from SE #6 (Figure 4.4b) are useful for comparing how IWSZs with varying depths are affected by higher influent NO_3^- concentrations. Since NO_3^- was almost completely removed in most of the 45 and 60 cm effluent samples during the other storm events, SE #6 data provides a more quantifiable view of the extent of NO_3^- removal. During the one hour detention time, NO_3^- removal efficiency from the samples for each column were relatively equal; however, greater removal efficiencies were observed in the 45 and 60 cm columns than the 30 column at higher detention times. This was also observed during SE #2, SE #3, SE #4 (Figure 4.4a), SE #5 and SE #9, which were all operated under the same flow conditions but varying ADCs. These results provide evidence that dispersion consistently affects NO_3^- removal efficiencies in storm events that have varying influent NO_3^- concentrations and ADCs.

NO_3^- removal efficiency data from SE #7 (Figure 4.4c) are useful for comparing how IWSZs with varying depths are affected by higher flow rates. The decrease in NO_3^- removal efficiency during the initial stage could be explained by water mixing and DOC flushing processes, as previously discussed. However, the differences in NO_3^- mass removal efficiencies between each of the columns were relatively small compared to the other storm events that were operated with lower flow rates. This is consistent with the tracer study results, where the estimated Pe values during lower detention times (1 hr) indicated moderate dispersion from each of the columns. These results provide additional evidence that dispersion limits NO_3^- removal efficiencies to a lesser degree at higher flow rates, but will play a more prominent role at lower flow rates.

66

NO_3^- removal efficiency data from the constant two hour detention time storm event (Figure 4.5) illustrate how dispersion affects NO_3^- removal efficiency for a specific IWSZ depth and detention time. As indicated by the tracer study results, taller IWSZs tend to operate closer to plug flow conditions compared to shorter IWSZs; hence, the taller column (60 cm) was observed to have a greater NO_3^- mass removal efficiency than the 30 and 45 cm columns. Similar results were also observed during the three hour detention time storm event (SE #11). However, during the one hour detention time (SE #8), NO_3^- mass removal efficiencies for each column were almost equal. This is consistent with the one hour detention time tracer tests where moderate dispersion was observed in all of the columns.

This study clearly demonstrates that dispersion plays a role in limiting NO_3^- removal efficiencies in IWSZs and its degree of impact depends both on depth and hydraulic loading rate. However, this study only evaluated one media type under laboratory conditions, where the effect of dispersion under varying environmental conditions and media types may be different. For example, Nachabe et al. (1999) studied solute transport in soil and observed that hydraulic efficiency is greater in unsaturated compared to saturated soils. In addition, Cameron and Schipper (2012) evaluated the hydraulic efficiency of various carbon-containing media types for use in denitrifying bioreactors and observed that dispersion played a minor role in affecting NO_3^- removal efficiency. However, their tracer study was conducted at one flow rate, where dispersion may have not affected NO_3^- removal efficiency.

Dispersion and advection may not be the only flow related processes that affect NO_3^- removal efficiencies in IWSZs. It is quite possible that the pore velocity can change the pore

67

water/ biofilm mass transfer coefficient (Nath and Chand, 1996; Mudlar et al., 2008) or the biofilm thickness (Delay et al., 2013) of attached growth systems, such as IWSZs. Future research should investigate the degree in which the changes in the dispersion coefficient, mass transfer coefficient and biofilm thickness as a function of the Reynolds Number affect the transport of chemicals through different types of porous media systems.

4.5 Conclusions

Hydrodynamics and water quality performance were evaluated in three IWSZs for bioretention systems with varying depths (30, 45 and 60 cm). Results from tracer tests indicate that taller IWSZs are more hydraulically efficient than shorter IWSZs. An alternative equation for estimating dispersion in saturated porous media was introduced. Results from the storm event studies indicated that NO_3^- removal efficiencies of taller IWSZs were greater than shorter IWSZs even when these reactors were operated with equal detention times; however, at higher flow rates, NO_3^- removal efficiencies of taller and shorter IWSZs were similar. These results provide evidence that dispersion affects the NO_3^- removal efficiency of IWSZs. Based on these results, the minimum recommended depth for IWSZs in bioretention systems was 45 cm.

Table 4.1. Estimated dispersive parameters that were calculated from the data obtained during each tracer test.

Column	IWSZ detention time (hr)	Pe [a]	D x 10^{-2} (cm^2/s)	t_{50} (hr) [b]	MDI [c]
30 cm	1	13.1 (8.4 – 20.8)	2.7	2.0	2.3
	3	2.5 (2.1 – 2.9)	4.8	4.8	4.4
	4	1.5 (1.2 – 1.9)	5.9	5.7	4.5
45 cm	1	12.2 (7.2 – 21.4)	6.2	2.0	2.3
	3	7.9 (5.8 – 10.6)	3.2	5.5	3.1
	4	4.4 (3.8 – 5.0)	4.4	6.6	4.4
60 cm	1	14.8 (9.8 – 23.2)	8.8	1.8	2.4
	3	6.2 (4.2 – 9.1)	7.0	5.6	3.8
	4	6.8 (5.4 – 8.5)	4.8	6.9	3.6

[a] Values in parenthesis represent Fisher's 95% confidence interval
[b] t_{50} the time when 50% of the tracer mass has passed through the columns
[c] MDI represents the Morrill Dispersion Index

Table 4.2. Overall water quality results of the three IWSZs (30, 45 and 60 cm) during the storm event study.

	Mean concentration [a]				Mass removal efficiency (%)		
	Influent	Column			Column		
		30 cm	45 cm	60 cm	30 cm	45 cm	60 cm
Parameter							
NO_3^--N	2.13 (0.55)	0.44 (0.39)	0.30 (0.38)	0.30 (0.41)	78	85	85
TKN	0.3 (0.1)	0.5 (0.1)	0.5 (0.1)	0.5 (0.1)	-43	-42	-49
TN	2.5 (0.6)	1.0 (0.4)	0.8 (0.4)	0.9 (0.4)	60	66	65
$PO_4^{3-}-P$	0.12 (0.03)	0.07 (0.16)	0.07 (0.18)	0.09 (0.22)	58	60	49
$SO_4^{2-}-S$	65.3 (5.7)	54.5 (21.2)	54.6 (21.4)	54.9 (21.6)	10	9	9
TSS	6.1 (2.2)	2.8 (0.9)	2.5 (0.9)	2.4 (0.7)	55	59	61
VSS	1.8 (0.7)	0.6 (0.5)	0.5 (0.5)	0.5 (0.3)	64	68	72
TOC	4.8 (0.4)	10.1 (13.1)	13.4 (20.8)	12.0 (18.8)	-72	-119	-100
pH [b]	7.6 (0.3)	7.1 (0.2)	7.0 (0.2)	7.0 (0.2)	-0.5	-0.6	-0.6

[a] Values shown are in mg/L except for pH and values shown in parenthesis represent the standard deviation.
[b] Mass removal efficiency pH values represent the weighted increase in effluent pH compared to influent.

69
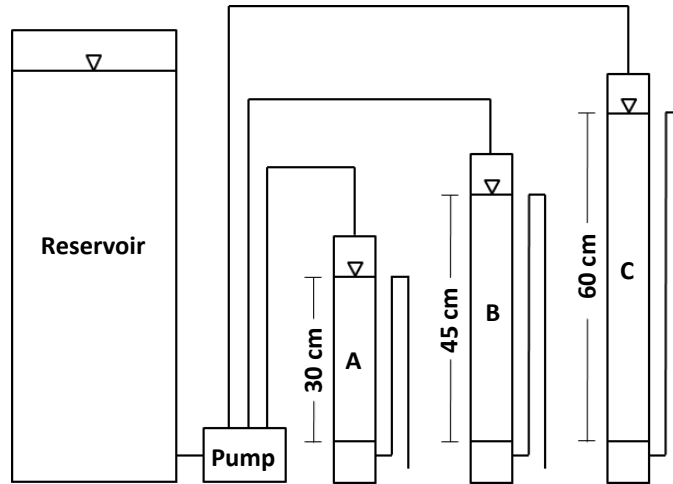
Figure 4.1. General laboratory setup for the storm event studies. The 30 (A), 45 (B) and 60 (C) cm columns were operated with equivalent detention times by varying the flow rate.
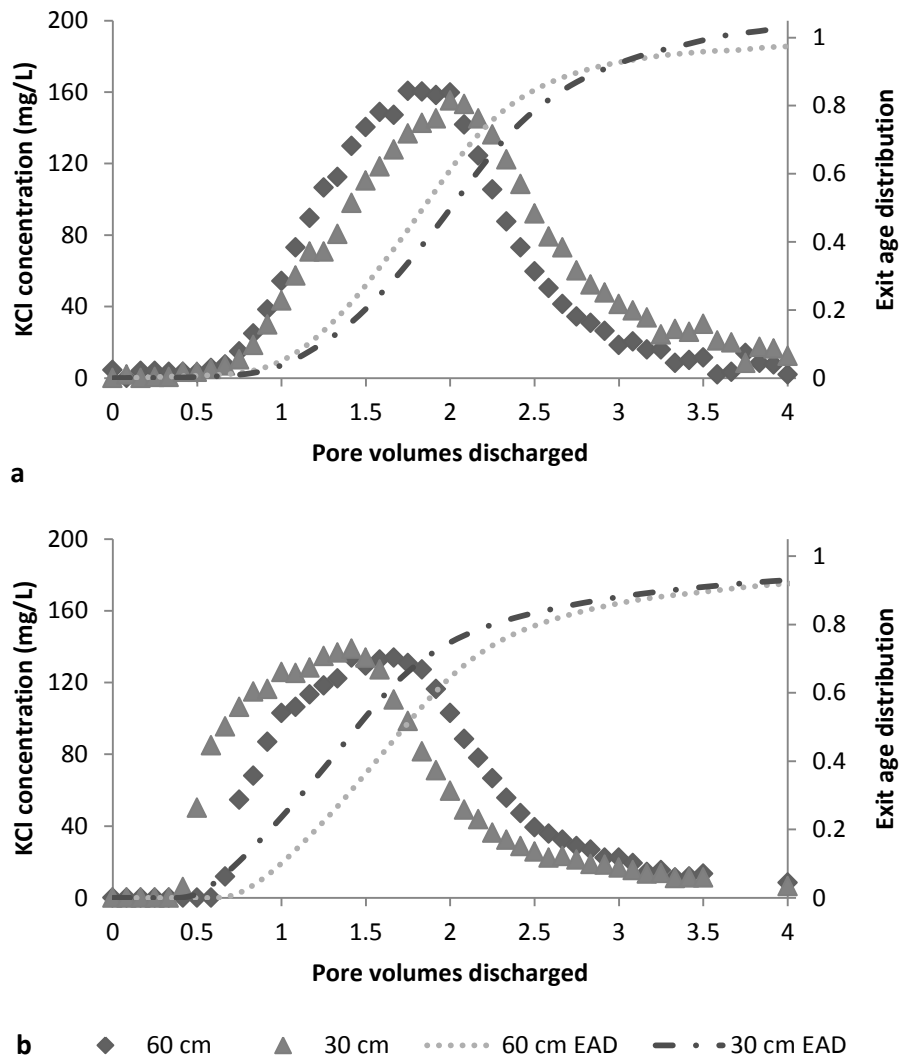
Figure 4.2. Tracer study data and cumulative distribution curves from the 30 and 60 cm columns operated with a detention time of one (a) and four (b) hours. EAD represents the cumulative exit age distribution curve.

71
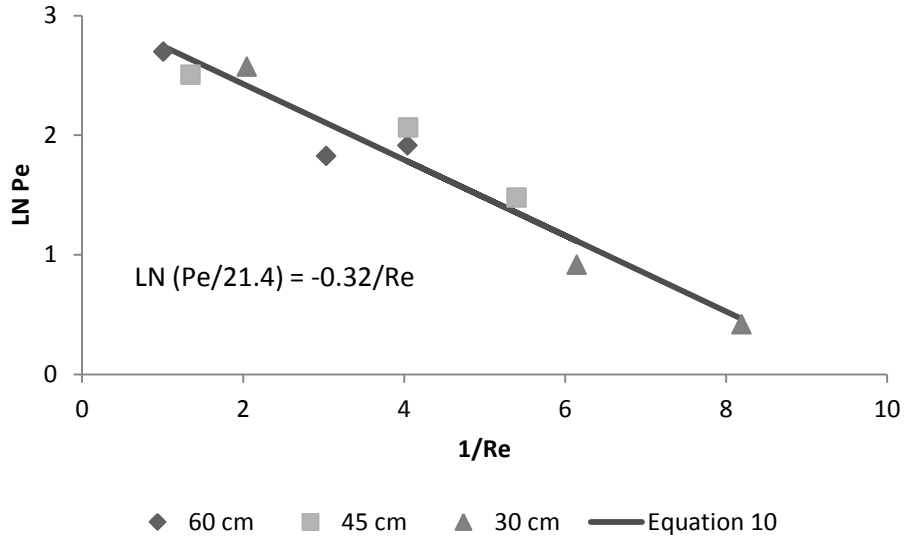
Figure 4.3. Estimated Pe values in relation to Re from each tracer test and Eq. 4.10 ($r^2 = 0.94$) and the model used to calculate Pe as a function of Re (Eq. 4.10).
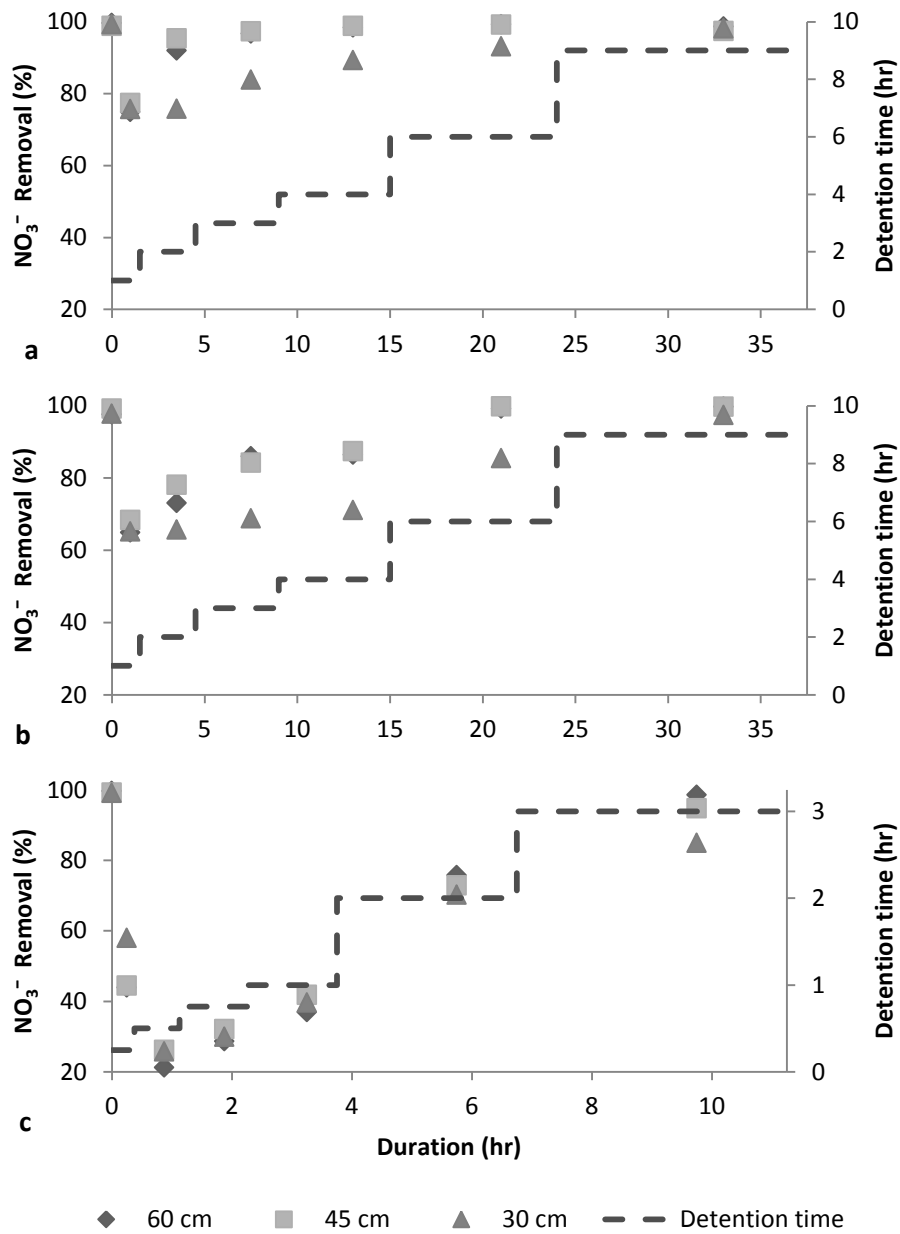
Figure 4.4. NO_3^- removal efficiency data from the 8 day ADC base case (SE #4; Fig. 4a), higher influent NO_3^- concentration (SE #6; Fig. 4b) and the higher flow rate (SE #7; Fig. 4c) storm events.
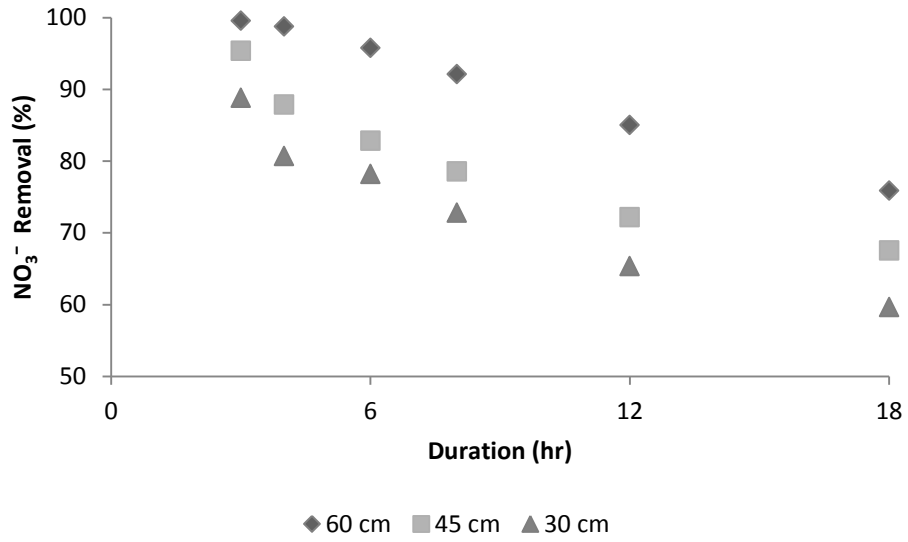
Figure 4.5. NO_3^- removal efficiency data from the constant two hour detention time storm event (SE #10).

<center>**Chapter 5:**</center>

<center>**A Nitrogen Loading Model for Bioretention Systems[3]**</center>

5.1 Introduction

Excess nutrient (nitrogen and phosphorus) loadings from urban areas promote eutrophication in nearby surface waters. This has contributed to the need for implementation of Numeric Nutrient Criteria (NNC) for rivers, lakes, and/or streams in 24 states within the United States, which will likely increase to 31 in 2016 (USEPA, 2014). Numeric Nutrient Criteria standards pose a significant challenge to stormwater system designers because selected treatment technologies will need to provide a quantifiable nutrient (e.g., nitrogen and phosphorus) reduction benefit instead of being selected based on assumed removal efficiencies or the most practical option available (Clark and Pitt, 2012). To quantify nutrient loadings, it is necessary to accurately model the hydrologic, hydraulic and transformation processes that occur in stormwater systems, such as bioretention systems.

A bioretention system is an emerging stormwater treatment technology that is capable of reducing peak flow rates and runoff volumes (Davis et al., 2009). Conventional bioretention systems include a ponding area, plants, an unsaturated layer, and can also include a storage layer and an under-drain pipe. These systems are known to have poor nitrate removal efficiencies (See

---

[3] Note: Portions of this chapter are being prepared for submission to the Journal of "Environmental Engineering – ASCE". The co-authors of the manuscript included Thomas Lynn, Mahmood Nachabe and Sarina Ergas. Research questions, experimental design, drafting, data interpretation and comments were provided by all authors.

review by Collins et al., 2010). To solve this problem, modified bioretention systems were introduced (Kim et al., 2003). A modified bioretention system includes a submerged internal water storage zone (IWSZ) that contains a carbon-based medium to promote denitrification.

A number of field, laboratory and modeling studies have evaluated nutrient removal and hydraulic performance in conventional and modified bioretention systems (See reviews by Collins et al., 2010; Ahiablame et al., 2012; and Hunt et al., 2012). However, a model is needed that allows designers to appropriately size bioretention systems to meet hydrologic and nutrient reduction goals (Roy-Poirier et al., 2010; Ahiablame et al., 2012). To meet this challenge, understanding how to model the fate and transport of nitrogen in bioretention systems is essential. Modeling nitrogen loadings in bioretention systems is difficult because: (1) complex hydraulic and water quality processes need to be modeled together to estimate nitrogen loadings; (2) several nitrogen species are found in stormwater runoff (Taylor et al., 2005); (3) appropriate data sets that include nitrogen speciation concentrations in stormwater runoff are only available for some species, such as Total Kjedahl Nitrogen (TKN) or nitrate + nitrite (Pitt et al., 2005); and (4) numerous nitrogen transformation processes occur in bioretention systems (Lucas and Greenway, 2011) and are not well understood (Davis et al., 2009).

Several stormwater modeling programs have been developed to aid the design of bioretention systems. Some models are broad in scope, where the properties of the catchment area largely govern system performance; however, these models assume that constant percent removal efficiencies dictate actual bioretention system performance (Ahiablame et al., 2012; Park et al., 2014; Wanielista et al., 2014). Other models employ mechanistic approaches to

model the hydrologic, hydraulic, physical, chemical and/or biological processes occurring in bioretention systems (Atchison et al., 2006; Dietz, 2007; Elliott and Trowsdale, 2007; Palgehyi, 2010; Ahiablame et al., 2012; Brown et al., 2013; Gao et al., 2013). In particular, the Stormwater Management Model (SWMM-5) is a continuous simulation model that provides designers the capability of modeling multiple interconnected and/or disconnected stormwater managment systems (bioretention, retention, pervious pavement, etc.) with one simulation (Elliott and Trowdale, 2007). This allows designers to quickly analyze all of the hydrologic, hydraulic, and water quality aspects of an entire stormwater management system, instead of analyzing a performance metric for a single bioretention system.

To develop a mechanistic nitrogen loading model, large data sets are needed to create process-driven equations that can be used with stormwater modeling programs. However, few studies have used actual data to verify the accuracy of a nitrogen loading model. Imteaz et al. (2013) compared total nitrogen (TN) removal efficiencies from experimental data with results from the Model for Urban Stormwater Improvement Conceptualisation (MUSIC). They found that the model overestimated TN removal efficiency, possibly due to TN leaching from the bioretention cell media. Deng et al. (2012) developed a variable residence time denitrification reaction model for predicting nitrate (NO_3^-) removal from stormwater; however, the model was only validated with data from studies where wastewater was the source water and from one data point where stormwater was the source water.

The model presented in this study represents a simplified approach in modeling the actual hydraulic/water quality processes that occur in bioretention systems. Hydraulic models such as

RECARGA (Atchinson, 2006) and water quality models such as RT3D (Clement, 1997) would provide a more detailed representation of the processes that occur in bioretention systems; however, the model described in this paper was developed to prioritize application over a detailed representation. Additional considerations that were used to develop the model included: (1) the ability to use the model in conjunction with stormwater modeling software programs that can output time interval flow data, such as SWMM-5; (2) the ability of stormwater software developers to incorporate the model into their programs; (3) enabling designers without backgrounds in both water resources and environmental engineering to understand and apply the model; (4) including a reasonable amount of hydraulic/water quality processes to characterize the dynamic nature of bioretention systems; and (5) reducing computational time.

The overall goal of this study was to develop a mechanistic model that can quantify nitrogen transport and transformation processes in bioretention systems. The specific objectives of this study were to: (1) develop a simplified approach to model saturated and unsaturated flows through modified bioretention systems using SWMM-5 software; (2) develop a nitrogen transformation model that can be used with SWMM-5; and (3) conduct a case study that evaluates annual nitrogen load reductions by implementing various bioretention system designs. This model was developed from prior experimental studies that were conducted in the laboratories at the University of South Florida, Tampa, Florida (see Chapters 3 and 4) and the University of Maryland, College Park, Maryland (Davis et al., 2006).

5.2 Methods

5.2.1 Model Development

The model was broken down into two components: hydraulic and water quality. The equations for the hydraulic component were inserted into SWMM-5 to obtain time interval flow rate data. The flow rate data was exported to Excel, which was used to simulate the water quality component. The water quality component included nitrogen transformation mechanisms for each bioretention cell layer (unsaturated, IWSZ, and under-drain). The parameters that were incorporated into the model are shown in Table 5.1. Note, that if the parameters listed in this section contain the subscript "i", then that parameter is subject to change with each time step.

5.2.1.1 Hydraulics. A generalized schematic of transport processes in a bioretention system is shown in Figure 5.1. During the initial phase of a storm event, rainfall infiltrates into the ground. Runoff is generated when the rainfall intensity exceeds the infiltration capacity of the soil. As runoff discharges into the bioretention system ponding area, transport through the bioretention cell occurs. Effluent either infiltrates into the ground or is discharged from the site through an under-drain pipe. During high rainfall storm events, runoff can increase the water surface elevation in the ponding area to the point where it is conveyed over a weir (or over the bank of the pond) and is discharged from the site. After a storm event, the water elevation gradually decreases as runoff continues to filter through the bioretention cell. When the water elevation is above the pond bottom area, flow is a function of the hydraulic gradient, where a decrease in the hydraulic gradient results in a linear decrease in flow. When the ponding area finally becomes empty, unsaturated drainage conditions begin to occur in the unsaturated layer.

79

During these conditions, flow is a function of moisture content, where a decrease in moisture content results in an exponential decrease in flow.

To simplify the hydraulic component of the model, the volume of the ponding area and drainable porosity ($\Theta_s - \Theta_r$) of the media layers were grouped together into a single storage unit. This strategy required the following assumptions: (1) the initial runoff that enters the storage unit will "drop" into and fill the sand media pore volume (Nachabe, 2006); (2) a single rating curve that utilizes programming controls in SWMM-5 can be created to estimate flow during saturated or unsaturated conditions; and (3) headloss in the gravel-containing IWSZ and under-drain layers is negligible.

5.2.1.1.1 Saturated Drainage. Darcy's Law was used to estimate flow under saturated conditions:

$$Q_i = AK_{sat}\frac{h_{1i} - h_{2i}}{L} \tag{5.1}$$

where, Q is the saturated flow rate (cm^3/s), A is the filtration cell cross-sectional area (cm^2), K_{sat} is the saturated hydraulic conductivity of the unsaturated layer (cm/s), h_1 is the head elevation at the filtration node (cm), h_2 is the head elevation at the filtration discharge node (cm), i is the time step node and L is the unsaturated layer depth (cm). A rating curve was generated to estimate saturated flow as a function of head ($h_{1i} - h_{2i}$).

5.2.1.1.2 Unsaturated Drainage. During unsaturated drainage conditions, flow rate is a function of moisture content:

$$Q_{Ui} = AK_{sat}K_{ri}(\Theta)[1] \tag{5.2a}$$

80

where, Q_U is the unsaturated flow rate (cm^3/s), $K_r(\Theta)$ is the unsaturated layer relative hydraulic conductivity (unitless) and [1] is the unit hydraulic gradient which is equal to 1 during unsaturated drainage conditions. $K_r(\Theta)$ was estimated from the classical unsaturated flow equations presented by Mualem (1976):

$$K_{ri}(\Theta) = [S_e]^\alpha \tag{5.2b}$$

and

$$S_e = \frac{\Theta_i - \Theta_r}{\Theta_s - \Theta_r} \tag{5.2c}$$

where, S_e is the effective saturation in the unsaturated layer (unitless), α is the unsaturated flow power function constant (unitless), Θ_i is the current moisture content, Θ_r is the residual moisture content and Θ_s is the saturated moisture content (all unitless). A mass balance was then used to relate Equation 5.2c with the modeled water elevation in the unsaturated layer.

A plot-series relationship between drainage flux (q_U, which is equal to $K_{sat}K_r(\Theta)$) and S_e for sand media was generated using the HYDRUS-1D Software Package. During these simulations, the unsaturated layer was assumed to be initially saturated. Ten day simulations were executed using varying unsaturated layer depths between 30 and 152 cm in increments of 15.24 cm. Values of α for each unsaturated layer depth were determined by minimizing the sum of squares residuals (SSR) between Equation 5.2a (Q_{Ui}/A) and the HYDRUS-1D output velocity data. Coefficient of determination (r^2) values that compared Equation 5.2a and the HYDRUS-1D output bottom drainage flux data were determined.

SWMM-5 can only model a single rating curve between the bioretention cell node and the discharge outlet node; however, Equations 5.1 and 5.2a need to be characterized as ratings

81

curves between these nodes. Therefore, program controls were utilized in SWMM-5 to allow the program to model a single rating curve based on saturated conditions, while accounting for the change in flow behavior that occurs during unsaturated flow conditions. A new unifying equation that incorporated both saturated and unsaturated flow conditions with the aid of program controls is:

$$Q_i = f A K_{sat} \frac{h_{1i} - h_{2i}}{L} \tag{5.3a}$$

where,

$$f = \frac{Q_U}{Q} \tag{5.3b}$$

f is the flow rate multiplier used to estimate unsaturated flow under saturated conditions. In Equation 5.3(a-b), f is equal to 1 when the water surface elevation is above the top elevation of the unsaturated layer; however, f is less than 1 and can change when the water surface elevation is below the top of the unsaturated layer.

To find f, the hydraulic gradient term in Equation 5.3a was assumed to be approximately equal to the water elevation ratio (water elevation divided by unsaturated layer depth) in the unsaturated layer. This allowed f to be estimated for a specific water elevation ratio value. Control rules were then constructed in SWMM-5 to adjust f for a given range of water elevation ratio values. For example, when the water elevation ratio equals 0.5, the f value used represented the value for the range of water elevation ratio values between 0.4 and 0.6.

5.2.1.2 Water Quality. A general schematic of the water quality component of a bioretention system is shown in Figure 5.2. To allow the model to calculate nitrogen loadings from the bioretention cell, the following information was required: (1) time interval flow data;

(2) event mean concentrations (EMC) of TN, dissolved oxygen (DO) and dissolved organic

carbon (DOC); and (3) physical dimensions and media parameters for the unsaturated, IWSZ,

and under-drain layers. The first step of the water quality component included the conversion of

influent TN concentrations to influent TKN concentrations (Equation 5.4a) and influent TN

concentrations to influent NO_3^--N concentrations (Equation 5.4b).

$$TKN_O = f_{TKN}TN_O \qquad (5.4a)$$

$$NO_3N_O = f_{NO3N}TN_O \qquad (5.4b)$$

where, TN_O is the influent total nitrogen concentration (mg/L), TKN_O is the influent TKN

concentration (mg/L), f_{TKN} is the influent TKN fraction of TN_O, NO_3N_O is the influent NO_3^--N

concentration (mg/L) and f_{NO3N} is the influent NO_3^--N fraction of TN_O. Appropriate f_{TKN} and

f_{NO3N} values were extrapolated from land use data provided by Pitt et al. (2005).

5.2.1.2.1 Unsaturated Layer. Data from Davis et al. (2006) were used to develop

equations that characterize nitrogen transformation in the unsaturated layer. Davis et al. (2006)

evaluated the TKN removal performance of two bioretention boxes of different depths (61 and

91 cm). Each box contained sandy loam soil, a mulch layer and *Creeping juniper* plants. Total

Kjeldahl Nitrogen removal performance was evaluated with varying hydraulic loading rates,

storm event durations, influent pH values and influent TKN concentrations.

The unsaturated layer was used as an overall representation of the nitrogen

transformation processes that occur from the sand media, mulch and plants. Due to the unknown

factors (and their rates) that control many of these processes, nitrogen transformation processes

were simplified and assumed to be caused by a pseudo-TKN-nitrification process. Nitrification

83

of TKN was characterized by a first-order plug flow reactor (PFR) equation as shown in Equation 5.5.

$$TKN_{Ii} = TKN_O exp^{-\left(\frac{k_n V_s}{3600 Q_i}\right)}$$ (5.5)

where, k_n is the nitrification rate constant (hr^{-1}), V_s is the pore volume of the unsaturated layer (cm^3) and TKN_I is the concentration of TKN that enters the IWSZ (mg/L). Mean TKN removal efficiency data (as a function of detention time) from Davis et al. (2006) was extrapolated to estimate k_n, by minimizing the SSR between Equation 5.5 and the data from Davis et al. (2006). The r^2 value between Equation 5.5 and the data was then determined.

Total Kjeldahl Nitrogen that was removed in Equation 5.5 was assumed to undergo complete nitrification as shown in Equation 5.6.

$$NO_3N_{Ii} = NO_3N_{Oi} + TKN_{Oi} - TKN_{Ii}$$ (5.6)

where, NO_3N_I is the concentration of NO_3^--N that enters the IWSZ (mg/L). Based on stoichiometry, DO was assumed to be removed during nitrification as shown in Equation 5.7.

$$O_{2Ii} = O_{2Oi} - f_{O2C}(TKN_{Oi} - TKN_{Ii})$$ (5.7)

where, f_{O2C} is the mass of DO consumed per mass of TKN removed during nitrification (mg/mg), O_{2O} is the influent DO concentration (mg/L), and O_{2I} is the concentration of DO that enters the IWSZ (mg/L). The influent bio-available dissolved organic carbon concentration ($bDOC_O$ (mg/L)) was assumed to be a constant fraction of the influent dissolved organic carbon concentration (DOC_O (mg/L)) as shown in Equation 5.8.

$$bDOC_{Ii} = bDOC_O = f_{bDOC} DOC_O$$ (5.8)

where, f_{bDOC} is the bDOC fraction of DOC_O and $bDOC_I$ is the concentration of bDOC that enters the IWSZ (mg/L). bDOC removal or production in the unsaturated layer was considered

negligible, as competing elements either remove (e.g. sand filter or plants) or produce (e.g. mulch or plants) bDOC in the unsaturated layer.

5.2.1.2.2 IWSZ Layer. Data from Chapters 3 and 4 were used to develop equations that characterize nitrogen transformation processes in the IWSZ layer. Chapters 3 and 4 evaluated the NO_3^- removal, TKN production and DOC production performance of IWSZ microcosms and three IWSZs columns of different depths (30, 45 and 60 cm). Each IWSZ contained a 2:1 (vol/vol) ratio of pea gravel and eucalyptus wood chips. The influent and effluent of each constituent was evaluated under varying detention times, durations, flow regimes, influent NO_3^- concentrations and antecedent dry conditions.

Based on the results provided in Chapters 3 and 4, NO_3^- removal, TKN leaching and hydrolysis were assumed to occur in the IWSZ. In addition, NO_3^- removal was assumed to be caused by denitrification because a carbon source was available and low effluent DO concentrations were consistently measured in the IWSZs. The IWSZ layer was modeled to allow hydrolysis, denitrification, TKN leaching and mixing to proceed in successive order for each time interval.

The denitrification rate constant including limitation (k_1 (hr^{-1})) (Equation 5.19a) from each time step was a function of DO inhibition and bDOC limitation:

$$k_{1i} = k \times O_{fi} \times bDOC_{fi} \tag{5.9a}$$

where,

$$O_{fi} = \frac{K_{O_2}}{K_{O_2} + O_{2Ii}} \tag{5.9b}$$

85

and

$$bDOC_{fi} = \frac{bDOC_{Ei-1} + bDOC_H \Delta t/3600}{bDOC_{Ei-1} + bDOC_H \Delta t/3600 + K_{bDOC}} \tag{5.9c}$$

where, $bDOC_f$ is the bDOC limitation factor, O_f is the oxygen inhibition factor, k is the

maximum denitrification rate constant (hr^{-1}), K_{O2} is the oxygen inhibition coefficient for

denitrification (mg/L), Δt is the time step (s), $bDOC_H$ is the hydrolysis rate (mg/L-hr), K_{bDOC} is

the bDOC half-maximum rate concentration for denitrification (mg/L) and $bDOC_{Ei-1}$ is the

bDOC concentration in the IWSZ from the previous time step (mg/L). The following

assumptions were used to develop Equations 5.9(a-c): (1) the maximum denitrification rate

followed first-order kinetics; (2) O_f was a function of the influent DO concentration (see Chapter

3); (3) $bDOC_f$ was a function of $bDOC_E$ from the previous time step and DOC_H; and (4)

hydrolyzed organic carbon passed through biofilm and the end-product that enters the IWSZ

pore water was biodegradable.

Equations 5.10(a-b) were used to quantify how dispersion affects denitrification in the

IWSZ. The Peclet Number (Pe) was calculated as (see Chapter 4):

$$Pe_i = 21.4e^{-\left(\frac{0.32}{Re_i + Re_d}\right)} \tag{5.10a}$$

where, Re_d is the Reynolds Number dead constant, Re is the Reynolds Number (which is equal to

$v_i\phi d/\nu$), v is the IWSZ pore velocity (cm/s), d is the average diameter of media in the IWSZ

(cm), ϕ is the porosity and ν is the kinematic viscosity (cm^2/s). The minimum allowable Pe

value determined from Equation 5.10a was set to 0.5 (see Chapter 4). The flow rate for each

time interval (Q_i) was obtained from the SWMM-5 modeling results and used to calculate v_i.

The remaining variables (d, A, ϕ, ν, Re_d) were assumed to be constant. The Pe for each time

86

interval was used to estimate the number of equivalent tanks-in-series (n) (presented by Crittenden et al., 2005) that are required to accurately model the IWSZ.

$$n_i = [2/Pe_i - 2(1/Pe_i)^2(1 - exp^{-Pe_i})]^{-1} \qquad (5.10b)$$

The denitrification process was assumed to occur at steady-state at each time interval. The tanks-in-series equation (presented by Crittenden et al. (2005)) was used to calculate the concentration of NO_3^--N that enters the IWSZ after denitrification has occurred (NO_3N_R (mg/L):

$$NO_3N_{Ri} = NO_3N_{Ii}[(1 + k_{1i}V/(3600Q_in_i))^{-n_i}] \qquad (5.11)$$

where, V is the IWSZ pore volume (cm^3). The sub-variable, NO_3N_R, is also the concentration of NO_3^--N that enters the IWSZ before mixing begins for each time step interval.

Based on experimental data that was obtained from Chapters 3 and 4, TKN production occurs in the IWSZ. This was assumed to be caused by TKN stripping in the IWSZ. In this model, TKN production was assumed to be linearly correlated with the IWSZ pore velocity, as shown below:

$$TKN_{Ri} = TKN_{Ii} + 0.08v_i/60 + 0.06 \qquad (5.12)$$

Equation 5.12 calculates the concentration of TKN that enters the IWSZ after TKN production in the IWSZ has occurred (TKN_R (mg/L)). Data from Chapters 3 and 4 were used to calculate the mean TKN concentration that was produced for a given v. Equation 5.12 was developed by minimizing the SSR between the data and a linear function that relates TKN production with v. Subsequently, the r^2 value between TKN production data and Equation 5.12 was calculated. The relationship between TKN production data and Equation 5.12 is shown in the results section of this study.

87

Mass balance equations for NO_3^--N (Equation 5.13a), TKN (Equation 5.13b) and bDOC (Equation 5.13c) were used to calculate effluent concentrations that were discharged from the IWSZ at each time interval.

$$NO_3N_{Ei} = \frac{NO_3N_{Ri}Q_i\Delta t + NO_3N_{Ei-1}V}{Q_i\Delta t + V} \tag{5.13a}$$

$$TKN_{Ei} = \frac{TKN_{Ri}Q_i\Delta t + TKN_{Ei-1}V}{Q_i\Delta t + V} \tag{5.13b}$$

$$bDOC_{Ei} = \frac{bDOC_{Ri}Q_i\Delta t + bDOC_H V\Delta t/3600 + bDOC_{Ei-1}V}{Q_i\Delta t + V} \tag{5.13c}$$

where, NO_3N_E is the concentration of NO_3^--N that enters the under-drain layer (mg/L), TKN_E is the concentration of TKN that enters the under-drain layer (mg/L) and $bDOC_E$ is concentration of bDOC that enters the under-drain layer (mg/L). Equations 5.13(a-c) calculate the effect of mixing after the reaction processes have been completed. Since nitrogen speciation reactions do not occur during this stage (an exception is discussed later), mass balance equations for completely mixed flow reactors (CMFR) without reaction were used in Equations 5.13(a-b); however, Equation 13c includes hydrolysis within a CMFR. Equations 5.13(a-c) were also used to calculate the NO_3^--N, TKN, and bDOC concentration in the IWSZ pore water for each time interval.

Experimental data from Chapters 3 and 4 were used to calibrate the denitrification portion (Equations 5.9-5.11 and 5.13) of the IWSZ model. Chapters 3 and 4 contain IWSZ grab sample measurements of flow rate and influent and effluent concentrations of NO_3^-, DOC, and DO. The unknown variables that were needed to calibrate the model were k and K_{bDOC}. The storm events that were used to either calibrate or validate the model are shown in Table 3.1 (see page 44). Storm Events #4, 5, 6 and 10 were used for calibration, while the remaining storm

88

events were used for validation. The SSR between storm event sampling data and model were used for comparison. The SSR from each of the storm events were summed together and minimized with the best fit k and K_{bDOC} values.

The evolutionary solving method from Excel was used to calibrate k and K_{bDOC}. The boundary constraints of 0.01 to 10 hr^{-1} were used for k and the boundary constraints of 0.01 to 100 mg/L were used for K_{bDOC}. The model was considered validated if the NO_3^- removal efficiency of the model: (1) was within 10% of the experimental data for each storm event; and (2) conservatively estimated NO_3^- removal efficiency when compared to experimental data.

5.2.1.2.3 Under-Drain Layer. The under-drain layer was the last layer included in the model before runoff discharges into the under-drain pipe. The effluent from the IWSZ layer is the influent for the under-drain layer. The under-drain layer was modeled as a CMFR without reaction.

5.2.1.2.4 Conditional Statements. Additional expressions were included in the model to account for the expected change in biological behavior during low flow or dormant conditions (more details provided in Section 5.4.2.1). Conditional statements were incorporated into the denitrification portion of the model with the assumptions that NO_3^- will be completely removed when the detention time of the IWSZ layer exceeds 24 hours and when the detention time of the under-drain layer exceeds 48 hours. In addition, the maximum allowable $bDOC_{Ei}$ concentration was assumed to equal 100 mg/L.

89

5.2.1.3 Model Output. The model output included effluent under-drain NO_3^--N (NO_3N_D) and TKN (TKN_D) concentrations for each time interval. These data were used to compute input and output nitrogen speciation loads during a continuous simulation. As an example, the discharged NO_3^--N input (Equation 5.14a) and output (Equation 5.14b) loads were calculated with the following equations:

$$NO_3N \ input \ load = \sum Q_O \Delta t NO_3 N_{Oi} \qquad (5.14a)$$

$$NO_3N \ output \ load = \sum Q_D \Delta t NO_3 N_{Di} \qquad (5.14b)$$

where, Q_O is the unsaturated layer flow rate (L/s) and Q_D is the under-drain layer flow rate (L/s). Input and output loads for TN were then computed by summing the input and output loads of NO_3^--N and TKN.

5.2.2 Case Study

A hypothetical case study was modeled based on a highly urbanized two-acre site located in Tampa, Florida. Three alternative bioretention system designs of varying IWSZ depths (30, 45 and 60 cm) were evaluated, and are shown in Figure 5.3. The 30 (Figure 5.3a), 45 (Figure 5.3b) and 60 (Figure 5.3c) cm IWSZ bioretention cells encompassed the entire, two-thirds and one-half of the ponding bottom area, respectively. However, the total IWSZ volume of each bioretention cell was equal. Additional features that were used to design these systems are shown in Table 5.2.

The systems were designed to comply with general stormwater permitting requirements for the State of Florida and included: detain and filter the first one inch of runoff from the contributing area; and discharge the post-development 25-yr, 24-hr maximum discharge rate at a

90

rate less than the pre-development 25-yr, 24-hr maximum discharge rate. The systems were modeled using SWMM-5. To comply with the general permitting requirements, the curve number method was selected for site infiltration and the dynamic wave method was used for routing.

The TN and nitrogen speciation removal performance of the three bioretention system designs were evaluated in a year-long continuous simulation with 15-minute precipitation data from the Hillsborough River (Station 02304500) during 2012 (USGS, 2014). During this simulation, the Green-Ampt (site hydraulic conductivity = 0.5 in/hr or 1.3 cm/hr) method was selected for infiltration and the dynamic wave method was selected for routing. For practical purposes, the influent (rainfall that falls onto the surface of the site) TN EMCs were used. The pre-development TN EMC was assumed to be 1.8 mg/L (mixed open space) and the pos-development TN EMC was assumed to be 2.0 mg/L (mixed residential) (Pitt et al., 2005). Relatively high pre-development TN EMCs were used since the hypothetical site is located within an urbanized environment. A TKN/NO_3^--N ratio of 2.33 was extrapolated from Pitt et al. (2005).

A nitrogen speciation loading analysis was conducted for the bioretention cells and the sites. The bioretention cell loading analysis evaluated nitrogen speciation removal performance only from cell processes. The site loading analysis evaluated the overall nitrogen speciation removal performance from cell processes, site infiltration and weir overflow. TN removal efficiencies of 100% were assumed for stormwater that infiltrated into the ground. TN removal efficiencies of 0% were assumed for stormwater that was conveyed over the weir in the

91

bioretention system. However, the nitrogen removal efficiency of runoff that discharged from the bioretention cell was assumed to vary according to the nitrogen loading model.

5.3 Results

5.3.1 Model Development

5.3.1.1 Hydraulics. The plot-series relationship that compares q_U with duration and S_e for a 30 cm sand column depth with the use of HYDRUS is shown in Figure 5.4. Within one hour, q_u rapidly decreased from 25.8 to 1.2 cm/hr (Figure 5.4a) and the moisture content decreased from 1.00 to 0.61 (data not shown). In addition, q_U was observed to exponentially decrease with a decrease in S_e, as shown in Figure 5.4b. The S_e of the 30 cm sand column was greater than 0.4 throughout the entire 10-day simulation. Determined α values decreased with an increase unsaturated layer depth (Table 5.3). Over the course of every simulation, S_e was always greater than 0.25; however, final S_e values decreased with an increase in the sand column depth (data not shown). A high r^2 (> 0.996) between q_U and the HYDRUS-1D output data for all unsaturated layer depths was calculated.

The estimated f values for specific water elevation ratios within the unsaturated layer are shown in Table 5.4. A decrease in the water elevation ratio decreased the value of f. The list of f values that were used in the SWMM-5 Control Rules for a given range of water elevation ratios within the unsaturated layer are also shown in Table 5.4.

5.3.1.2 Water Quality. The relationship between TKN removal efficiencies that were determined from the model (Equation 5.5) and from Davis et al. (2006) is shown in Figure 5.5.

92

TKN removal efficiency generally increased with increasing detention time in both the model and data; however, only a modest correlation ($r^2 = 0.63$) was observed between Equation 5.5 (that was used to calculate % TKN removal) and data reported in Davis et al. (2006).

The relationship between TKN production and IWSZ pore velocity is shown in Figure 5.6. TKN production generally increased with an increase in IWSZ pore velocity; however, there was a variability of TKN production for each pore velocity. The relationship between mean TKN production and Equation 5.13 (used to calculate TKN production) was modestly correlated ($r^2 = 0.67$).

A comparison of the denitrification portion of the IWSZ model with the experimental NO_3^--N data reported in Chapter 4 is shown in Figure 5.7. In the model, close to 100% NO_3^- removal efficiency was observed from the first sample taken, as shown in Figures 5.7(a-c). After the initial pore water was discharged, NO_3^- removal efficiency decreased. Subsequently, NO_3^- removal efficiency increased as the detention time increased. The model output data from SE #10 indicates that NO_3^- removal efficiency decreases over the duration of a constant detention time storm event, as shown in Figure 5.7d. The experimental data followed similar NO_3^- removal efficiency patterns when compared to the model, as shown in Figures 5.7(a-d).

A summary of the IWSZ NO_3^- removal efficiency modeling results and experimental results reported in Chapter 4 are shown in Table 5.5. Overall, NO_3^- removal efficiencies of 80% were calculated from the model and NO_3^- removal efficiencies of 83% were calculated from the experimental data. For all storm events and IWSZ columns, the model predicted NO_3^- removal

93

efficiencies that were within 10% of the experimental results. In addition, when compared to the experimental results the model conservatively predicted NO_3^- removal efficiencies for every storm event and IWSZ column with the exception of SE #8.

5.3.2 Case Study

SWMM-5 output volume results are shown in Table 5.6. All of the sites with bioretention systems (30, 45 and 60 cm IWSZ cells) received the same volume of rainfall. As expected, a greater volume of rainfall infiltrated during pre-development when compared to developed conditions. The 30 cm IWSZ cell filtered the greatest amount of stormwater and the 60 cm IWSZ cell filtered the least amount of stormwater.

The annual output loading results for NO_3^--N, TKN and TN are shown in Figure 5.8(a-c). The 30 cm IWSZ cell received slightly higher NO_3^--N loadings compared to the other cells, as shown in Figure 5.8a. Input IWSZ NO_3^--N loads for the 30 cm IWSZ cell (10.7 kg/yr), the 45 cm IWSZ cell (9.6 kg/yr) and the 60 cm IWSZ cell (8.8 kg/yr) were observed to decrease with an increase in IWSZ cell depth. The 60 cm IWSZ cell removed NO_3^- most efficiently (88%) and removed the greatest mass of NO_3^--N (4.3 kg/year) compared to the other cells. In contrast, IWSZ TKN input loadings were the highest for the 30 cm IWSZ cell, as shown in Figure 5.8b. In addition, the 30 cm IWSZ cell removed TKN most efficiently (46%) and removed the greatest mass of TKN (5.2 kg/year) compared to the other cells. A TKN load increase between the IWSZ cell input and IWSZ cell output for the 30 cm IWSZ cell (0.62 kg/yr), the 45 cm IWSZ cell (0.64 kg/yr) and the 60 cm IWSZ cell (0.66 kg/yr) were observed to increase with an increase in IWSZ cell depth. Site TN removal efficiencies for the bioreention systems were observed to increase

94

with a decrease in IWSZ cell depth, as shown in Figure 8c. Similarly, cell TN removal

efficiencies increased with a decrease in IWSZ cell depth. The 30 cm IWSZ bioretention system

(7.1 kg/year) was the only system that discharged lower TN loadings compared to pre-

development conditions (8.2 kg/yr).

5.4 Discussion

5.4.1 Hydraulics

Data from the HYDRUS-1D drainage simulations can be used to understand how

unsaturated flow rates exponentially decrease with an increase in drainage duration (Figure 5.4a)

or a decrease in saturation (Figure 5.4b). These phenomena are caused by capillary retention in

the unsaturated layer, which creates a negative suction head relative to the direction of the flow.

Since S_e was always greater than zero during all of the 10-day simulations, water retained by

capillary suction will likely reduce the available storage capacity of the unsaturated layer for the

next storm event. Lucas (2010) created a hydrologic model for bioretention systems in SWMM-

5 but did not include unsaturated flow processes in the unsaturated layer. However, computed

flow rates in continuous drainage simulations are a function of available storage capacity. Data

from the drainage simulations indicates that the available storage capacity of the unsaturated

layer may be overestimated if unsaturated flow processes are not included in continuous

simulation drainage models for bioretention systems.

The determined values for α (Table 5.3) are useful in understanding how unsaturated

layer depths affect unsaturated flow rates in the unsaturated layer. When the depth of the

unsaturated layer increases, α decreases. This indicates that capillary suction plays a decreased

role in reducing flow rates for deeper unsaturated layers. Therefore, if two unsaturated layer designs are equal in volume, the deeper sand layer will have a higher available storage capacity for the next storm event compared to a shallower unsaturated layer. Different conclusions could be made if evaporation and plant uptake were also considered; however, the exclusion of these processes would result in a conservative bioretention system design.

The determined values for f (Table 5.4) are useful in understanding the relationship between saturated and unsaturated flow regimes. If the saturated flow equation (Equation 5.1a) was utilized when the modeled water elevation is below the top of the sand layer, then an overestimate of the output flow rate would occur. The determined f values are also useful for designers in using program controls to model saturated and unsaturated flows through the unsaturated layer with one rating curve. SWMM-5 utilizes an alternative approach to compute saturated/unsaturated flows in bioretention systems; however, the program cannot quantify how varying unsaturated layer depths affect flow rates (MSDGC, 2013). The f values that were incorporated into SWMM-5 program controls (Table 5.5) are an approximation of the expected flow rate for a given value of S_e. This is because program controls can only be constructed for a given range of elevations (that are used to calculate S_e) instead of using an actual formula. RECARGA would be more accurate in modeling unsaturated flows in bioretention systems; however, RECARGA models the bioretention ponding area as a vertical box (Atchison et al., 2006), which may not be permissible in regions more prone to flooding, such as Florida.

96

5.4.2 Water Quality

5.4.2.1 Overview. SWMM-5 uses a unique method in calculating water quality treatment processes (Rossman, 2010). The program uses influent concentrations to calculate the concentration of a constituent after a reaction has occurred. This reaction equation is calculated before any reacted water enters into the receiving node. Once the reacted water enters the node, the program allows the node concentration to mix with the reacted concentration that enters the node. The model presented in this study uses the same methodology. The one exception is how bDOC concentrations are modeled, where the bDOC concentration from the previous time step is used in the treatment expression (this will be discussed later). This exception is fairly simple to configure in the SWMM-5 treatment module since the program already calculates constituent concentrations for each node.

In reality, reaction and mixing processes occur simultaneously in bioretention cells. This poses a challenge in modeling nitrogen removal processes with the methodology utilized by SWMM-5 during low flow and/or dormant conditions. For example, when the volume of runoff from a storm event is less than the IWSZ pore volume, runoff will enter and stay in the IWSZ until the next storm event. This provides enough contact time for denitrifying bacteria to remove most or all of the NO_3^- that was contained in the runoff. Moreover, sloughed denitrifying bacteria, excess bDOC and low DO concentrations from the IWSZ will be transported to the under-drain layer through diffusive and/or low flow advective processes and create an environment that is suitable to promote denitrification. After NO_3^- is removed in the IWSZ, SO_4^{2-} reduction is observed (see Chapter 3), which may be due to biological sulfate reduction. After SO_4^{2-} is removed, an anaerobic environment can develop in the IWSZ that promotes the growth

97

of methanogenic bacteria (Rittman and McCarty, 2003). Methanogenic bacteria growth may continue until the bDOC consumption rate equals $bDOC_H$. This would prevent bDOC concentrations in the IWSZ to continually increase over long dormant periods (one month or longer).

Based on the example provided above, the conditional statements that were incorporated into the model were considered appropriate due to the following circumstances: (1) NO_3^- was completely removed in IWSZ microcosms within six hours (see Chapter 3); (2) when the IWSZ detention time exceeds 24 hours, influent entering the IWSZ will likely remain in the IWSZ until the next storm event occurs; (3) low DO and high DOC concentrations were consistently measured in samples that were detained in the IWSZ prior to each storm event (see Chapter 4); (4) initial DOC concentrations that exited the IWSZ from the 30 day ADC storm event was less than the 16 day ADC storm event (see Chapter 4); and (5) initial DOC concentrations that exited from the 30 day ADC storm event were less than 100 mg/L (see Chapter 4).

5.4.2.2 Processes in Each Layer.

5.4.2.2.1 Unsaturated Layer. Nitrogen transformation processes that are known to occur in the unsaturated layer include: immobilization, plant uptake, nitrification (Lucas and Greenway, 2011) and hydrolysis of organic nitrogen. However, the major factors (and their rates) that control TKN transformation processes in the unsaturated layer are unknown. Until these factors are better understood, a simplified approach to modeling nitrogen transformation mechanisms in the unsaturated layer is justifiable. The model presented in this study used a 'lumped' approach with the assumption that detention time was the only factor that controls

TKN transformations. Consequently, only a modest correlation between Equation 6 and the experimental data from Davis et al. (2006) was observed when TKN removal efficiency was calculated as a function of detention time. More research on this topic is warranted.

The pseudo-TKN-nitrification model may conservatively estimate TKN removal efficiencies if mulch and/or high organic content media are excluded from unsaturated layer designs. Barrett el al. (2013) evaluated the TKN removal performance of 12 different media types and/or cell configurations that presumably contained little organic matter (<0.5%) in the unsaturated layer. The authors observed TKN removal efficiencies that were between 65 and 94% for all media types and/or cell configurations. However, the model presented in this study used data from Davis et al. (2006) that included an organic mulch layer in the unsaturated layer, where mean TKN removal efficiencies were observed to be between 12 and 83%.

5.4.2.2.2 IWSZ Layer. Total Kjeldahl Nitrogen production in the IWSZ most likely occurs from the leaching of organic media (Clark and Pitt, 2009); however, the controlling factors are relatively unknown. This study assumed that the stripping of biofilm/organic media was the main factor that controlled TKN production in the IWSZ and that stripping was a function of pore velocity. Therefore, data from Figure 5.6 was used to develop Equation 5.12. Even though TKN production and pore velocity were moderately correlated, there was high variability in the data. This is likely due to factors other than pore velocity that influence TKN production, and additional research on this topic is warranted. In addition, readers should be cautioned that data from Figure 5.6 was obtained from a permanently saturated IWSZ. If the IWSZ is not permanently saturated, higher TKN leaching rates may occur (see Chapter 3).

Data from Figure 5.7 indicates that the denitrification portion of the IWSZ model is similar to the expected behavior of NO_3^- removal in the IWSZ. The effects of mixing (first two samples taken) and detention time (remaining samples taken) on NO_3^- removal efficiency are clearly evident in Figures 5.7(a-c). In addition, the decrease in bDOC concentrations resulted in decreased NO_3^- removal efficiencies after multiple IWSZ pore flushes in both the model and the experimental data (Figure 5.7d). The modeling results in Table 5.5 indicate that steady state equations can be used for each time interval to model the dynamics of NO_3^- removal in the IWSZ. For greater accuracy, models that include additional processes and use transient equations may be more appropriate than the denitrification model presented in this study. Deng et al. (2012) developed a denitrification model that includes dispersion, mass transfer of NO_3^- into the biofilm, microbial growth, oxygen inhibition, DOC substrate limitation and temperature; however, multiple rate constants from wastewater literature were assumed rather than calibrating the model with data from stormwater systems. The denitrification model presented in this study used multiple rate constants that were calibrated from our prior research, which was carried out under controlled conditions with stormwater spiked to give NO_3^- concentrations typical of urban runoff (see Chapters 3 and 4).

5.4.3 Reactor Modeling. A variety of reactors were utilized to characterize the hydraulic performance of each layer in the bioretention cell. Pseudo-TKN-nitrification in the unsaturated layer was modeled as a PFR because the hydraulic efficiency was expected to be greater than the saturated layers (Nachabe, 1999). Denitrification in the IWSZ was modeled as a non-ideal reactor since there is available data to support the mixing conditions in IWSZs (See Chapter 4). TKN production in the IWSZ was modeled as an empirical reactor because the actual processes

that control this phenomenon are not well understood. Similarly, hydrolysis in the IWSZ was modeled as a CMFR because the process kinetics were assumed to be constant and there is limited data to quantify the actual processes that control hydrolysis. The under-drain layer was modeled as a CMFR because reactions in this layer only occur on a conditional basis and SWMM-5 is already configured to model storage units as a CMFR. Non-ideal reactors may be more accurate to approximate the actual hydraulic performance of each layer and/or process; however, simple reactor types were chosen to support the modeling capabilities of SWMM-5.

5.4.4 Case Study

The hypothetical bioretention systems were designed with an impermeable liner that encompassed all layers in the cell, and the systems were located on a site with poorly-drained soils in an open drainage basin with a high water table. The hydrological processes that were incorporated into the SWMM-5 model setup included: site infiltration, under-drain flow from the bioretention cell and weir flow from the ponding area. The bioretention design and hydrological processes included in this case study do not necessarily represent all bioretention designs and processes that should be used for all regions and environmental conditions. The case study only represents the minimum number of processes that are expected to occur in bioretention systems with an IWSZ. At the designers' discretion, additional processes can be incorporated into the SWMM-5 model to better represent the site characteristics for each unique site and/or bioretention system design. Additional processes that could be incorporated may include: on-site depressional storage, evaporation, infiltration from the ponding area, and percolation from the bioretention cell layers.

101

The SWMM-5 output volume results show how the volume of stormwater treated is controlled by the dimensions of the bioretention cell. However, the case study results revealed that only a 2% increase of untreated runoff volume occurs when the bioretention cell footprint area was reduced by 50%. This aspect is important for designers who need to comply with volume-based treatment and attenuation requirements. Based on these results, the designer would likely select the 60 cm IWSZ cell from a materials and cost perspective, since only a small increase in untreated runoff will occur compared to the other cells that have a larger cell area. However, if the bioretention cell area is too small, a larger increase in untreated runoff volume will occur. In this case, a larger bioretention cell area may be necessary to comply with treatment and attenuation regulations.

The annual output loading results (Figures 5.8(a-c)) are useful in understanding how nitrogen transformation processes affected nitrogen loadings. Nitrification occurs as runoff passes through the unsaturated layer and discharges into the IWSZ. This causes a reduction in TKN loadings (Figure 5.8b) and an increase of NO_3^- (Figure 5.8a) loadings into the IWSZ. The 30 cm IWSZ cell discharged the greatest NO_3^- loadings and the least TKN loadings into the IWSZ. This was likely due to the larger sand layer volume that was used in the 30 cm IWSZ cell design. When runoff passes through the IWSZ and discharges from the cell, denitrification and TKN production occurs. At this location, denitrification reduced NO_3^- loadings (Figure 5.8a) and TKN production increased TKN loadings (Figure 5.8b). The greatest NO_3^- loadings were removed in the 60 cm IWSZ, possibly due to lower dispersion in this cell when compared to the 30 and 45 cm IWSZ cells (see Chapter 4). Even though the 60 cm IWSZ cell removed higher NO_3^- loadings, the 30 cm IWSZ cell removed the highest TN loadings for the site and the cell

102

(Figure 5.8c). This may have occurred because: (1) more TKN loadings were removed in the 30 cm IWSZ cell (Figure 5.8b) when compared to NO_3^--N loadings that were removed in the 60 cm IWSZ cell (Figure 5.8a); and (2) the 30 cm IWSZ cell treated a greater volume of runoff than the 60 cm IWSZ cell (Table 5.6). Since the 30 cm IWSZ bioretention system discharged less TN than the pre-development conditions, the hypothetical development could use this system to meet nitrogen loading permitting requirements.

5.5 Conclusions

Increased nutrient control standards for stormwater runoff are being implemented throughout the United States. However, comprehensive models that estimate nutrient loadings from stormwater treatment systems are unavailable. In this study, a quantitative nitrogen loading model was developed for modified bioretention systems. Experimental and programming simulation data were used to develop and calibrate process-driven equations that characterize the hydraulic and water quality components of the model. The processes incorporated into the model include: unsaturated flow, saturated flow, pseudo-nitrification, denitrification and TKN leaching. A new unifying equation was developed to approximate saturated and unsaturated flows in SWMM-5. An in-depth analysis revealed that unsaturated flow processes reduce the available storage capacity of the unsaturated layer and that unsaturated flow processes should be included in multiple storm event simulation studies. Denitrification in the IWSZ was validated with experimental data. Other modeling results revealed that TKN removal in the unsaturated layer is positively correlated with detention time and TKN production in the IWSZ is positively correlated with pore velocity; however, additional research that identifies the factors (and rates) that control these processes are recommended. A hypothetical case study was modeled in

103

SWMM-5 to assess the nitrogen removal performance of various bioretention designs that have equal IWSZ volumes. The results indicate that bioretention systems with taller IWSZs remove greater NO_3^- loadings; however, systems with shorter IWSZs remove greater TKN and TN loadings. The model presented in this study provides a tool for designers to quantify nitrogen loadings as a function of the bioretention system design.

Table 5.1. Terminology and parameters used to develop the nitrogen loading model.

Symbol	Name	Value	Units	Reference
$bDOC_H$	hydrolysis rate	0.28	mg/L-hr	Chapter 3
f_{bDOC}	bDOC fraction of DOC_O	0.1	mg/mg	Assumed
f_{TKN}	Influent TKN fraction of TN_O	0.7	mg/mg	Collins et al. (2010)
f_{O2C}	mass of DO consumed per mass of TKN removed during nitrification	3.96	mg/mg	Rittman and McCarty (2005)
f_{NO3N}	Influent NO_3^--N fraction of TN_O	0.7	mg/mg	Collins et al. (2010)
i	Time step node	-	-	
k	Denitrification rate constant	4.46	hr^{-1}	This study
k_n	Nitrification rate constant	0.19	hr^{-1}	This study
K_{bDOC}	bDOC half-maximum rate concentration for denitrification	0.61	mg/L	This study
K_{O2}	Oxygen inhibition coefficient for denitrification	2.18	mg/L	Chapter 3
Re_d	Re dead constant	10^{-6}	-	Chapter 4
Δt	Time step	180	s	This study
Θ_r	Residual moisture content for sand	0.045	-	Loheide et al. (2005)
Θ_s	Saturated moisture content for sand	0.43	-	Loheide et al. (2005)
ϕ	IWSZ porosity	0.42	-	Chapter 3
ν	Kinematic viscosity	1.004×10^{-2}	cm^2/s	Crittenden et al. (2005)

104

Table 5.2. Main parameters used to design the three bioretention systems.

Parameter	U.S. Units	SI Units
$CN_{pervious}$	80	80
25 yr, 24 hr rainfall depth	8.0 in	20.3 cm
Bottom of pond area	9216 ft^2	856 m^2
Top of pond area	12800 ft^2	1189 m^2
Pond depth	2 ft	61 cm
Freeboard	0.5 ft	15 cm
Weir invert height relative to pond bottom	0.75 ft	22.9 cm
Actual impervious area	70%	70%
Equivalent impervious area	75%	75%

Table 5.3. Determined values of α from Equation 3 for a specific unsaturated layer depth.

Unsaturated layer depth (cm)	α	Mean square residual	r^2
30	5.5	0.18	0.999
46	4.6	0.26	0.999
61	4.2	0.24	0.999
76	4.3	0.19	0.999
91	3.9	0.39	0.998
107	3.8	0.40	0.997
122	3.7	0.42	0.997
137	3.7	0.41	0.997
152	3.7	0.42	0.997

Table 5.4. Estimated f values for specific water elevation ratio values within the unsaturated layer and the range of water elevation ratio values within the sand layer used in the SWMM-5 Control Rules for a given f value.

Water elevation ratio values	f	Water elevation ratio values used for a given f value
0.1	0.00003	0 – 0.2
0.2	0.0007	-
0.3	0.004	0.2 – 0.4
0.4	0.016	-
0.5	0.04	0.4 – 0.6
0.6	0.10	-
0.7	0.20	0.6 – 0.8
0.8	0.37	-
0.9	0.62	0.8 – 1.0
1.0 or greater	1.00	1.0 or greater

Table 5.5. NO_3^- removal efficiency experimental and modeling results for the eleven storm events analyzed. Storm event #11 was not included in the overall results calculations. Sum of squares residuals (SSR) were calculated in NO_3^--N mg/L.

Storm event	Influent as NO_3^--N (mg/L)	Experimental			Model			Difference		
		60 cm	45 cm	30 cm	60 cm	45 cm	30 cm	Mean	Standard deviation	SSR
1	1.96	83	86	82	82	81	78	3.2	2.55	0.99
2	1.98	97	97	89	90	88	86	6.7	3.15	0.61
3	2.00	97	96	90	87	86	83	8.7	1.74	0.69
4	1.92	96	97	89	89	88	85	6.6	2.54	0.41
5	1.87	87	86	80	86	84	81	0.7	1.84	0.79
6	3.64	88	89	78	87	85	82	0.2	4.03	1.19
7	2.22	61	62	60	61	61	60	0.5	0.52	1.19
8	1.94	59	58	59	63	63	62	-4.3	0.93	0.71
9	2.04	97	97	88	88	86	84	7.9	3.36	0.72
10	1.91	90	80	73	77	77	74	4.7	7.18	0.47
11	2.02	86	84	73	-	-	-	-	-	-
Overall	2.15	85	85	79	81	80	78	3.2	2.02	-
Total overall	2.15	83			80			3.2	4.68	7.76

Table 5.6. Computed SWMM-5 output volumes (kL) from pre-development conditions and from the bioretention systems with IWSZ depths of 30, 45 and 60 cm.

System	Rainfall	Infiltration	Weir[a]	Bioretention cell
Pre-development	9,250	4,706	4,544	-
30 cm IWSZ	9,250	1,015	57	8,172
45 cm IWSZ	9,250	1,015	140	8,100
60 cm IWSZ	9,250	1,015	223	8,017

[a] Values represent surface runoff from the site or overflow
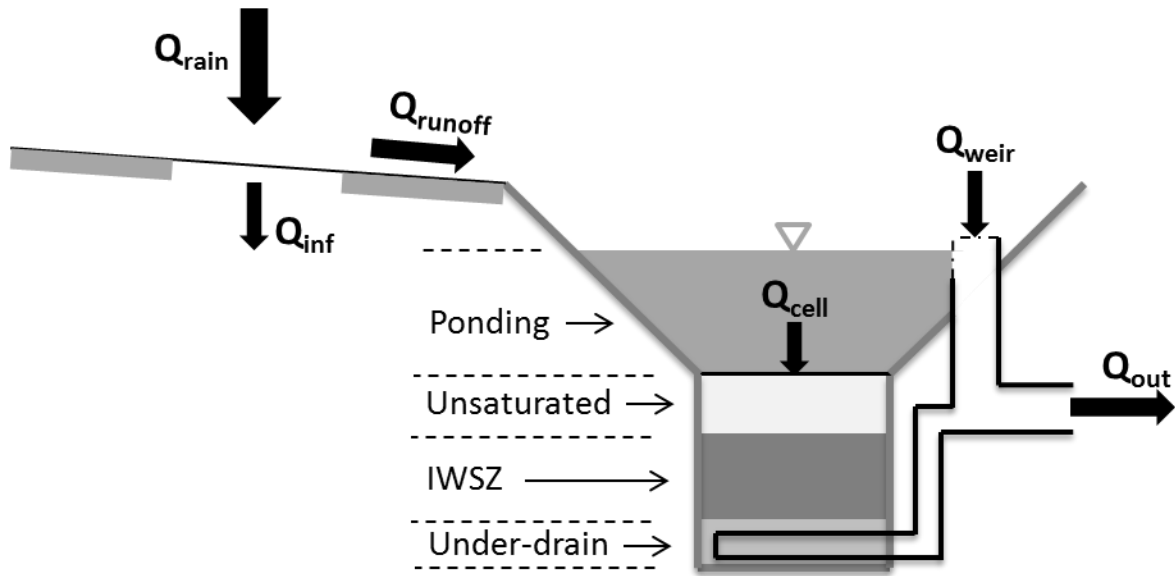
Figure 5.1. General schematic showing how rainfall is transported from a site that includes a modified bioretention system.
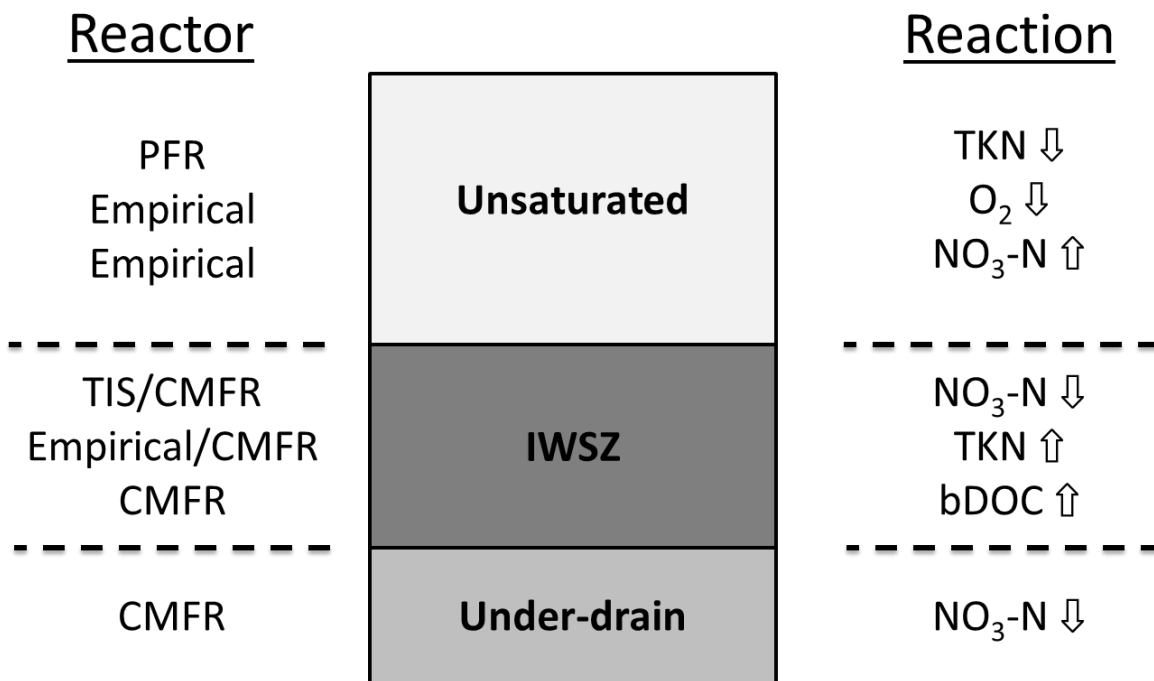
Figure 5.2. A general schematic of the transformations that were included in the water quality component.
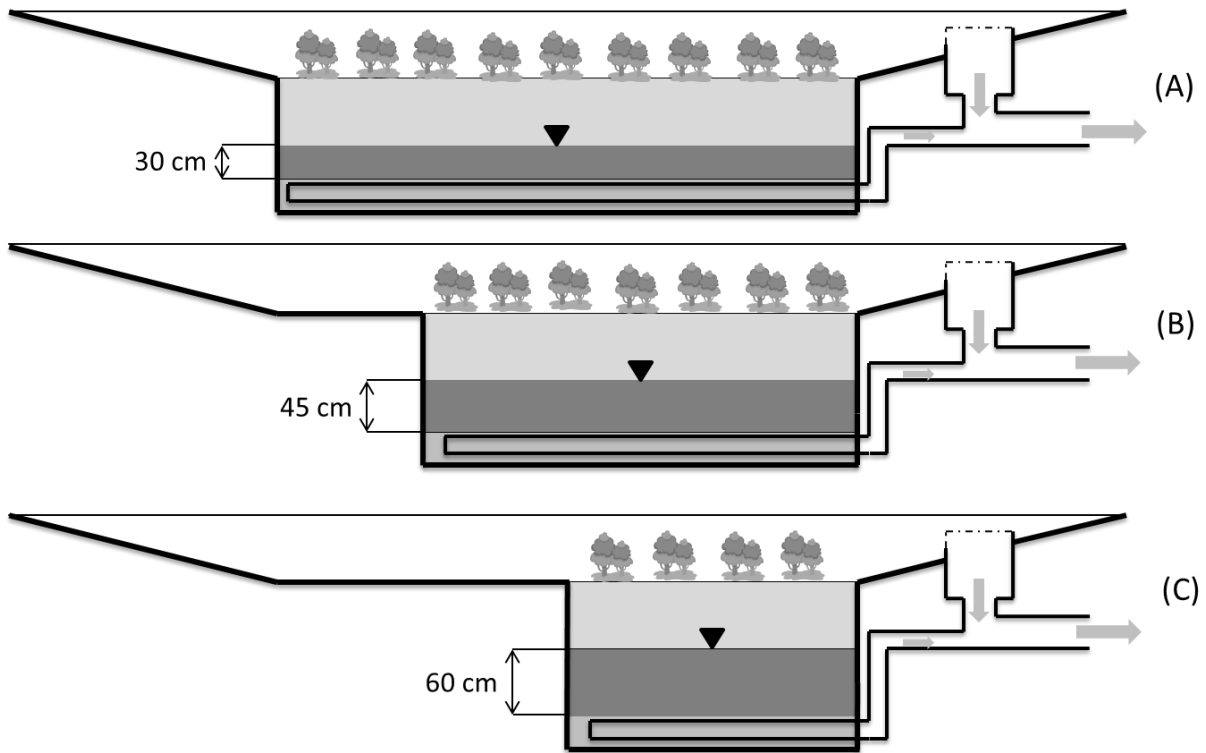
Figure 5.3. Bioretention systems analyzed in the case study. All systems were designed to have equivalent IWSZ volumes, unsaturated layer depths, under-drain layer depths, pond dimensions and weir dimensions.
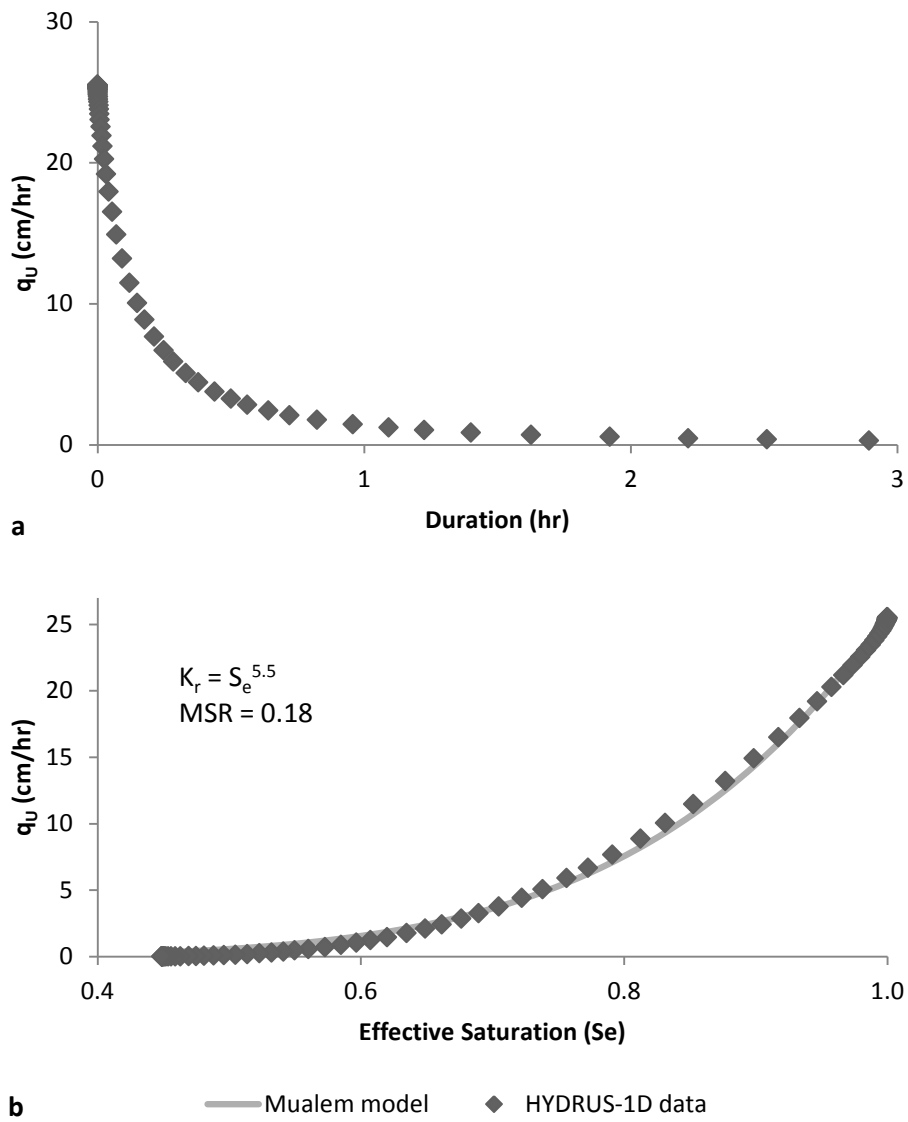
Figure 5.4. Plot-series relationship comparing q_U with duration (a) and S_e (b) for an initially saturated sand column with a depth of 30 cm.
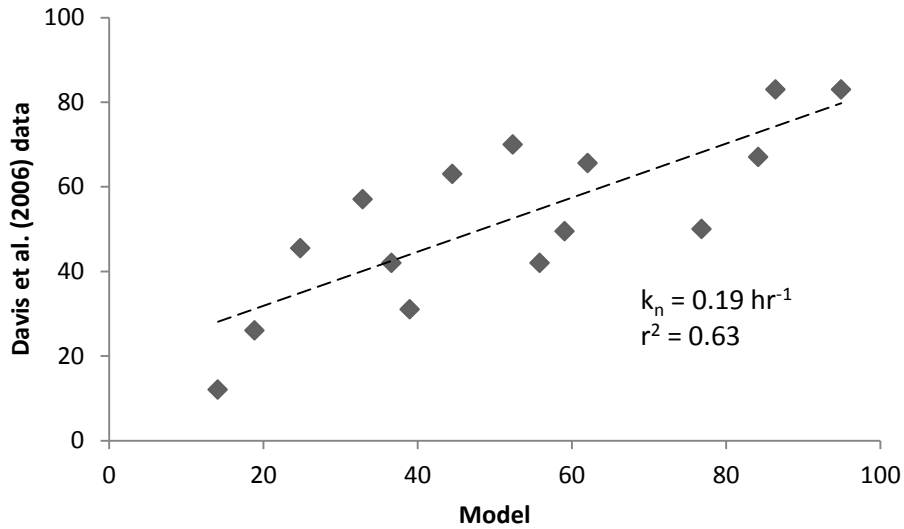
Figure 5.5. The relationship between TKN removal efficiency data from Equation 6 and mean TKN removal efficiency data from Davis et al. (2006). Dotted line represents the trend line.
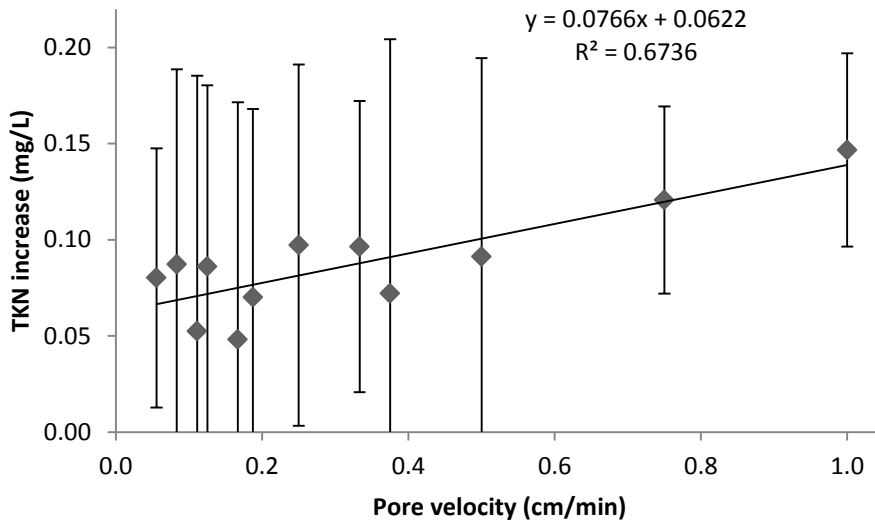
Figure 5.6. IWSZ experimental data taken during the study from Chapters 3 and 4. The dotted line represents the linear relationship between TKN increase and pore velocity. Error bars represent the standard deviation.

110
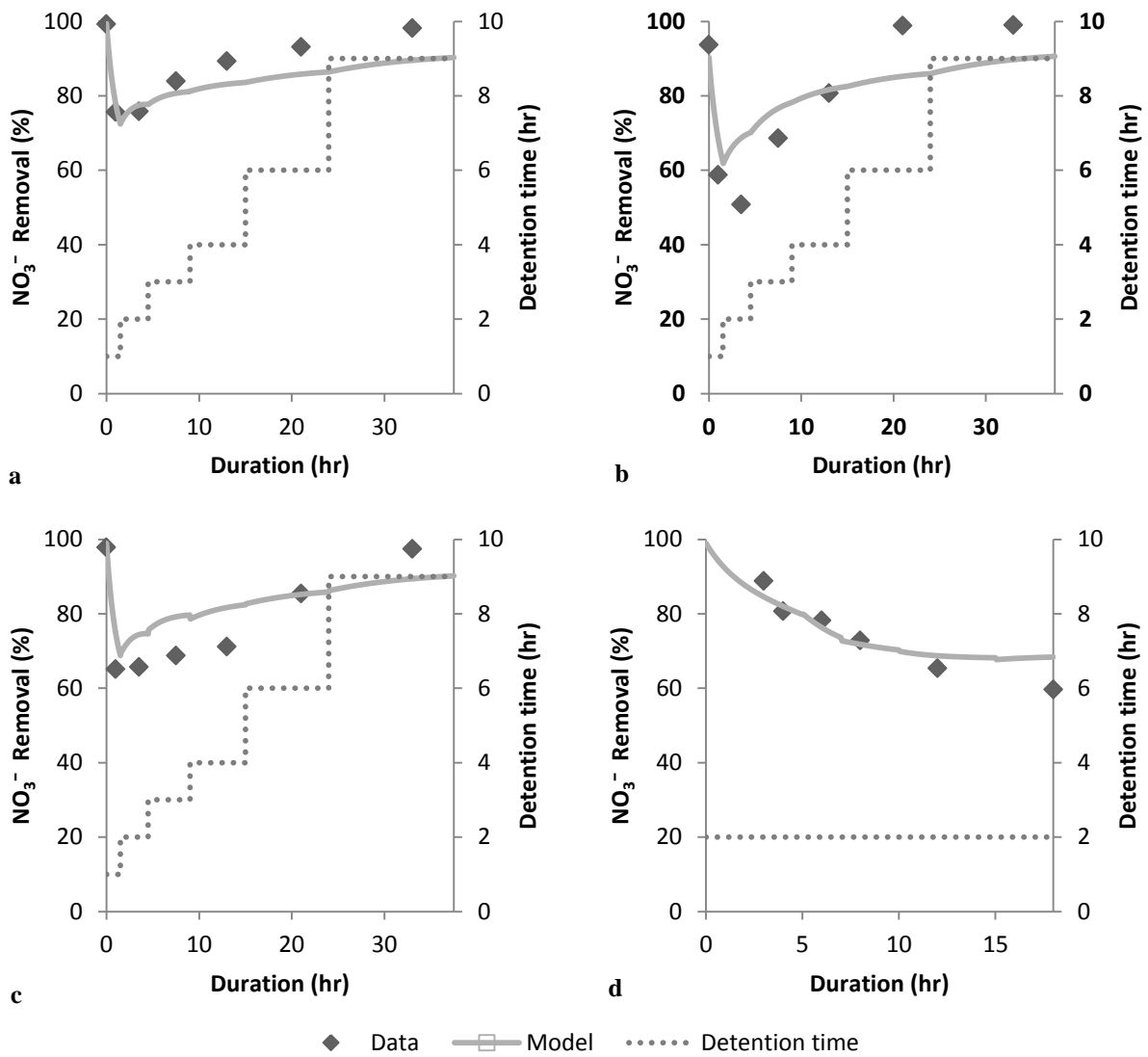
Figure 5.7. 30 cm column data and modeling results for the 8 day ADC base case (SE #4, Fig. 7a), 0 day ADC (SE #5, Fig. 7b), higher influent NO_3^- concentration (SE #6, Fig. 7c and constant 2 hour detention time (SE #10, Fig. 7d) storm events.
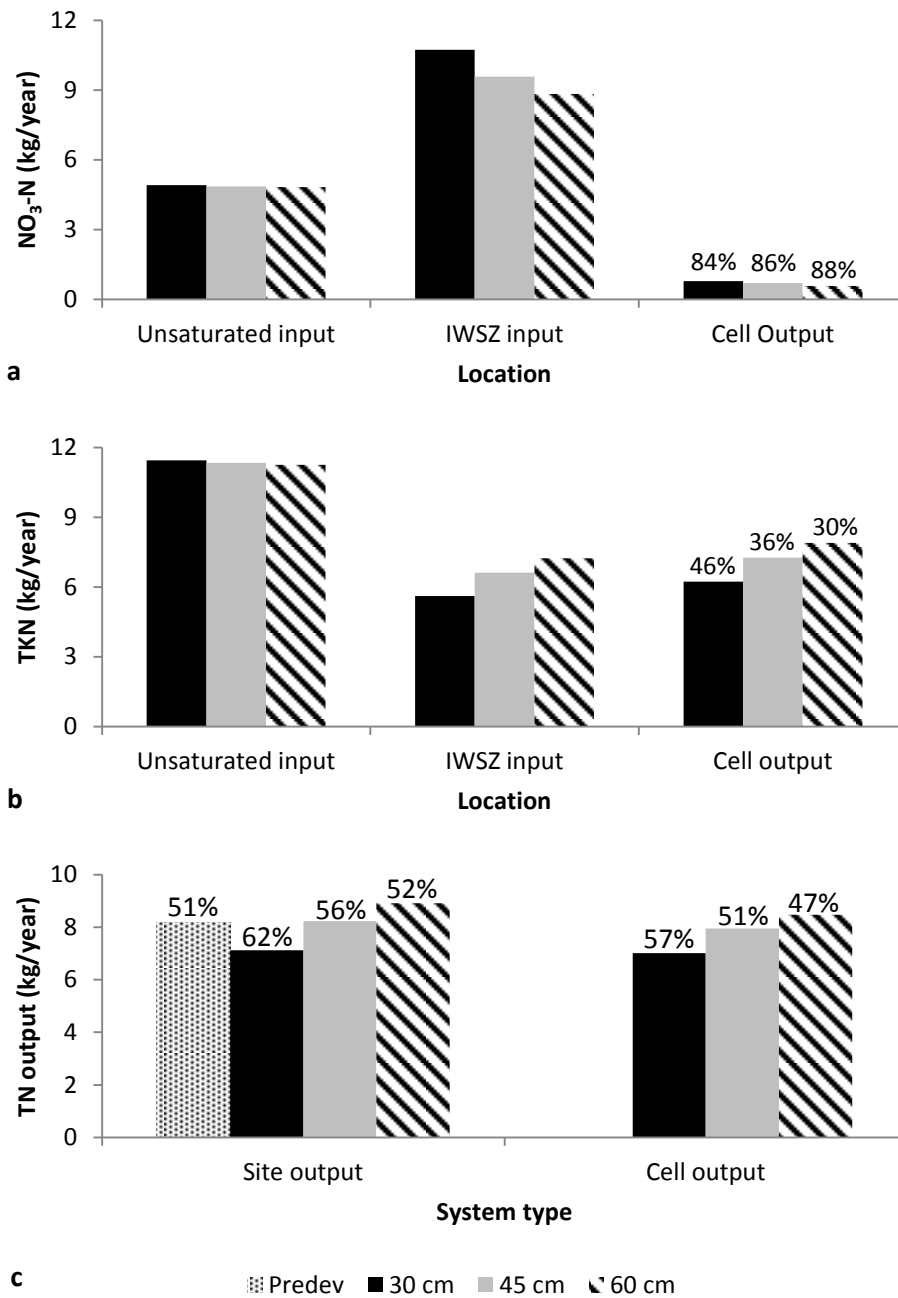
Figure 5.8. Annual output loading results for NO_3^--N (a), TKN (b) and TN (c) from pre-development conditions and from the 30, 45 and 60 cm IWSZ bioretention systems during the case study. Values shown above the columns represent overall mass removal efficiency.

112

Chapter 6:

Conclusions

A bioretention system is an innovative stormwater treatment technology that utilizes a variety of physical, chemical and biological transformation processes to treat stormwater runoff. Many of these processes are well known; however, the driving factors (detention time, cell dimensions, etc.) that affect these processes are not well understood. This prevents designers from having the ability to appropriately size bioretention systems for nutrient removal. Without scientifically-based design guidelines, the following issues will likely impede the implementation of bioretention systems: (1) regulators are less certain that bioretention systems will reduce nutrient loadings to downstream surface waters; (2) previous design guidelines be more expensive than is necessary; and (3) a model that accurately predicts the nitrogen removal performance of bioretention systems is unavailable.

Conventional bioretention systems have been shown to remove NO_3^- poorly. However, these systems can be modified to include an IWSZ to promote denitrification. This dissertation focused on understanding: (1) how biological processes affect NO_3^- removal; (2) how IWSZ dimensions affect NO_3^- removal; and (3) how a model can be developed to quantify NO_3^- removal in the IWSZ. This research contains guidelines that can be used by designers and regulators to decide how IWSZs in bioretention systems should be designed to meet the hydrologic and nitrogen loading goals for a development.

113

Environmental conditions play a significant role in promoting denitrification in the IWSZ. These conditions include: the presence of denitrifying bacteria, anaerobic conditions and the bio-availability of carbon-containing media in the IWSZ. Without these conditions, NO_3^- removal will likely occur at a slow to negligible rate. The results from the un-acclimated microcosm experiments indicated that an acclimation period is necessary before denitrifying bacteria respire NO_3^- at a high rate. In addition, NO_3^- removal rates were faster during anaerobic compared to aerobic conditions. Another interesting finding was how the hydrolysis of carbon-containing media affects NO_3^- removal. Hydrolysis increases dissolved organic carbon concentrations in the IWSZ pores which enable denitrifying organisms to consume NO_3^- at a higher rate. Hydrolysis occurs at a faster rate in un-saturated as compared to saturated IWSZs. However, an increase in hydrolysis rates reduces the lifespan of organic media to provide a carbon source. In addition, high TKN production rates in unsaturated compared to saturated IWSZs will reduce the benefits of incorporating an IWSZ to reduce nitrogen loadings.

The physical dimensions of the IWSZ can affect NO_3^- removal efficiencies. This phenomenon appears to be caused by dispersion. When IWSZs are operated at equal detention times, taller IWSZs will remove NO_3^- at a faster rate than shorter IWSZs. Shorter IWSZs are operated with slower pore velocities where dispersive processes play a more pronounced role in transporting NO_3^- through the IWSZ; however, if IWSZs are operated with lower detention times (< 1 hr), dispersive processes may not have a major effect on NO_3^- removal. The effects of dispersion can also be compounded in IWSZs. When IWSZs are operated under conditions similar to plug flow reactors (low dispersion), denitrifying bacteria have more time to respire

114

NO_3^-. In this dissertation, a model was developed to estimate the Peclet Number as a function of the Reynolds Number; however, other media types and flow rates would need to be evaluated to further validate the model. Future research that investigates how dispersion affects biological systems, such as IWSZs, is recommended.

Large data sets from the experimental portion of this research were used to develop a model that can predict NO_3^- removal in IWSZs. However, a model that predicts TN loadings from bioretention systems would be more useful for application. Additional equations pertaining to other nitrogen transformation (nitrification and TKN leaching) and hydraulic (saturated and unsaturated flow) processes were developed and combined with data from Davis et al. (2006) and the denitrification model to predict TN loadings from bioretention systems. Even though modest correlations between the model (nitrification and TKN stripping portion) and the extrapolated data sets were calculated, additional research is recommended to verify the factors and kinetics that control nitrogen transformation processes other than NO_3^- removal in the IWSZ. The unsaturated flow equation that was presented in this dissertation is a simplified way to quantify unsaturated flows in the sand layer. This unsaturated flow equation is particularly useful because numerous hydrologic/hydraulic/water quality processes need to be simplified to develop a user-friendly nitrogen loading model for bioretention systems.

The model that was developed from this dissertation will allow designers to predict TN loadings from various bioretention systems that are designed under various hydrological conditions. In terms of stormwater quality modeling for site development projects, this model is highly advanced. However, many processes and kinetics that occur in stormwater treatment

115

systems are poorly understood. Through this rationale, it was prudent to develop a simple model that can also model the dynamic behavior of bioretention systems. The terms "simplified" and "assumed" were used thoroughly in this dissertation. These terms were used to satisfy the concerns of readers with a background in only environmental engineering or only water resources engineering, since more complex models in other specialized areas (e.g., wastewater treatment) may be more accurate for one particular aspect of the model.

This dissertation advances our knowledge of how NO_3^- is removed in the IWSZ of bioretention systems. Even though this research provides solutions to many issues, more research is necessary to understand how bioretention systems should be designed to improve water quality. In broader terms, similar research should be conducted for other stormwater treatment systems (e.g., wet detention, dry retention) to provide designers a greater understanding in selecting the most beneficial system for each unique site. Until then, our goal of designing sustainable stormwater management systems to meet the needs of our environment, economy and society is still a work in progress.

References

Ahiablame, L.M., Engel, B.A., and Chaubey, I. (2012). "Effectiveness of Low Impact Development Practices: Literature Review and Suggestions for Future Research." *Water Air & Soil Pollution*, 223, 4253-4273.

Akan, A.O., and Houghtalen, R.J. (2003). "Urban Hydrology, Hydraulics, and Stormwater Quality: Engineering Applications and Computer Modeling". John Wiley & Sons, Inc. Hoboken, New Jersey.

Atchison, D., Potter, K., and Severson, L. (2006). "Design Guidelines for Stormwater Bioretention Facilities." University of Wisconsin Water Resources Institute.

Barker, P.S., and Dold, P.L. (1997). "General Model for Biological Nutrient Removal in Activated Sludge Systems: Model Presentation." *Water Environment Research*, 69(5), 969-984.

Barrett, M.E., Limouzin, M., and Lawler, D.F. (2013). "Effects of Media and Plant Selection on Biofiltration Performance." *Journal of Environmental Engineering – ASCE*, 139(4), 462-470.

Bear, J. (1972). "Dynamics of Fluids in Porous Media." Elsevier, New York.

Bedient, P.B., and Huber, W.C. (2002). "Hydrology and Floodplain Analysis". 3rd Ed. Prentice Hall, Inc. Upper Saddle River, NJ.

Bertrand-Krajewski, J., Chebbo, G, and Saget, A. (1998). "Distribution of Pollutant Mass vs. Volume in Stormwater Discharges and the First Flush Phenomenon." *Water Research,* 32(8), 2341-2356.

Betts, W.B., Dart, R.K., Ball, A.S., and Pedlar, S.L. (1991). "Biosynthesis and Structure of Lignocellulose." In: Betts WB (Ed) Biodegradation: Natural and Synthetic Materials. Springer, Verlag, Berlin, Germany.

Bratieres, K., Fletcher, T.D., Deletic, A., and Zinger, Y. (2008). "Nutrient and Sediment Removal by Stormwater Biofilters: A Large-Scale Design Optimisation Study." *Water Research*, 42, 3930-3940.

Brown, R.A., and Hunt, W.F. (2011). "Underdrain Configuration to Enhance Bioretention Exfiltration to Reduce Pollutant Loads." *Journal of Environmental Engineering – ASCE*, 137(11), 1082-1091.

Brown, R.A., Skaggs, R.W., Hunt II, W.F. (2013). "Calibration and Validation of DRAINMOD to Model Bioretention Hydrology." *Journal of Hydrology*, 486, 430-442.

Cameron, S.G., and Schipper, L.A. (2010). "Nitrate Removal and Hydraulic Performance of Organic Carbon for Use in Denitrification Beds." *Ecological Engineering*, 36, 1588-1595.

Cameron, S.G., and Schipper, L.A. (2012). "Hydraulic Properties, Hydraulic Efficiency and Nitrate Removal of Organic Carbon Media for Use in Denitrification Beds." *Ecological Engineering*, 41, 1-7.

Charbeneau, R.J. (2006). "Groundwater Hydraulics and Pollutant Transport", Waveland Press, Long Grove, Illinois.

Chen, X., Peltier, E., Sturm, B.S.M., and Young, C.B. (2013). "Nitrogen Removal and Nitrifying and Denitrifying Bacteria Quantification in a Stormwater Bioretention System." *Water Research,* 47, 1691-1700.

Cho, K., Yoon, M, Song, K., and Ahn, K. (2011). "The Effects of Antecedent Dry Days on the Nitrogen Removal in Layered Soil Infiltration Systems for Storm Run-off Control." *Environmental Technology*, 32(7), 747-755.

Christianson, L.E., Bhandari, A., and Helmers, M.J. (2012). "A Practice-oriented Review of Woodchip Bioreactors for Subsurface Agricultural Drainage." *Applied Engineering in Agriculture*, 28(6), 861-874.

Chu, L. and Wang, J. (2013). "Denitrifcation Performance and Biofilm Characteristics Using Biodegradable Polymers PCL as Carriers and Carbon Source." *Chemosphere*, 91, 1310-1316.

Chun, J.A., Cook, R.A., Eheart, J.W., and Kang, M.S. (2009). "Estimation of Flow and Transport Parameters for Woodchip-Based Bioreactors: I. Laboratory-scale Bioreactor." *Biosystems Engineering*, 104, 384-395.

Clark, S., and Pitt, R. (2009). "Storm-Water Filter Media Pollutant Retention under Aerobic versus Anaerobic Conditions." *Journal of Environmental Engineering – ASCE*, 5, 367-371.

Clark, S.E., and Pitt, R. (2012). "Targeting Treatment Technologies to Address Specific Stormwater Pollutants and Numeric Discharge Limits." *Water Research*, 46, 6715-6730.

Clement, T.P. (1997). "A Modular Computer Code for Simulating Reactive Multi-Species Transport in 3-Dimensional Groundwater Systems." The U.S. Department of Energy. Pacific Northwest National Laboratory, Richland, Washington, PNNL-11720.

Collins, K.A., Lawrence, T.J., Stander, E.K., Jontos, R., Kaushal, S.S., Newcomer, T.A., Grimm, N.B., and Eckberg, M.L.C. (2010). "Opportunities and Challenges for Managing Nitrogen in Urban Stormwater: A Review and Synthesis." *Ecological Engineering*, 36, 1507-1519.

Coyne, M.S. (2008). "Biological Denitrification." In: Schepers, J.S., Raun, W. (Eds.), Nitrogen in Agricultural Systems. ASA-CSSSA-SSSA, Agronomy Monograph, 49, Madison, WI, 197-249.

Crittenden, J.C., Trussell, R.R., Hand, D.W., Howe, K.J., and Tchobanoglous, G. (2005). "Water Treatment: Principles and Design." John Wiley & Sons, Inc. Hoboken, NJ.

Davis, A.P., Shokouhian, M., Sharma, H., and Minami, C. (2001). "Laboratory Study of Biological Retention for Urban Stormwater Management." *Water Environment Research*, 73(1), 5-14.

Davis, A.P., Shokouhian, M., Sharma, H., and Minami, C. (2006). "Water Quality Improvement through Bioretention Media: Nitrogen and Phosphorous Removal." *Water Environment Research*, 78(3), 284-293.

Davis, A.P., Hunt, W., Traver, R.G., and Clar, M. (2009). "Bioretention Technology: Overview of Current Practice and Future Needs." *Journal of Environmental Engineering – ASCE*, 135, 109-117.

Delay, F., Porel, G., and Chatelier, M. (2013). "A Dual Flowing Continuum Approach to Model Denitrification Experiments in Porous Media Colonized by Biofilms." *Journal of Contaminant Hydrology*, 150, 12-24.

Delgado, J.M.P.Q. (2006). "A Critical Review of Dispersion in Packed Beds." *Heat Mass Transfer*, 42, 279-310.

Deng, Z., Sun, S., and Gang, D.D. (2012). "Modeling Nitrate-Nitrogen Removal Process in First-Flush Reactor for Stormwater Treatment." *Bioprocess Biosystems Engineering*, 35, 865-874.

Desvaux, M. (2006). "Unravelling Carbon Metabolism in Anaerobic Cellulolytic Bacteria." *Biotechnol. Prog,* 22, 1229-1238.

Dietz, M.E. and Clausen, J.C. (2006). "Saturation to Improve Pollutant Retention in a Rain Garden." *Environment Science & Technology*, 40(4), 1335-1340.

Dietz, M.E. (2007). "Low Impact Development Practices: A Review of Current Research and Recommendations for Future Directions." *Water, Air and Soil Pollution*, 186, 351-363.

Elgood, Z., Robertson, W.D., Schiff, S.L., and Elgood, R. (2010). "Nitrate Removal and Greenhouse Gas Production in a Stream-Bed Denitrifying Bioreactor." *Ecological Engineering*, 36, 1575-1580.

Elliott, A.H., and Trowsdale, S.A. (2011). "A Review of Models for Low Impact Urban Stormwater Drainage." *Environmental Modelling & Software*, 22, 394-405.

Ergas, S.J., Sengupta, S., Siegel, R., Pandit, A., Yao, Y., and Yuan, X. (2010). "Performance of Nitrogen-Removing Bioretention Systems for Control of Agricultural Runoff." *Journal of Environmental Engineering – ASCE,* 136(10), 1105-1112.

Facility for Advancing Water Biofiltration (FAWB) (2008). "Advancing the Design of Stormwater Biofiltration." Monash University. Australia.

Gao, C.; Liu, J., Zhu, J., Wang, Z. (2013). "Review of Current Research on Urban Low-impact Development Practices." *Research Journal of Chemistry and Environment*, 17(S1), 209-214.

Gibert, O., Pomierny, S., Rowe, I., and Kalin, R. M. (2008). "Selection of Organic Substrates as Potential Reactive Materials for Use in a Denitrification Permeable Reactive Barrier (PRB)." *Bioresource Technology*, 99, 7587-7596.

Grebel, J.E., Mohanty, S.K., Torkelson, A.A., Boehm, A.B., Higgins, C.P., Maxwell, R.M., Nelson, K.L., and Sedlak, D.L. (2013). "Engineered Infiltration Systems for Urban Stormwater Reclamation." *Environmental Engineering Science*, 30(8), 437-454.

Greenway, M., and Lucas, B. (2010) "Improved Media and Plant Species for Long Term Sustainability of Nutrient Retention in Bioretention Systems." Pesented at *STORMWATER 2010 Stormwater Industry Association National Conference*, November 9-11, Sydney, Australia; Stormwater Industry Association of Australia: Sydney, Australia.

Grismer, M.E., Hogan, M.P., and Steinfeld, D. (2012). "Column Analyses of Chloride Breakthrough and Lead Retention in Amended Sandy Soils." *Journal of Environmental Science and Engineering A*, 1, 503-513.

Gunn, D.J. and Pryce, C. (1969). "Dispersion in Packed Beds." *Trans IChemE*, 47, T341-T350.

Gurr, E., and Nnadi, F. (2009). "Non-Point Source Nutrient Loading in an Urban Watershed." *World Environmental and Water Resources Congress 2009: Great Rivers*. ASCE.

Harper, H.H., and Baker, D.M. (2007). "Evaluation of Current Stormwater Design Criteria within the State of Florida: Final Report." Environmental Research & Design, Inc. Prepared for the Florida Department of Environmental Protection. June 2007.

Hatt, B.E., Fletcher, T.D., and Deletic, A. (2007). "Treatment Performance of Gravel Filter Media: Implications for Design and Application of Stormwater Infiltration Systems." *Water Research*, 41, 2513-2524.

Herbert, R.B. Jr. (2011). "Implications of Non-equilibrium Transport in Heterogeneous Reactive Barrier Systems: Evidence from Laboratory Denitrification Experiments." *Journal of Contaminant Hydrology*, 123, 30-39.

Hsieh, C., and Davis, A.P. (2005a). "Multiple-Event Study of Bioretention for Treatment of Urban Stormwater Runoff." *Water Science & Technology*, 51(3-4), 177-181.

Hsieh, C., and Davis, A.P. (2005b) "Evaluation and Optimization of Bioretention Media for Treatment of Urban Stormwater Runoff." *Journal of Environmental Engineering*, 131(11), 1521-1531.

Hsieh, C., Davis, A.P., and Needelman, B.A. (2007). "Nitrogen Removal from Urban Stormwater Runoff through Layered Bioretention Columns." *Water Environment Research*, 79(2), 177-184.

Hunt, W.F., Jarrett, A.R., Smith, J.T., and Sharkey, L.J. (2006). "Evaluating Bioretention Hydrology and Nutrient Removal at Three Field Sites in North Carolina." *J. Irrig. Drain. Eng*, 132(6), 600-608.

Hunt, W.F., Davis, A.P., and Traver, R.G. (2012). "Meeting Hydrologic and Water Quality Goals through Targeted Bioretention Design." *Journal of Environmental Engineering – ASCE*, 138(6), 698-707.

Imteaz, M.A., Ahsan, A., Rahman, A., and Mekanik, F. (2013). "Modelling Stormwater Treatment Systems using MUSIC: Accuracy." *Resources, Conservation and Recycling*, 71, 15-21.

International Stormwater Best Management Practices Database (2010) "Categorical Summary of BMP Performance Data for Nutrients Contained in the International Stormwater Database Attachment 1." Prepared by Geosyntec Consultants and Wright Water Engineers, Inc. http://www.bmpdatabase.org/Docs/Attachment1_Categorical_BMP_StatsReport_Nutrients_Final.pdf . last accessed: May 30, 2012.

Kadlec, R.H., Tanner, C.C., Hally, V.M., and Gibbs, M.M. (2009). "Treatment Wetlands." 2nd Ed. CRC Press: Boca Raton, Florida.

Kemmer, G. and Keller, S. (2010). "Nonlinear Least-Squares Data Fitting in Excel Spreadsheets." *Nature Protocols*, 5, 267-281.

Kim, H., Seagren, E.A., and Davis, A.P. (2003) "Engineered Bioretention for Removal of Nitrate from Stormwater Runoff." *Water Environment Research*, 75, 355-367.

Kobayashi, T., Sugiyama, A., Kawase, Y., Saito, T., Mergaert, J., and Swings, J. (1999). "Biochemical and Genetic Characterization of an Extracellular Poly (3-Hydroxybutyrate) Depolymerase from *Acidovorax* Sp. Strain TP4." *Journal of Environmental Polymer Degradation*, 7(1), 9-18.

Kosugi, A., Murashima, K., and Doi, R.H. (2001). "Characterization of Xylanolytic Enzymes in Clostridium cellulovorans: Expression of Xylanase Activity Dependent on Growth Substrates." *J. Bacteriol*, 183(24), 7037-7043.

Kramer, H., and Westererp, K.R. (1963). "*Elements of Chemical Reactor Design and Operation.*" Academic Press, Inc., New York, NY.

Laurenson, G., Laurenson, S., Bolan, N., Beecham, S., and Clark, I. (2013) "The Role of Bioretention Systems in the Treatment of Stormwater." *Advances in Agronomy*, 120, 223-274.

Lee, L.Y., Tan, L., Wu, W., Yeo, S.K.Q., and Ong, S.L. (2013). "Nitrogen Removal in Saturated Zone with Vermicompost as Organic Carbon Source." *Sustain. Environ. Res.*, 23(2), 85-92.

Leschine, S.B. (1995). "Cellulose Degradation in Anaerobic Environments." *Annu. Rev. Microbiol*, 49, 399-426.

Loheide II, S.P., Butler Jr., J.J., Gorelick, S.M. (2005). "Estimation of Groundwater Consumption by Phreatophytes Using Diurnal Water Table Fluctuations: A Saturated-Unsaturated Flow Assessement." *Water Resources Research*, 41, W07030.

Lucas, W.C. (2010). "Design of Integrated Biofiltration-Detention Urban Retrofits with Design Storm and Continuous Simulation Methods." *Journal of Hydrol. Eng.*, 15(6), 486-498.

Lucas, W.C., and Greenway, M. (2011a). "Hydraulic Response and Nitrogen Retention in Bioretention Mesocosms with Regulated Outlets: Part I-Hydraulic Response." *Water Environment Research*, 83, 692-702.

Lucas, W.C., and Greenway, M. (2011b). "Hydraulic Response and Nitrogen Retention in Bioretention Mesocosms with Regulated Outlets: Part II-Nitrogen Retention." *Water Environment Research*, 83, 703-713.

Luell, S.K, Hunt, W.F., and Winston, R.J. (2011). "Evaluation of Undersized Bioretention Stormwater Control Measures for Treatment of Highway Bridge Deck Runoff." *Water Science & Technology*, 64(4), 974-978.

Malherbe, S., and Cloete, T.E. (2002). "Lignocellulose Biodegradation: Fundamentals and Applications." *Reviews in Environmental Science & Bio/Technology*, 1, 105-114.

Masi, M. (2011). "A SWMM-5 Model of a Denitrifying Bioretention System to Estimate Nitrogen Removal from Stormwater Runoff." November 2, 2011. *Thesis*.

Mergaert, J., Boley, A., Cnockaert, M.C., Muller, W., and Swings, J. (2001). "Identity and Potential Functions of Heterotrophic Bacterial Isolates from a Continuous-Upflow Fixed-Bed Reactor for Denitrification of Drinking Water with Bacterial Polyester as Source of Carbon and Electron Donor." *System Appl. Microbiol*, 24, 303-310.

Metropolitan Sewer District of Greater Cincinnati (MSDGC) (2013). "MSDGC Modeling Guidelines and Standards Volume I System Wide Model." Revision 3. February 2013.

Moorman, T.B., Parkin, T.B., Kaspar, T.C., and Jaynes, D.B. (2010). "Denitrification Actrivity, Wood Loss, and N2O Emissions Over 9 Years from a Wood Chip Bioreactor." *Ecological Engineering*, 36, 1567-1574.

Morzaria-Luna, H.N., Schaepe, K.S., Cutforth, L.B., and Veltman, R.L. (2004). "Implementation of Bioretention Systems: A Wisconsin Case Study." *Journal of the American Water Resources Association*, August, 1053-1061.

Mualem, Y. (1976). "A New Model for Predicting the Hydraulic Conductivity of Unsaturated Porous Media." *Water Resources Research*, 12(3), 513-522.

Nachabe, M.H., Ahuja, L.R., Butters, G. (1999). "Bromide Transport Under Sprinkler and Flood Irrigation for No-till Soil Condition." *Journal of Hydrology*, 214, 8-17.

Nachabe, M.H. (2006). "Equivalence Between Topmodel and the NRCS Curve Number Method in Predicting Variable Runoff Source Areas." *Journal of the American Water Resources Association*, 42(1):225-235.

Nath, S., and Chand, S. (1996). "Mass Transfer and Biochemical Reaction in Immobilized Cell Packed Bed Reactors: Correlation of Experiment with Theory." *J. Chem. Tech. Biotechnol.*, 66, 286-292.

Palhegyi, G.E. (2010). "Modeling and Sizing Bioretention using flow duration Control." *Journal of Hydrologic Engingeering*, 15(6), 417-425.

Park, Y.S., Engel, B.A., and Harbor, J. (2014). "A Web-Based Model to Estimate the Impact of Best Management Practices." *Water*, 6, 455-471.

Payne, E.G., Fletcher, T.D., Cook, P.L., Deletic, A., and Hatt, B. E. (2013). "Processes and Drivers of Nitrogen Removal in Stormwater Biofiltration." *Critical Reviews in Environmental Science and Technology*, Accepted for publication, August 2013.

Perez, J., Munoz-Dorado, J., Rubia, T. de la, and Martinez, J. (2002). "Biodegradation and Biological Treatments of Cellulose, Hemicellulose and Lignin: An Overview." *Int Microbiol*, 5, 53-63.

Philippot, L., Hallin, S., Schloter, M. (2007). "Ecology of Denitrifying Prokaryotes in Agricultural Soil." *Advances in Agronomy*, 96, 249-305.

Pitt, R., Maestre, A., and Morquecho, R. (2005). "The National Stormwater Quality Database (NSQD, version 1.1)." Department of Civil and Environmental Engineering, University of Alabama, Tuscaloosa, AL.

Recous, S., Machet, J.M., and Mary, B. (1992). "The Partitioning of Fertilizer-N Between Soil and Crop: Comparison of Ammonium and Nitrate Applications." *Plant Soil*, 144, 101-111.

Rittmann, B.E., and McCarty, P.L. (2001). "Environmental Biotechnology: Principles and Applications." McGraw-Hill. New York, NY.

123

Robertson, W.D., Vogan, J.L., and Lombardo, P.S. (2008). "Nitrate Removal Rates in a 15-Year-Old Permeable Reactive Barrier Treating Septic System Nitrate." *Ground Water Monitoring & Remediation*, 28(3), 65-72.

Rossman, L.A. (2010). "Storm Water Management Model User's Manual – Version. 5.0.", United States Environmental Protection Agency, Water Supply and Water Resources Division, National Risk Management Research Laboratory, Cincinnati, Ohio.

Rovira, P., and Vallejo, V.R. (2002). "Labile and Recalcitrant Pools of Carbon and Nitrogen in Organic Matter Decomposing at Different Depths in Soil: An Acid Hydrolysis Approach." *Geoderma*, 107, 109-141.

Roy-Poirier, A., Champagne, P., and Filion, Y. (2010). "Review of Bioretention System Research and Design: Past, Present, and Future" *Journal of Environmental Engineering – ASCE*, 136(9), 878-889.

Schipper, L.A., Robertson, W.D., Gold, A.J., Jaynes, D.B., and Cameron, S.C. (2010). "Denitrifying Bioreactors – An Approach for Reducing Nitrate Loads to Receiving Waters." *Ecological Engineering*, 36, 1532-1543.

Schueler, T.B. (1987). "Controlling Urban Runoff: A Practical Maual for Planning and Designing Urban BMPs." Washington Metropolitan Water Resources Planning Board, Washington, DC.

Schueler, T. (2003). "Impacts of Impervious Cover on Aquatic Systems." Watershed Protection Research Monograph No. 1, Center for Watershed Protection, Ellicot City, MD.

Schwartz, W.H. (2001). "The Cellulosome and Cellulose Degradation by Anaerobic Bacteria." *Appl. Microbiol. Biotechnol*, 56, 634-649.

Shen, Z., Zhou, Y., Hu, J., and Wang, J. (2013). "Denitrification performance and Microbial Diversity in a Packed-Bed Bioreactor Using Biodegradable Polymer as Carbon Source and Biofilm Support." *Journal of Hazardous Materials*, 250-251, 431-438.

Smith, D.P. (2008). "Sorptive Media Biofiltration for Inorganic Nitrogen Removal from Storm Water." *Journal of Irrigation and Drainage Engineering – ASCE*, 134, 624-629.

Smith, V. (2003). "Eutrophication of Freshwater and Coastal Marine Ecosystems." *Environmental Science & Pollution Research*, 10(2), 126-139.

Standard Methods for the Examination of Water and Wastewater (2012). 22nd Ed., American Public Health Association, American Water Works Association, and Water Environment Federation, Washington.

Sulaiman, W.R.W., and Lee, E.S. (2012). "Pyrolysis of Eucalyptus Wood in a Fluidized-Bed Reactor." *Research on Chemical Intermediates*, 38, 2025-2029.

Taylor, G.D., Fletcher, T.D., Wong, T.H.F., Breen, P.F., and Duncan, H.P. (2005). "Nitrogen Composition in Urban Runoff – Implications for Stormwater Management." *Water Research*, 39, 1982-1989.

Tchobanoglous, G., Burton, F.L., and Stensel, H.D. (2003). "Wastewater Engineering: Treatment and Reuse." 4th Ed. McGraw-Hill. New York, New York.

Tiedje, J.M., Sexstone, A.J., Myrold, D.D., and Robinson, J.A. (1982). "Denitrification: Ecological Niches, Competition and Survival." *Antonie van Leeuwenhoek*, 48, 569-583.

Tomme, P., Warren, R.A., and Gilkes, N.R. (1995). "Cellulose hydrolysis by Bacteria and Fungi." *Adv. Microb. Physiol*, 37, 1-81.

United States Environmental Protection Agency (USEPA) (1997). "Method 300.1: Methods for the Determination of Inorganic anions in Drinking Water Using Ion Chromatography." *EPA/815-R-00-014*, Cincinnati, Ohio.

USEPA (1999). "Storm Water Technology Fact Sheet: Bioretention." US Environmental Protection Agency. EPA-832-F-99-012.

USEPA (2000). "National Water Quality Inventory." 305(b) List. Washington, DC: EPA Office of Water.

USEPA (2010). "Nutrient Control Design Manual." Cincinnati, Ohio: EPA Office of Research and Development.

USEPA (2014). "State Development of Numeric Criteria for Nitrogen and Phosphorus Pollution." http://cfpub.epa.gov/wqsits/nnc-development/ . Date accessed: 3-21-2014.

United States Geological Survey (USGS). (2014) "USGS Current Water Data for Florida." http://waterdata.usgs.gov/fl/nwis/rt . Date accessed: 3-21-2014.

Vaccari, D.A., Strom, P.F., and Alleman, J.E. (2006). "Environmental Biology for Engineers and Scientists." John Wiley & Sons, Inc. Hoboken, New Jersey.

Van Genuchten, M.T., and Alves, W.J. (1982). "Analytical solutions for the one-dimensional convective-dispersive solute Transport Equation." U.S. Department of Agriculture Technical Bulletin No. 1661. Washington, D.C.: U.S. GPO.

Vidon, P., Hubbard, L.E., Soyeux, E. (2009). "Seasonal Solute Dynamics Across Land Uses During Storms in Glaciated Landscape of the US Midwest." *Journal of Hydrology*, 376, 34-47.

Viesman, W., Hammer, M.J., Perez, E.M., and Chadik, P.A. (2009). "Water Supply and Pollution Control." Pearson Education, Inc. Upper Saddle River, NJ.

125

Wanielista, M., Hardin, M., Kuzlo, P., and Gogo-Abite, I. (2014). "User's Manual for the BMPTRAINS Model." University of Central Florida Stormwater Management Academy. Florida Department of Transportation, February 1, 2014.

Warneke, S., Schipper, L.A., Matiasek, M., Scow, K.M., Cameron, S., Bruesewitz, D., and McDonald, I.R. (2011). "Nitrate Removal, Communities of Denitrifiers and Adverse Effects in Different Carbon Substrates for Use in Denitrification Beds." *Water Research*, 45, 5463-5475.

Yang, J.S., Ni, J.R., Yuan, H.L. (2007). "Biodegradation of Three Different Wood Chips by Pseudomonas sp PKE117." *International Biodeterioration & Biodegradation*, 60(2), 90-95.

Young, J.M., Leschine, S.B., Reguera, G. (2012). "Reversible Control of Biofilm Formation by Cellulomonas spp. in Response to Nitrogen Availability." *Environmental Microbiology*, 14(3), 594-604.

Wallenstein, M.D., Myrold, D.D., Firestone, M., and Voytek, M. (2006). "Environmental Controls on Denitrifying Communities and Denitrification Rates: Insights from Molecular Methods." *Ecological Applications*, 16(6), 2143-2152.

Wild, D., Schulthess, R., and Gujer, W. (1995). "Structured Modelling of Denitrification Intermediates." *Water, Science and Technology*, 31(2), 45-54.

Zhang, L., Seagren, E.A., Davis, A.P., Karns, J.S. (2010). "The Capture and Destruction of *Escherichia coli* from Simulated Urban Runoff Using Conventional Bioretention Media and Iron Oxide-coated Sand." *Water Environment Research*, 82, 701-714.

Zhang, L., Seagren, E.A., Davis, A.P., and Karns, J.S. (2012). "Effects of Temperature on Bacterial Transport and Destruction in Bioretention Media: Field and Laboratory Evaluations." *Water Environment Research*, 84(6), 485-496.

Zhang, Z., Rengel, Z., Liaghati, T., Anoniette, T., and Meney, K. (2011). "Influence of Plant Species and Submerged Zone with Carbon Addition on Nutrient Removal in Stormwater Biofilter." *Ecological Engineering*, 37, 1833-1841.

Zhu, G., Wang, S., Wang, W., Wang, Y., Zhou, L., Jiang, B., Op den Camp, H.J.M., Risgaard-Petersen, N., Schwark, L., Peng, Y., Hefting, M.M, Jetten, M.S.M., Yin, C. (2013). "Hotspots of anaerobic ammonium oxidation at Land-Freshwater Interfaces." *Nature Geoscience*. 6, 103-107.

Zinger, Y., Fletcher, T.D., Deletic, A., Blecken, G.T., and Viklander, M. (2007a). "Optimisation of the Nitrogen Retention Capacity of Stormwater Biofiltration Systems." *Proceedings of the 6th International Conference NOVATECH 2007, Sustainable Techniques and Strategies in Urban Water Management*, June 24-28, Lyon, France, Graie: Villeurbanne, France, 893-900.

126

Zinger, Y., Deletic, A., Fletcher, T. D. (2007b). "The Effect of Various Intermittent Wet-Dry Cycles on Nitrogen Removal Capacity in Biofilters Systems." *Conference on Rainwater and Urban Design*. Sydney, Australia. August 21-23, 2007.

127

Appendix A:

Microcosm Study Data

Table A.1. Acclimated anoxic microcosm TN data.

Media	Incubation time (hr)	Sample 1 (hr)	Sample 2 (hr)	Sample 3 (hr)	Average (mg/L)	Standard deviation (mg/L)
Sand	0	2.11	2.03	2.37	2.17	0.18
Sand	6	2.38	2.15	2.44	2.32	0.15
Gravel	0	2.11	2.03	2.37	2.17	0.18
Gravel	6	2.24	2.15	2.27	2.22	0.06
Wood	0	2.11	2.03	2.37	2.17	0.18
Wood	6	0.29	0.31	0.33	0.31	0.02
Tire	0	2.11	2.03	2.37	2.17	0.18
Tire	6	0.44	0.39	0.46	0.43	0.04
Sand-Wood	0	2.20	2.11	2.24	2.18	0.07
Sand-Wood	6	0.61	0.65	0.73	0.67	0.06
Gravel-Wood	0	2.20	2.11	2.24	2.18	0.07
Gravel-Wood	6	0.34	0.39	0.42	0.38	0.04
Sand-Tire	0	2.20	2.11	2.24	2.18	0.07
Sand-Tire	6	0.79	0.64	0.92	0.79	0.14
Gravel-Tire	0	2.20	2.11	2.24	2.18	0.07
Gravel-Tire	6	0.35	0.35	0.45	0.39	0.06

128

Table A.2. Acclimated anoxic microcosm DOC data.

Media	Incubation time (hr)	Sample 1 (hr)	Sample 2 (hr)	Sample 3 (hr)	Average (mg/L)	Standard deviation (mg/L)
Sand	0	2.73	2.70	3.22	2.88	0.29
Sand	6	4.10	2.92	3.34	3.45	0.60
Gravel	0	2.73	2.70	3.22	2.88	0.29
Gravel	6	3.33	2.68	3.05	3.02	0.33
Wood	0	2.73	2.70	3.22	2.88	0.29
Wood	6	8.21	6.23	6.00	6.81	1.22
Tire	0	2.73	2.70	3.22	2.88	0.29
Tire	6	8.01	5.83	5.60	6.48	1.33
Sand-Wood	0	2.85	2.96	3.16	2.99	0.16
Sand-Wood	6	5.73	4.36	3.75	4.61	1.01
Gravel-Wood	0	2.85	2.96	3.16	2.99	0.16
Gravel-Wood	6	4.61	3.75	3.83	4.06	0.48
Sand-Tire	0	2.85	2.96	3.16	2.99	0.16
Sand-Tire	6	4.99	4.76	3.59	4.45	0.75
Gravel-Tire	0	2.85	2.96	3.16	2.99	0.16
Gravel-Tire	6	4.30	3.62	3.85	3.92	0.35

Table A.3. Acclimated anoxic microcosm DO data.

Media	Incubation time (hr)	Sample 1 (hr)	Sample 2 (hr)	Sample 3 (hr)	Average (mg/L)	Standard deviation (mg/L)
Sand	0	0.99	1.00	1.00	1.00	0.01
Sand	6	0.80	1.02	1.08	0.97	0.15
Gravel	0	0.99	1.00	1.00	1.00	0.01
Gravel	6	0.24	0.83	0.25	0.44	0.34
Wood	0	0.99	1.00	1.00	1.00	0.01
Wood	6	0.38	1.05	0.06	0.50	0.51
Tire	0	0.99	1.00	1.00	1.00	0.01
Tire	6	0.78	0.36	0.19	0.44	0.30
Sand-Wood	0	0.99	1.00	1.00	1.00	0.01
Sand-Wood	6	0.66	0.46	0.17	0.43	0.25
Gravel-Wood	0	0.99	1.00	1.00	1.00	0.01
Gravel-Wood	6	0.44	0.28	1.04	0.59	0.40
Sand-Tire	0	0.99	1.00	1.00	1.00	0.01
Sand-Tire	6	0.42	0.46	0.56	0.48	0.07
Gravel-Tire	0	0.99	1.00	1.00	1.00	0.01
Gravel-Tire	6	0.26	0.37	0.18	0.27	0.10

Table A.4. Acclimated anoxic microcosm pH data.

Media	Incubation time (hr)	Sample 1 (hr)	Sample 2 (hr)	Sample 3 (hr)	Average (mg/L)	Standard deviation (mg/L)
Sand	0	7.79	8.13	7.88	7.93	0.18
Sand	6	7.10	7.53	8.05	7.56	0.48
Gravel	0	7.79	8.13	7.88	7.93	0.18
Gravel	6	7.57	7.70	7.93	7.73	0.18
Wood	0	7.79	8.13	7.88	7.93	0.18
Wood	6	6.95	7.06	7.03	7.01	0.06
Tire	0	7.79	7.13	7.88	7.60	0.41
Tire	6	7.55	7.67	7.53	7.58	0.08
Sand-Wood	0	7.85	8.13	8.06	8.01	0.15
Sand-Wood	6	7.36	7.21	7.10	7.22	0.13
Gravel-Wood	0	7.85	8.13	8.06	8.01	0.15
Gravel-Wood	6	7.33	7.80	7.46	7.53	0.24
Sand-Tire	0	7.85	8.13	8.06	8.01	0.15
Sand-Tire	6	7.70	7.68	7.41	7.60	0.16
Gravel-Tire	0	7.85	8.13	8.06	8.01	0.15
Gravel-Tire	6	7.70	7.36	7.92	7.66	0.28

Table A.5. Acclimated anoxic microcosm NH_4^+-N data.

Media	Incubation time (hr)	Sample 1 (hr)	Sample 2 (hr)	Sample 3 (hr)	Average (mg/L)	Standard deviation (mg/L)
Sand	0	0.02	0.01	0.04	0.02	0.02
Sand	1	0.00	0.01	0.00	0.00	0.01
Sand	2	0.00	0.01	0.00	0.00	0.01
Sand	4	0.00	0.01	0.00	0.00	0.01
Sand	6	0.00	0.01	0.00	0.00	0.01
Gravel	0	0.02	0.01	0.04	0.02	0.02
Gravel	1	0.00	0.01	0.00	0.00	0.01
Gravel	2	0.00	0.01	0.00	0.00	0.01
Gravel	4	0.00	0.01	0.00	0.00	0.01
Gravel	6	0.00	0.01	0.00	0.00	0.01
Wood	0	0.02	0.01	0.04	0.02	0.02
Wood	1	0.00	0.01	0.00	0.00	0.01
Wood	2	0.00	0.01	0.00	0.00	0.01
Wood	4	0.00	0.01	0.00	0.00	0.01
Wood	6	0.00	0.01	0.00	0.00	0.01
Tire	0	0.02	0.01	0.04	0.02	0.02
Tire	1	0.00	0.01	0.00	0.00	0.01
Tire	2	0.00	0.01	0.00	0.00	0.01
Tire	4	0.00	0.01	0.00	0.00	0.01
Tire	6	0.00	0.01	0.02	0.01	0.01
Sand-Wood	0	0.00	0.01	0.03	0.01	0.02
Sand-Wood	1	0.00	0.01	0.00	0.00	0.01
Sand-Wood	2	0.00	0.01	0.00	0.00	0.01
Sand-Wood	4	0.00	0.01	0.00	0.00	0.01
Sand-Wood	6	0.00	0.01	0.00	0.00	0.01
Gravel-Wood	0	0.00	0.01	0.03	0.01	0.02
Gravel-Wood	1	0.00	0.01	0.00	0.00	0.01
Gravel-Wood	2	0.00	0.01	0.00	0.00	0.01
Gravel-Wood	4	0.00	0.01	0.00	0.00	0.01
Gravel-Wood	6	0.00	0.01	0.18	0.06	0.10
Sand-Tire	0	0.00	0.01	0.03	0.01	0.02
Sand-Tire	1	0.00	0.01	0.00	0.00	0.01
Sand-Tire	2	0.00	0.01	0.00	0.00	0.01
Sand-Tire	4	0.00	0.01	0.00	0.00	0.01
Sand-Tire	6	0.00	0.01	0.00	0.00	0.01
Gravel-Tire	0	0.00	0.01	0.03	0.01	0.02
Gravel-Tire	1	0.00	0.01	0.02	0.01	0.01
Gravel-Tire	2	0.00	0.01	0.00	0.00	0.01
Gravel-Tire	4	0.00	0.01	0.00	0.00	0.01
Gravel-Tire	6	0.00	0.01	0.15	0.05	0.08

131

Table A.6. Acclimated anoxic microcosm NO_2^--N data.

Media	Incubation time (hr)	Sample 1 (hr)	Sample 2 (hr)	Sample 3 (hr)	Average (mg/L)	Standard deviation (mg/L)
Sand	0	0.00	0.00	0.01	0.00	0.01
Sand	1	0.00	0.00	0.01	0.00	0.01
Sand	2	0.00	0.00	0.01	0.00	0.01
Sand	4	0.00	0.00	0.00	0.00	0.00
Sand	6	0.00	0.00	0.01	0.00	0.01
Gravel	0	0.00	0.00	0.01	0.00	0.01
Gravel	1	0.00	0.00	0.00	0.00	0.00
Gravel	2	0.00	0.00	0.01	0.00	0.01
Gravel	4	0.00	0.00	0.01	0.00	0.01
Gravel	6	0.01	0.00	0.01	0.01	0.01
Wood	0	0.00	0.00	0.01	0.00	0.01
Wood	1	0.07	0.09	0.14	0.10	0.04
Wood	2	0.07	0.17	0.23	0.16	0.08
Wood	4	0.01	0.08	0.07	0.05	0.04
Wood	6	0.01	0.00	0.01	0.01	0.01
Tire	0	0.00	0.00	0.01	0.00	0.01
Tire	1	0.13	0.04	0.03	0.07	0.06
Tire	2	0.03	0.01	0.01	0.02	0.01
Tire	4	0.01	0.00	0.01	0.01	0.01
Tire	6	0.01	0.00	0.02	0.01	0.01
Sand-Wood	0	0.01	0.00	0.01	0.01	0.01
Sand-Wood	1	0.01	0.01	0.01	0.01	0.00
Sand-Wood	2	0.04	0.02	0.03	0.03	0.01
Sand-Wood	4	0.04	0.03	0.03	0.03	0.01
Sand-Wood	6	0.03	0.03	0.02	0.03	0.01
Gravel-Wood	0	0.01	0.00	0.01	0.01	0.01
Gravel-Wood	1	0.05	0.09	0.10	0.08	0.03
Gravel-Wood	2	0.11	0.15	0.17	0.14	0.03
Gravel-Wood	4	0.04	0.12	0.17	0.11	0.07
Gravel-Wood	6	0.01	0.02	0.05	0.03	0.02
Sand-Tire	0	0.01	0.00	0.01	0.01	0.01
Sand-Tire	1	0.10	0.09	0.02	0.07	0.04
Sand-Tire	2	0.01	0.17	0.04	0.07	0.09
Sand-Tire	4	0.12	0.12	0.04	0.09	0.05
Sand-Tire	6	0.00	0.05	0.02	0.02	0.03
Gravel-Tire	0	0.01	0.00	0.01	0.01	0.01
Gravel-Tire	1	0.04	0.04	0.03	0.04	0.01
Gravel-Tire	2	0.04	0.03	0.04	0.04	0.01
Gravel-Tire	4	0.03	0.02	0.02	0.02	0.01
Gravel-Tire	6	0.00	0.00	0.01	0.00	0.01

132

Table A.7. Acclimated anoxic microcosm NO_3^--N data.

Media	Incubation time (hr)	Sample 1 (hr)	Sample 2 (hr)	Sample 3 (hr)	Average (mg/L)	Standard deviation (mg/L)
Sand	0	1.90	1.92	2.06	1.96	0.09
Sand	1	2.15	1.95	1.99	2.03	0.11
Sand	2	2.10	1.93	1.97	2.00	0.09
Sand	4	2.19	1.91	1.45	1.85	0.37
Sand	6	1.91	1.91	2.01	1.94	0.06
Gravel	0	1.90	1.92	2.06	1.96	0.09
Gravel	1	2.16	1.95	2.01	2.04	0.11
Gravel	2	2.11	1.95	1.99	2.02	0.08
Gravel	4	2.15	1.97	2.00	2.04	0.10
Gravel	6	2.16	1.94	2.03	2.04	0.11
Wood	0	1.90	1.92	2.06	1.96	0.09
Wood	1	1.01	0.98	0.90	0.96	0.06
Wood	2	0.41	0.46	0.40	0.42	0.03
Wood	4	0.02	0.05	0.03	0.03	0.02
Wood	6	0.00	0.00	0.00	0.00	0.00
Tire	0	1.90	1.92	2.06	1.96	0.09
Tire	1	0.43	0.42	0.50	0.45	0.04
Tire	2	0.03	0.04	0.06	0.04	0.02
Tire	4	0.00	0.00	0.00	0.00	0.00
Tire	6	0.01	0.00	0.00	0.00	0.01
Sand-Wood	0	1.90	1.92	1.94	1.92	0.02
Sand-Wood	1	1.52	1.45	1.55	1.51	0.05
Sand-Wood	2	1.16	1.17	1.23	1.19	0.04
Sand-Wood	4	0.60	0.65	0.68	0.64	0.04
Sand-Wood	6	0.19	0.37	0.33	0.30	0.09
Gravel-Wood	0	1.90	1.92	1.94	1.92	0.02
Gravel-Wood	1	1.06	1.02	1.21	1.10	0.10
Gravel-Wood	2	0.49	0.59	0.80	0.63	0.16
Gravel-Wood	4	0.02	0.14	0.28	0.15	0.13
Gravel-Wood	6	0.00	0.00	0.02	0.01	0.01
Sand-Tire	0	1.90	1.92	1.94	1.92	0.02
Sand-Tire	1	1.28	1.29	1.52	1.36	0.14
Sand-Tire	2	0.78	0.80	1.13	0.90	0.20
Sand-Tire	4	0.24	0.23	0.54	0.34	0.18
Sand-Tire	6	0.01	0.13	0.17	0.10	0.08
Gravel-Tire	0	1.90	1.92	1.94	1.92	0.02
Gravel-Tire	1	1.23	1.00	1.17	1.13	0.12
Gravel-Tire	2	0.74	0.64	0.77	0.72	0.07
Gravel-Tire	4	0.22	0.19	0.25	0.22	0.03
Gravel-Tire	6	0.00	0.00	0.02	0.01	0.01

Table A.8. Acclimated anoxic microcosm Org-N data.

Media	Incubation time (hr)	Sample 1 (hr)	Sample 2 (hr)	Sample 3 (hr)	Average (mg/L)	Standard deviation (mg/L)
Sand	0	0.9	0.10	0.26	0.42	0.42
Sand	6	0.47	0.23	0.42	0.37	0.13
Gravel	0	0.19	0.10	0.26	0.18	0.08
Gravel	6	0.08	0.21	0.23	0.17	0.08
Wood	0	0.19	0.10	0.26	0.18	0.08
Wood	6	0.28	0.30	0.31	0.30	0.02
Tire	0	0.19	0.10	0.26	0.18	0.08
Tire	6	0.42	0.38	0.42	0.41	0.02
Sand-Wood	0	0.30	0.18	0.27	0.25	0.06
Sand-Wood	6	0.39	0.24	0.38	0.34	0.08
Gravel-Wood	0	0.30	0.18	0.27	0.25	0.06
Gravel-Wood	6	0.33	0.36	0.17	0.29	0.10
Sand-Tire	0	0.30	0.18	0.27	0.25	0.06
Sand-Tire	6	0.79	0.46	0.74	0.66	0.18
Gravel-Tire	0	0.30	0.18	0.27	0.25	0.06
Gravel-Tire	6	0.36	0.34	0.27	0.32	0.05

134

Table A.9. Acclimated anoxic microcosm PO_4^{3-} data.

Media	Incubation time (hr)	Sample 1 (hr)	Sample 2 (hr)	Sample 3 (hr)	Average (mg/L)	Standard deviation (mg/L)
Sand	0	0.08	0.08	0.12	0.09	0.02
Sand	1	0.15	0.10	0.13	0.13	0.03
Sand	2	0.12	0.10	0.13	0.12	0.02
Sand	4	0.24	0.11	0.05	0.13	0.10
Sand	6	0.15	0.11	0.14	0.13	0.02
Gravel	0	0.08	0.08	0.12	0.09	0.02
Gravel	1	0.11	0.14	0.13	0.13	0.02
Gravel	2	0.12	0.11	0.13	0.12	0.01
Gravel	4	0.11	0.11	0.14	0.12	0.02
Gravel	6	0.13	0.13	0.13	0.13	0.00
Wood	0	0.08	0.08	0.12	0.09	0.02
Wood	1	0.14	0.08	0.11	0.11	0.03
Wood	2	0.09	0.07	0.11	0.09	0.02
Wood	4	0.08	0.07	0.11	0.09	0.02
Wood	6	0.09	0.07	0.11	0.09	0.02
Tire	0	0.08	0.08	0.12	0.09	0.02
Tire	1	0.03	0.00	0.03	0.02	0.02
Tire	2	0.03	0.00	0.03	0.02	0.02
Tire	4	0.04	0.00	0.04	0.03	0.02
Tire	6	0.05	0.00	0.05	0.03	0.03
Sand-Wood	0	0.08	0.08	0.11	0.09	0.02
Sand-Wood	1	0.05	0.05	0.05	0.05	0.00
Sand-Wood	2	0.04	0.03	0.03	0.03	0.01
Sand-Wood	4	0.03	0.02	0.00	0.02	0.02
Sand-Wood	6	0.03	0.03	0.00	0.02	0.02
Gravel-Wood	0	0.08	0.08	0.11	0.09	0.02
Gravel-Wood	1	0.06	0.04	0.06	0.05	0.01
Gravel-Wood	2	0.05	0.03	0.04	0.04	0.01
Gravel-Wood	4	0.05	0.02	0.03	0.03	0.02
Gravel-Wood	6	0.07	0.03	0.02	0.04	0.03
Sand-Tire	0	0.08	0.08	0.11	0.09	0.02
Sand-Tire	1	0.05	0.05	0.06	0.05	0.01
Sand-Tire	2	0.03	0.04	0.05	0.04	0.01
Sand-Tire	4	0.00	0.03	0.03	0.02	0.02
Sand-Tire	6	0.00	0.05	0.03	0.03	0.03
Gravel-Tire	0	0.08	0.08	0.11	0.09	0.02
Gravel-Tire	1	0.07	0.05	0.06	0.06	0.01
Gravel-Tire	2	0.05	0.04	0.05	0.05	0.01
Gravel-Tire	4	0.04	0.05	0.03	0.04	0.01
Gravel-Tire	6	0.06	0.05	0.06	0.06	0.01

135

Table A.10. Acclimated anoxic microcosm SO_4^{2-}-S data.

Media	Incubation time (hr)	Sample 1 (hr)	Sample 2 (hr)	Sample 3 (hr)	Average (mg/L)	Standard deviation (mg/L)
Sand	0	19.27	18.11	23.25	20.21	2.70
Sand	1	20.58	18.29	23.22	20.70	2.47
Sand	2	20.05	18.02	22.90	20.32	2.45
Sand	4	26.74	17.95	20.69	21.79	4.50
Sand	6	21.85	17.92	22.94	20.90	2.64
Gravel	0	19.27	18.11	23.25	20.21	2.70
Gravel	1	20.88	18.24	23.04	20.72	2.40
Gravel	2	20.40	18.17	22.47	20.35	2.15
Gravel	4	20.22	18.30	22.52	20.35	2.11
Gravel	6	20.87	18.01	22.70	20.53	2.36
Wood	0	19.27	18.11	23.25	20.21	2.70
Wood	1	19.70	17.47	21.93	19.70	2.23
Wood	2	19.09	17.09	21.45	19.21	2.18
Wood	4	16.76	17.13	20.78	18.22	2.22
Wood	6	18.24	15.73	19.64	17.87	1.98
Tire	0	19.27	18.11	23.25	20.21	2.70
Tire	1	17.93	16.71	21.03	18.56	2.23
Tire	2	17.11	16.50	20.64	18.08	2.24
Tire	4	15.42	15.38	19.24	16.68	2.22
Tire	6	13.83	13.47	17.58	14.96	2.28
Sand-Wood	0	20.34	19.00	22.86	20.73	1.96
Sand-Wood	1	20.20	18.20	22.90	20.43	2.36
Sand-Wood	2	19.89	18.42	22.41	20.24	2.02
Sand-Wood	4	19.73	18.41	22.56	20.23	2.12
Sand-Wood	6	19.99	18.92	22.51	20.47	1.84
Gravel-Wood	0	20.34	19.00	22.86	20.73	1.96
Gravel-Wood	1	19.63	18.25	22.11	20.00	1.96
Gravel-Wood	2	19.16	18.36	22.08	19.87	1.96
Gravel-Wood	4	18.70	17.88	21.88	19.49	2.11
Gravel-Wood	6	17.39	18.01	21.27	18.89	2.08
Sand-Tire	0	20.34	19.00	22.86	20.73	1.96
Sand-Tire	1	20.18	18.26	22.72	20.39	2.24
Sand-Tire	2	20.26	18.46	22.67	20.46	2.11
Sand-Tire	4	20.26	17.95	22.52	20.24	2.29
Sand-Tire	6	16.36	18.06	22.32	18.91	3.07
Gravel-Tire	0	20.34	19.00	22.86	20.73	1.96
Gravel-Tire	1	19.92	18.12	22.12	20.05	2.00
Gravel-Tire	2	19.69	18.11	22.33	20.04	2.13
Gravel-Tire	4	18.97	18.01	22.21	19.73	2.20
Gravel-Tire	6	18.20	18.24	22.17	19.54	2.28

136

Table A.11. Acclimated anoxic microcosm TSS data.

Media	Incubation time (hr)	Sample 1 (hr)	Sample 2 (hr)	Sample 3 (hr)	Average (mg/L)	Standard deviation (mg/L)
Sand	0	3.40	5.45	3.40	4.08	1.18
Sand	6	6.70	6.50	6.99	6.73	0.25
Gravel	0	3.40	5.45	3.40	4.08	1.18
Gravel	6	5.90	7.31	6.58	6.60	0.71
Wood	0	3.40	5.45	3.40	4.08	1.18
Wood	6	43.00	16.77	15.56	25.11	15.51
Tire	0	3.40	5.45	3.40	4.08	1.18
Tire	6	12.30	8.53	15.04	11.96	3.27
Sand-Wood	0	2.05	6.22	4.67	4.31	2.11
Sand-Wood	6	6.10	17.50	10.00	11.20	5.79
Gravel-Wood	0	2.05	6.22	4.67	4.31	2.11
Gravel-Wood	6	21.60	19.19	18.53	19.77	1.62
Sand-Tire	0	2.05	6.22	4.67	4.31	2.11
Sand-Tire	6	7.90	9.40	4.93	7.41	2.27
Gravel-Tire	0	2.05	6.22	4.67	4.31	2.11
Gravel-Tire	6	14.90	15.84	14.48	15.07	0.70

Table A.12. Acclimated anoxic microcosm VSS data.

Media	Incubation time (hr)	Sample 1 (hr)	Sample 2 (hr)	Sample 3 (hr)	Average (mg/L)	Standard deviation (mg/L)
Sand	0	4.00	4.67	3.07	3.91	0.80
Sand	6	4.90	4.19	4.18	4.42	0.41
Gravel	0	4.00	4.67	3.07	3.91	0.80
Gravel	6	2.30	3.93	4.08	3.44	0.99
Wood	0	4.00	4.67	3.07	3.91	0.80
Wood	6	39.10	14.80	14.16	22.69	14.22
Tire	0	4.00	4.67	3.07	3.91	0.80
Tire	6	11.00	7.13	11.92	10.02	2.54
Sand-Wood	0	1.50	4.93	3.70	3.38	1.74
Sand-Wood	6	8.70	13.21	6.94	9.62	3.23
Gravel-Wood	0	1.50	4.93	3.70	3.38	1.74
Gravel-Wood	6	14.80	13.93	12.43	13.72	1.20
Sand-Tire	0	1.50	4.93	3.70	3.38	1.74
Sand-Tire	6	4.60	5.52	4.12	4.75	0.71
Gravel-Tire	0	1.50	4.93	3.70	3.38	1.74
Gravel-Tire	6	7.30	7.21	7.45	7.32	0.12

137

Table A.13. Aerobic, anoxic and killed control gravel-wood microcosm TN data.

Condition	Incubation time (hr)	Sample 1 (hr)	Sample 2 (hr)	Sample 3 (hr)	Average (mg/L)	Standard deviation (mg/L)
Anoxic	0	2.32	2.32	2.32	2.32	0.00
Anoxic	6	0.48	0.46	0.53	0.49	0.04
Aerobic	0	2.53	2.53	2.53	2.53	0.00
Aerobic	6	0.54	0.82	0.87	0.74	0.18
Killed control	0	2.23	2.23	2.23	2.23	0.00
Killed control	6	4.73	4.84	4.82	4.80	0.06

Table A.14. Aerobic, anoxic and killed control gravel-wood microcosm DOC data.

Condition	Incubation time (hr)	Sample 1 (hr)	Sample 2 (hr)	Sample 3 (hr)	Average (mg/L)	Standard deviation (mg/L)
Anoxic	0	3.93	3.93	3.93	3.93	0.00
Anoxic	6	5.16	4.77	4.76	4.90	0.23
Aerobic	0	3.86	3.86	3.86	3.86	0.00
Aerobic	6	4.45	4.95	4.36	4.59	0.32
Killed control	0	3.83	3.83	3.83	3.83	0.00
Killed control	6	66.48	76.5	71.2	71.39	5.01

Table A.15. Aerobic, anoxic and killed control gravel-wood microcosm DO data.

Condition	Incubation time (hr)	Sample 1 (hr)	Sample 2 (hr)	Sample 3 (hr)	Average (mg/L)	Standard deviation (mg/L)
Anoxic	0	1.00	1.00	1.00	1.00	0.00
Anoxic	6	0.03	0.05	0.00	0.03	0.03
Aerobic	0	4.92	4.62	5.92	5.15	0.68
Aerobic	1	1.13	1.64	1.91	1.56	0.40
Aerobic	2	0.58	0.82	1.11	0.84	0.27
Aerobic	3	0.57	0.7	0.15	0.47	0.29
Aerobic	4	0.37	0.53	0.05	0.32	0.24
Aerobic	6	0.31	0.03	0.01	0.12	0.17
Killed control	0	1.00	1.00	1.00	1.00	0.00

138

Table A.16. Aerobic, anoxic and killed control gravel-wood microcosm NH_4^+-N data.

Condition	Incubation time (hr)	Sample 1 (hr)	Sample 2 (hr)	Sample 3 (hr)	Average (mg/L)	Standard deviation (mg/L)
Anoxic	0	0.04	0.04	0.04	0.04	0.00
Anoxic	1	0.00	0.00	0.00	0.00	0.00
Anoxic	2	0.00	0.00	0.00	0.00	0.00
Anoxic	3	0.00	0.00	0.00	0.00	0.00
Anoxic	4	0.00	0.00	0.00	0.00	0.00
Anoxic	6	0.00	0.00	0.00	0.00	0.00
Aerobic	0	0.01	0.01	0.01	0.01	0.00
Aerobic	1	0.00	0.00	0.00	0.00	0.00
Aerobic	2	0.00	0.00	0.00	0.00	0.00
Aerobic	3	0.00	0.00	0.00	0.00	0.00
Aerobic	4	0.00	0.00	0.00	0.00	0.00
Aerobic	6	0.00	0.00	0.00	0.00	0.00
Killed control	0	0.00	0.00	0.00	0.00	0.00
Killed control	1	0.16	0.31	0.45	0.31	0.15
Killed control	2	0.00	0.43	0.61	0.35	0.31
Killed control	3	0.61	0.66	0.77	0.68	0.08
Killed control	4	0.77	0.77	0.86	0.80	0.05
Killed control	6	0.89	0.95	1.01	0.95	0.06

139

Table A.17. Aerobic, anoxic and killed control gravel-wood microcosm NO_2^--N data.

Condition	Incubation time (hr)	Sample 1 (hr)	Sample 2 (hr)	Sample 3 (hr)	Average (mg/L)	Standard deviation (mg/L)
Anoxic	0	0.07	0.07	0.07	0.07	0.00
Anoxic	1	0.07	0.08	0.08	0.08	0.01
Anoxic	2	0.07	0.10	0.08	0.08	0.02
Anoxic	3	0.08	0.10	0.08	0.09	0.01
Anoxic	4	0.07	0.10	0.08	0.08	0.02
Anoxic	6	0.08	0.08	0.07	0.08	0.01
Aerobic	0	0.03	0.03	0.03	0.03	0.00
Aerobic	1	0.03	0.02	0.02	0.02	0.01
Aerobic	2	0.03	0.03	0.03	0.03	0.00
Aerobic	3	0.04	0.02	0.03	0.03	0.01
Aerobic	4	0.04	0.04	0.04	0.04	0.00
Aerobic	6	0.04	0.04	0.04	0.04	0.00
Killed control	0	0.08	0.08	0.08	0.08	0.00
Killed control	1	0.08	0.08	0.08	0.08	0.00
Killed control	2	0.08	0.08	0.09	0.08	0.01
Killed control	3	0.08	0.08	0.09	0.08	0.01
Killed control	4	0.09	0.09	0.09	0.09	0.00
Killed control	6	0.09	0.09	0.09	0.09	0.00

Table A.18. Aerobic, anoxic and killed control gravel-wood microcosm NO_3^--N data.

Condition	Incubation time (hr)	Sample 1 (hr)	Sample 2 (hr)	Sample 3 (hr)	Average (mg/L)	Standard deviation (mg/L)
Anoxic	0	1.88	1.88	1.88	1.88	0.00
Anoxic	1	1.45	1.21	1.40	1.35	0.13
Anoxic	2	1.09	0.99	1.02	1.03	0.05
Anoxic	3	0.76	0.40	0.69	0.62	0.19
Anoxic	4	0.49	0.26	0.43	0.39	0.12
Anoxic	6	0.05	0.04	0.13	0.07	0.05
Aerobic	0	1.96	1.96	1.96	1.96	0.00
Aerobic	1	1.43	1.23	1.52	1.39	0.15
Aerobic	2	1.17	1.26	1.37	1.27	0.10
Aerobic	3	0.88	0.57	1.18	0.88	0.31
Aerobic	4	0.63	0.69	0.97	0.76	0.18
Aerobic	6	0.19	0.42	0.55	0.39	0.18
Killed control	0	1.92	1.92	1.92	1.92	0.00
Killed control	1	1.80	1.76	1.79	1.78	0.02
Killed control	2	1.76	2.01	1.77	1.85	0.14
Killed control	3	1.80	1.78	1.77	1.78	0.02
Killed control	4	1.87	1.78	1.78	1.81	0.05
Killed control	6	1.82	1.82	1.87	1.84	0.03

Table A.19. Aerobic, anoxic and killed control gravel-wood microcosm Org-N data.

Condition	Incubation time (hr)	Sample 1 (hr)	Sample 2 (hr)	Sample 3 (hr)	Average (mg/L)	Standard deviation (mg/L)
Anoxic	0	0.33	0.33	0.33	0.33	0.00
Anoxic	6	0.36	0.33	0.33	0.34	0.02
Aerobic	0	0.54	0.54	0.54	0.54	0.00
Aerobic	6	0.31	0.36	0.28	0.32	0.04
Killed control	0	0.22	0.22	0.22	0.22	0.00
Killed control	6	1.93	1.97	1.86	1.92	0.06

141

Table A.20. Aerobic, anoxic and killed control gravel-wood microcosm PO_4^{3-}-P data.

Condition	Incubation time (hr)	Sample 1 (hr)	Sample 2 (hr)	Sample 3 (hr)	Average (mg/L)	Standard deviation (mg/L)
Anoxic	0	0.18	0.18	0.18	0.18	0.00
Anoxic	1	0.16	0.18	0.17	0.17	0.01
Anoxic	2	0.15	0.16	0.16	0.16	0.01
Anoxic	3	0.15	0.16	0.16	0.16	0.01
Anoxic	4	0.15	0.16	0.16	0.16	0.01
Anoxic	6	0.15	0.16	0.15	0.15	0.01
Aerobic	0	0.12	0.12	0.12	0.12	0.00
Aerobic	1	0.10	0.09	0.11	0.10	0.01
Aerobic	2	0.09	0.08	0.10	0.09	0.01
Aerobic	3	0.09	0.00	0.09	0.06	0.05
Aerobic	4	0.09	0.08	0.10	0.09	0.01
Aerobic	6	0.09	0.08	0.08	0.08	0.01
Killed control	0	0.08	0.08	0.08	0.08	0.00
Killed control	1	0.37	0.29	0.27	0.31	0.05
Killed control	2	0.45	0.40	0.41	0.42	0.03
Killed control	3	0.62	0.56	0.51	0.56	0.06
Killed control	4	0.73	0.64	0.56	0.64	0.09
Killed control	6	0.83	0.74	0.66	0.74	0.09

Table A.21. Aerobic, anoxic and killed control gravel-wood microcosm SO_4^{2-}-S data.

Condition	Incubation time (hr)	Sample 1 (hr)	Sample 2 (hr)	Sample 3 (hr)	Average (mg/L)	Standard deviation (mg/L)
Anoxic	0	35.40	35.40	35.40	35.40	0.00
Anoxic	1	34.69	34.75	35.24	34.89	0.30
Anoxic	2	34.51	34.55	35.16	34.74	0.36
Anoxic	3	34.96	35.02	34.88	34.95	0.07
Anoxic	4	34.31	34.73	34.63	34.56	0.22
Anoxic	6	33.91	34.41	34.21	34.18	0.25
Aerobic	0	35.63	35.63	35.63	35.63	0.00
Aerobic	1	35.00	30.02	35.23	33.42	2.94
Aerobic	2	35.26	35.08	35.42	35.25	0.17
Aerobic	3	34.37	24.10	35.36	31.28	6.23
Aerobic	4	35.45	35.41	35.27	35.38	0.09
Aerobic	6	35.63	35.72	35.40	35.58	0.17
Killed control	0	38.84	38.84	38.84	38.84	0.00
Killed control	1	43.45	42.89	43.70	43.35	0.41
Killed control	2	43.12	44.58	44.71	44.14	0.88
Killed control	3	45.78	46.45	46.22	46.15	0.34
Killed control	4	46.80	47.67	47.71	47.39	0.51
Killed control	6	50.56	51.87	49.93	50.79	0.99

Table A.22. Aerobic, anoxic and killed control gravel-wood microcosm TSS data.

Condition	Incubation time (hr)	Sample 1 (hr)	Sample 2 (hr)	Sample 3 (hr)	Average (mg/L)	Standard deviation (mg/L)
Anoxic	0	2.62	2.62	2.62	2.62	0.00
Anoxic	6	37.00	25.95	27.25	30.07	6.04
Aerobic	0	3.28	3.28	3.28	3.28	0.00
Aerobic	6	28.90	21.60	17.15	22.55	5.93
Killed control	0	2.20	2.20	2.20	2.20	0.00
Killed control	6	37.85	34.20	29.30	33.78	4.29

143

Table A.23. Aerobic, anoxic and killed control gravel-wood microcosm VSS data.

Condition	Incubation time (hr)	Sample 1 (hr)	Sample 2 (hr)	Sample 3 (hr)	Average (mg/L)	Standard deviation (mg/L)
Anoxic	0	1.22	1.22	1.22	1.22	0.00
Anoxic	6	26.65	19.55	21.05	22.42	3.74
Aerobic	0	2.60	2.60	2.60	2.60	0.00
Aerobic	6	19.35	12.50	14.35	15.40	3.54
Killed control	0	1.87	1.87	1.87	1.87	0.00
Killed control	6	34.35	30.45	24.25	29.68	5.09

Storm Event Study Data

Table B.1. Storm event start time.

Storm event	Month	Day	Year	Time	AM/PM
1	11	18	2012	12:56	PM
2	12	5	2012	10:35	PM
3	12	10	2012	11:15	AM
4	12	19	2012	3:45	PM
5	12	21	2012	6:15	AM
6	12	30	2012	4:00	PM
7	1	8	2013	7:10	AM
8	1	17	2013	5:48	AM
9	2	17	2013	7:00	AM
10	3	29	2013	8:45	PM
11	5	6	2013	6:45	PM

Table B.2. Storm event #1 flow data for the 30 cm column.

Theoretical detention time (hr)	Theoretical flow rate (mL/min)	Flow rate 1 (mL/min)	Flow rate 2 (mL/min)	Average flow rate (mL/min)
1	29.27	30	31	30.5
2	14.63	15	15	15
3	9.76	10	8	9
4	7.32	7	7.25	7.1
6	4.88	5	5	5
9	3.25	3.25	3.5	3.4

145

Table B.3. Storm event #1 flow data for the 45 cm column.

Theoretical detention time (hr)	Theoretical flow rate (mL/min)	Flow rate 1 (mL/min)	Flow rate 2 (mL/min)	Average flow rate (mL/min)
1	44.43	44	48	46
2	22.22	23	23	23
3	14.81	15	14	14.5
4	11.11	11	11	11
6	7.41	7.5	7.5	7.5
9	4.94	5	4.5	4.8

Table B.4. Storm event #1 flow data for the 60 cm column.

Theoretical detention time (hr)	Theoretical flow rate (mL/min)	Flow rate 1 (mL/min)	Flow rate 2 (mL/min)	Average flow rate (mL/min)
1	59.33	59	60	59.5
2	29.67	30	31	30.5
3	19.78	20	20	20
4	14.83	15	14	14.5
6	9.89	9.5	10	9.8
9	6.59	6.75	6.5	6.6

Table B.5. Storm event #1 Influent TN data.

Sample time (hr)	Theoretical detention time (hr)	Sample 1 (mg/L)	Sample 2 (mg/L)	Sample 3 (mg/L)	Average (mg/L)	Standard deviation (mg/L)
0.25	-	2.29	2.26	2.31	2.29	0.02
1.25	1	2.35	2.29	2.30	2.31	0.03
4	2	2.30	2.23	2.31	2.28	0.04
8.25	3	2.25	2.22	2.30	2.26	0.04
14	4	2.32	2.29	2.30	2.31	0.01
22.5	6	2.30	2.28	2.26	2.28	0.02
35.25	9	2.37	2.34	2.42	2.38	0.04

146

Table B.6. Storm event #1 TN data for the 30 cm column.

Sample time (hr)	Theoretical detention time (hr)	Sample 1 (mg/L)	Sample 2 (mg/L)	Sample 3 (mg/L)	Average (mg/L)	Standard deviation (mg/L)
0.25	-	0.48	0.47	0.47	0.47	0.01
1.25	1	0.92	0.92	0.94	0.93	0.01
4	2	1.37	1.40	1.41	1.39	0.02
8.25	3	1.06	1.07	1.07	1.07	0.01
14	4	0.94	0.93	0.94	0.94	0.00
22.5	6	0.62	0.62	0.61	0.62	0.01
35.25	9	0.45	0.44	0.45	0.45	0.01

Table B.7. Storm event #1 TN data for the 45 cm column.

Sample time (hr)	Theoretical detention time (hr)	Sample 1 (mg/L)	Sample 2 (mg/L)	Sample 3 (mg/L)	Average (mg/L)	Standard deviation (mg/L)
0.25	-	0.44	0.45	0.45	0.45	0.01
1.25	1	0.67	0.67	0.68	0.67	0.01
4	2	1.35	1.33	1.35	1.34	0.01
8.25	3	0.95	1.00	0.99	0.98	0.03
14	4	0.69	0.71	0.72	0.71	0.02
22.5	6	0.47	0.47	0.48	0.47	0.01
35.25	9	0.44	0.45	0.46	0.45	0.01

Table B.8. Storm event #1 TN data for the 60 cm column.

Sample time (hr)	Theoretical detention time (hr)	Sample 1 (mg/L)	Sample 2 (mg/L)	Sample 3 (mg/L)	Average (mg/L)	Standard deviation (mg/L)
0.25	-	0.46	0.47	0.48	0.47	0.01
1.25	1	0.80	0.82	0.85	0.83	0.03
4	2	1.42	1.46	1.46	1.45	0.02
8.25	3	1.09	1.05	1.07	1.07	0.02
14	4	0.67	0.64	0.67	0.66	0.02
22.5	6	0.38	0.40	0.40	0.40	0.01
35.25	9	0.43	0.42	0.42	0.42	0.01

147

Table B.9. Storm event #1 Influent DOC data.

Sample time (hr)	Theoretical detention time (hr)	Sample 1 (mg/L)	Sample 2 (mg/L)	Sample 3 (mg/L)	Average (mg/L)	Standard deviation (mg/L)
0.25	-	3.87	3.95	3.97	3.93	0.05
1.25	1	4.65	4.65	4.67	4.65	0.01
4	2	4.50	4.58	4.67	4.58	0.08
8.25	3	4.31	4.18	4.33	4.27	0.08
14	4	4.03	4.14	4.11	4.09	0.06
22.5	6	4.03	3.99	4.14	4.05	0.08
35.25	9	4.55	4.72	4.67	4.65	0.08

Table B.10. Storm event #1 DOC data for the 30 cm column.

Sample time (hr)	Theoretical detention time (hr)	Sample 1 (mg/L)	Sample 2 (mg/L)	Sample 3 (mg/L)	Average (mg/L)	Standard deviation (mg/L)
0.25	-	7.50	7.74	7.74	7.66	0.14
1.25	1	6.16	6.22	6.29	6.22	0.07
4	2	4.66	4.48	4.59	4.57	0.09
8.25	3	5.00	4.93	4.96	4.96	0.03
14	4	4.87	4.84	5.01	4.91	0.09
22.5	6	5.20	5.09	5.21	5.17	0.06
35.25	9	6.07	5.96	6.14	6.06	0.09

Table B.11. Storm event #1 DOC data for the 45 cm column.

Sample time (hr)	Theoretical detention time (hr)	Sample 1 (mg/L)	Sample 2 (mg/L)	Sample 3 (mg/L)	Average (mg/L)	Standard deviation (mg/L)
0.25	-	9.82	10.03	10.06	9.97	0.13
1.25	1	6.99	6.88	6.80	6.89	0.09
4	2	4.79	4.76	4.82	4.79	0.03
8.25	3	4.99	5.02	5.04	5.02	0.03
14	4	4.37	4.30	4.29	4.32	0.04
22.5	6	5.60	5.40	5.52	5.51	0.10
35.25	9	6.77	6.68	6.92	6.79	0.12

Table B.12. Storm event #1 DOC data for the 60 cm column.

Sample time (hr)	Theoretical detention time (hr)	Sample 1 (mg/L)	Sample 2 (mg/L)	Sample 3 (mg/L)	Average (mg/L)	Standard deviation (mg/L)
0.25	-	8.47	8.19	8.33	8.33	0.14
1.25	1	6.10	6.07	6.25	6.14	0.10
4	2	4.81	4.83	4.99	4.88	0.10
8.25	3	4.83	4.61	4.70	4.71	0.11
14	4	4.37	4.53	4.53	4.47	0.09
22.5	6	5.40	5.56	5.53	5.50	0.08
35.25	9	6.05	6.00	6.07	6.04	0.03

Table B.13. Storm event #1 DO data.

Sample time (hr)	Theoretical detention time (hr)	Influent (mg/L)	60 cm column (mg/L)	45 cm column (mg/L)	30 cm column (mg/L)
0.25	-	5.76	0	0	0
1.25	1	9.7	0.25	0.15	0.01
4	2	8	0	0.1	0.21
8.25	3	6.2	0.14	0.07	0.19
14	4	5.5	0	0.07	0.08
22.5	6	5.3	0.07	0.23	0.09
35.25	9	5	0.01	0.05	0.06

Table B.14. Storm event #1 pH data.

Sample time (hr)	Theoretical detention time (hr)	Influent (mg/L)	60 cm column (mg/L)	45 cm column (mg/L)	30 cm column (mg/L)
0.25	-	6.94	6.85	6.85	6.85
1.25	1	7.23	6.93	6.89	6.96
4	2	7.46	6.83	6.83	6.88
8.25	3	7.35	6.94	6.88	6.94
14	4	7.46	6.9	6.92	6.94
22.5	6	7.45	6.94	6.93	6.94
35.25	9	7.42	6.94	6.88	6.97

149

Table B.15. Storm event #1 NH_4^+-N data.

Sample time (hr)	Theoretical detention time (hr)	Influent (mg/L)	60 cm column (mg/L)	45 cm column (mg/L)	30 cm column (mg/L)
0.25	-	0.00	0.00	0.00	0.00
1.25	1	0.00	0.00	0.00	0.00
4	2	0.00	0.00	0.00	0.00
8.25	3	0.00	0.00	0.00	0.00
14	4	0.00	0.00	0.00	0.00
22.5	6	0.00	0.00	0.00	0.00
35.25	9	0.00	0.00	0.00	0.00

Table B.16. Storm event #1 NO_2^--N data.

Sample time (hr)	Theoretical detention time (hr)	Influent (mg/L)	60 cm column (mg/L)	45 cm column (mg/L)	30 cm column (mg/L)
0.25	-	0.01	0.03	0.03	0.03
1.25	1	0.01	0.02	0.02	0.03
4	2	0.01	0.06	0.08	0.03
8.25	3	0.02	0.09	0.10	0.08
14	4	0.01	0.11	0.11	0.08
22.5	6	0.02	0.02	0.02	0.04
35.25	9	0.01	0.00	0.02	0.02

Table B.17. Storm event #1 NO_3^--N data.

Sample time (hr)	Theoretical detention time (hr)	Influent (mg/L)	60 cm column (mg/L)	45 cm column (mg/L)	30 cm column (mg/L)
0.25	-	2.00	0.01	0.01	0.01
1.25	1	1.97	0.36	0.26	0.46
4	2	1.95	0.92	0.82	0.90
8.25	3	1.95	0.56	0.47	0.55
14	4	1.95	0.18	0.25	0.39
22.5	6	1.95	0.11	0.01	0.06
35.25	9	1.95	0.13	0.01	0.01

150

Table B.18. Storm event #1 Org-N data.

Sample time (hr)	Theoretical detention time (hr)	Influent (mg/L)	60 cm column (mg/L)	45 cm column (mg/L)	30 cm column (mg/L)
0.25	-	0.28	0.43	0.41	0.44
1.25	1	0.33	0.45	0.39	0.44
4	2	0.32	0.47	0.44	0.46
8.25	3	0.29	0.41	0.41	0.44
14	4	0.34	0.37	0.34	0.46
22.5	6	0.32	0.26	0.45	0.52
35.25	9	0.41	0.29	0.42	0.42

Table B.19. Storm event #1 PO_4^{3-}-P data.

Sample time (hr)	Theoretical detention time (hr)	Influent (mg/L)	60 cm column (mg/L)	45 cm column (mg/L)	30 cm column (mg/L)
0.25	-	0.09	0.10	0.07	0.11
1.25	1	0.09	0.08	0.07	0.08
4	2	0.09	0.00	0.00	0.00
8.25	3	0.09	0.00	0.00	0.00
14	4	0.09	0.00	0.00	0.00
22.5	6	0.09	0.05	0.03	0.03
35.25	9	0.09	0.04	0.07	0.10

Table B.20. Storm event #1 SO_4^{2-}-S data.

Sample time (hr)	Theoretical detention time (hr)	Influent (mg/L)	60 cm column (mg/L)	45 cm column (mg/L)	30 cm column (mg/L)
0.25	-	54.76	36.23	30.75	36.58
1.25	1	54.83	45.28	43.28	44.76
4	2	54.61	55.29	54.56	54.46
8.25	3	54.62	55.47	54.34	55.28
14	4	54.79	52.93	54.65	54.61
22.5	6	54.62	53.38	54.00	53.53
35.25	9	54.56	45.84	49.49	50.49

151

Table B.21. Storm event #1 TSS data.

Sample time (hr)	Theoretical detention time (hr)	Influent (mg/L)	60 cm column (mg/L)	45 cm column (mg/L)	30 cm column (mg/L)
0.25	-	6.28	1.46	1.18	2.84
1.25	1	6.28	3.94	4.06	3.96
4	2	6.14	3.32	3.30	2.93
8.25	3	6.30	2.40	2.80	2.40
14	4	5.92	2.91	2.25	2.06
22.5	6	4.86	2.13	2.04	2.14
35.25	9	4.04	1.99	1.76	1.87

Table B.22. Storm event #1 VSS data.

Sample time (hr)	Theoretical detention time (hr)	Influent (mg/L)	60 cm column (mg/L)	45 cm column (mg/L)	30 cm column (mg/L)
0.25	-	1.68	0.68	0.00	0.18
1.25	1	1.68	1.14	0.82	0.76
4	2	2.02	1.12	1.42	0.00
8.25	3	1.24	0.27	0.02	0.63
14	4	1.90	0.40	0.67	0.48
22.5	6	1.16	0.47	0.00	0.00
35.25	9	1.34	0.41	0.04	0.00

Table B.23. Storm event #2 flow data for the 30 cm column.

Theoretical detention time (hr)	Theoretical flow rate (mL/min)	Flow rate 1 (mL/min)	Flow rate 2 (mL/min)	Average flow rate (mL/min)
1	29.27			
2	14.63			
3	9.76			
4	7.32			
6	4.88			
9	3.25			

152

Table B.24. Storm event #2 flow data for the 45 cm column.

Theoretical detention time (hr)	Theoretical flow rate (mL/min)	Flow rate 1 (mL/min)	Flow rate 2 (mL/min)	Average flow rate (mL/min)
1	44.43	44.5	44	44.3
2	22.22	22.25	21.5	21.9
3	14.81	15	14	14.5
4	11.11	11	11.25	11.1
6	7.41	7.75	7.75	7.75
9	4.94	5	5	5

Table B.25. Storm event #2 flow data for the 60 cm column.

Theoretical detention time (hr)	Theoretical flow rate (mL/min)	Flow rate 1 (mL/min)	Flow rate 2 (mL/min)	Average flow rate (mL/min)
1	59.33	59.33	59.33	59.33
2	29.67	29.5	29.5	29.5
3	19.78	20	19	19.5
4	14.83	14.75	14.75	14.75
6	9.89	9.75	9.5	9.6
9	6.59	6.5	6.5	6.5

Table B.26. Storm event #2 Influent TN data.

Sample time (hr)	Theoretical detention time (hr)	Sample 1 (mg/L)	Sample 2 (mg/L)	Sample 3 (mg/L)	Average (mg/L)	Standard deviation (mg/L)
0.25	-	2.37	2.34	2.42	2.38	0.04
1.25	1	2.45	2.52	2.54	2.50	0.04
4	2	2.57	2.59	2.62	2.59	0.03
8.25	3	2.40	2.34	2.43	2.39	0.05
14	4	2.42	2.40	2.41	2.41	0.01
22.5	6	2.46	2.54	2.54	2.51	0.05
35.25	9	2.40	2.31	2.38	2.36	0.05

153

Table B.27. Storm event #2 TN data for the 30 cm column.

Sample time (hr)	Theoretical detention time (hr)	Sample 1 (mg/L)	Sample 2 (mg/L)	Sample 3 (mg/L)	Average (mg/L)	Standard deviation (mg/L)
0.25	-	0.68	0.66	0.69	0.68	0.02
1.25	1	1.17	1.17	1.14	1.16	0.01
4	2	0.80	0.80	0.81	0.80	0.01
8.25	3	0.90	0.89	0.90	0.90	0.00
14	4	0.79	0.78	0.79	0.78	0.00
22.5	6	0.52	0.53	0.56	0.54	0.02
35.25	9	0.42	0.41	0.44	0.42	0.01

Table B.28. Storm event #2 TN data for the 45 cm column.

Sample time (hr)	Theoretical detention time (hr)	Sample 1 (mg/L)	Sample 2 (mg/L)	Sample 3 (mg/L)	Average (mg/L)	Standard deviation (mg/L)
0.25	-	0.66	0.62	0.63	0.64	0.02
1.25	1	1.17	1.23	1.20	1.20	0.03
4	2	0.45	0.44	0.45	0.45	0.00
8.25	3	0.46	0.45	0.45	0.45	0.00
14	4	0.52	0.51	0.51	0.51	0.01
22.5	6	0.45	0.45	0.45	0.45	0.00
35.25	9	0.42	0.40	0.42	0.41	0.01

Table B.29. Storm event #2 TN data for the 60 cm column.

Sample time (hr)	Theoretical detention time (hr)	Sample 1 (mg/L)	Sample 2 (mg/L)	Sample 3 (mg/L)	Average (mg/L)	Standard deviation (mg/L)
0.25	-	0.74	0.70	0.70	0.71	0.02
1.25	1	1.27	1.26	1.30	1.28	0.02
4	2	0.50	0.52	0.52	0.52	0.01
8.25	3	0.48	0.46	0.48	0.47	0.01
14	4	0.56	0.54	0.56	0.56	0.01
22.5	6	0.44	0.43	0.43	0.43	0.01
35.25	9	0.40	0.37	0.37	0.38	0.01

154

Table B.30. Storm event #2 Influent DOC data.

Sample time (hr)	Theoretical detention time (hr)	Sample 1 (mg/L)	Sample 2 (mg/L)	Sample 3 (mg/L)	Average (mg/L)	Standard deviation (mg/L)
0.25	-	4.55	4.72	4.67	4.65	0.08
1.25	1	5.05	4.92	5.05	5.01	0.07
4	2	4.60	4.56	4.75	4.64	0.10
8.25	3	4.31	4.41	4.47	4.40	0.08
14	4	4.49	4.41	4.38	4.43	0.05
22.5	6	4.86	4.83	4.93	4.87	0.05
35.25	9	5.10	4.96	4.98	5.01	0.08

Table B.31. Storm event #2 DOC data for the 30 cm column.

Sample time (hr)	Theoretical detention time (hr)	Sample 1 (mg/L)	Sample 2 (mg/L)	Sample 3 (mg/L)	Average (mg/L)	Standard deviation (mg/L)
0.25	-	86.70	84.41	84.57	85.22	1.28
1.25	1	38.52	38.82	37.41	38.25	0.74
4	2	7.53	7.41	7.28	7.41	0.13
8.25	3	4.88	5.02	5.11	5.00	0.12
14	4	4.77	4.79	4.73	4.76	0.03
22.5	6	4.89	4.83	4.83	4.85	0.03
35.25	9	5.74	5.54	5.56	5.62	0.11

Table B.32. Storm event #2 DOC data for the 45 cm column.

Sample time (hr)	Theoretical detention time (hr)	Sample 1 (mg/L)	Sample 2 (mg/L)	Sample 3 (mg/L)	Average (mg/L)	Standard deviation (mg/L)
0.25	-	126.87	130.95	132.54	130.12	2.92
1.25	1	53.43	51.30	52.39	52.37	1.07
4	2	6.45	6.51	6.65	6.54	0.10
8.25	3	5.28	5.14	5.34	5.25	0.10
14	4	5.05	5.04	5.11	5.07	0.04
22.5	6	5.02	4.84	4.96	4.94	0.09
35.25	9	5.75	5.65	5.76	5.72	0.06

155

Table B.33. Storm event #2 DOC data for the 60 cm column.

Sample time (hr)	Theoretical detention time (hr)	Sample 1 (mg/L)	Sample 2 (mg/L)	Sample 3 (mg/L)	Average (mg/L)	Standard deviation (mg/L)
0.25	-	125.85	123.00	126.74	125.20	1.95
1.25	1	44.96	43.85	44.53	44.44	0.56
4	2	5.85	5.91	6.04	5.93	0.10
8.25	3	5.15	5.17	5.25	5.19	0.06
14	4	4.67	4.75	4.67	4.70	0.05
22.5	6	5.21	5.25	5.23	5.23	0.02
35.25	9	5.55	5.61	5.75	5.64	0.11

Table B.34. Storm event #2 DO data.

Sample time (hr)	Theoretical detention time (hr)	Influent (mg/L)	60 cm column (mg/L)	45 cm column (mg/L)	30 cm column (mg/L)
0.25	-	5	0.05	0	0
1.25	1	4.98	0	0	0.12
4	2	4.82	0	0	0
8.25	3	5.24	0.09	0	0.03
14	4	5.8	0	0	0.01
22.5	6	6.2	0.06	0	0.06
35.25	9	4.92	0.04	0.05	0.11

Table B.35. Storm event #2 pH data.

Sample time (hr)	Theoretical detention time (hr)	Influent (mg/L)	60 cm column (mg/L)	45 cm column (mg/L)	30 cm column (mg/L)
0.25	-	7.42			
1.25	1	7.41	6.31	6.23	6.5
4	2	7.35	6.73	6.72	6.77
8.25	3	7.38	7.01	7.01	7.23
14	4	7.37	6.85	6.86	6.88
22.5	6	7.38	6.9	6.87	6.91
35.25	9	7.37	6.95	6.89	6.92

Figure B.36. Storm event #2 NH$_4^+$-N data.

Sample time (hr)	Theoretical detention time (hr)	Influent (mg/L)	60 cm column (mg/L)	45 cm column (mg/L)	30 cm column (mg/L)
0.25	-	0.00	0.07	0.02	0.06
1.25	1	0.00	0.05	0.02	0.03
4	2	0.00	0.00	0.00	0.00
8.25	3	0.00	0.00	0.00	0.00
14	4	0.00	0.00	0.00	0.00
22.5	6	0.00	0.00	0.00	0.00
35.25	9	0.00	0.00	0.00	0.00

Table B.37. Storm event #2 NO$_2^-$-N data.

Sample time (hr)	Theoretical detention time (hr)	Influent (mg/L)	60 cm column (mg/L)	45 cm column (mg/L)	30 cm column (mg/L)
0.25	-	0.01	0.07	0.07	0.07
1.25	1	0.01	0.04	0.07	0.05
4	2	0.02	0.02	0.02	0.03
8.25	3	0.02	0.02	0.03	0.01
14	4	0.01	0.03	0.03	0.00
22.5	6	0.02	0.02	0.03	0.03
35.25	9	0.02	0.03	0.02	0.01

Table B.38. Storm event #2 NO$_3^-$-N data.

Sample time (hr)	Theoretical detention time (hr)	Influent (mg/L)	60 cm column (mg/L)	45 cm column (mg/L)	30 cm column (mg/L)
0.25	-	1.92	0.01	0.02	0.01
1.25	1	1.99	0.56	0.51	0.61
4	2	1.98	0.04	0.00	0.23
8.25	3	1.99	0.02	0.03	0.50
14	4	1.99	0.06	0.06	0.30
22.5	6	1.98	0.01	0.03	0.09
35.25	9	1.97	0.01	0.02	0.00

157

Table B.39. Storm event #2 Org-N data.

Sample time (hr)	Theoretical detention time (hr)	Influent (mg/L)	60 cm column (mg/L)	45 cm column (mg/L)	30 cm column (mg/L)
0.25	-	0.44	0.56	0.52	0.54
1.25	1	0.50	0.63	0.60	0.47
4	2	0.59	0.45	0.43	0.54
8.25	3	0.44	0.43	0.39	0.38
14	4	0.38	0.47	0.43	0.48
22.5	6	0.51	0.41	0.38	0.41
35.25	9	0.37	0.35	0.37	0.41

Table B.40. Storm event #2 PO_4^{3-}-P data.

Sample time (hr)	Theoretical detention time (hr)	Influent (mg/L)	60 cm column (mg/L)	45 cm column (mg/L)	30 cm column (mg/L)
0.25	-	0.09	0.37	0.25	0.15
1.25	1	0.11	0.07	0.05	0.07
4	2	0.12	0.00	0.00	0.00
8.25	3	0.12	0.00	0.00	0.00
14	4	0.12	0.00	0.00	0.00
22.5	6	0.11	0.00	0.00	0.00
35.25	9	0.11	0.00	0.00	0.00

Table B.41. Storm event #2 SO_4^{2-}-S data.

Sample time (hr)	Theoretical detention time (hr)	Influent (mg/L)	60 cm column (mg/L)	45 cm column (mg/L)	30 cm column (mg/L)
0.25	-	54.08	1.03	0.72	1.04
1.25	1	62.41	33.08	35.60	39.17
4	2	62.10	60.40	60.04	59.00
8.25	3	62.59	60.58	61.15	62.05
14	4	62.73	58.01	55.07	61.80
22.5	6	62.30	60.79	61.33	61.06
35.25	9	62.47	59.14	59.64	59.22

158

Table B.42. Storm event #2 TSS data.

Sample time (hr)	Theoretical detention time (hr)	Influent (mg/L)	60 cm column (mg/L)	45 cm column (mg/L)	30 cm column (mg/L)
0.25	-	4.04	2.58	2.98	2.80
1.25	1	3.77	3.12	3.72	3.06
4	2	5.49	3.96	4.09	3.55
8.25	3	4.33	3.33	3.48	3.28
14	4	4.45	2.41	2.53	2.60
22.5	6	4.08	2.96	1.64	1.82
35.25	9	4.36	1.59	1.56	1.90

Table B.43. Storm event #2 VSS data.

Sample time (hr)	Theoretical detention time (hr)	Influent (mg/L)	60 cm column (mg/L)	45 cm column (mg/L)	30 cm column (mg/L)
0.25	-	1.34	0.00	0.00	0.38
1.25	1	1.27	0.30	0.84	0.64
4	2	2.29	1.09	0.67	0.85
8.25	3	1.51	0.40	0.57	0.65
14	4	1.72	0.23	0.72	0.10
22.5	6	1.55	0.31	0.72	0.23
35.25	9	1.19	0.20	0.06	0.08

Table B.44. Storm event #3 flow data for the 30 cm column.

Theoretical detention time (hr)	Theoretical flow rate (mL/min)	Flow rate 1 (mL/min)	Flow rate 2 (mL/min)	Average flow rate (mL/min)
1	29.27	29.5	29.5	29.5
2	14.63	14.5	14.5	14.5
3	9.76	9.5	9.5	9.5
4	7.32	7.3	7.25	7.3
6	4.88	5	4.75	5.9
9	3.25	3.25	3.25	3.25

159

Table B.45. Storm event #3 flow data for the 45 cm column.

Theoretical detention time (hr)	Theoretical flow rate (mL/min)	Flow rate 1 (mL/min)	Flow rate 2 (mL/min)	Average flow rate (mL/min)
1	44.43	45	46	45.5
2	22.22	22.5	22.5	22.5
3	14.81	15	14.75	14.9
4	11.11	11	10.75	10.9
6	7.41	7.5	7.5	7.5
9	4.94	4.75	4.75	4.75

Table B.46. Storm event #3 flow data for the 60 cm column.

Theoretical detention time (hr)	Theoretical flow rate (mL/min)	Flow rate 1 (mL/min)	Flow rate 2 (mL/min)	Average flow rate (mL/min)
1	59.33	59.5	60	59.75
2	29.67	29.5	29	29.25
3	19.78	19.5	20	19.75
4	14.83	15	15	15
6	9.89	10	9.75	9.8
9	6.59	6.75	6.5	6.6

Table B.47. Storm event #3 Influent TN data.

Sample time (hr)	Theoretical detention time (hr)	Sample 1 (mg/L)	Sample 2 (mg/L)	Sample 3 (mg/L)	Average (mg/L)	Standard deviation (mg/L)
0.25	-	2.40	2.31	2.38	2.36	0.05
1.25	1	2.33	2.35	2.31	2.33	0.02
4	2	2.44	2.42	2.37	2.41	0.04
8.25	3	2.31	2.33	2.28	2.31	0.02
14	4	2.39	2.31	2.34	2.35	0.04
22.5	6	2.41	2.35	2.43	2.40	0.04
35.25	9	2.33	2.35	2.40	2.36	0.03

160

Table B.48. Storm event #3 TN data for the 30 cm column.

Sample time (hr)	Theoretical detention time (hr)	Sample 1 (mg/L)	Sample 2 (mg/L)	Sample 3 (mg/L)	Average (mg/L)	Standard deviation (mg/L)
0.25	-	0.58	0.56	0.58	0.58	0.01
1.25	1	0.97	0.93	0.95	0.95	0.02
4	2	1.02	1.02	1.04	1.03	0.01
8.25	3	0.88	0.86	0.86	0.87	0.01
14	4	0.86	0.86	0.86	0.86	0.00
22.5	6	0.56	0.55	0.54	0.55	0.01
35.25	9	0.40	0.40	0.43	0.41	0.02

Table B.49. Storm event #3 TN data for the 45 cm column.

Sample time (hr)	Theoretical detention time (hr)	Sample 1 (mg/L)	Sample 2 (mg/L)	Sample 3 (mg/L)	Average (mg/L)	Standard deviation (mg/L)
0.25	-	0.58	0.60	0.62	0.60	0.02
1.25	1	0.91	0.89	0.92	0.90	0.02
4	2	0.82	0.81	0.80	0.81	0.01
8.25	3	0.64	0.64	0.65	0.64	0.01
14	4	0.57	0.56	0.56	0.56	0.01
22.5	6	0.47	0.51	0.48	0.48	0.02
35.25	9	0.41	0.41	0.41	0.41	0.00

Table B.50. Storm event #3 TN data for the 60 cm column.

Sample time (hr)	Theoretical detention time (hr)	Sample 1 (mg/L)	Sample 2 (mg/L)	Sample 3 (mg/L)	Average (mg/L)	Standard deviation (mg/L)
0.25	-	0.56	0.55	0.55	0.55	0.01
1.25	1	0.96	0.91	0.96	0.94	0.03
4	2	0.74	0.75	0.75	0.75	0.01
8.25	3	0.51	0.54	0.53	0.53	0.02
14	4	0.50	0.49	0.49	0.49	0.01
22.5	6	0.40	0.41	0.43	0.41	0.02
35.25	9	0.41	0.43	0.41	0.42	0.01

161

Table B.51. Storm event #3 Influent DOC data.

Sample time (hr)	Theoretical detention time (hr)	Sample 1 (mg/L)	Sample 2 (mg/L)	Sample 3 (mg/L)	Average (mg/L)	Standard deviation (mg/L)
0.25	-	5.10	4.96	4.98	5.01	0.08
1.25	1	4.59	4.45	4.52	4.52	0.07
4	2	4.67	4.58	4.63	4.63	0.04
8.25	3	4.55	4.49	4.65	4.56	0.08
14	4	4.61	4.61	4.62	4.62	0.01
22.5	6	4.99	5.04	5.07	5.03	0.04
35.25	9	5.02	4.89	4.85	4.92	0.09

Table B.52. Storm event #3 DOC data for the 30 cm column.

Sample time (hr)	Theoretical detention time (hr)	Sample 1 (mg/L)	Sample 2 (mg/L)	Sample 3 (mg/L)	Average (mg/L)	Standard deviation (mg/L)
0.25	-	10.88	10.89	10.66	10.81	0.13
1.25	1	8.74	8.45	8.82	8.67	0.19
4	2	5.28	5.21	5.25	5.25	0.04
8.25	3	5.04	5.16	5.26	5.15	0.11
14	4	5.04	4.91	4.96	4.97	0.06
22.5	6	4.55	4.65	4.73	4.65	0.09
35.25	9	5.01	4.98	5.16	5.05	0.10

Table B.53. Storm event #3 DOC data for the 45 cm column.

Sample time (hr)	Theoretical detention time (hr)	Sample 1 (mg/L)	Sample 2 (mg/L)	Sample 3 (mg/L)	Average (mg/L)	Standard deviation (mg/L)
0.25	-	14.78	15.11	15.24	15.04	0.24
1.25	1	9.90	9.88	10.11	9.96	0.13
4	2	5.15	5.31	5.29	5.25	0.09
8.25	3	5.29	5.17	5.18	5.21	0.07
14	4	5.50	5.33	5.40	5.41	0.08
22.5	6	5.42	5.40	5.50	5.44	0.05
35.25	9	5.91	5.77	5.90	5.86	0.08

162

Table B.54. Storm event #3 DOC data for the 60 cm column.

Sample time (hr)	Theoretical detention time (hr)	Sample 1 (mg/L)	Sample 2 (mg/L)	Sample 3 (mg/L)	Average (mg/L)	Standard deviation (mg/L)
0.25	-	13.75	13.61	13.75	13.70	0.08
1.25	1	8.47	8.58	8.75	8.60	0.14
4	2	5.19	5.09	5.10	5.13	0.06
8.25	3	4.89	5.00	5.07	4.98	0.09
14	4	4.71	4.86	4.75	4.77	0.08
22.5	6	5.09	5.13	5.28	5.17	0.10
35.25	9	5.33	5.30	5.20	5.28	0.07

Table B.55. Storm event #3 DO data.

Sample time (hr)	Theoretical detention time (hr)	Influent (mg/L)	60 cm column (mg/L)	45 cm column (mg/L)	30 cm column (mg/L)
0.25	-	4.92	0	0	0.08
1.25	1	4.5	0.05	0.07	0.01
4	2	5.4	0.05	0	0.09
8.25	3	4.7	0.11	0.26	0.11
14	4	5.72	0.05	0.11	0.23
22.5	6	5.9	0.28	0.19	0.2
35.25	9	6.45	0.26	0.16	0.18

Table B.56. Storm event #3 pH data.

Sample time (hr)	Theoretical detention time (hr)	Influent (mg/L)	60 cm column (mg/L)	45 cm column (mg/L)	30 cm column (mg/L)
0.25	-	7.37	6.82	6.78	6.91
1.25	1	8.12	6.94	6.97	7.09
4	2	7.92	6.99	6.98	7
8.25	3	8.06	7.24	7.16	7.27
14	4	8.05	7.15	7.2	7.23
22.5	6	7.89	7.05	7.12	7.19
35.25	9	7.89	6.88	6.87	6.98

163

Table B.57. Storm event #3 NH$_4^+$-N data.

Sample time (hr)	Theoretical detention time (hr)	Influent (mg/L)	60 cm column (mg/L)	45 cm column (mg/L)	30 cm column (mg/L)
0.25	-	0.00	0.04	0.03	0.05
1.25	1	0.00	0.00	0.00	0.05
4	2	0.00	0.00	0.00	0.03
8.25	3	0.00	0.00	0.00	0.00
14	4	0.00	0.00	0.00	0.00
22.5	6	0.00	0.00	0.00	0.00
35.25	9	0.00	0.00	0.00	0.00

Table B.58. Storm event #3 NO$_2^-$-N data.

Sample time (hr)	Theoretical detention time (hr)	Influent (mg/L)	60 cm column (mg/L)	45 cm column (mg/L)	30 cm column (mg/L)
0.25	-	0.02	0.08	0.06	0.08
1.25	1	0.02	0.04	0.05	0.07
4	2	0.02	0.00	0.00	0.00
8.25	3	0.03	0.04	0.00	0.11
14	4	0.02	0.02	0.02	0.13
22.5	6	0.02	0.02	0.03	0.03
35.25	9	0.02	0.02	0.02	0.01

Table B.59. Storm event #3 NO$_3^-$-N data.

Sample time (hr)	Theoretical detention time (hr)	Influent (mg/L)	60 cm column (mg/L)	45 cm column (mg/L)	30 cm column (mg/L)
0.25	-	1.97	0.01	0.01	0.01
1.25	1	1.98	0.41	0.36	0.37
4	2	1.96	0.19	0.21	0.44
8.25	3	1.98	0.02	0.09	0.30
14	4	1.98	0.03	0.05	0.27
22.5	6	2.06	0.00	0.01	0.07
35.25	9	2.02	0.00	0.01	0.00

164

Table B.60. Storm event #3 Org-N data.

Sample time (hr)	Theoretical detention time (hr)	Influent (mg/L)	60 cm column (mg/L)	45 cm column (mg/L)	30 cm column (mg/L)
0.25	-	0.37	0.43	0.50	0.44
1.25	1	0.33	0.49	0.49	0.46
4	2	0.42	0.56	0.59	0.56
8.25	3	0.30	0.46	0.55	0.45
14	4	0.35	0.44	0.49	0.45
22.5	6	0.30	0.38	0.44	0.44
35.25	9	0.32	0.39	0.38	0.39

Table B.61. Storm event #3 PO_4^{3-}-P data.

Sample time (hr)	Theoretical detention time (hr)	Influent (mg/L)	60 cm column (mg/L)	45 cm column (mg/L)	30 cm column (mg/L)
0.25	-	0.11	0.30	0.23	0.26
1.25	1	0.12	0.19	0.19	0.20
4	2	0.09	0.00	0.00	0.03
8.25	3	0.12	0.00	0.00	0.00
14	4	0.12	0.00	0.00	0.00
22.5	6	0.12	0.03	0.00	0.02
35.25	9	0.12	0.06	0.05	0.05

Table B.62. Storm event #3 SO_4^{2-}-S data.

Sample time (hr)	Theoretical detention time (hr)	Influent (mg/L)	60 cm column (mg/L)	45 cm column (mg/L)	30 cm column (mg/L)
0.25	-	62.47	9.17	12.81	14.55
1.25	1	64.97	42.78	39.47	38.19
4	2	65.11	64.16	65.03	63.15
8.25	3	66.41	66.12	65.79	64.75
14	4	65.51	65.77	65.62	65.44
22.5	6	68.17	63.80	63.62	63.61
35.25	9	68.35	60.69	60.87	60.70

Table B.63. Storm event #3 TSS data.

Sample time (hr)	Theoretical detention time (hr)	Influent (mg/L)	60 cm column (mg/L)	45 cm column (mg/L)	30 cm column (mg/L)
0.25	-	4.36	1.93	1.39	1.30
1.25	1	4.56	1.86	2.65	3.24
4	2	5.18	2.46	2.53	2.82
8.25	3	4.43	2.06	2.20	2.37
14	4	4.24	1.54	1.54	1.72
22.5	6	4.40	1.46	1.60	1.93
35.25	9	1.72	1.61	1.42	1.47

Table B.64. Storm event #3 VSS data.

Sample time (hr)	Theoretical detention time (hr)	Influent (mg/L)	60 cm column (mg/L)	45 cm column (mg/L)	30 cm column (mg/L)
0.25	-	1.19	0.05	0.00	0.08
1.25	1	1.60	0.29	0.51	0.88
4	2	2.04	0.30	0.70	0.88
8.25	3	1.32	0.46	0.33	0.70
14	4	1.46	0.44	0.34	0.52
22.5	6	1.40	0.33	0.31	0.73
35.25	9	0.29	0.20	0.00	0.17

Table B.65. Storm event #4 flow data for the 30 cm column.

Theoretical detention time (hr)	Theoretical flow rate (mL/min)	Flow rate 1 (mL/min)	Flow rate 2 (mL/min)	Average flow rate (mL/min)
1	29.27	29.5	29.5	29.5
2	14.63	14.75	14.75	14.75
3	9.76	9.5	9.25	9.4
4	7.32	7.25	7	7.1
6	4.88	5	5	5
9	3.25	3.5	3.5	5

166

Table B.66. Storm event #4 flow data for the 45 cm column.

Theoretical detention time (hr)	Theoretical flow rate (mL/min)	Flow rate 1 (mL/min)	Flow rate 2 (mL/min)	Average flow rate (mL/min)
1	44.43	44.5	44.5	44.5
2	22.22	22.25	22.5	22.4
3	14.81	14.5	14.5	14.5
4	11.11	11.25	10.75	11.0
6	7.41	7.75	7.75	7.75
9	4.94	5	4.75	4.9

Table B.67. Storm event #4 flow data for the 60 cm column.

Theoretical detention time (hr)	Theoretical flow rate (mL/min)	Flow rate 1 (mL/min)	Flow rate 2 (mL/min)	Average flow rate (mL/min)
1	59.33	59.5	60	59.75
2	29.67	29.67	29.5	29.6
3	19.78	20	20	20
4	14.83	14.75	14.75	14.75
6	9.89	10	10	10
9	6.59	6.5	6.5	6.5

Table B.68. Storm event #4 Influent TN data.

Sample time (hr)	Theoretical detention time (hr)	Sample 1 (mg/L)	Sample 2 (mg/L)	Sample 3 (mg/L)	Average (mg/L)	Standard deviation (mg/L)
0.25	-	2.33	2.35	2.40	2.36	0.03
1.25	1	2.28	2.25	2.30	2.27	0.02
4	2	2.30	2.29	2.30	2.30	0.00
8.25	3	2.38	2.36	2.46	2.40	0.05
14	4	2.34	2.37	2.35	2.35	0.02
22.5	6	2.28	2.36	2.31	2.32	0.04
35.25	9	2.29	2.28	2.36	2.31	0.05

167

Table B.69. Storm event #4 TN data for the 30 cm column.

Sample time (hr)	Theoretical detention time (hr)	Sample 1 (mg/L)	Sample 2 (mg/L)	Sample 3 (mg/L)	Average (mg/L)	Standard deviation (mg/L)
0.25	-	0.64	0.66	0.64	0.65	0.01
1.25	1	1.00	1.01	1.00	1.00	0.01
4	2	1.01	1.01	1.03	1.02	0.01
8.25	3	0.96	0.93	0.96	0.95	0.01
14	4	0.75	0.74	0.75	0.75	0.01
22.5	6	0.63	0.63	0.62	0.63	0.01
35.25	9	0.50	0.51	0.50	0.50	0.01

Table B.70. Storm event #4 TN data for the 45 cm column.

Sample time (hr)	Theoretical detention time (hr)	Sample 1 (mg/L)	Sample 2 (mg/L)	Sample 3 (mg/L)	Average (mg/L)	Standard deviation (mg/L)
0.25	-	0.64	0.61	0.63	0.62	0.02
1.25	1	0.98	0.96	0.98	0.97	0.01
4	2	0.55	0.56	0.57	0.56	0.01
8.25	3	0.59	0.57	0.59	0.58	0.01
14	4	0.49	0.46	0.49	0.48	0.02
22.5	6	0.48	0.48	0.49	0.49	0.01
35.25	9	0.50	0.51	0.50	0.50	0.01

Table B.71. Storm event #4 TN data for the 60 cm column.

Sample time (hr)	Theoretical detention time (hr)	Sample 1 (mg/L)	Sample 2 (mg/L)	Sample 3 (mg/L)	Average (mg/L)	Standard deviation (mg/L)
0.25	-	0.78	0.74	0.76	0.76	0.02
1.25	1	1.07	1.06	1.13	1.09	0.04
4	2	0.76	0.78	0.78	0.77	0.01
8.25	3	0.59	0.63	0.65	0.62	0.03
14	4	0.54	0.53	0.54	0.54	0.01
22.5	6	0.50	0.48	0.48	0.49	0.01
35.25	9	0.45	0.44	0.45	0.45	0.01

168

Table B.72. Storm event #4 Influent DOC data.

Sample time (hr)	Theoretical detention time (hr)	Sample 1 (mg/L)	Sample 2 (mg/L)	Sample 3 (mg/L)	Average (mg/L)	Standard deviation (mg/L)
0.25	-	5.02	4.89	4.85	4.92	0.09
1.25	1	5.25	5.20	5.23	5.22	0.02
4	2	4.98	4.94	5.16	5.02	0.11
8.25	3	5.61	5.42	5.56	5.53	0.10
14	4	4.79	4.72	4.84	4.78	0.06
22.5	6	4.93	4.80	4.80	4.84	0.07
35.25	9	4.95	4.81	4.84	4.87	0.07

Table B.73. Storm event #4 DOC data for the 30 cm column.

Sample time (hr)	Theoretical detention time (hr)	Sample 1 (mg/L)	Sample 2 (mg/L)	Sample 3 (mg/L)	Average (mg/L)	Standard deviation (mg/L)
0.25	-	24.65	24.36	24.77	24.59	0.21
1.25	1	16.30	15.86	16.28	16.15	0.25
4	2	5.73	5.87	5.99	5.86	0.13
8.25	3	5.69	5.49	5.70	5.63	0.12
14	4	4.95	5.04	5.05	5.01	0.05
22.5	6	5.25	5.26	5.45	5.32	0.11
35.25	9	5.63	5.67	5.61	5.64	0.03

Table B.74. Storm event #4 DOC data for the 45 cm column.

Sample time (hr)	Theoretical detention time (hr)	Sample 1 (mg/L)	Sample 2 (mg/L)	Sample 3 (mg/L)	Average (mg/L)	Standard deviation (mg/L)
0.25	-	50.37	48.49	49.26	49.38	0.95
1.25	1	22.64	21.80	21.98	22.14	0.44
4	2	5.72	5.57	5.79	5.70	0.11
8.25	3	5.55	5.52	5.64	5.57	0.06
14	4	5.20	5.14	5.34	5.23	0.10
22.5	6	6.22	5.96	6.22	6.13	0.15
35.25	9	6.18	6.11	6.30	6.20	0.10

169

Table B.75. Storm event #4 DOC data for the 60 cm column.

Sample time (hr)	Theoretical detention time (hr)	Sample 1 (mg/L)	Sample 2 (mg/L)	Sample 3 (mg/L)	Average (mg/L)	Standard deviation (mg/L)
0.25	-	41.97	41.56	41.40	41.64	0.29
1.25	1	18.65	18.81	18.85	18.77	0.10
4	2	5.83	5.78	6.01	5.87	0.13
8.25	3	5.83	5.75	5.92	5.84	0.09
14	4	5.15	5.06	5.03	5.08	0.06
22.5	6	5.50	5.63	5.70	5.61	0.10
35.25	9	5.59	5.59	5.59	5.59	0.00

Table B.76. Storm event #4 DO data.

Sample time (hr)	Theoretical detention time (hr)	Influent (mg/L)	60 cm column (mg/L)	45 cm column (mg/L)	30 cm column (mg/L)
0.25	-	6.45	0.04	0.11	0
1.25	1	4.99	0.1	0	0
4	2	5.1	0.09	0.08	0.07
8.25	3	5.2	0	0	0
14	4	5.09	0	0.04	0
22.5	6	5.08	0	0.02	0.05
35.25	9	5.73	0.05	0	0

Table B.77. Storm event #4 pH data.

Sample time (hr)	Theoretical detention time (hr)	Influent (mg/L)	60 cm column (mg/L)	45 cm column (mg/L)	30 cm column (mg/L)
0.25	-	7.89	6.59	6.48	6.6
1.25	1	7.86	6.79	6.66	6.88
4	2	8.09	7.03	7.02	7.15
8.25	3	7.9	7.06	7.01	7.13
14	4	7.75	7.01	7	7.22
22.5	6	7.86	7.14	7.13	7.45
35.25	9	7.56	6.94	6.93	7.13

Table B.78. Storm event #4 NH_4^+-N data.

Sample time (hr)	Theoretical detention time (hr)	Influent (mg/L)	60 cm column (mg/L)	45 cm column (mg/L)	30 cm column (mg/L)
0.25	-	0.00	0.10	0.05	0.06
1.25	1	0.00	0.10	0.07	0.09
4	2	0.00	0.02	0.00	0.03
8.25	3	0.00	0.03	0.03	0.03
14	4	0.00	0.03	0.03	0.03
22.5	6	0.00	0.05	0.03	0.04
35.25	9	0.00	0.03	0.00	0.05

Table B.79. Storm event #4 NO_2^--N data.

Sample time (hr)	Theoretical detention time (hr)	Influent (mg/L)	60 cm column (mg/L)	45 cm column (mg/L)	30 cm column (mg/L)
0.25	-	0.02	0.06	0.06	0.07
1.25	1	0.01	0.05	0.06	0.04
4	2	0.05	0.10	0.05	0.12
8.25	3	0.01	0.05	0.03	0.13
14	4	0.02	0.03	0.02	0.10
22.5	6	0.01	0.07	0.03	0.06
35.25	9	0.03	0.02	0.05	0.04

Table B.80. Storm event #4 NO_3^--N data.

Sample time (hr)	Theoretical detention time (hr)	Influent (mg/L)	60 cm column (mg/L)	45 cm column (mg/L)	30 cm column (mg/L)
0.25	-	2.06	0.01	0.02	0.01
1.25	1	1.89	0.47	0.43	0.46
4	2	1.90	0.15	0.09	0.46
8.25	3	1.90	0.06	0.05	0.31
14	4	1.91	0.03	0.02	0.20
22.5	6	1.91	0.01	0.01	0.13
35.25	9	1.91	0.03	0.05	0.04

171

Table B.81. Storm event #4 Org-N data.

Sample time (hr)	Theoretical detention time (hr)	Influent (mg/L)	60 cm column (mg/L)	45 cm column (mg/L)	30 cm column (mg/L)
0.25	-	0.28	0.59	0.50	0.51
1.25	1	0.37	0.47	0.42	0.41
4	2	0.34	0.50	0.42	0.41
8.25	3	0.48	0.49	0.48	0.48
14	4	0.43	0.44	0.41	0.41
22.5	6	0.39	0.36	0.41	0.40
35.25	9	0.37	0.37	0.39	0.38

Table B.82. Storm event #4 PO_4^{3-}-P data.

Sample time (hr)	Theoretical detention time (hr)	Influent (mg/L)	60 cm column (mg/L)	45 cm column (mg/L)	30 cm column (mg/L)
0.25	-	0.12	0.28	0.19	0.22
1.25	1	0.13	0.17	0.13	0.18
4	2	0.13	0.00	0.00	0.00
8.25	3	0.13	0.00	0.00	0.00
14	4	0.13	0.00	0.00	0.00
22.5	6	0.13	0.00	0.00	0.00
35.25	9	0.13	0.05	0.04	0.04

Table B.83. Storm event #4 SO_4^{2-}-S data.

Sample time (hr)	Theoretical detention time (hr)	Influent (mg/L)	60 cm column (mg/L)	45 cm column (mg/L)	30 cm column (mg/L)
0.25	-	69.98	2.35	2.62	4.33
1.25	1	70.81	48.07	41.57	37.67
4	2	71.35	70.45	70.16	70.38
8.25	3	71.08	71.95	76.34	70.99
14	4	70.45	71.95	70.85	71.87
22.5	6	70.35	70.72	70.12	71.13
35.25	9	70.67	69.40	68.72	70.39

172

Table B.84. Storm event #4 TSS data.

Sample time (hr)	Theoretical detention time (hr)	Influent (mg/L)	60 cm column (mg/L)	45 cm column (mg/L)	30 cm column (mg/L)
0.25	-	1.72	1.73	1.29	1.45
1.25	1	10.30	2.16	2.57	2.48
4	2	7.01	1.81	2.48	3.33
8.25	3	6.11	1.97	2.42	2.32
14	4	6.72	1.83	1.72	1.92
22.5	6	5.44	1.68	1.70	0.94
35.25	9	4.98	1.32	1.31	1.56

Table B.85. Storm event #4 VSS data.

Sample time (hr)	Theoretical detention time (hr)	Influent (mg/L)	60 cm column (mg/L)	45 cm column (mg/L)	30 cm column (mg/L)
0.25	-	0.29	0.09	0.00	0.00
1.25	1	4.12	0.40	0.18	0.38
4	2	0.86	0.31	0.55	0.91
8.25	3	3.77	0.40	0.20	0.41
14	4	2.28	0.38	0.38	0.22
22.5	6	1.34	0.76	0.22	0.00
35.25	9	1.32	0.01	0.00	0.00

Table B.86. Storm event #5 flow data for the 30 cm column.

Theoretical detention time (hr)	Theoretical flow rate (mL/min)	Flow rate 1 (mL/min)	Flow rate 2 (mL/min)	Average flow rate (mL/min)
1	29.27	29.5	29.5	29.5
2	14.63	14.75	14.75	14.75
3	9.76	9.75	9.75	9.75
4	7.32	7.25	7.25	7.25
6	4.88	5	5	5
9	3.25	3.25	3.25	3.25

173

Table B.87. Storm event #5 flow data for the 45 cm column.

Theoretical detention time (hr)	Theoretical flow rate (mL/min)	Flow rate 1 (mL/min)	Flow rate 2 (mL/min)	Average flow rate (mL/min)
1	44.43	44.5	44	44.25
2	22.22	22	21.5	21.75
3	14.81	14.75	14.75	14.75
4	11.11	11.25	11	11.1
6	7.41	7.5	8	7.75
9	4.94	5	4.5	4.75

Table B.88. Storm event #5 flow data for the 60 cm column.

Theoretical detention time (hr)	Theoretical flow rate (mL/min)	Flow rate 1 (mL/min)	Flow rate 2 (mL/min)	Average flow rate (mL/min)
1	59.33	59.5	61	60.25
2	29.67	29.5	29	29.25
3	19.78	19.5	20	19.75
4	14.83	14.75	14.75	14.75
6	9.89	10	10.25	10.1
9	6.59	6.5	5.75	12.25

Table B.89. Storm event #5 Influent TN data.

Sample time (hr)	Theoretical detention time (hr)	Sample 1 (mg/L)	Sample 2 (mg/L)	Sample 3 (mg/L)	Average (mg/L)	Standard deviation (mg/L)
0.25	-	2.29	2.28	2.36	2.31	0.05
1.25	1	2.28	2.32	2.38	2.33	0.05
4	2	2.35	2.38	2.31	2.35	0.03
8.25	3	2.35	2.26	2.31	2.31	0.05
14	4	2.37	2.31	2.40	2.36	0.04
22.5	6	2.22	2.17	2.24	2.21	0.04
35.25	9	2.28	2.23	2.30	2.27	0.04

174

Table B.90. Storm event #5 TN data for the 30 cm column.

Sample time (hr)	Theoretical detention time (hr)	Sample 1 (mg/L)	Sample 2 (mg/L)	Sample 3 (mg/L)	Average (mg/L)	Standard deviation (mg/L)
0.25	-	0.60	0.61	0.62	0.61	0.01
1.25	1	1.27	1.25	1.30	1.27	0.02
4	2	1.53	1.57	1.58	1.56	0.02
8.25	3	1.28	1.35	1.31	1.31	0.03
14	4	1.09	1.08	1.11	1.09	0.01
22.5	6	0.64	0.64	0.66	0.64	0.01
35.25	9	0.65	0.64	0.65	0.64	0.01

Table B.91. Storm event #5 TN data for the 45 cm column.

Sample time (hr)	Theoretical detention time (hr)	Sample 1 (mg/L)	Sample 2 (mg/L)	Sample 3 (mg/L)	Average (mg/L)	Standard deviation (mg/L)
0.25	-	0.50	0.49	0.48	0.49	0.01
1.25	1	1.51	1.49	1.47	1.49	0.02
4	2	1.46	1.42	1.44	1.44	0.02
8.25	3	0.97	0.99	0.99	0.98	0.01
14	4	0.56	0.59	0.55	0.57	0.02
22.5	6	0.51	0.50	0.52	0.51	0.01
35.25	9	0.55	0.53	0.55	0.54	0.01

Table B.92. Storm event #5 TN data for the 60 cm column.

Sample time (hr)	Theoretical detention time (hr)	Sample 1 (mg/L)	Sample 2 (mg/L)	Sample 3 (mg/L)	Average (mg/L)	Standard deviation (mg/L)
0.25	-	0.51	0.52	0.53	0.52	0.01
1.25	1	1.64	1.65	1.71	1.67	0.04
4	2	1.53	1.53	1.50	1.52	0.02
8.25	3	0.91	0.92	0.93	0.92	0.01
14	4	0.56	0.56	0.58	0.56	0.01
22.5	6	0.61	0.64	0.64	0.63	0.02
35.25	9	0.77	0.75	0.75	0.75	0.01

175

Table B.93. Storm event #5 Influent DOC data.

Sample time (hr)	Theoretical detention time (hr)	Sample 1 (mg/L)	Sample 2 (mg/L)	Sample 3 (mg/L)	Average (mg/L)	Standard deviation (mg/L)
0.25	-	4.95	4.81	4.84	4.87	0.07
1.25	1	4.84	4.75	4.74	4.78	0.05
4	2	4.89	4.84	4.73	4.82	0.08
8.25	3	5.37	5.30	5.35	5.34	0.04
14	4	5.86	5.98	5.91	5.92	0.06
22.5	6	5.85	5.87	5.83	5.85	0.02
35.25	9	6.01	5.77	5.84	5.87	0.13

Table B.94. Storm event #5 DOC data for the 30 cm column.

Sample time (hr)	Theoretical detention time (hr)	Sample 1 (mg/L)	Sample 2 (mg/L)	Sample 3 (mg/L)	Average (mg/L)	Standard deviation (mg/L)
0.25	-	5.57	5.55	5.62	5.58	0.04
1.25	1	5.45	5.29	5.25	5.33	0.11
4	2	5.04	4.84	4.95	4.94	0.10
8.25	3	4.85	4.85	4.93	4.88	0.05
14	4	5.84	5.86	5.98	5.89	0.07
22.5	6	5.72	5.86	5.97	5.85	0.12
35.25	9	6.09	5.87	5.99	5.98	0.11

Table B.95. Storm event #5 DOC data for the 45 cm column.

Sample time (hr)	Theoretical detention time (hr)	Sample 1 (mg/L)	Sample 2 (mg/L)	Sample 3 (mg/L)	Average (mg/L)	Standard deviation (mg/L)
0.25	-	5.63	5.62	5.78	5.68	0.09
1.25	1	5.84	5.71	5.80	5.79	0.06
4	2	4.67	4.59	4.60	4.62	0.04
8.25	3	4.81	4.66	4.72	4.73	0.07
14	4	4.92	5.10	5.10	5.04	0.10
22.5	6	5.36	5.39	5.40	5.38	0.02
35.25	9	6.11	6.10	6.11	6.10	0.01

176

Table B.96. Storm event #5 DOC data for the 60 cm column.

Sample time (hr)	Theoretical detention time (hr)	Sample 1 (mg/L)	Sample 2 (mg/L)	Sample 3 (mg/L)	Average (mg/L)	Standard deviation (mg/L)
0.25	-	5.85	5.81	5.95	5.87	0.07
1.25	1	5.94	5.71	5.80	5.82	0.11
4	2	4.75	4.69	4.64	4.69	0.06
8.25	3	4.74	4.68	4.74	4.72	0.03
14	4	4.99	4.96	5.11	5.02	0.08
22.5	6	6.66	6.47	6.67	6.60	0.11
35.25	9	6.98	6.85	6.87	6.90	0.07

Table B.97. Storm event #5 DO data.

Sample time (hr)	Theoretical detention time (hr)	Influent (mg/L)	60 cm column (mg/L)	45 cm column (mg/L)	30 cm column (mg/L)
0.25	-	5.73	0	0.19	0
1.25	1	5.73	0	0.48	0.56
4	2	5.24	0	0	0.31
8.25	3	4.47	0	0	0
14	4	5.42	0	0.15	0
22.5	6	5.31	0	0	0
35.25	9	5.60	0	0	0

Table B.98. Storm event #5 pH data.

Sample time (hr)	Theoretical detention time (hr)	Influent (mg/L)	60 cm column (mg/L)	45 cm column (mg/L)	30 cm column (mg/L)
0.25	-	7.56	7.05	7.04	7.09
1.25	1	7.56	7.02	7.02	7.09
4	2	7.8	6.92	6.98	7.07
8.25	3	7.51	6.86	7	7.13
14	4	7.39	7.05	7.04	7.15
22.5	6	7.34	7.08	7.05	7.23
35.25	9	7.29	7.01	7.03	7.19

177

Table B.99. Storm event #5 NH$_4^+$-N data.

Sample time (hr)	Theoretical detention time (hr)	Influent (mg/L)	60 cm column (mg/L)	45 cm column (mg/L)	30 cm column (mg/L)
0.25	-	0.00	0.08	0.05	0.08
1.25	1	0.02	0.03	0.03	0.05
4	2	0.00	0.00	0.03	0.03
8.25	3	0.00	0.03	0.03	0.03
14	4	0.00	0.05	0.04	0.05
22.5	6	0.00	0.15	0.10	0.14
35.25	9	0.18	0.19	0.09	0.19

Table B.100. Storm event #5 NO$_2^-$-N data.

Sample time (hr)	Theoretical detention time (hr)	Influent (mg/L)	60 cm column (mg/L)	45 cm column (mg/L)	30 cm column (mg/L)
0.25	-	0.03	0.05	0.05	0.02
1.25	1	0.02	0.02	0.02	0.02
4	2	0.01	0.16	0.16	0.15
8.25	3	0.01	0.28	0.25	0.20
14	4	0.01	0.02	0.00	0.16
22.5	6	0.02	0.01	0.04	0.04
35.25	9	0.03	0.04	0.05	0.02

Table B.101. Storm event #5 NO$_3^-$-N data.

Sample time (hr)	Theoretical detention time (hr)	Influent (mg/L)	60 cm column (mg/L)	45 cm column (mg/L)	30 cm column (mg/L)
0.25	-	1.91	0.01	0.01	0.12
1.25	1	1.76	1.04	0.84	0.73
4	2	1.91	0.92	0.84	0.94
8.25	3	1.93	0.18	0.31	0.61
14	4	1.86	0.03	0.09	0.36
22.5	6	1.82	0.01	0.01	0.02
35.25	9	1.82	0.01	0.00	0.02

178

Table B.102. Storm event #5 Org-N data.

Sample time (hr)	Theoretical detention time (hr)	Influent (mg/L)	60 cm column (mg/L)	45 cm column (mg/L)	30 cm column (mg/L)
0.25	-	0.37	0.39	0.39	0.39
1.25	1	0.53	0.57	0.59	0.47
4	2	0.42	0.44	0.41	0.44
8.25	3	0.37	0.44	0.40	0.47
14	4	0.49	0.47	0.44	0.52
22.5	6	0.36	0.46	0.36	0.44
35.25	9	0.25	0.51	0.41	0.41

Table B.103. Storm event #5 PO_4^{3-}-P data.

Sample time (hr)	Theoretical detention time (hr)	Influent (mg/L)	60 cm column (mg/L)	45 cm column (mg/L)	30 cm column (mg/L)
0.25	-	0.13	0.07	0.06	0.06
1.25	1	0.13	0.04	0.04	0.06
4	2	0.13	0.00	0.00	0.03
8.25	3	0.12	0.00	0.00	0.03
14	4	0.12	0.00	0.00	0.03
22.5	6	0.11	0.08	0.07	0.07
35.25	9	0.22	0.23	0.15	0.16

Table B.104. Storm event #5 SO_4^{2-}-S data.

Sample time (hr)	Theoretical detention time (hr)	Influent (mg/L)	60 cm column (mg/L)	45 cm column (mg/L)	30 cm column (mg/L)
0.25	-	70.67	69.51	68.94	70.37
1.25	1	65.82	71.93	71.65	70.78
4	2	71.41	73.62	73.42	73.29
8.25	3	72.11	74.05	73.75	73.61
14	4	70.80	73.26	71.97	72.82
22.5	6	72.33	73.03	71.55	70.92
35.25	9	62.56	67.27	68.14	69.48

179

Table B.105. Storm event #5 TSS data.

Sample time (hr)	Theoretical detention time (hr)	Influent (mg/L)	60 cm column (mg/L)	45 cm column (mg/L)	30 cm column (mg/L)
0.25	-	4.98	1.27	1.87	2.85
1.25	1	5.59	3.92	4.70	3.83
4	2	8.41	2.37	3.68	2.88
8.25	3	9.20	2.16	2.49	2.98
14	4	11.33	2.28	1.83	3.07
22.5	6	9.96	2.18	2.47	1.93
35.25	9	5.49	1.49	2.16	2.92

Table B.106. Storm event #5 VSS data.

Sample time (hr)	Theoretical detention time (hr)	Influent (mg/L)	60 cm column (mg/L)	45 cm column (mg/L)	30 cm column (mg/L)
0.25	-	1.32	0.22	0.68	0.89
1.25	1	1.38	1.00	1.31	0.92
4	2	2.16	0.73	0.83	0.67
8.25	3	2.02	1.09	0.47	0.68
14	4	1.82	0.29	0.28	0.45
22.5	6	1.76	0.08	0.84	0.75
35.25	9	1.00	0.00	0.59	0.54

Table B.107. Storm event #6 flow data for the 30 cm column.

Theoretical detention time (hr)	Theoretical flow rate (mL/min)	Flow rate 1 (mL/min)	Flow rate 2 (mL/min)	Average flow rate (mL/min)
1	29.27	29.5	30.5	30.0
2	14.63	14.5	14.6	14.6
3	9.76	9.75	9.6	9.7
4	7.32	7.5	7.4	7.5
6	4.88	4.5	5.25	4.9
9	3.25	3.25	3.25	3.25

180

Table B.108. Storm event #6 flow data for the 45 cm column.

Theoretical detention time (hr)	Theoretical flow rate (mL/min)	Flow rate 1 (mL/min)	Flow rate 2 (mL/min)	Average flow rate (mL/min)
1	44.43	44.5	44.5	44.5
2	22.22	22.5	22	22.25
3	14.81	14.5	14.5	14.5
4	11.11	11.25	11	11.1
6	7.41	7.5	7.6	7.6
9	4.94	5.25	5.25	5.25

Table B.109. Storm event #6 flow data for the 60 cm column.

Theoretical detention time (hr)	Theoretical flow rate (mL/min)	Flow rate 1 (mL/min)	Flow rate 2 (mL/min)	Average flow rate (mL/min)
1	59.33	59.3	60.5	59.9
2	29.67	29.5	29	29.25
3	19.78	19.5	19	19.25
4	14.83	14.75	15	14.9
6	9.89	9.75	9.5	9.6
9	6.59	6.75	6.75	6.8

Table B.110. Storm event #6 Influent TN data.

Sample time (hr)	Theoretical detention time (hr)	Sample 1 (mg/L)	Sample 2 (mg/L)	Sample 3 (mg/L)	Average (mg/L)	Standard deviation (mg/L)
0.25	-	2.28	2.23	2.30	2.27	0.04
1.25	1	4.07	3.95	3.98	4.00	0.06
4	2	4.17	4.30	4.30	4.26	0.07
8.25	3	4.32	4.21	4.20	4.24	0.06
14	4	4.06	4.12	4.20	4.13	0.07
22.5	6	4.04	4.01	4.18	4.08	0.09
35.25	9	4.26	4.13	4.24	4.21	0.07

181

Table B.111. Storm event #6 TN data for the 30 cm column.

Sample time (hr)	Theoretical detention time (hr)	Sample 1 (mg/L)	Sample 2 (mg/L)	Sample 3 (mg/L)	Average (mg/L)	Standard deviation (mg/L)
0.25	-	0.68	0.70	0.69	0.69	0.01
1.25	1	1.84	1.78	1.78	1.80	0.04
4	2	2.05	2.06	2.06	2.06	0.00
8.25	3	1.95	1.95	1.98	1.96	0.02
14	4	1.81	1.76	1.82	1.80	0.03
22.5	6	1.18	1.18	1.14	1.17	0.02
35.25	9	0.63	0.62	0.63	0.62	0.00

Table B.112. Storm event #6 TN data for the 45 cm column.

Sample time (hr)	Theoretical detention time (hr)	Sample 1 (mg/L)	Sample 2 (mg/L)	Sample 3 (mg/L)	Average (mg/L)	Standard deviation (mg/L)
0.25	-	0.66	0.67	0.66	0.66	0.00
1.25	1	1.69	1.64	1.69	1.68	0.03
4	2	1.67	1.71	1.73	1.70	0.03
8.25	3	1.49	1.50	1.48	1.49	0.01
14	4	1.23	1.26	1.27	1.25	0.02
22.5	6	0.48	0.47	0.49	0.48	0.01
35.25	9	0.49	0.46	0.48	0.48	0.01

Table B.113. Storm event #6 TN data for the 60 cm column.

Sample time (hr)	Theoretical detention time (hr)	Sample 1 (mg/L)	Sample 2 (mg/L)	Sample 3 (mg/L)	Average (mg/L)	Standard deviation (mg/L)
0.25	-	0.79	0.79	0.80	0.79	0.01
1.25	1	1.93	1.88	1.89	1.90	0.03
4	2	1.95	1.88	1.91	1.91	0.04
8.25	3	1.54	1.52	1.52	1.52	0.01
14	4	1.35	1.38	1.34	1.36	0.02
22.5	6	0.59	0.54	0.57	0.57	0.03
35.25	9					

182

Table B.114. Storm event #6 Influent DOC data.

Sample time (hr)	Theoretical detention time (hr)	Sample 1 (mg/L)	Sample 2 (mg/L)	Sample 3 (mg/L)	Average (mg/L)	Standard deviation (mg/L)
0.25	-	6.01	5.77	5.84	5.87	0.13
1.25	1	4.95	4.86	4.84	4.88	0.06
4	2	5.17	5.13	5.24	5.18	0.06
8.25	3	5.15	4.86	5.10	5.04	0.15
14	4	4.96	5.13	5.09	5.06	0.09
22.5	6	5.05	4.97	5.05	5.02	0.05
35.25	9	5.46	5.45	5.35	5.42	0.06

Table B.115. Storm event #6 DOC data for the 30 cm column.

Sample time (hr)	Theoretical detention time (hr)	Sample 1 (mg/L)	Sample 2 (mg/L)	Sample 3 (mg/L)	Average (mg/L)	Standard deviation (mg/L)
0.25	-	27.89	27.74	27.26	27.63	0.33
1.25	1	14.17	14.73	14.31	14.40	0.29
4	2	5.17	5.01	5.05	5.08	0.08
8.25	3	4.65	4.60	4.62	4.62	0.02
14	4	5.12	5.05	5.25	5.14	0.10
22.5	6	5.33	5.22	5.16	5.24	0.09
35.25	9	5.52	5.48	5.53	5.51	0.03

Table B.116. Storm event #6 DOC data for the 45 cm column.

Sample time (hr)	Theoretical detention time (hr)	Sample 1 (mg/L)	Sample 2 (mg/L)	Sample 3 (mg/L)	Average (mg/L)	Standard deviation (mg/L)
0.25	-	50.80	52.12	52.28	51.73	0.81
1.25	1	19.41	18.88	19.21	19.17	0.27
4	2	5.76	5.78	5.95	5.83	0.10
8.25	3	5.39	5.23	5.22	5.28	0.10
14	4	4.42	4.34	4.29	4.35	0.06
22.5	6	5.48	5.49	5.46	5.48	0.01
35.25	9	5.18	5.26	5.25	5.23	0.04

183

Table B.117. Storm event #6 DOC data for the 60 cm column.

Sample time (hr)	Theoretical detention time (hr)	Sample 1 (mg/L)	Sample 2 (mg/L)	Sample 3 (mg/L)	Average (mg/L)	Standard deviation (mg/L)
0.25	-	43.98	44.28	44.10	44.12	0.15
1.25	1	16.37	16.44	16.14	16.32	0.16
4	2	5.14	5.00	5.06	5.06	0.07
8.25	3	5.22	5.21	5.31	5.25	0.06
14	4	4.28	4.26	4.19	4.24	0.05
22.5	6	5.20	5.03	5.08	5.10	0.09
35.25	9					

Table B.118. Storm event #6 DO data.

Sample time (hr)	Theoretical detention time (hr)	Influent (mg/L)	60 cm column (mg/L)	45 cm column (mg/L)	30 cm column (mg/L)
0.25	-	5.6	0.08	0	0
1.25	1	6.07	0	0.02	0.02
4	2	6.08	0.05	0.08	0.12
8.25	3	5.69	0.06	0.04	0.03
14	4	5.44	0.21	0.25	0.23
22.5	6	5.36	0.2	0.18	0.17
35.25	9	5.83	0.09	0.11	0.37

Table B.119. Storm event #6 pH data.

Sample time (hr)	Theoretical detention time (hr)	Influent (mg/L)	60 cm column (mg/L)	45 cm column (mg/L)	30 cm column (mg/L)
0.25	-	7.29	6.75	6.77	7.04
1.25	1	8.05	6.88	7.04	7.04
4	2	8.1	7.13	7.11	7.29
8.25	3	8.09	7.15	7.15	7.3
14	4	7.91	7.19	7.25	7.37
22.5	6	7.7	7.23	7.23	7.39
35.25	9	7.54	7.15	7.12	7.39

184

Table B.120. Storm event #6 NH$_4^+$-N data.

Sample time (hr)	Theoretical detention time (hr)	Influent (mg/L)	60 cm column (mg/L)	45 cm column (mg/L)	30 cm column (mg/L)
0.25	-	0.17	0.14	0.04	0.05
1.25	1	0.00	0.18	0.10	0.09
4	2	0.00	0.08	0.02	0.07
8.25	3	0.00	0.04	0.06	0.06
14	4	0.00	0.06	0.06	0.06
22.5	6	0.00	0.08	0.06	0.06
35.25	9	0.00	0.11	0.07	0.08

Table B.121. Storm event #6 NO$_2^-$-N data.

Sample time (hr)	Theoretical detention time (hr)	Influent (mg/L)	60 cm column (mg/L)	45 cm column (mg/L)	30 cm column (mg/L)
0.25	-	0.03	0.12	0.11	0.11
1.25	1	0.02	0.06	0.07	0.06
4	2	0.03	0.46	0.39	0.26
8.25	3	0.03	0.56	0.44	0.37
14	4	0.02	0.46	0.36	0.33
22.5	6	0.03	0.05	0.05	0.17
35.25	9	0.03	0.05	0.05	0.03

Table B.122. Storm event #6 NO$_3^-$-N data.

Sample time (hr)	Theoretical detention time (hr)	Influent (mg/L)	60 cm column (mg/L)	45 cm column (mg/L)	30 cm column (mg/L)
0.25	-	1.78	0.04	0.01	0.04
1.25	1	3.80	1.33	1.20	1.32
4	2	3.84	1.03	0.84	1.32
8.25	3	3.99	0.56	0.63	1.25
14	4	3.78	0.51	0.48	1.09
22.5	6	3.83	0.03	0.01	0.56
35.25	9	3.93	0.01	0.01	0.10

Table B.123. Storm event #6 Org-N data.

Sample time (hr)	Theoretical detention time (hr)	Influent (mg/L)	60 cm column (mg/L)	45 cm column (mg/L)	30 cm column (mg/L)
0.25	-	0.29	0.49	0.50	0.49
1.25	1	0.18	0.33	0.31	0.33
4	2	0.38	0.33	0.45	0.41
8.25	3	0.23	0.37	0.36	0.28
14	4	0.32	0.32	0.35	0.31
22.5	6	0.22	0.41	0.36	0.34
35.25	9	0.25	0.31	0.35	0.40

Table B.124. Storm event #6 PO_4^{3-}-P data.

Sample time (hr)	Theoretical detention time (hr)	Influent (mg/L)	60 cm column (mg/L)	45 cm column (mg/L)	30 cm column (mg/L)
0.25	-	0.21	0.42	0.40	0.36
1.25	1	0.11	0.22	0.16	0.18
4	2	0.11	0.00	0.00	0.03
8.25	3	0.12	0.00	0.00	0.00
14	4	0.11	0.00	0.00	0.00
22.5	6	0.12	0.00	0.00	0.00
35.25	9	0.12	0.04	0.03	0.04

Table B.125. Storm event #6 SO_4^{2-}-S data.

Sample time (hr)	Theoretical detention time (hr)	Influent (mg/L)	60 cm column (mg/L)	45 cm column (mg/L)	30 cm column (mg/L)
0.25	-	69.85	2.59	1.89	2.92
1.25	1	65.91	42.96	41.13	38.31
4	2	66.67	68.58	65.44	59.83
8.25	3	68.19	69.15	69.38	69.99
14	4	65.16	67.97	67.23	66.16
22.5	6	65.50	67.43	67.37	67.14
35.25	9	67.57	64.29	64.14	66.61

186

Table B.126. Storm event #6 TSS data.

Sample time (hr)	Theoretical detention time (hr)	Influent (mg/L)	60 cm column (mg/L)	45 cm column (mg/L)	30 cm column (mg/L)
0.25	-	5.49	1.27	1.64	2.51
1.25	1	7.66	2.74	2.46	4.44
4	2	8.53	3.19	3.36	3.65
8.25	3	9.39	2.86	3.01	3.95
14	4	10.72	2.80	2.68	3.63
22.5	6	9.36	2.74	2.36	3.30
35.25	9	1.78	2.13	2.64	1.78

Table B.127. Storm event #6 VSS data.

Sample time (hr)	Theoretical detention time (hr)	Influent (mg/L)	60 cm column (mg/L)	45 cm column (mg/L)	30 cm column (mg/L)
0.25	-	1.00	0.00	0.01	0.74
1.25	1	2.30	0.84	0.65	0.42
4	2	2.17	0.99	1.72	0.68
8.25	3	3.12	0.71	1.18	2.47
14	4	2.82	0.54	0.87	1.48
22.5	6	2.48	0.38	0.56	0.50
35.25	9	1.46	0.93	0.18	0.89

Table B.128. Storm event #7 flow data for the 30 cm column.

Theoretical detention time (hr)	Theoretical flow rate (mL/min)	Flow rate 1 (mL/min)	Flow rate 2 (mL/min)	Average flow rate (mL/min)
0.25	117.1	116		116
0.5	58.5	56		56
0.75	39	39		39
1	29.3	29		29
2	14.6	14.5		14.5
3	9.8	9.5		9.5

187

Table B.129. Storm event #7 flow data for the 45 cm column.

Theoretical detention time (hr)	Theoretical flow rate (mL/min)	Flow rate 1 (mL/min)	Flow rate 2 (mL/min)	Average flow rate (mL/min)
0.25	177.7	180		180
0.5	88.9	88		88
0.75	59.2	59		59
1	44.4	44		44
2	22.2	21.5		21.5
3	14.8	14.8		14.8

Table B.130. Storm event #7 flow data for the 60 cm column.

Theoretical detention time (hr)	Theoretical flow rate (mL/min)	Flow rate 1 (mL/min)	Flow rate 2 (mL/min)	Average flow rate (mL/min)
0.25	237.3	244		244
0.5	118.7	120		120
0.75	79.1	78		78
1	59.3	59		59
2	29.7	29.5		29.5
3	19.8	19		19

Table B.131. Storm event #7 Influent TN data.

Sample time (hr)	Theoretical detention time (hr)	Sample 1 (mg/L)	Sample 2 (mg/L)	Sample 3 (mg/L)	Average (mg/L)	Standard deviation (mg/L)
0.1	-	4.26	4.13	4.24	4.21	0.07
0.31	0.25	2.17	2.16	2.24	2.19	0.04
1	0.5	2.32	2.25	2.33	2.30	0.04
2.1	0.75	2.38	2.34	2.33	2.35	0.03
3.5	1	2.30	2.24	2.31	2.28	0.04
6.25	2	2.19	2.21	2.16	2.19	0.03
10.5	3	2.31	2.35	2.39	2.35	0.04

Table B.132. Storm event #7 TN data for the 30 cm column.

Sample time (hr)	Theoretical detention time (hr)	Sample 1 (mg/L)	Sample 2 (mg/L)	Sample 3 (mg/L)	Average (mg/L)	Standard deviation (mg/L)
0.1	-	0.60	0.62	0.61	0.61	0.01
0.31	0.25	1.21	1.18	1.21	1.20	0.02
1	0.5	1.83	1.80	1.87	1.83	0.03
2.1	0.75	1.83	1.83	1.81	1.82	0.01
3.5	1	1.54	1.49	1.52	1.52	0.02
6.25	2	1.17	1.13	1.20	1.17	0.03
10.5	3	0.78	0.80	0.79	0.79	0.01

Table B.133. Storm event #7 TN data for the 45 cm column.

Sample time (hr)	Theoretical detention time (hr)	Sample 1 (mg/L)	Sample 2 (mg/L)	Sample 3 (mg/L)	Average (mg/L)	Standard deviation (mg/L)
0.1	-	0.65	0.64	0.68	0.66	0.02
0.31	0.25	1.47	1.49	1.47	1.47	0.01
1	0.5	1.77	1.73	1.78	1.76	0.03
2.1	0.75	1.69	1.71	1.75	1.72	0.03
3.5	1	1.63	1.61	1.62	1.62	0.01
6.25	2	1.07	1.08	1.11	1.09	0.02
10.5	3	0.54	0.57	0.55	0.55	0.02

Table B.134. Storm event #7 TN data for the 60 cm column.

Sample time (hr)	Theoretical detention time (hr)	Sample 1 (mg/L)	Sample 2 (mg/L)	Sample 3 (mg/L)	Average (mg/L)	Standard deviation (mg/L)
0.1	-	0.75	0.72	0.74	0.74	0.01
0.31	0.25	1.46	1.51	1.51	1.49	0.03
1	0.5	1.87	1.90	1.90	1.89	0.01
2.1	0.75	1.82	1.75	1.78	1.78	0.03
3.5	1	1.60	1.57	1.66	1.61	0.05
6.25	2	1.09	1.07	1.12	1.09	0.02
10.5	3	0.53	0.49	0.53	0.52	0.02

189

Table B.135. Storm event #7 Influent DOC data.

Sample time (hr)	Theoretical detention time (hr)	Sample 1 (mg/L)	Sample 2 (mg/L)	Sample 3 (mg/L)	Average (mg/L)	Standard deviation (mg/L)
0.1	-	5.46	5.45	5.35	5.42	0.06
0.31	0.25	4.43	4.50	4.53	4.49	0.05
1	0.5	5.14	5.06	5.05	5.08	0.05
2.1	0.75	4.29	4.15	4.20	4.22	0.07
3.5	1	4.44	4.33	4.32	4.36	0.06
6.25	2	4.37	4.45	4.46	4.43	0.05
10.5	3	4.89	4.70	4.81	4.80	0.10

Table B.136. Storm event #7 DOC data for the 30 cm column.

Sample time (hr)	Theoretical detention time (hr)	Sample 1 (mg/L)	Sample 2 (mg/L)	Sample 3 (mg/L)	Average (mg/L)	Standard deviation (mg/L)
0.1	-	21.87	22.65	22.36	22.29	0.39
0.31	0.25	13.60	13.56	13.85	13.67	0.16
1	0.5	5.42	5.30	5.47	5.40	0.09
2.1	0.75	5.07	4.98	5.01	5.02	0.05
3.5	1	4.09	4.12	4.19	4.13	0.05
6.25	2	4.11	4.11	4.18	4.13	0.04
10.5	3	4.47	4.40	4.43	4.43	0.04

Table B.137. Storm event #7 DOC data for the 45 cm column.

Sample time (hr)	Theoretical detention time (hr)	Sample 1 (mg/L)	Sample 2 (mg/L)	Sample 3 (mg/L)	Average (mg/L)	Standard deviation (mg/L)
0.1	-	40.47	39.09	40.24	39.93	0.74
0.31	0.25	16.01	15.63	15.98	15.87	0.21
1	0.5	4.62	4.64	4.72	4.66	0.05
2.1	0.75	4.21	4.21	4.27	4.23	0.03
3.5	1	4.92	4.80	4.89	4.87	0.06
6.25	2	4.53	4.47	4.50	4.50	0.03
10.5	3	4.16	4.06	4.07	4.10	0.06

190

Table B.138. Storm event #7 DOC data for the 60 cm column.

Sample time (hr)	Theoretical detention time (hr)	Sample 1 (mg/L)	Sample 2 (mg/L)	Sample 3 (mg/L)	Average (mg/L)	Standard deviation (mg/L)
0.1	-	34.69	35.39	35.01	35.03	0.35
0.31	0.25	12.82	12.54	12.96	12.78	0.21
1	0.5	4.22	4.28	4.28	4.26	0.03
2.1	0.75	4.64	4.65	4.80	4.70	0.09
3.5	1	4.15	4.19	4.27	4.20	0.06
6.25	2	3.99	4.01	4.11	4.04	0.07
10.5	3	4.52	4.42	4.38	4.44	0.07

Table B.139. Storm event #7 DO data.

Sample time (hr)	Theoretical detention time (hr)	Influent (mg/L)	60 cm column (mg/L)	45 cm column (mg/L)	30 cm column (mg/L)
0.1	-	5.83	0.14	0.2	0.15
0.31	0.25	7.48	1.02	1.1	1.1
1	0.5	5.62	0.76		
2.1	0.75	5.73	0.5	0.4	0.34
3.5	1	4.89	0.1	0.15	0.2
6.25	2	5.41	0.1	0.02	0.21
10.5	3	5.72	0.12	0.07	0.13

Table B.140. Storm event #7 pH data.

Sample time (hr)	Theoretical detention time (hr)	Influent (mg/L)	60 cm column (mg/L)	45 cm column (mg/L)	30 cm column (mg/L)
0.1	-	7.54	6.96	6.83	6.97
0.31	0.25	7.49	7.02	7.01	6.88
1	0.5	7.53	7.12	7.03	7.16
2.1	0.75	7.5	7.1	7.07	7.18
3.5	1	7.55	7.06	7.04	7.13
6.25	2	7.56	7.05	7.12	7.23
10.5	3	7.6	7.11	7.14	7.31

191

Table B.141. Storm event #7 NH_4^+-N data.

Sample time (hr)	Theoretical detention time (hr)	Influent (mg/L)	60 cm column (mg/L)	45 cm column (mg/L)	30 cm column (mg/L)
0.1	-	0.00	0.16	0.10	0.09
0.31	0.25	0.00	0.10	0.06	0.06
1	0.5	0.00	0.06	0.00	0.02
2.1	0.75	0.00	0.00	0.00	0.00
3.5	1	0.04	0.00	0.00	0.00
6.25	2	0.00	0.00	0.00	0.00
10.5	3	0.00	0.02	0.01	0.02

Table B.142. Storm event #7 NO_2^--N data.

Sample time (hr)	Theoretical detention time (hr)	Influent (mg/L)	60 cm column (mg/L)	45 cm column (mg/L)	30 cm column (mg/L)
0.1	-	0.03	0.09	0.09	0.10
0.31	0.25	0.02	0.05	0.05	0.07
1	0.5	0.03	0.04	0.03	0.03
2.1	0.75	0.02	0.01	0.01	0.02
3.5	1	0.02	0.00	0.00	0.00
6.25	2	0.02	0.25	0.18	0.20
10.5	3	0.03	0.00	0.00	0.00

Table B.143. Storm event #7 NO_3^--N data.

Sample time (hr)	Theoretical detention time (hr)	Influent (mg/L)	60 cm column (mg/L)	45 cm column (mg/L)	30 cm column (mg/L)
0.1	-	3.98	0.01	0.03	0.04
0.31	0.25	2.03	1.14	1.13	0.85
1	0.5	1.98	1.56	1.46	1.47
2.1	0.75	1.97	1.40	1.34	1.38
3.5	1	2.03	1.28	1.18	1.23
6.25	2	2.02	0.49	0.55	0.60
10.5	3	2.01	0.03	0.11	0.30

192

Table B.144. Storm event #7 Org-N data.

Sample time (hr)	Theoretical detention time (hr)	Influent (mg/L)	60 cm column (mg/L)	45 cm column (mg/L)	30 cm column (mg/L)
0.1	-	0.20	0.48	0.43	0.38
0.31	0.25	0.14	0.21	0.23	0.22
1	0.5	0.30	0.23	0.26	0.31
2.1	0.75	0.36	0.36	0.37	0.43
3.5	1	0.20	0.33	0.43	0.29
6.25	2	0.14	0.36	0.36	0.37
10.5	3	0.30	0.47	0.44	0.47

Table B.145. Storm event #7 PO_4^{3-}-P data.

Sample time (hr)	Theoretical detention time (hr)	Influent (mg/L)	60 cm column (mg/L)	45 cm column (mg/L)	30 cm column (mg/L)
0.1	-	0.12	0.35	0.19	0.30
0.31	0.25	0.17	0.24	0.20	0.21
1	0.5	0.16	0.04	0.04	0.06
2.1	0.75	0.15	0.00	0.00	0.00
3.5	1	0.16	0.00	0.00	0.00
6.25	2	0.16	0.00	0.00	0.00
10.5	3	0.15	0.00	0.00	0.00

Table B.146. Storm event #7 SO_4^{2-}-S data.

Sample time (hr)	Theoretical detention time (hr)	Influent (mg/L)	60 cm column (mg/L)	45 cm column (mg/L)	30 cm column (mg/L)
0.1	-	68.80	1.89	2.07	3.10
0.31	0.25	65.08	43.84	42.54	34.82
1	0.5	64.08	64.70	64.22	62.86
2.1	0.75	64.26	65.12	64.11	63.87
3.5	1	64.53	63.82	64.59	64.03
6.25	2	64.42	65.25	64.74	65.87
10.5	3	65.07	65.42	66.22	67.41

193

Table B.147. Storm event #7 TSS data.

Sample time (hr)	Theoretical detention time (hr)	Influent (mg/L)	60 cm column (mg/L)	45 cm column (mg/L)	30 cm column (mg/L)
0.1	-	7.64	2.56	1.56	3.06
0.31	0.25	4.32	2.12	3.34	6.02
1	0.5	6.05	3.00	4.53	2.62
2.1	0.75	5.76	3.32	2.69	3.67
3.5	1	4.57	3.09	3.42	3.07
6.25	2	4.70	2.68	3.87	3.33
10.5	3	3.73	2.67	2.72	3.58

Table B.148. Storm event #7 VSS data.

Sample time (hr)	Theoretical detention time (hr)	Influent (mg/L)	60 cm column (mg/L)	45 cm column (mg/L)	30 cm column (mg/L)
0.1	-	1.46	0.70	0.00	1.74
0.31	0.25	1.47	0.74	0.60	1.98
1	0.5	2.03	0.64	1.15	0.67
2.1	0.75	1.84	0.49	1.39	1.16
3.5	1	1.84	1.03	1.00	0.78
6.25	2	1.59	0.58	1.23	1.18
10.5	3	1.08	0.00	0.83	0.72

Table B.149. Storm event #8 flow data for the 30 cm column.

Theoretical detention time (hr)	Theoretical flow rate (mL/min)	Flow rate 1 (mL/min)	Flow rate 2 (mL/min)	Average flow rate (mL/min)
1	29.27	29.5		29.5
1	29.27	30		30
1	29.27	30		30
1	29.27	30		30
1	29.27	30		30
1	29.27	30		30

194

Table B.150. Storm event #8 flow data for the 45 cm column.

Theoretical detention time (hr)	Theoretical flow rate (mL/min)	Flow rate 1 (mL/min)	Flow rate 2 (mL/min)	Average flow rate (mL/min)
1	44.43	44.5		44.5
1	44.43	44.5		44.5
1	44.43	45		45
1	44.43	45		45
1	44.43	45		45
1	44.43	45		45

Table B.151. Storm event #8 flow data for the 60 cm column.

Theoretical detention time (hr)	Theoretical flow rate (mL/min)	Flow rate 1 (mL/min)	Flow rate 2 (mL/min)	Average flow rate (mL/min)
1	59.33	59.5		59.5
1	59.33	59.5		59.5
1	59.33	60		60
1	59.33	60		60
1	59.33	60		60
1	59.33	60		60

Table B.152. Storm event #8 Influent TN data.

Sample time (hr)	Theoretical detention time (hr)	Sample 1 (mg/L)	Sample 2 (mg/L)	Sample 3 (mg/L)	Average (mg/L)	Standard deviation (mg/L)
0.25	-	2.31	2.35	2.39	2.35	0.04
1.25	1	2.28	2.20	2.31	2.26	0.06
1.5	1	2.22	2.22	2.27	2.24	0.03
2	1	2.29	2.25	2.22	2.25	0.03
3	1	2.17	2.17	2.26	2.20	0.05
5	1	2.16	2.22	2.22	2.20	0.03
9	1	2.17	2.18	2.18	2.18	0.01

195

Table B.153. Storm event #8 TN data for the 30 cm column.

Sample time (hr)	Theoretical detention time (hr)	Sample 1 (mg/L)	Sample 2 (mg/L)	Sample 3 (mg/L)	Average (mg/L)	Standard deviation (mg/L)
0.25	-	0.57	0.56	0.57	0.57	0.00
1.25	1	0.84	0.83	0.83	0.83	0.01
1.5	1	0.97	0.96	0.95	0.96	0.01
2	1	1.05	1.09	1.10	1.08	0.03
3	1	1.26	1.27	1.31	1.28	0.02
5	1	1.46	1.54	1.53	1.51	0.04
9	1	1.67	1.67	1.71	1.69	0.02

Table B.154. Storm event #8 TN data for the 45 cm column.

Sample time (hr)	Theoretical detention time (hr)	Sample 1 (mg/L)	Sample 2 (mg/L)	Sample 3 (mg/L)	Average (mg/L)	Standard deviation (mg/L)
0.25	-	0.61	0.61	0.63	0.61	0.01
1.25	1	0.78	0.78	0.80	0.79	0.01
1.5	1	0.95	0.95	0.96	0.95	0.01
2	1	0.80	0.80	0.85	0.82	0.03
3	1	1.17	1.14	1.16	1.15	0.02
5	1	1.74	1.75	1.73	1.74	0.01
9	1	1.80	1.77	1.83	1.80	0.03

Table B.155. Storm event #8 TN data for the 60 cm column.

Sample time (hr)	Theoretical detention time (hr)	Sample 1 (mg/L)	Sample 2 (mg/L)	Sample 3 (mg/L)	Average (mg/L)	Standard deviation (mg/L)
0.25	-	0.62	0.61	0.64	0.62	0.02
1.25	1	0.81	0.79	0.81	0.80	0.01
1.5	1	0.87	0.84	0.86	0.86	0.02
2	1	1.06	1.05	1.10	1.07	0.03
3	1	1.24	1.23	1.25	1.24	0.01
5	1	1.47	1.48	1.50	1.48	0.02
9	1	1.78	1.77	1.82	1.79	0.03

196

Table B.156. Storm event #8 Influent DOC data.

Sample time (hr)	Theoretical detention time (hr)	Sample 1 (mg/L)	Sample 2 (mg/L)	Sample 3 (mg/L)	Average (mg/L)	Standard deviation (mg/L)
0.25	-	4.89	4.70	4.81	4.80	0.10
1.25	1	4.77	4.72	4.87	4.78	0.08
1.5	1	4.57	4.66	4.66	4.63	0.05
2	1	4.77	4.80	4.80	4.79	0.02
3	1	4.50	4.36	4.49	4.45	0.08
5	1	4.50	4.45	4.39	4.45	0.05
9	1	4.20	4.28	4.36	4.28	0.08

Table B.157. Storm event #8 DOC data for the 30 cm column.

Sample time (hr)	Theoretical detention time (hr)	Sample 1 (mg/L)	Sample 2 (mg/L)	Sample 3 (mg/L)	Average (mg/L)	Standard deviation (mg/L)
0.25	-	25.63	26.19	25.81	25.88	0.29
1.25	1	23.00	22.41	22.77	22.73	0.30
1.5	1	10.08	9.76	9.95	9.93	0.16
2	1	5.85	5.78	5.77	5.80	0.04
3	1	4.80	4.72	4.84	4.79	0.07
5	1	4.47	4.38	4.36	4.40	0.06
9	1	4.33	4.20	4.36	4.30	0.09

Table B.158. Storm event #8 DOC data for the 45 cm column.

Sample time (hr)	Theoretical detention time (hr)	Sample 1 (mg/L)	Sample 2 (mg/L)	Sample 3 (mg/L)	Average (mg/L)	Standard deviation (mg/L)
0.25	-	47.52	46.57	47.36	47.15	0.51
1.25	1	32.49	32.34	33.67	32.83	0.73
1.5	1	12.58	12.78	12.93	12.77	0.18
2	1	6.12	6.04	6.20	6.12	0.08
3	1	4.75	4.63	4.65	4.68	0.07
5	1	5.06	5.04	5.22	5.10	0.10
9	1	4.97	4.85	5.00	4.94	0.08

197

Table B.159. Storm event #8 DOC data for the 60 cm column.

Sample time (hr)	Theoretical detention time (hr)	Sample 1 (mg/L)	Sample 2 (mg/L)	Sample 3 (mg/L)	Average (mg/L)	Standard deviation (mg/L)
0.25	-	45.05	44.21	44.62	44.63	0.42
1.25	1	29.32	28.26	29.10	28.89	0.56
1.5	1	9.93	9.71	9.79	9.81	0.11
2	1	5.91	5.94	5.88	5.91	0.03
3	1	4.40	4.41	4.44	4.42	0.02
5	1	4.21	4.27	4.20	4.23	0.03
9	1	4.29	4.27	4.17	4.24	0.07

Table B.160. Storm event #8 DO data.

Sample time (hr)	Theoretical detention time (hr)	Influent (mg/L)	60 cm column (mg/L)	45 cm column (mg/L)	30 cm column (mg/L)
0.25	-	5.72	0.03	0.1	0
1.25	1	4.53			
1.5	1	2.82			
2	1	4.8			
3	1	4.8			
5	1	4.95			
9	1	5.30	0.23	0.42	0.34

Table B.161. Storm event #8 pH data.

Sample time (hr)	Theoretical detention time (hr)	Influent (mg/L)	60 cm column (mg/L)	45 cm column (mg/L)	30 cm column (mg/L)
0.25	-	7.6	6.68	6.75	6.94
1.25	1	7.48			
1.5	1	7.51			
2	1	7.59			
3	1	7.52			
5	1	7.52			
9	1	7.48			

198

Table B.162. Storm event #8 NH$_4^+$-N data.

Sample time (hr)	Theoretical detention time (hr)	Influent (mg/L)	60 cm column (mg/L)	45 cm column (mg/L)	30 cm column (mg/L)
0.25	-	0.00	0.06	0.05	0.03
1.25	1	0.00	0.13	0.10	0.07
1.5	1	0.00	0.22	0.23	0.14
2	1	0.00	0.16	0.14	0.14
3	1	0.00	0.04	0.08	0.04
5	1	0.00	0.00	0.00	0.00
9	1	0.00	0.00	0.00	0.00

Table B.163. Storm event #8 NO$_2^-$-N data.

Sample time (hr)	Theoretical detention time (hr)	Influent (mg/L)	60 cm column (mg/L)	45 cm column (mg/L)	30 cm column (mg/L)
0.25	-	0.03	0.16	0.16	0.11
1.25	1	0.03	0.10	0.11	0.14
1.5	1	0.03	0.06	0.06	0.09
2	1	0.02	0.08	0.04	0.06
3	1	0.03	0.06	0.06	0.07
5	1	0.03	0.05	0.05	0.06
9	1	0.03	0.03	0.06	0.04

Table B.164. Storm event #8 NO$_3^-$-N data.

Sample time (hr)	Theoretical detention time (hr)	Influent (mg/L)	60 cm column (mg/L)	45 cm column (mg/L)	30 cm column (mg/L)
0.25	-	1.95	0.02	0.04	0.03
1.25	1	1.95	0.20	0.19	0.24
1.5	1	1.96	0.22	0.25	0.44
2	1	1.92	0.30	0.25	0.51
3	1	1.90	0.66	0.58	0.77
5	1	1.95	1.03	1.10	1.06
9	1	1.96	1.37	1.36	1.10

199

Table B.165. Storm event #8 Org-N data.

Sample time (hr)	Theoretical detention time (hr)	Influent (mg/L)	60 cm column (mg/L)	45 cm column (mg/L)	30 cm column (mg/L)
0.25	-	0.36	0.39	0.37	0.40
1.25	1	0.29	0.37	0.39	0.38
1.5	1	0.25	0.36	0.41	0.29
2	1	0.31	0.53	0.38	0.37
3	1	0.27	0.48	0.44	0.39
5	1	0.22	0.40	0.58	0.39
9	1	0.19	0.39	0.38	0.56

Table B.166. Storm event #8 PO_4^{3-}-P data.

Sample time (hr)	Theoretical detention time (hr)	Influent (mg/L)	60 cm column (mg/L)	45 cm column (mg/L)	30 cm column (mg/L)
0.25	-	0.15	0.62	0.40	0.31
1.25	1	0.17	0.43	0.39	0.22
1.5	1	0.17	0.15	0.32	0.12
2	1	0.17	0.07	0.13	0.06
3	1	0.17	0.00	0.00	0.02
5	1	0.17	0.00	0.00	0.00
9	1	0.17	0.00	0.00	0.00

Table B.167. Storm event #8 SO_4^{2-}-S data.

Sample time (hr)	Theoretical detention time (hr)	Influent (mg/L)	60 cm column (mg/L)	45 cm column (mg/L)	30 cm column (mg/L)
0.25	-	63.57	2.53	4.26	3.89
1.25	1	67.67	21.38	21.27	20.54
1.5	1	67.75	54.05	52.02	49.73
2	1	66.57	64.11	60.05	59.76
3	1	66.07	66.67	65.89	66.22
5	1	67.23	67.04	70.31	70.78
9	1	67.49	67.17	72.00	55.81

200

Table B.168. Storm event #9 flow data for the 30 cm column.

Theoretical detention time (hr)	Theoretical flow rate (mL/min)	Flow rate 1 (mL/min)	Flow rate 2 (mL/min)	Average flow rate (mL/min)
1	29.27	30	30	30.0
2	14.63	14.5	14.5	14.5
3	9.76	10	10	10.0
4	7.32	7	7	7.0
6	4.88	4.75	4.75	4.75
9	3.25	3.25	3.25	3.25

Table B.169. Storm event #9 flow data for the 45 cm column.

Theoretical detention time (hr)	Theoretical flow rate (mL/min)	Flow rate 1 (mL/min)	Flow rate 2 (mL/min)	Average flow rate (mL/min)
1	44.43	43	42	42.5
2	22.22	21.5	21	21.25
3	14.81	14.5	14.5	14.5
4	11.11	11.25	11.25	11.25
6	7.41	7.5	7.5	7.5
9	4.94	5	5	5

Table B.170. Storm event #9 flow data for the 60 cm column.

Theoretical detention time (hr)	Theoretical flow rate (mL/min)	Flow rate 1 (mL/min)	Flow rate 2 (mL/min)	Average flow rate (mL/min)
1	59.33	60	60	60.0
2	29.67	29.5	29.5	29.5
3	19.78	19.5	19.5	19.5
4	14.83	15	15	15
6	9.89	10	10	10
9	6.59	6.75	6.75	6.75

201

Table B.171. Storm event #9 Influent TN data.

Sample time (hr)	Theoretical detention time (hr)	Sample 1 (mg/L)	Sample 2 (mg/L)	Sample 3 (mg/L)	Average (mg/L)	Standard deviation (mg/L)
0.25	-	2.17	2.18	2.18	2.18	0.01
1.25	1	2.45	2.53	2.49	2.49	0.04
4	2	2.35	2.29	2.35	2.33	0.03
8.25	3	2.38	2.34	2.44	2.38	0.05
14	4	2.35	2.35	2.38	2.36	0.02
22.5	6	2.51	2.48	2.47	2.49	0.02
35.25	9	2.43	2.46	2.44	2.44	0.02

Table B.172. Storm event #9 TN data for the 30 cm column.

Sample time (hr)	Theoretical detention time (hr)	Sample 1 (mg/L)	Sample 2 (mg/L)	Sample 3 (mg/L)	Average (mg/L)	Standard deviation (mg/L)
0.25	-	0.58	0.58	0.58	0.58	0.00
1.25	1	1.31	1.24	1.24	1.27	0.04
4	2	1.04	1.04	1.05	1.04	0.01
8.25	3	0.99	1.04	1.06	1.03	0.03
14	4	0.92	0.94	0.91	0.92	0.02
22.5	6	0.74	0.76	0.77	0.76	0.02
35.25	9	0.53	0.52	0.54	0.53	0.01

Table B.173. Storm event #9 TN data for the 45 cm column.

Sample time (hr)	Theoretical detention time (hr)	Sample 1 (mg/L)	Sample 2 (mg/L)	Sample 3 (mg/L)	Average (mg/L)	Standard deviation (mg/L)
0.25	-	0.65	0.68	0.67	0.67	0.01
1.25	1	1.06	1.06	1.06	1.06	0.00
4	2	0.61	0.62	0.64	0.62	0.01
8.25	3	0.59	0.57	0.59	0.58	0.01
14	4	0.64	0.62	0.65	0.64	0.02
22.5	6	0.48	0.50	0.50	0.49	0.01
35.25	9	0.47	0.44	0.45	0.45	0.02

Table B.174. Storm event #9 TN data for the 60 cm column.

Sample time (hr)	Theoretical detention time (hr)	Sample 1 (mg/L)	Sample 2 (mg/L)	Sample 3 (mg/L)	Average (mg/L)	Standard deviation (mg/L)
0.25	-	0.59	0.61	0.61	0.60	0.01
1.25	1	1.13	1.16	1.17	1.16	0.02
4	2	0.66	0.69	0.68	0.68	0.01
8.25	3	0.55	0.56	0.56	0.55	0.01
14	4	0.53	0.56	0.57	0.55	0.02
22.5	6	0.55	0.57	0.55	0.56	0.01
35.25	9	0.44	0.44	0.43	0.44	0.01

Table B.175. Storm event #9 Influent DOC data.

Sample time (hr)	Theoretical detention time (hr)	Sample 1 (mg/L)	Sample 2 (mg/L)	Sample 3 (mg/L)	Average (mg/L)	Standard deviation (mg/L)
0.25	-	4.20	4.28	4.36	4.28	0.08
1.25	1	4.91	4.97	5.12	5.00	0.11
4	2	4.85	4.75	4.94	4.85	0.10
8.25	3	4.49	4.69	4.70	4.63	0.12
14	4	4.95	4.86	4.98	4.93	0.06
22.5	6	4.99	4.90	5.09	4.99	0.09
35.25	9	4.67	4.63	4.76	4.68	0.06

Table B.176. Storm event #9 DOC data for the 30 cm column.

Sample time (hr)	Theoretical detention time (hr)	Sample 1 (mg/L)	Sample 2 (mg/L)	Sample 3 (mg/L)	Average (mg/L)	Standard deviation (mg/L)
0.25	-	63.24	60.80	61.86	61.97	1.23
1.25	1	21.39	21.05	21.22	21.22	0.17
4	2	7.31	7.54	7.55	7.47	0.14
8.25	3	5.88	5.78	5.65	5.77	0.12
14	4	5.37	5.28	5.43	5.36	0.08
22.5	6	5.82	5.77	5.80	5.80	0.03
35.25	9	5.28	5.26	5.40	5.31	0.07

Table B.177. Storm event #9 DOC data for the 45 cm column.

Sample time (hr)	Theoretical detention time (hr)	Sample 1 (mg/L)	Sample 2 (mg/L)	Sample 3 (mg/L)	Average (mg/L)	Standard deviation (mg/L)
0.25	-	90.12	87.67	90.32	89.37	1.48
1.25	1	30.68	30.07	30.77	30.51	0.38
4	2	7.43	7.31	7.34	7.36	0.06
8.25	3	5.56	5.41	5.57	5.51	0.09
14	4	6.19	6.02	6.04	6.08	0.10
22.5	6	5.91	5.73	5.79	5.81	0.09
35.25	9	5.96	5.88	5.82	5.89	0.07

Table B.178. Storm event #9 DOC data for the 60 cm column.

Sample time (hr)	Theoretical detention time (hr)	Sample 1 (mg/L)	Sample 2 (mg/L)	Sample 3 (mg/L)	Average (mg/L)	Standard deviation (mg/L)
0.25	-	76.82	75.39	74.46	75.56	1.19
1.25	1	20.28	20.00	20.60	20.29	0.30
4	2	5.83	5.85	5.80	5.83	0.02
8.25	3	4.79	4.91	4.84	4.85	0.06
14	4	5.15	5.05	5.27	5.16	0.11
22.5	6	5.60	5.42	5.64	5.55	0.12
35.25	9	5.10	5.12	5.30	5.17	0.11

Table B.179. Storm event #9 DO data.

Sample time (hr)	Theoretical detention time (hr)	Influent (mg/L)	60 cm column (mg/L)	45 cm column (mg/L)	30 cm column (mg/L)
0.25	-	5.3			
1.25	1	5.89			
4	2	6.39			
8.25	3	5.99			
14	4	6			
22.5	6				
35.25	9				

204

Table B.180. Storm event #9 pH data.

Sample time (hr)	Theoretical detention time (hr)	Influent (mg/L)	60 cm column (mg/L)	45 cm column (mg/L)	30 cm column (mg/L)
0.25	-	7.48	6.57	6.6	6.64
1.25	1	7.57	6.24	6.44	6.57
4	2	7.67	6.57	6.77	6.86
8.25	3	7.56	6.82	7.01	7.06
14	4	7.49	7.18	7.3	7.41
22.5	6	7.88	7.25	7.25	7.39
35.25	9	7.87	7.24	7.31	7.46

Table B.181. Storm event #9 NH_4^+-N data.

Sample time (hr)	Theoretical detention time (hr)	Influent (mg/L)	60 cm column (mg/L)	45 cm column (mg/L)	30 cm column (mg/L)
0.25	-	0.00	0.00	0.00	0.03
1.25	1	0.00	0.06	0.00	0.07
4	2	0.00	0.04	0.05	0.05
8.25	3	0.00	0.06	0.04	0.03
14	4	0.03	0.05	0.03	0.03
22.5	6	0.06	0.04	0.00	0.05
35.25	9	0.05	0.03	0.00	0.05

Table B.182. Storm event #9 NO_2^--N data.

Sample time (hr)	Theoretical detention time (hr)	Influent (mg/L)	60 cm column (mg/L)	45 cm column (mg/L)	30 cm column (mg/L)
0.25	-	0.02	0.19	0.18	0.17
1.25	1	0.00	0.00	0.00	0.02
4	2	0.00	0.00	0.00	0.00
8.25	3	0.00	0.00	0.00	0.00
14	4	0.00	0.00	0.00	0.00
22.5	6	0.00	0.01	0.04	0.00
35.25	9	0.06	0.04	0.04	0.07

205

Table B.183. Storm event #9 NO$_3^-$-N data.

Sample time (hr)	Theoretical detention time (hr)	Influent (mg/L)	60 cm column (mg/L)	45 cm column (mg/L)	30 cm column (mg/L)
0.25	-	2.01	0.01	0.01	0.01
1.25	1	2.00	0.50	0.39	0.65
4	2	1.97	0.08	0.05	0.37
8.25	3	2.06	0.04	0.07	0.41
14	4	2.05	0.06	0.09	0.33
22.5	6	2.10	0.05	0.02	0.12
35.25	9	2.09	0.01	0.01	0.03

Table B.184. Storm event #9 Org-N data.

Sample time (hr)	Theoretical detention time (hr)	Influent (mg/L)	60 cm column (mg/L)	45 cm column (mg/L)	30 cm column (mg/L)
0.25	-	0.15	0.40	0.47	0.36
1.25	1	0.49	0.60	0.67	0.52
4	2	0.36	0.56	0.52	0.62
8.25	3	0.32	0.45	0.47	0.59
14	4	0.28	0.44	0.51	0.56
22.5	6	0.33	0.47	0.44	0.59
35.25	9	0.24	0.35	0.41	0.38

Table B.185. Storm event #9 PO$_4^{3-}$-P data.

Sample time (hr)	Theoretical detention time (hr)	Influent (mg/L)	60 cm column (mg/L)	45 cm column (mg/L)	30 cm column (mg/L)
0.25	-	0.16	1.58	1.39	1.20
1.25	1	0.11	0.06	0.06	0.04
4	2	0.11	0.00	0.00	0.00
8.25	3	0.12	0.00	0.00	0.00
14	4	0.11	0.00	0.00	0.00
22.5	6	0.12	0.00	0.00	0.00
35.25	9	0.13	0.00	0.00	0.03

Table B.186. Storm event #9 SO_4^{2-}-S data.

Sample time (hr)	Theoretical detention time (hr)	Influent (mg/L)	60 cm column (mg/L)	45 cm column (mg/L)	30 cm column (mg/L)
0.25	-	68.42	0.60	0.77	0.81
1.25	1	75.68	58.44	54.50	58.08
4	2	74.16	73.56	72.54	73.22
8.25	3	77.01	72.78	71.58	75.24
14	4	76.00	75.33	75.78	75.02
22.5	6	77.65	76.76	74.93	74.52
35.25	9	76.12	74.24	73.44	73.85

Table B.187. Storm event #9 TSS data.

Sample time (hr)	Theoretical detention time (hr)	Influent (mg/L)	60 cm column (mg/L)	45 cm column (mg/L)	30 cm column (mg/L)
0.25	-		0.03	1.80	2.00
1.25	1	4.92	2.63	0.00	4.20
4	2	5.55	2.73	1.75	2.89
8.25	3	5.17	2.63	2.50	2.82
14	4	4.22			
22.5	6				
35.25	9	3.13	1.13	1.45	3.98

Table B.188. Storm event #9 VSS data.

Sample time (hr)	Theoretical detention time (hr)	Influent (mg/L)	60 cm column (mg/L)	45 cm column (mg/L)	30 cm column (mg/L)
0.25	-		0.00	0.00	0.00
1.25	1		1.43	0.00	0.00
4	2		0.37	0.00	0.58
8.25	3				
14	4				
22.5	6				
35.25	9				

207

Table B.189. Storm event #10 flow data for the 30 cm column.

Theoretical detention time (hr)	Theoretical flow rate (mL/min)	Flow rate 1 (mL/min)	Flow rate 2 (mL/min)	Average flow rate (mL/min)
2	14.63			
2	14.63			
2	14.63			
2	14.63			
2	14.63			
2	14.63			

Table B.190. Storm event #10 flow data for the 45 cm column.

Theoretical detention time (hr)	Theoretical flow rate (mL/min)	Flow rate 1 (mL/min)	Flow rate 2 (mL/min)	Average flow rate (mL/min)
2	22.22			
2	22.22			
2	22.22			
2	22.22			
2	22.22			
2	22.22			

Table B.191. Storm event #10 flow data for the 60 cm column.

Theoretical detention time (hr)	Theoretical flow rate (mL/min)	Flow rate 1 (mL/min)	Flow rate 2 (mL/min)	Average flow rate (mL/min)
2	29.67			
2	29.67			
2	29.67			
2	29.67			
2	29.67			
2	29.67			

Table B.192. Storm event #10 DO data.

Sample time (hr)	Theoretical detention time (hr)	Influent (mg/L)	60 cm column (mg/L)	45 cm column (mg/L)	30 cm column (mg/L)
0	-		0	0	0
3	2	5.12	0	0.06	0.15
4	2	5.12	0.1	0.04	0.14
6	2	6.25	0.15	0.07	0
8	2	5.82	0	0	0
12	2	6.09	0.07	0	0.02
18	2	6.00	0	0	0

Table B.193. Storm event #10 NH_4^+-N data.

Sample time (hr)	Theoretical detention time (hr)	Influent (mg/L)	60 cm column (mg/L)	45 cm column (mg/L)	30 cm column (mg/L)
0	-		0.03	0.03	0.01
3	2	0.01	0.12	0.04	0.05
4	2	0.01	0.13	0.03	0.03
6	2	0.01	0.07	0.03	0.03
8	2	0.01	0.03	0.01	0.01
12	2	0.01	0.01	0.01	0.01
18	2	0.01	0.01	0.01	0.01

Table B.194. Storm event #10 NO_2^--N data.

Sample time (hr)	Theoretical detention time (hr)	Influent (mg/L)	60 cm column (mg/L)	45 cm column (mg/L)	30 cm column (mg/L)
0	-		0.23	0.20	0.28
3	2	0.12	0.23	0.16	0.16
4	2	0.12	0.20	0.18	0.15
6	2	0.12	0.10	0.11	0.11
8	2	0.15	0.03	0.07	0.09
12	2	0.12	0.03	0.07	0.14
18	2	0.12	0.02	0.08	0.11

209

Table B.195. Storm event #10 NO$_3^-$-N data.

Sample time (hr)	Theoretical detention time (hr)	Influent (mg/L)	60 cm column (mg/L)	45 cm column (mg/L)	30 cm column (mg/L)
0	-		0.02	0.01	0.02
3	2	1.94	0.01	0.09	0.22
4	2	1.94	0.02	0.24	0.37
6	2	1.97	0.08	0.34	0.43
8	2	1.91	0.15	0.41	0.52
12	2	1.89	0.28	0.53	0.65
18	2	1.86	0.45	0.60	0.75

Table B.196. Storm event #10 PO$_4^{3-}$-P data.

Sample time (hr)	Theoretical detention time (hr)	Influent (mg/L)	60 cm column (mg/L)	45 cm column (mg/L)	30 cm column (mg/L)
0	-		0.44	0.10	0.33
3	2	0.10	0.13	0.05	0.12
4	2	0.09	0.03	0.00	0.05
6	2	0.09	0.00	0.00	0.00
8	2	0.09	0.00	0.00	0.00
12	2	0.09	0.00	0.00	0.00
18	2	0.09	0.00	0.00	0.00

Table B.197. Storm event #10 SO$_4^{2-}$-S data.

Sample time (hr)	Theoretical detention time (hr)	Influent (mg/L)	60 cm column (mg/L)	45 cm column (mg/L)	30 cm column (mg/L)
0	-		5.70	11.99	10.00
3	2	60.99	50.71	44.58	46.65
4	2	60.99	61.37	56.91	56.88
6	2	62.66	61.82	60.47	61.83
8	2	61.53	63.99	61.44	62.14
12	2	60.90	64.18	62.87	62.99
18	2	60.16	63.75	62.45	62.95

Table B.198. Storm event #11 flow data for the 30 cm column.

Theoretical detention time (hr)	Theoretical flow rate (mL/min)	Flow rate 1 (mL/min)	Flow rate 2 (mL/min)	Average flow rate (mL/min)
3	9.76			
3	9.76			
3	9.76			
3	9.76			
3	9.76			

Table B.199. Storm event #11 flow data for the 45 cm column.

Theoretical detention time (hr)	Theoretical flow rate (mL/min)	Flow rate 1 (mL/min)	Flow rate 2 (mL/min)	Average flow rate (mL/min)
3	14.81			
3	14.81			
3	14.81			
3	14.81			
3	14.81			

Table B.200. Storm event #11 flow data for the 60 cm column.

Theoretical detention time (hr)	Theoretical flow rate (mL/min)	Flow rate 1 (mL/min)	Flow rate 2 (mL/min)	Average flow rate (mL/min)
3	19.78			
3	19.78			
3	19.78			
3	19.78			
3	19.78			

Table B.201. Storm event #11 NH_4^+-N data.

Sample time (hr)	Theoretical detention time (hr)	Influent (mg/L)	60 cm column (mg/L)	45 cm column (mg/L)	30 cm column (mg/L)
12	3	0.01	0.12	0.05	0.05
24	3	0.01	0.03	0.01	0.01
42.75	3	0.01	0.03	0.01	0.01
61.25	3	0.01	0.01	0.01	0.01
86.25	3	0.01	0.01	0.01	0.01

211

Table B.202. Storm event #11 NO_2^--N data.

Sample time (hr)	Theoretical detention time (hr)	Influent (mg/L)	60 cm column (mg/L)	45 cm column (mg/L)	30 cm column (mg/L)
12	3	0.15	0.10	0.10	0.12
24	3	0.18	0.02	0.05	0.13
42.75	3	0.12	0.01	0.10	0.12
61.25	3	0.11	0.12	0.10	0.13
86.25	3	0.05	0.05	0.04	0.08

Table B.203. Storm event #11 NO_3^--N data.

Sample time (hr)	Theoretical detention time (hr)	Influent (mg/L)	60 cm column (mg/L)	45 cm column (mg/L)	30 cm column (mg/L)
12	3	1.99	0.04	0.14	0.37
24	3	2.01	0.23	0.30	0.57
42.75	3	2.12	0.27	0.40	0.70
61.25	3	2.04	0.47	0.43	0.65
86.25	3	1.93	0.48	0.42	0.53

Table B.204. Storm event #11 PO_4^{3-}-P data.

Sample time (hr)	Theoretical detention time (hr)	Influent (mg/L)	60 cm column (mg/L)	45 cm column (mg/L)	30 cm column (mg/L)
12	3	0.06	0.00	0.00	0.00
24	3	0.08	0.00	0.00	0.00
42.75	3	0.06	0.00	0.00	0.00
61.25	3	0.11	0.00	0.00	0.00
86.25	3	0.11	0.00	0.00	0.00

Table B.205. Storm event #11 SO_4^{2-}-S data.

Sample time (hr)	Theoretical detention time (hr)	Influent (mg/L)	60 cm column (mg/L)	45 cm column (mg/L)	30 cm column (mg/L)
12	3	62.43	61.99	64.21	63.51
24	3	61.97	64.63	64.83	65.05
42.75	3	62.66	62.94	64.61	63.65
61.25	3	60.49	62.42	62.17	61.79
86.25	3	60.25	60.36	61.21	60.43

213

Appendix C;

Tracer Study Data

Table C.1. 60 cm column one hour detention time tracer study data.

Time (min)	KCL eq. (mg/L)		Time (min)	KCL eq. (mg/L)		Time (min)	KCL eq. (mg/L)
0	4		85	130		170	31
5	0		90	140		175	26
10	4		95	149		180	18
15	4		100	147		185	20
20	3		105	161		190	16
25	3		110	160		195	16
30	3		115	158		200	8
35	5		120	160		205	10
40	7		125	142		210	11
45	15		130	124		215	2
50	25		135	105		220	3
55	38		140	88		225	14
60	54		145	73		230	8
65	73		150	60		235	7
70	90		155	50		240	2
75	106		160	41			
80	112		165	34			

214

Table C.2. 45 cm column one hour detention time tracer study data.

Time (min)	KCL eq. (mg/L)		Time (min)	KCL eq. (mg/L)		Time (min)	KCL eq. (mg/L)
0	2		85	102		170	43
5	1		90	113		175	40
10	0		95	123		180	31
15	2		100	128		185	28
20	2		105	139		190	25
25	3		110	146		195	27
30	3		115	151		200	17
35	6		120	160		205	15
40	7		125	158		210	16
45	12		130	151		215	11
50	21		135	138		220	10
55	34		140	122		225	9
60	47		145	105		230	10
65	62		150	86		235	9
70	70		155	72		240	6
75	74		160	60			
80	88		165	53			

Table C.3. 30 cm column one hour detention time tracer study data.

Time (min)	KCL eq. (mg/L)		Time (min)	KCL eq. (mg/L)		Time (min)	KCL eq. (mg/L)
0	0		85	98		170	52
5	2		90	110		175	48
10	0		95	118		180	41
15	0		100	128		185	38
20	0		105	137		190	34
25	3		110	143		195	24
30	3		115	145		200	27
35	5		120	155		205	26
40	7		125	153		210	30
45	10		130	145		215	21
50	18		135	136		220	20
55	30		140	122		225	8
60	43		145	108		230	17
65	57		150	92		235	16
70	71		155	79		240	12
75	71		160	73			
80	81		165	60			

215

Table C.4. 60 cm column three hour detention time tracer study data.

Time (min)	KCL eq. (mg/L)		Time (min)	KCL eq. (mg/L)		Time (min)	KCL eq. (mg/L)
0	3		255	110		510	33
15	3		270	114		525	25
30	4		285	126		540	24
45	3		300	127		555	24
60	4		315	120		570	18
75	4		330	120		585	18
90	0		345	113		600	19
105	11		360	102		615	18
120	16		375	95		630	17
135	34		390	85		660	15
150	54		405	78		690	18
165	69		420	72		720	14
180	73		435	63		750	16
195	80		450	48		840	17
210	96		465	43		1000	7
225	97		480	43			
240	101		495	37			

Table C.5. 45 cm column three hour detention time tracer study data.

Time (min)	KCL eq. (mg/L)		Time (min)	KCL eq. (mg/L)		Time (min)	KCL eq. (mg/L)
0	0		255	115		510	34
15	3		270	126		525	25
30	4		285	132		540	26
45	6		300	134		555	22
60	4		315	130		570	20
75	2		330	131		585	18
90	1		345	126		600	18
105	5		360	118		615	20
120	13		375	110		630	18
135	31		390	99		660	15
150	51		405	86		690	18
165	68		420	75		720	14
180	79		435	61		750	16
195	92		450	50		840	16
210	100		465	43		1000	5
225	103		480	43			
240	106		495	36			

Table C.6. 30 cm column three hour detention time tracer study data.

Time (min)	KCL eq. (mg/L)		Time (min)	KCL eq. (mg/L)		Time (min)	KCL eq. (mg/L)
0	4		255	127		510	25
15	0		270	134		525	20
30	2		285	129		540	18
45	4		300	126		555	15
60	6		315	107		570	14
75	8		330	100		585	12
90	19		345	88		600	12
105	40		360	77		615	13
120	58		375	64		630	15
135	78		390	60		660	12
150	99		405	47		690	14
165	107		420	42		720	13
180	112		435	37		750	11
195	120		450	29		840	12
210	122		465	26		1000	7
225	122		480	31			
240	123		495	24			

Table C.7. 60 cm column four hour detention time tracer study data.

Time (min)	KCL eq. (mg/L)		Time (min)	KCL eq. (mg/L)		Time (min)	KCL eq. (mg/L)
0	0		340	134		680	27
20	0		360	129		700	22
40	0		380	133		720	22
60	0		400	134		740	19
80	0		420	131		760	14
100	0		440	127		780	15
120	0		460	116		800	11
140	0		480	103		820	12
160	12		500	88		840	13
180	55		520	78		960	8
200	68		540	67		1440	3
220	87		560	56		1680	4
240	103		580	47		1920	3
260	106		600	39		1940	3
280	113		620	36		1960	3
300	118		640	32			
320	122		660	29			

217

Table C.8. 45 cm column four hour detention time tracer study data.

Time (min)	KCL eq. (mg/L)		Time (min)	KCL eq. (mg/L)		Time (min)	KCL eq. (mg/L)
0	0		340	136		680	20
20	0		360	135		700	18
40	0		380	135		720	19
60	0		400	131		740	14
80	0		420	125		760	17
100	0		440	114		780	14
120	9		460	100		800	10
140	35		480	87		820	11
160	51		500	70		840	12
180	67		520	61		960	7
200	76		540	58		1440	4
220	87		560	42		1680	3
240	102		580	38		1920	4
260	109		600	31		1940	4
280	118		620	27		1960	4
300	123		640	25			
320	127		660	24			

Table C.9. 30 cm column four hour detention time tracer study data.

Time (min)	KCL eq. (mg/L)		Time (min)	KCL eq. (mg/L)		Time (min)	KCL eq. (mg/L)
0	0		340	139		680	19
20	0		360	134		700	18
40	0		380	127		720	17
60	0		400	110		740	15
80	0		420	98		760	13
100	6		440	82		780	14
120	50		460	71		800	11
140	85		480	60		820	11
160	95		500	49		840	11
180	106		520	44		960	6
200	115		540	36		1440	4
220	116		560	32		1680	4
240	126		580	29		1920	4
260	125		600	26		1940	4
280	128		620	22		1960	4
300	135		640	23			
320	137		660	21			

218

Appendix D:

SWMM-5 Data

Case Study

01/01/2012 00:03:09

219
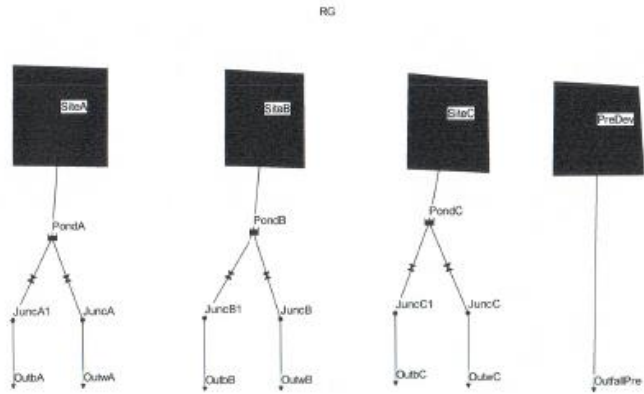
Case Study

```
[TITLE]
Case Study

[OPTIONS]
FLOW_UNITS            CFS
INFILTRATION          GREEN_AMPT
FLOW_ROUTING          DYNWAVE
START_DATE            01/01/2012
START_TIME            00:00:00
REPORT_START_DATE     01/01/2012
REPORT_START_TIME     00:00:00
END_DATE              12/31/2012
END_TIME              23:59:00
SWEEP_START           01/01
SWEEP_END             12/31
DRY_DAYS              0
REPORT_STEP           00:03:00
WET_STEP              00:03:00
DRY_STEP              00:03:00
ROUTING_STEP          0:00:01
ALLOW_PONDING         YES
INERTIAL_DAMPING      PARTIAL
VARIABLE_STEP         0.75
LENGTHENING_STEP      0
MIN_SURFAREA          0
NORMAL_FLOW_LIMITED   BOTH
SKIP_STEADY_STATE     NO
FORCE_MAIN_EQUATION   H-W
LINK_OFFSETS          DEPTH
MIN_SLOPE             0

[EVAPORATION]
;;Type       Parameters
;;---------- -----------
CONSTANT     0.0
DRY_ONLY     NO

[RAINGAGES]
;;            Rain      Time   Snow   Data
;;Name        Type      Intrvl Catch  Source
;;----------- --------- ------ ------ ----------
RG            VOLUME    0:15   1.0    TIMESERIES 2012HR

[SUBCATCHMENTS]
;;                                    Total  Pcnt.         Pcnt.  Curb    Snow
;;Name        Raingage   Outlet       Area   Imperv  Width Slope  Length  Pack
;;----------- ---------- ------------ -----  ------  ----- -----  ------  ------
SiteA         RG         PondA        2      75      200   0.5    0
SiteB         RG         PondB        2      75      200   0.5    0
SiteC         RG         PondC        2      75      200   0.5    0
PreDev        RG         OutfallPre   2      0       200   0.5    0
```

```
[SUBAREAS]
;;Subcatchment   N-Imperv   N-Perv   S-Imperv   S-Perv   PctZero   RouteTo   PctRouted
;;------------   --------   ------   --------   ------   -------   -------   ---------
SiteA            0.01       0.1      0          0        100       OUTLET
SiteB            0.01       0.1      0          0        100       OUTLET
SiteC            0.01       0.1      0          0        100       OUTLET
PreDev           0.01       0.1      0          0        100       OUTLET

[INFILTRATION]
;;Subcatchment   Suction    HydCon   IMDmax
;;------------   -------    ------   ------
SiteA            1.93       0.05     0.375
SiteB            1.93       0.05     0.375
SiteC            1.93       0.05     0.375
PreDev           1.93       0.05     0.375

[JUNCTIONS]
;;               Invert     Max.     Init.      Surcharge   Ponded
;;Name           Elev.      Depth    Depth      Depth       Area
;;------------   ------     -----    -----      ---------   ------
JuncA            0          6        3          0           0
JuncB            0          6        3          0           0
JuncC            0          6        3          0           0
JuncA1           0          6        3          0           0
JuncB1           0          6        3          0           0
JuncC1           0          6        3          0           0

[OUTFALLS]
;;               Invert     Outfall  Stage/Table   Tide
;;Name           Elev.      Type     Time Series   Gate
;;------------   ------     -------  -----------   ----
OutwA            0          FIXED    2.5           NO
OutwB            0          FIXED    2.5           NO
OutwC            0          FIXED    2.5           NO
OutfallPre       0          FIXED    2.5           NO
OutbA            0          FIXED    2.5           NO
OutbB            0          FIXED    2.5           NO
OutbC            0          FIXED    2.5           NO

[STORAGE]
;;               Invert   Max.    Init.   Storage   Curve                 Ponded   Evap.
;;Name           Elev.    Depth   Depth   Curve     Params                Area     Frac.    Infiltration Parameters
;;------------   ------   -----   -----   -------   --------   --------   ------   -----    -----------------------
PondA            0        6       3       TABULAR   StorageA              0        0
PondB            0.5      5.5     2.5     TABULAR   StorageB              0        0
PondC            1        5       2       TABULAR   StorageC              0        0

[CONDUITS]
;;               Inlet              Outlet                    Manning   Inlet     Outlet    Init.    Max.
;;Name           Node               Node          Length      N         Offset    Offset    Flow     Flow
```

Case Study

```
;;----------  ------------  ----------  ---------  ---------  ---  ---------  ---------  ----------
CulvertA     JuncA         OutwA       10         0.01       3    2.5        0          0
CulvertB     JuncB         OutwB       10         0.01       3    2.5        0          0
CulvertC     JuncC         OutwC       10         0.01       3    2.5        0          0
CulvertA1    JuncA1        OutbA       10         0.01       3    2.5        0          0
CulvertB1    JuncB1        OutbB       10         0.01       3    2.5        0          0
CulvertC1    JuncC1        OutbC       10         0.01       3    2.5        0          0
```

```
[WEIRS]
;;           Inlet         Outlet      Weir       Crest      Disch.     Flap End    End
;;Name       Node          Node        Type       Height     Coeff.     Gate Con.   Coeff.
;;----------  ------------  ----------  ---------  ---------  ---------  ---- ----   ----------
WeirA        PondA         JuncA       TRANSVERSE 4.75       3.33       NO   2      0
WeirB        PondB         JuncB       TRANSVERSE 4.25       3.33       NO   2      0
WeirC        PondC         JuncC       TRANSVERSE 3.75       3.33       NO   2      0
WeirAo       PondA         JuncA       TRANSVERSE 5.5        3.33       NO   2      0
WeirBo       PondB         JuncB       TRANSVERSE 5.0        3.33       NO   0      0
WeirCo       PondC         JuncC       TRANSVERSE 4.5        3.33       NO   0      0
```

```
[OUTLETS]
;;           Inlet         Outlet      Outflow    Outlet     Qcoeff/                Flap
;;Name       Node          Node        Height     Type       QTable     Qexpon      Gate
;;----------  ------------  ----------  ---------  ---------  ---------  ----------  ----
BioA         PondA         JuncA1      3          TABULAR/HEAD RCA                   NO
BioB         PondB         JuncB1      2.5        TABULAR/HEAD RCB                   NO
BioC         PondC         JuncC1      2          TABULAR/HEAD RCC                   NO
```

```
[XSECTIONS]
;;Link        Shape         Geom1       Geom2      Geom3      Geom4    Barrels
;;----------  ------------  ----------  ---------  ---------  -------  ----------
CulvertA     CIRCULAR      1           0          0          0        1
CulvertB     CIRCULAR      1           0          0          0        1
CulvertC     CIRCULAR      1           0          0          0        1
CulvertA1    CIRCULAR      1.0         0          0          0        1
CulvertB1    CIRCULAR      1.0         0          0          0        1
CulvertC1    CIRCULAR      1.0         0          0          0        1
WeirA        RECT_OPEN     0.75        4          0          0
WeirB        RECT_OPEN     0.75        4          0          0
WeirC        RECT_OPEN     0.75        4          0          0
WeirAo       RECT_OPEN     0.50        10.17      0          0
WeirBo       RECT_OPEN     0.5         10.17      0          0
WeirCo       RECT_OPEN     0.5         10.17      0          0
```

```
[LOSSES]
;;Link        Inlet     Outlet    Average    Flap Gate
;;----------  --------  --------  ---------  ----------
CulvertA     0.5       1.0       0          NO
CulvertB     0.5       1.0       0          NO
CulvertC     0.5       1.0       0          NO
CulvertA1    0.5       1.0       0          NO
CulvertB1    0.5       1.0       0          NO
```

```
CulvertC1         0.5        1.0        0         NO

[CONTROLS]
Rule 1RCA
IF NODE PondA DEPTH <= 4.0
AND NODE PondA DEPTH > 3.8
THEN OUTLET BioA SETTING = 0.62

Rule 2RCA
IF NODE PondA DEPTH <= 3.8
AND NODE PondA DEPTH > 3.6
THEN OUTLET BioA SETTING = 0.20

Rule 3RCA
IF NODE PondA DEPTH <= 3.6
AND NODE PondA DEPTH > 3.4
THEN OUTLET BioA SETTING = 0.04

Rule 4RCA
IF NODE PondA DEPTH <= 3.4
AND NODE PondA DEPTH > 3.2
THEN OUTLET BioA SETTING = 0.004

Rule 5RCA
IF NODE PondA DEPTH <= 3.2
AND NODE PondA DEPTH > 3.0
THEN OUTLET BioA SETTING = 0.00003

Rule 1RCB
IF NODE PondB DEPTH <= 3.5
AND NODE PondB DEPTH > 3.3
THEN OUTLET BioB SETTING = 0.62

Rule 2RCB
IF NODE PondB DEPTH <= 3.3
AND NODE PondB DEPTH > 3.1
THEN OUTLET BioB SETTING = 0.20

Rule 3RCB
IF NODE PondB DEPTH <= 3.1
AND NODE PondB DEPTH > 2.9
THEN OUTLET BioB SETTING = 0.04

Rule 4RCB
IF NODE PondB DEPTH <= 2.9
AND NODE PondB DEPTH > 2.7
THEN OUTLET BioB SETTING = 0.004

Rule 5RCB
IF NODE PondB DEPTH <= 2.7
AND NODE PondB DEPTH > 2.5
```

```
THEN OUTLET BioB SETTING = 0.00003

Rule 1RCC
IF NODE PondC DEPTH <= 3.0
AND NODE PondC DEPTH > 2.8
THEN OUTLET BioC SETTING = 0.62

Rule 2RCC
IF NODE PondC DEPTH <= 2.8
AND NODE PondC DEPTH > 2.6
THEN OUTLET BioC SETTING = 0.20

Rule 3RCC
IF NODE PondC DEPTH <= 2.6
AND NODE PondC DEPTH > 2.4
THEN OUTLET BioC SETTING = 0.04

Rule 4RCC
IF NODE PondC DEPTH <= 2.4
AND NODE PondC DEPTH > 2.2
THEN OUTLET BioC SETTING = 0.004

Rule 5RCC
IF NODE PondC DEPTH <= 2.2
AND NODE PondC DEPTH > 2.0
THEN OUTLET BioC SETTING = 0.00003
```

```
[LANDUSES]
;;                Cleaning    Fraction    Last
;;Name            Interval    Available   Cleaned
;;--------------- ----------- ----------- -----------
Residential       0           0           0

[COVERAGES]
;;Subcatchment    Land Use            Percent
;;--------------- ------------------- -----------
SiteA             Residential         100
SiteB             Residential         100
SiteC             Residential         100

[CURVES]
;;Name            Type        X-Value     Y-Value
;;--------------- ----------- ----------- -----------
RCA               Rating      0           0.000
RCA                           0.1         0.109
RCA                           0.2         0.217
RCA                           0.3         0.326
```

RCA		0.4	0.434
RCA		0.5	0.543
RCA		0.6	0.651
RCA		0.7	0.760
RCA		0.8	0.868
RCA		0.9	0.977
RCA		1	1.086
RCA		1.1	1.194
RCA		1.2	1.303
RCA		1.3	1.411
RCA		1.4	1.520
RCA		1.5	1.628
RCA		1.6	1.737
RCA		1.7	1.845
RCA		1.8	1.954
RCA		1.9	2.063
RCA		2	2.171
RCA		2.1	2.280
RCA		2.2	2.388
RCA		2.3	2.497
RCA		2.4	2.605
RCA		2.5	2.714
RCA		2.6	2.822
RCA		2.7	2.931
RCA		2.8	3.040
RCA		2.9	3.148
RCA		3	3.257
RCA		3.1	3.365
RCA		3.2	3.474
RCA		3.3	3.582
RCA		3.4	3.691
RCA		3.5	3.799
RCA		3.6	3.908
RCA		3.7	4.017
RCA		3.8	4.125
RCA		3.9	4.234
RCA		4	4.342
RCB	Rating	0	0.000
RCB		0.1	0.145
RCB		0.2	0.289
RCB		0.3	0.434
RCB		0.4	0.579
RCB		0.5	0.724
RCB		0.6	0.868
RCB		0.7	1.013
RCB		0.8	1.158
RCB		0.9	1.303
RCB		1	1.447
RCB		1.1	1.592
RCB		1.2	1.737

225

RCB		1.3	1.882
RCB		1.4	2.026
RCB		1.5	2.171
RCB		1.6	2.316
RCB		1.7	2.461
RCB		1.8	2.605
RCB		1.9	2.750
RCB		2	2.895
RCB		2.1	3.040
RCB		2.2	3.184
RCB		2.3	3.329
RCB		2.4	3.474
RCB		2.5	3.619
RCB		2.6	3.763
RCB		2.7	3.908
RCB		2.8	4.053
RCB		2.9	4.198
RCB		3	4.342
RCB		3.1	4.487
RCB		3.2	4.632
RCB		3.3	4.776
RCB		3.4	4.921
RCB		3.5	5.066
RCB		3.6	5.211
RCB		3.7	5.355
RCB		3.8	5.500
RCB		3.9	5.645
RCB		4	5.790
RCC	Rating	0	0.000
RCC		0.1	0.217
RCC		0.2	0.434
RCC		0.3	0.651
RCC		0.4	0.868
RCC		0.5	1.086
RCC		0.6	1.303
RCC		0.7	1.520
RCC		0.8	1.737
RCC		0.9	1.954
RCC		1	2.171
RCC		1.1	2.388
RCC		1.2	2.605
RCC		1.3	2.822
RCC		1.4	3.040
RCC		1.5	3.257
RCC		1.6	3.474
RCC		1.7	3.691
RCC		1.8	3.908
RCC		1.9	4.125
RCC		2	4.342
RCC		2.1	4.559

226

Case Study

```
RCC                     2.2      4.776
RCC                     2.3      4.994
RCC                     2.4      5.211
RCC                     2.5      5.428
RCC                     2.6      5.645
RCC                     2.7      5.862
RCC                     2.8      6.079
RCC                     2.9      6.296
RCC                     3        6.513
RCC                     3.1      6.730
RCC                     3.2      6.948
RCC                     3.3      7.165
RCC                     3.4      7.382
RCC                     3.5      7.599
RCC                     3.6      7.816
RCC                     3.7      8.033
RCC                     3.8      8.250
RCC                     3.9      8.467
RCC                     4        8.685

StorageA     Storage    0        1935.4
StorageA                1        1935.4
StorageA                3        1935.4
StorageA                3.001    1774
StorageA                4        1774
StorageA                4.001    9216
StorageA                5        10944
StorageA                6        12800

StorageB     Storage    0        2580.5
StorageB                1        2580.5
StorageB                2.5      2580.5
StorageB                2.501    2365
StorageB                3.5      2365
StorageB                3.501    9216
StorageB                4.5      10944
StorageB                5.5      12800

StorageC     Storage    0        3870.7
StorageC                1        3870.7
StorageC                2        3870.7
StorageC                2.001    3548
StorageC                3        3548
StorageC                3.001    9216
StorageC                4        10944
StorageC                5        12800

[TIMESERIES]
;;Name          Date       Time       Value
;;------------- ---------- ---------- ----------
25yr24hr                   0          0
```

Case Study

```
25yr24hr              0:30      0.048
25yr24hr              1         0.048
25yr24hr              1:30      0.056
25yr24hr              2         0.048
25yr24hr              2:30      0.056
25yr24hr              3         0.056
25yr24hr              3:30      0.064
25yr24hr              4         0.056
25yr24hr              4:30      0.064
25yr24hr              5         0.072
25yr24hr              5:30      0.072
25yr24hr              6         0.072
25yr24hr              6:30      0.08
25yr24hr              7         0.088
25yr24hr              7:30      0.096
25yr24hr              8         0.096
25yr24hr              8:30      0.112
25yr24hr              9         0.128
25yr24hr              9:30      0.136
25yr24hr              10        0.16
25yr24hr              10:30     0.2
25yr24hr              11        0.256
25yr24hr              11:30     0.4
25yr24hr              12        2.392
25yr24hr              12:30     0.896
25yr24hr              13        0.304
25yr24hr              13:30     0.224
25yr24hr              14        0.176
25yr24hr              14:30     0.152
25yr24hr              15        0.128
25yr24hr              15:30     0.12
25yr24hr              16        0.104
25yr24hr              16:30     0.096
25yr24hr              17        0.088
25yr24hr              17:30     0.088
25yr24hr              18        0.072
25yr24hr              18:30     0.08
25yr24hr              19        0.064
25yr24hr              19:30     0.072
25yr24hr              20        0.064
25yr24hr              20:30     0.056
25yr24hr              21        0.056
25yr24hr              21:30     0.056
25yr24hr              22        0.056
25yr24hr              22:30     0.056
25yr24hr              23        0.048
25yr24hr              23:30     0.048
25yr24hr              24        0.04

;15 min data from the Hillsborough River
2012HR        FILE "C:\Users\Tommy\Desktop\PhD\Research\bioretention\Data\Model\SWMM\2012HRcondensed15min.txt"
```

Case Study

```
[REPORT]
INPUT        YES
CONTROLS     NO
SUBCATCHMENTS ALL
NODES ALL
LINKS ALL

[TAGS]

[MAP]
DIMENSIONS 0.000 0.000 10000.000 10000.000
Units       None

[COORDINATES]
;;Node           X-Coord            Y-Coord
;;-------------- ------------------ ------------------
JuncA            -2264.151          5283.019
JuncB            325.901            5283.019
JuncC            2761.578           5351.630
JuncA1           -3173.242          5283.019
JuncB1           -686.106           5300.172
JuncC1           1818.182           5351.630
OutwA            -2264.151          4416.810
OutwB            325.901            4373.928
OutwC            2761.578           4399.657
OutfallPre       4395.369           4339.623
OutbA            -3173.242          4416.810
OutbB            -686.106           4373.928
OutbC            1818.182           4433.962
PondA            -2658.662          6355.060
PondB            -25.729            6415.094
PondC            2264.151           6526.587

[VERTICES]
;;Link           X-Coord            Y-Coord
;;-------------- ------------------ ------------------

[Polygons]
;;Subcatchment   X-Coord            Y-Coord
;;-------------- ------------------ ------------------
SiteA            -1925.386          8550.600
SiteA            -1933.962          7272.727
SiteA            -3151.801          7298.456
SiteA            -3143.225          8593.482
SiteB            638.937            8464.837
SiteB            647.513            7246.998
SiteB            -407.376           7281.304
SiteB            -398.799           8524.871
SiteC            3023.156           8370.497
SiteC            3040.309           7178.388
```

```
SiteC          1985.420         7229.846
SiteC          2002.573         8464.837
PreDev         4995.712         8284.734
PreDev         5064.322         7135.506
PreDev         3872.213         7135.506
PreDev         3889.365         8353.345

[SYMBOLS]
;;Gage         X-Coord          Y-Coord
;;-------------- -------------------- --------------------
RG             947.684          9099.485
```

```
                                   txt

EPA STORM WATER MANAGEMENT MODEL - VERSION 5.0 (Build 5.0.022)
--------------------------------------------------------------

Case Study

****************************************************************
NOTE: The summary statistics displayed in this report are
based on results found at every computational time step,
not just on results from each reporting time step.
****************************************************************

****************
Analysis Options
****************
Flow Units .............. CFS
Process Models:
  Rainfall/Runoff ........ YES
  Snowmelt ............... NO
  Groundwater ............ NO
  Flow Routing ........... YES
  Ponding Allowed ........ YES
  Water Quality .......... NO
Infiltration Method ...... GREEN_AMPT
Flow Routing Method ...... DYNWAVE
Starting Date ............ JAN-01-2012 00:00:00
Ending Date .............. DEC-31-2012 23:59:00
Antecedent Dry Days ...... 0.0
Report Time Step ......... 00:03:00
Wet Time Step ............ 00:03:00
Dry Time Step ............ 00:03:00
Routing Time Step ........ 1.00 sec


*************
Element Count
*************
Number of rain gages ...... 1
Number of subcatchments ... 4
Number of nodes ........... 16
Number of links ........... 15
Number of pollutants ...... 0
Number of land uses ....... 1


***************
Landuse Summary
***************
                        Sweeping    Maximum     Last
Name                    Interval    Removal     Swept
-----------------------------------------------------

Residential               0.00        0.00       0.00


****************
Raingage Summary
****************
                                        Data        Recording
Name            Data Source             Type        Interval
-----------------------------------------------------------
RG              2012HR                  VOLUME      15 min.
```

Page 1

```
                                            txt
*********************
Subcatchment Summary
*********************
Name                          Area      Width    %Imperv    %Slope    Rain Gage
Outlet
----------------

----------------
SiteA                         2.00     200.00     75.00     0.5000     RG
PondA
SiteB                         2.00     200.00     75.00     0.5000     RG
PondB
SiteC                         2.00     200.00     75.00     0.5000     RG
PondC
PreDev                        2.00     200.00      0.00     0.5000     RG
OutfallPre


*************
Node Summary
*************
                                                 Invert      Max.     Ponded    External
                                                 Elev.       Depth     Area      Inflow
Name                          Type
----------------
JuncA                         JUNCTION           0.00        6.00      0.0
JuncB                         JUNCTION           0.00        6.00      0.0
JuncC                         JUNCTION           0.00        6.00      0.0
JuncA1                        JUNCTION           0.00        6.00      0.0
JuncB1                        JUNCTION           0.00        6.00      0.0
JuncC1                        JUNCTION           0.00        6.00      0.0
OutwA                         OUTFALL            0.00        3.50      0.0
OutwB                         OUTFALL            0.00        3.50      0.0
OutwC                         OUTFALL            0.00        3.50      0.0
OutfallPre                    OUTFALL            0.00        0.00      0.0
OutbA                         OUTFALL            0.00        3.50      0.0
OutbB                         OUTFALL            0.00        3.50      0.0
OutbC                         OUTFALL            0.00        3.50      0.0
PondA                         STORAGE            0.00        6.00      0.0
PondB                         STORAGE            0.50        5.50      0.0
PondC                         STORAGE            1.00        5.00      0.0


*************
Link Summary
*************
Name                  From Node      To Node       Type          Length    %Slope
Roughness
----------------

------
CulvertA              JuncA          OutwA         CONDUIT        10.0      5.0063
0.0100
CulvertB              JuncB          OutwB         CONDUIT        10.0      5.0063
0.0100
CulvertC              JuncC          OutwC         CONDUIT        10.0      5.0063
0.0100
CulvertA1             JuncA1         OutbA         CONDUIT        10.0      5.0063
0.0100
CulvertB1             JuncB1         OutbB         CONDUIT        10.0      5.0063
0.0100
CulvertC1             JuncC1         OutbC         CONDUIT        10.0      5.0063
0.0100
WeirA                 PondA          JuncA         WEIR
                                    Page 2
```

```
                          txt
WeirB              PondB         JuncB          WEIR
WeirC              PondC         JuncC          WEIR
WeirAo             PondA         JuncA          WEIR
WeirBo             PondB         JuncB          WEIR
WeirCo             PondC         JuncC          WEIR
BioA               PondA         JuncA1         OUTLET
BioB               PondB         JuncB1         OUTLET
BioC               PondC         JuncC1         OUTLET
```

```
  **********************
  Cross Section Summary
  **********************
                                  Full     Full    Hyd.    Max.    No. of
Full
  Conduit          Shape          Depth    Area    Rad.    Width   Barrels
Flow
  -----------------------------------------------------------------------
  ---
  CulvertA         CIRCULAR       1.00     0.79    0.25    1.00    1
10.36
  CulvertB         CIRCULAR       1.00     0.79    0.25    1.00    1
10.36
  CulvertC         CIRCULAR       1.00     0.79    0.25    1.00    1
10.36
  CulvertA1        CIRCULAR       1.00     0.79    0.25    1.00    1
10.36
  CulvertB1        CIRCULAR       1.00     0.79    0.25    1.00    1
10.36
  CulvertC1        CIRCULAR       1.00     0.79    0.25    1.00    1
10.36
```

```
  ****************************      Volume          Depth
  Runoff Quantity Continuity       acre-feet        inches
  ****************************      ---------        -------
  Total Precipitation ......       30.000           45.000
  Evaporation Loss .........        0.000            0.000
  Infiltration Loss ........        6.305            9.458
  Surface Runoff ...........       23.745           35.618
  Final Surface Storage ....        0.000            0.000
  Continuity Error (%) .....       -0.168
```

```
  ****************************      Volume          Volume
  Flow Routing Continuity          acre-feet        10^6 gal
  ****************************      ---------        ---------
  Dry Weather Inflow .......        0.000            0.000
  Wet Weather Inflow .......       23.745            7.738
  Groundwater Inflow .......        0.000            0.000
  RDII Inflow .............         0.000            0.000
  External Inflow .........         0.000            0.000
  External Outflow ........        23.702            7.724
  Internal Outflow ........         0.000            0.000
  Storage Losses ..........         0.000            0.000
  Initial Stored Volume ....        0.459            0.150
  Final Stored Volume ......        0.502            0.164
  Continuity Error (%) .....       -0.001
```

```
  ****************************
```

Page 3

```
Time-Step Critical Elements
****************************
None


*******************************
Highest Flow Instability Indexes
*******************************
All links are stable.


**************************
Routing Time Step Summary
**************************
Minimum Time Step         :     0.84 sec
Average Time Step         :     1.00 sec
Maximum Time Step         :     1.00 sec
Percent in Steady State   :     0.00
Average Iterations per Step :   2.00


***************************
Subcatchment Runoff Summary
***************************
```

			Total	Total	Total	Total	Total
Total	Peak	Runoff	Precip	Runon	Evap	Infil	Runoff
Runoff	Runoff	Coeff	in	in	in	in	in
Subcatchment							
10^6 gal	CFS						

Subcatchment			Precip	Runon	Evap	Infil	Runoff
SiteA			45.00	0.00	0.00	4.94	40.15
2.18	8.43	0.892					
SiteB			45.00	0.00	0.00	4.94	40.15
2.18	8.43	0.892					
SiteC			45.00	0.00	0.00	4.94	40.15
2.18	8.43	0.892					
PreDev			45.00	0.00	0.00	23.00	22.01
1.20	5.24	0.489					

```
******************
Node Depth Summary
******************
```

Node	Type	Average Depth Feet	Maximum Depth Feet	Maximum HGL Feet	Time of Max Occurrence days hr:min	
JuncA	JUNCTION	3.00	3.58	3.58	218	17:16
JuncB	JUNCTION	3.00	3.49	3.49	218	17:19
JuncC	JUNCTION	3.00	3.33	3.33	218	17:28
JuncA1	JUNCTION	3.01	3.40	3.40	218	17:16
JuncB1	JUNCTION	3.01	3.46	3.46	218	17:19
JuncC1	JUNCTION	3.01	3.57	3.57	218	17:28
OutwA	OUTFALL	2.50	2.79	2.79	218	17:16

```
                                                txt
      OutwB          OUTFALL      2.50      2.75      2.75    218    17:19
      OutwC          OUTFALL      2.50      2.69      2.69    218    17:28
      OutfallPre     OUTFALL      0.00      0.00      0.00      0    00:00
      OutbA          OUTFALL      2.51      2.72      2.72    218    17:16
      OutbB          OUTFALL      2.51      2.74      2.74    218    17:19
      OutbC          OUTFALL      2.51      2.78      2.78    218    17:28
      PondA          STORAGE      3.27      5.02      5.02    218    17:16
      PondB          STORAGE      2.76      4.48      4.98    218    17:19
      PondC          STORAGE      2.26      3.91      4.91    218    17:28
```

```
  *********************
  Node Inflow Summary
  *********************
```

		Maximum Lateral Inflow	Maximum Total Inflow	Time of Max Occurrence	Lateral Inflow Volume	Total Inflow Volume
Node	Type	CFS	CFS	days hr:min	10^6 gal	10^6 gal
JuncA	JUNCTION	0.00	1.87	218 17:16	0.000	0.059
JuncB	JUNCTION	0.00	1.47	218 17:19	0.000	0.037
JuncC	JUNCTION	0.00	0.83	218 17:28	0.000	0.015
JuncA1	JUNCTION	0.00	1.09	218 17:16	0.000	2.118
JuncB1	JUNCTION	0.00	1.36	218 17:19	0.000	2.140
JuncC1	JUNCTION	0.00	1.81	218 17:28	0.000	2.159
OutwA	OUTFALL	0.00	1.87	218 17:16	0.000	0.059
OutwB	OUTFALL	0.00	1.47	218 17:19	0.000	0.037
OutwC	OUTFALL	0.00	0.83	218 17:28	0.000	0.015
OutfallPre	OUTFALL	5.24	5.24	218 17:00	1.196	1.196
OutbA	OUTFALL	0.00	1.09	218 17:16	0.000	2.118
OutbB	OUTFALL	0.00	1.36	218 17:19	0.000	2.140
OutbC	OUTFALL	0.00	1.81	218 17:28	0.000	2.159
PondA	STORAGE	8.43	8.43	218 17:00	2.181	2.224
PondB	STORAGE	8.43	8.43	218 17:00	2.181	2.229
PondC	STORAGE	8.43	8.43	218 17:00	2.181	2.238

```
**********************
Node Surcharge Summary
**********************

No nodes were surcharged.

**********************
Node Flooding Summary
**********************

No nodes were flooded.

**********************
Storage Volume Summary
**********************
```

| | Average | Avg | E&I | Maximum | Max | Time of Max | Maximum |
| | Volume | Pcnt | Pcnt | Volume | Pcnt | Occurrence | Outflow |
Storage Unit	1000 ft3	Full	Loss	1000 ft3	Full	days hr:min	CFS
PondA	6.297	21	0	17.900	61	218 17:16	2.96
PondB	7.083	23	0	18.697	61	218 17:19	2.84
PondC	8.653	26	0	20.367	61	218 17:28	2.64

```
**********************
Outfall Loading Summary
**********************
```

| | Flow Freq. | Avg. Flow | Max. Flow | Total Volume |
Outfall Node	Pcnt.	CFS	CFS	10^6 gal
OutwA	0.03	0.87	1.87	0.059
OutwB	0.03	0.71	1.47	0.037
OutwC	0.01	0.53	0.83	0.015
OutfallPre	2.42	0.22	5.24	1.196
OutbA	42.02	0.02	1.09	2.118
OutbB	48.99	0.02	1.36	2.140
OutbC	46.77	0.02	1.81	2.159
System	20.04	2.38	12.06	7.723

```
**********************
Link Flow Summary
**********************
```

```
                                    txt
                        Maximum   Time of Max    Maximum    Max/    Max/
                         |Flow|    Occurrence    |Veloc|    Full    Full
Link              Type    CFS    days  hr:min    ft/sec     Flow    Depth
------------------------------------------------------------------------
CulvertA          CONDUIT  1.87   218  17:16      5.71      0.18    0.43
CulvertB          CONDUIT  1.47   218  17:19      5.53      0.14    0.37
CulvertC          CONDUIT  0.83   218  17:28      5.10      0.08    0.26
CulvertA1         CONDUIT  1.09   218  17:16      5.30      0.11    0.31
CulvertB1         CONDUIT  1.36   218  17:19      5.47      0.13    0.35
CulvertC1         CONDUIT  1.81   218  17:28      5.69      0.17    0.42
WeirA             WEIR     1.87   218  17:16                        0.36
WeirB             WEIR     1.47   218  17:19                        0.31
WeirC             WEIR     0.83   218  17:28                        0.21
WeirAo            WEIR     0.00     0  00:00                        0.00
WeirBo            WEIR     0.00     0  00:00                        0.00
WeirCo            WEIR     0.00     0  00:00                        0.00
BioA              DUMMY    1.09   218  17:16
BioB              DUMMY    1.36   218  17:19
BioC              DUMMY    1.81   218  17:28


*******************************
Flow Classification Summary
*******************************
```

```
-----------------------------------------------------------------------
-----
              Adjusted    --- Fraction of Time in Flow Class ----   Avg.
Avg.          /Actual      Up   Down  Sub   Sup   Up   Down  Froude
Flow                                                                Number
  Conduit     Length  Dry  Dry  Dry   Crit  Crit  Crit  Crit
Change
-----------------------------------------------------------------------
-----
  CulvertA     1.00  0.47  0.00  0.00  0.52  0.00  0.00  0.00   0.00
0.0000
  CulvertB     1.00  0.48  0.00  0.00  0.52  0.00  0.00  0.00   0.00
0.0000
  CulvertC     1.00  0.60  0.00  0.00  0.40  0.00  0.00  0.00   0.00
0.0000
  CulvertA1    1.00  0.03  0.00  0.00  0.44  0.53  0.00  0.00   1.40
0.0000
  CulvertB1    1.00  0.03  0.00  0.00  0.44  0.53  0.00  0.00   1.39
0.0000
  CulvertC1    1.00  0.03  0.00  0.00  0.44  0.53  0.00  0.00   1.37
0.0000
```

```
*****************************
Conduit Surcharge Summary
*****************************

No conduits were surcharged.

Analysis begun on:  Mon Jun 30 11:35:38 2014
Analysis ended on:  Mon Jun 30 11:44:37 2014
Total elapsed time: 00:08:59
```